EXHIBIT A

Exponent®

Polymer Science and Materials Chemistry

Wave 2 General Report
Dr. Steven MacLean

United States District Court
For The Southern District Of
West Virginia
Charleston Division

This document relates to:
Ethicon Inc.,
Pelvic Repair System
Products Liability Litigation

Exponent

Expert Report of Dr. Steven MacLean

United States District Court
For The Southern District Of
West Virginia
Charleston Division

Prepared for

Chad R. Hutchinson
Butler Snow LLP
Renaissance at Colony Park
Suite 1400
1020 Highland Colony Parkway
Ridgeland, MS 39158-6010

Prepared by

Exponent
17000 Science Drive
Suite 200
Bowie, MD 20715

June 3, 2016

Contents

List of Figures

List of Tables

Limitations

At the request of Butler Snow LLP, Exponent reviewed relevant scientific literature, historic documented studies and expert reports for the pending litigation. Exponent investigated specific issues relevant to this report as requested by the client. The scope of services performed during this investigation may not adequately address the needs of other users of this report, and any reuse of this report or its findings, conclusions, or recommendations is at the sole risk of the user. The opinions and comments formulated during this investigation are based on observations and information available at the time of the investigation.

The findings presented herein are made to a reasonable degree of scientific and engineering certainty. We have endeavored to be accurate and complete in our assignment. If new data becomes available, or there are perceived omissions or misstatements in this report, we ask that they are brought to our attention as soon as possible so that we have the opportunity to address them.

Steven MacLean, Ph.D., P.E. Biography

I am a Principal Engineer in the Polymer Science and Materials Chemistry Practice at Exponent Failure Analysis Associates, Inc. ("Exponent"). My expertise and experience includes the chemical and physical behavior of polymeric materials in end-use applications, specifically in the evaluation of polymeric components in product safety assessments and product failure analysis. I have a B.S. and M.E. in Mechanical Engineering from Rensselaer Polytechnic Institute, and a M.S. in Material Science and Engineering from Rochester Institute of Technology. I also obtained a Ph.D. in Material Science from the University of Rochester in 2007. I am a registered Professional Engineer in New York and Maryland, a Senior Member of the Society of Plastics Engineers (SPE), and a board member of SPE's Failure Analysis and Prevention Special Interest Group.

During the pursuit of my advanced degrees in materials science, my chosen field of study was polymer science and engineering. Graduate courses taken during my academic career that specifically focused on polymers included, but were not limited to, polymer science, organic polymer chemistry, polymer physics, polymer rheology, polymer processing, bulk physical properties of polymers, adhesion theory, and analytical techniques for polymeric materials. Supplemental course work included mechanics of materials, fracture mechanics, thermodynamics of materials and electron microscopy practicum. At the master's degree level, my polymer research included characterizing the changes in chemical and physical properties of polycarbonate due to multiple heat histories from processing. At the doctoral level, my polymer research was focused on developing and investigating novel formulations of rubber-toughened polyphenylene ether polymers for use in pressurized, potable water systems. The primary emphasis of my dissertation included quantifying changes in select mechanical properties, including fracture toughness and tensile properties, due to the degrading effects from persistent exposure to chlorinated water at elevated temperatures.

In addition to my academic education and training, I have also been actively practicing in the field of polymer science and engineering for the past 20 years. Throughout that time, I have routinely utilized numerous polymer characterization techniques including, but not limited to, infrared spectroscopy, chromatography, mass spectrometry, and calorimetry as well as optical,

scanning electron and transmission electron microscopy. In particular, I have used these microscopic techniques to examine the topography and morphology of fracture surfaces created as a result of polymer cracking. I have also employed these techniques to characterize modes of polymer failure such as creep, fatigue, stress overload and environmentally-assisted stress cracking. In many instances, I have published the use of these analytical techniques to investigate polymer failures in commercialized products in peer-reviewed journal articles and scientific conference proceedings.

Prior to joining Exponent in 2011, I worked for over 15 years at General Electric Plastics (GE) and SABIC Innovative Plastics (SABIC) in a variety of technical roles of increasing responsibilities. Throughout my tenure, I was routinely involved in material selection, performance and testing for, among other things, high-demand applications, product safety assessments, and product failure analysis. As a result I have significant expertise and experience with industry standards and applicable regulations that prescribe the technical performance of polymeric materials in end-use applications, including those in the medical device industry.

At GE Plastics, I was trained extensively in the Six Sigma quality process, and became certified as a Six Sigma Black Belt. As a Certified Six Sigma Black Belt, my responsibilities included improving business processes by employing a variety of well-established statistical methods as well as mentoring and training Six Sigma Green Belts throughout the company.

Throughout my career, I have evaluated the suitability and performance of polymeric materials in end-use applications, including specifically, for the medical device industry. While at GE and SABIC, I worked with numerous medical device companies on material development, material specification, design and manufacturing for a wide variety of medical device applications. These efforts included, inter alia, developing and implementing tests related to the bulk physical properties of polymeric materials specified in said devices as well as material formulation development to meet unique device requirements that could not be met with off-the-shelf grades of resin. Formulation development often included the selection and refinement of base polymers or alloys, molecular weight, additives, stabilizers, processing aides, lubricants, colorants and inorganic fibers and fillers. In addition to proactive design and material selection assistance, I

have worked on hundreds of product safety assessments and failure analyses involving polymeric materials, many of which were performed on medical devices and components.

In my prior role as Director of Global Agency Relations and Product Safety at GE/SABIC, part of my leadership responsibilities included being an active member of the business' Healthcare Resins Advisory Board. The board developed internal processes and standards for the specification, use and sale of GE/SABIC resins in medical device applications. These efforts included ensuring that commercial resin grades within the GE/SABIC healthcare portfolio were assessed for biocompatibility using industry accepted test protocols such as United States Pharmacopeia (USP) Class VI, Tripartite Biocompatibility Guidance, or ISO 10993 Biological Evaluation of Medical Devices standards. For the past several decades, the latter two standards have been supported by the Food and Drug Administration (FDA) and commonly employed to assess the potential for cytotoxicity, hemolysis, pyrogenicity, sensitization issues, among other biological effects, when the human body is exposed to foreign materials. In addition, the board also ensured that "good manufacturing processes" were globally implemented to maximize the purity levels of all compounded materials within the healthcare resin portfolio.

In addition to my relevant training, education and industry experience, I have also reviewed and synthesized the available public literature pertaining to *in vivo* and *in vitro* studies of polymeric mesh devices, long-term implantation of polymeric medical devices, foreign body response to implantable materials, as well as select plaintiff reports which allege *in vivo* PROLENE mesh degradation. A complete list of the reviewed literature can be found in Appendix D.

Polypropylene

Chemical Structure of Polypropylene

Polypropylene is a widely produced polymer which possesses an excellent balance of physical properties, processability, and cost-effectiveness, and is commonly specified for use in a wide range of commercial applications.[1] Polypropylene is formed via a polymerization reaction where propylene molecules (monomers) are combined together in a step-wise fashion to ultimately form linear, chain-like macromolecules (Figure 1A). Polymerization is achieved through breaking the unsaturated (double) bond in propylene, and covalently reacting this bond with the polymer chain. In the current day commercial production of polypropylene, Ziegler-Natta or metallocene catalysts facilitate this reaction. Polypropylene is most commonly produced as a linear polymer (Figure 1B), meaning that the propylene monomers bond to the polymer at the end of the polymer chain, as opposed to forming a branching molecular architecture.

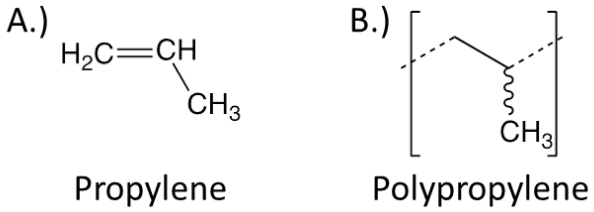

Figure 1. A.) Chemical structure of propylene and B.) Generalized chemical structure of linear polypropylene.

Polypropylene is a vinyl polymer with a lone pendant methyl group in its repeat unit as shown in Figure 1B. Chain growth using these catalysts is designed to attach in a head-to-tail manner such that the pendant methyl groups are regularly spaced. The collective orientation of these groups with respect to the backbone of the polymer, known as stereoregularity, can affect the final physical properties of the polymer.[1,2] As shown in Figure 2, the pendant methyl groups can be oriented in two different directions with respect to the polymer backbone, allowing

[1] Maier, C., Calafut, T. *Polypropylene: The Definitive User's Guide and Databook*. Norwich, NY: Plastics Design Library, 1998.
[2] Odian, G. G. *Principles of polymerization*, 4th ed.; Wiley-Interscience: Hoboken, N.J, 2004.

polypropylene to be produced in three different stereoregular conformations: isotactic (pendant methyl groups along the same side), syndiotactic (alternating sides), or atactic (random orientation). Control over which type of stereoregularity the polymer adopts is determined primarily by the choice of catalyst.[1,2] The majority of commercial polypropylene is manufactured in the isotactic conformation (*iso*-polypropylene).

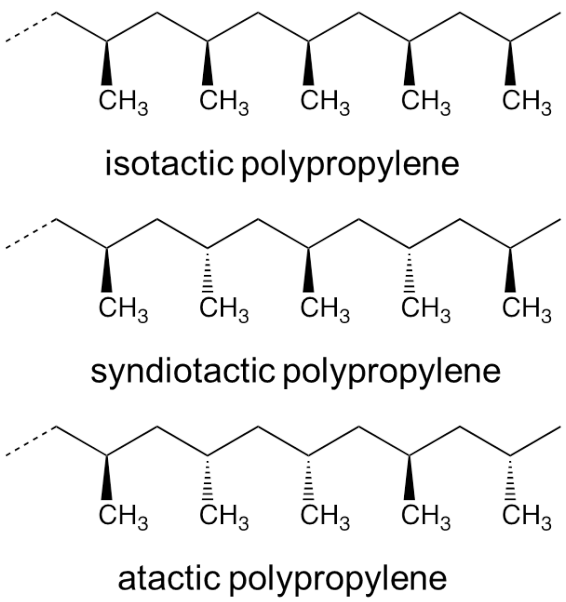

Figure 2. The three most common stereoregular conformations of polypropylene, isotactic (top), syndiotactic (middle), and atactic (bottom).

Crystallinity

Polypropylene is semi-crystalline in nature, meaning that both amorphous and crystalline regions are present throughout the polymer matrix. A typical range for the degree of crystallinity is 20% to 40% for commercially available *iso*-polypropylene.[3] The degree of crystallinity of the product is mainly determined by the stereoregularity and processing conditions. Isotactic polypropylene (*iso*-polypropylene) is the most crystalline conformation, due to the collective orientation of the pendant groups in the same direction allowing for neighboring polymer molecules to align and form a compact, ordered structure. The degree of crystallinity achieved by the material in its solid state directly influences bulk physical and thermodynamic properties.

[3] Sastri, V. R. "Commodity Thermoplastics." *Plastics in Medical Devices*. Elsevier, 2014.

With regard to expected mechanical properties, a higher crystallinity generally results in increased stiffness, yield stress, Young's modulus, and flexural strength among others, but a decreased toughness and impact strength.

Molecular Weight

During synthesis, propylene monomers are converted into polypropylene macromolecules of differing lengths. The lengths of polymeric chains are defined by the number average (M_n) and weight average (M_w) molecular weights. Typical M_w values for commercial polypropylene vary from 220,000 -700,000 g/mol[1] depending on a number of variables including the specific catalyst used.

Since there is a degree of randomness associated with the synthesis of most commercial polymers, the total number of monomeric units contained within each polymer chain will vary within a given sample. This range of polymer chain lengths is referred to as the molecular weight distribution (MWD) and is commonly reported as the polydispersity index (PDI). The PDI of a polymer is defined as the quotient of M_w and M_n (M_w/M_n) and is a measure of the broadness of the MWD, with a larger PDI corresponding to a broader MWD. Typical PDI values range from 2.1 – 11.0 for commercial polypropylene.[1]

Molecular weight and MWD directly influence the mechanical properties and processability of the bulk polymer. Polypropylene resins with a larger PDI are more shear sensitive, meaning the apparent melt viscosity decreases at a faster rate with increasing shear rate.

Thermal Properties of Polypropylene

Thermoplastic materials, including all variants of polypropylene, possess thermal transition temperatures that characterize the thermodynamic behavior of the polymer. These thermodynamic transitions are primarily based on the unique molecular structure and order of a specific polymer. The first of such thermal properties is the glass transition temperature, T_g, which is the temperature at which a polymer shifts from its glassy (more solid-like) phase to its rubbery phase. Typical T_g values for polypropylene range from -35 to 26°C.

The temperature at which crystalline domains are destroyed is known as the polymer's melting point (T_m). Once T_m has been eclipsed, the material's viscosity is sharply reduced and has the ability to readily flow in the presence of driving forces such as pressure or stress. Melting points for polypropylene can vary from 171°C for perfectly isotactic polypropylene to 130°C for syndiotactic polypropylene. In practice, commercially produced *iso*-polypropylene typically melts between 160-166°C due to small regions of atacticity (i.e. noncrystallinity).

Manufacturing of Polypropylene Resins

Industrial synthesis of bulk polypropylene is generally performed using either a bulk slurry (e.g. the Borstar® process or the Spheripol® process), or a gas phase reaction with a solid catalyst bed (e.g. Novolen®, Unipol® PP processes).[4,5] Depending on its end use, the polypropylene resins are then mixed with additives and stabilizers to aid in processing, provide color, enhance mechanical properties, or combat thermal or oxidative degradation. These additional formulation ingredients can be compounded into the finished polypropylene product either in batch mixing, or through continuous mixing (e.g. extrusion).

Processing of Polypropylene Fibers

Polypropylene has melt flow properties that make it well suited for the production of synthetic fibers. Polypropylene fibers are commonly produced via melt spinning, where the polypropylene is melted and extruded through a spinneret followed by cooling and solidification. The process of drawing a polypropylene fiber from the melt exerts uniaxial force on the polymer chains which, after cooling and solidification, results in the polymer chains being preferentially oriented along the drawing axis (i.e. the fiber length). Therefore, the crystalline character in polypropylene fibers is not only dependent on the rate of cooling during

[4] "*Process Analytics in Polypropylene (PP) Plants*", Siemens AG; 2007, pp:1-9.

[5] Mei, G.; Herben, P.; Cagnani, C.; Mazzucco A. *The Spherizone Process: A New PP Manufacturing Platform,* Macromol. Symp. 2006, 245–246, 677–680.

melt spinning but also on the induced molecular orientation from the mechanical drawing process.[6]

Polypropylene Applications

Numerous grades of resin with varying properties make polypropylene useful in a wide array of applications including components and devices for the medical industry, injection molded parts for the automotive industry, and other consumer products. Its ubiquitous specification and use is largely due to its excellent balance of bulk physical properties, ease of processing, chemical resistance, and ability to withstand moderate to elevated thermal environments.[1] In addition, polypropylene is generally unaffected when in contact with most solvents, acids, bases, disinfectants, and other common chemicals, which make it an excellent candidate material for many industries, including medical applications.

Polypropylene has found use in numerous applications, including medical devices, textiles, vehicle components and packaging. Polypropylene also finds wide usage in small medical equipment, mainly in hypodermic syringes,[3] but also in medical tubing, trays, sutures, vials and many others. The widespread use of polypropylene in the medical industry stems from its chemical resistance, mechanical strength, biocompatibility, ability to be sterilized, colorability and clarity. As a result, it has become a common material substitution for glass and other polymeric materials in the medical industry. Specifically in the case of sutures, polypropylene fibers are now a common material choice because of these desirable properties.

[6] Salem, D. R. *Structure Formation in Polymeric Fibers*. Munich : Cincinnati: Hanser Gardner Publications, 2001.

Chemistry of Oxidation and Formaldehyde Fixation

Oxidation of Polypropylene

Despite its semi-crystalline nature, polypropylene, in its neat form, can be susceptible to oxidation in its amorphous regions. Specifically, oxidation occurs at the pendant methyl groups present on the polymer backbone. Polypropylene can oxidize as a result of exposure to heat, oxygen in the air, acidic and basic environments, radiation and UV light.[1,7,8] The energy associated with any of these environments has the potential to break the bonds between a tertiary carbon atom and a neighboring hydrogen atom, resulting in the formation of radicals. These radicals are generally reactive and, in the presence of oxygen, can form hydroperoxides that eventually lead to the formation of carbonyl groups in the form of carboxylic acids, lactones, aldehydes, and esters (Figure 3).[9]

[7] Rosato, D. V., Mattia, D. P., Rosato, D. V. *Designing with Plastics and Composites: A Handbook*. Boston, MA: Springer US, 1991.

[8] Wieslawa Urbaniak-Domagala. *The Use of the Spectrometric Technique FTIR-ATR to Examine the Polymers Surface.* INTECH Open Access Publisher, 2012.

[9] Gijsman, P., Hennekens, J., Vincent, J. The Mechanism of the Low-Temperature Oxidation of Polypropylene. *Polym. Degrad. Stab.*, (1993) 42(1):95–105.

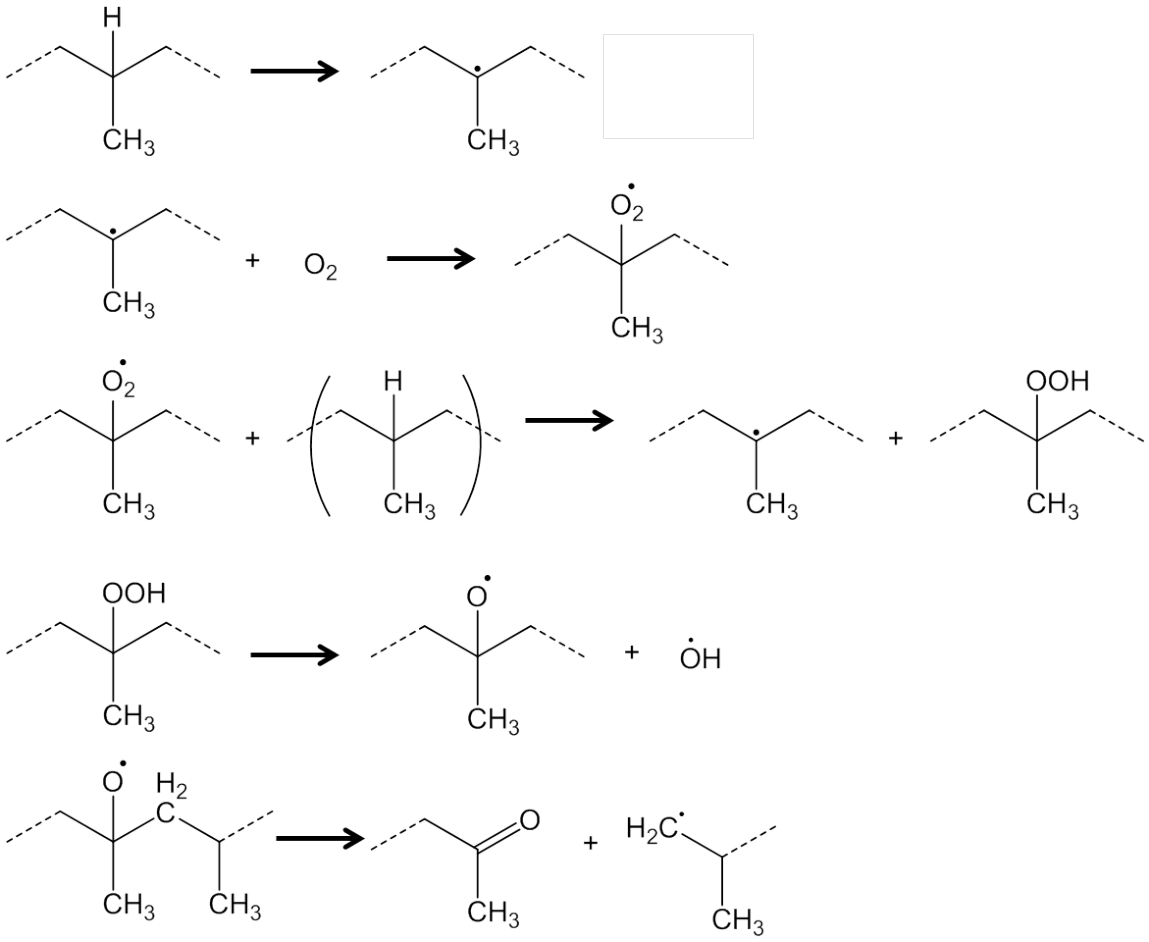

Figure 3. Reported oxidation reaction pathway of polypropylene.

As a result of oxidation, chemical, physical, and mechanical changes may occur in polypropylene. The potential chemical changes consist not only of the formation of carbonyl containing groups, but also a loss in average molecular weight and shifts in molecular weight distribution. Radicals formed during the oxidation process in polypropylene can lead to chain scission resulting in a reduction in molecular weight. Oxidation in polypropylene can also change the physical properties and appearance of the polymer. Polypropylene can turn "yellow-brown" in color and start to "flake away" after it begins to become oxidized.[10] Furthermore, the mechanical properties can also change as polypropylene becomes oxidized.[11] In general, it

[10] *Additives: Antioxidants*. Equistar. p:1–2.

[11] Gensler, R., Plummer, C. J.G., Kausch, H.-H., Kramer, E., et al. "Thermo-Oxidative Degradation of Isotactic Polypropylene at High Temperatures: Phenolic Antioxidants versus HAS." *Polym. Degrad. Stab.*, (2000) 67(2):195–208.

becomes more brittle as evidenced by a reduction in its elongation-at-break (ductility) when tensile tested.

In virtually all engineering applications, antioxidants are used to combat oxidation in polypropylene. These antioxidants are chemical additives which are added to the resin prior to processing and are typically divided into two groups known as primary and secondary antioxidants. Primary antioxidants are radical scavengers which are typically hindered phenolics and secondary aromatic amines.[1,10] These additives react with radicals and hydroperoxides in the polypropylene, thus eliminating the radicals from the polymer. The result is primary antioxidant species containing radicals, which are more stable than the polypropylene radical. Secondary antioxidants are peroxide decomposers which are typically phosphites and thioesters.,[10] These additives react with peroxides to form more stable alcohols. Often, both primary and secondary antioxidants are used together to protect polypropylene from oxidation.

Formaldehyde-Protein Crosslinking

Chemical fixation of tissues is a common technique used in histology for purposes of preservation and hardening.[12,13] While a number of different chemical fixatives are used in histology, formaldehyde is one of the most common. Formalin (a formaldehyde/water mixture) was first used to harden tissues in 1893 and has been a widely accepted chemical fixative since.[14] Formaldehyde works as a fixative by chemically cross-linking proteins, forming a large network polymer. The cross-linking chemical reaction in tissue between formaldehyde and proteins is outlined in Figure 4. Formaldehyde can react with amino acid chains in proteins to form methylene bridges between polypeptide chains.[12,13,14]

[12] Hewitson, T. D., Wigg, B., Becker, G. J. "Tissue Preparation for Histochemistry: Fixation, Embedding, and Antigen Retrieval for Light Microscopy." *Histology Protocols*. Ed. Tim D. Hewitson and Ian A. Darby. Vol. 611. Totowa, NJ: Humana Press, 2010.

[13] Thavarajah, R., Mudimbaimannar, V., Rao, U., Ranganathan, K., et al. "Chemical and Physical Basics of Routine Formaldehyde Fixation." *J. Oral Maxillofac. Pathol.*, (2012) 16(3):400–405.

[14] Puchtler, H., Meloan, S. N. "On the Chemistry of Formaldehyde Fixation and Its Effects on Immunohistochemical Reactions." *Histochemistry*, (1985) 82(3):201–204.

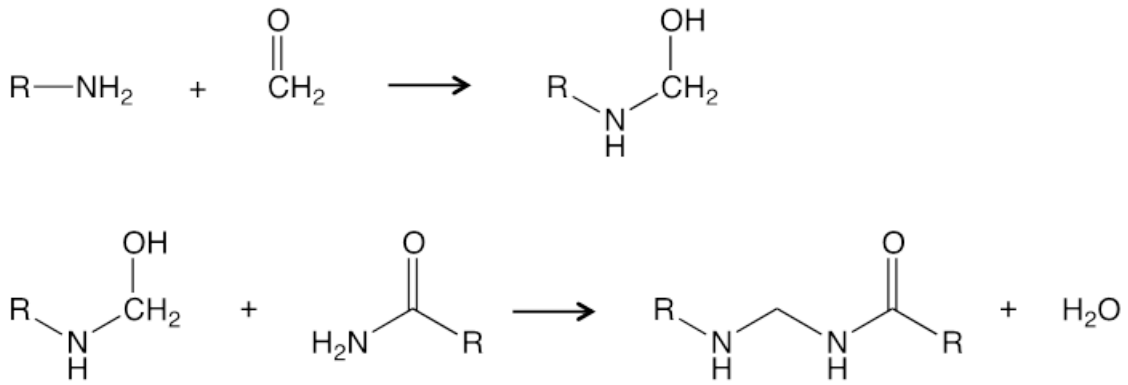

Figure 4. Simplified reaction schematic of proteins with formalin.

The resulting polymer has a much higher stiffness due to the newly formed chemical cross-links present. This increase in stiffness allows tissue samples to be sectioned by various techniques including microtoming.

PROLENE

Ethicon's antioxidant stabilized polypropylene-based resin is known by the tradename PROLENE. The resin was determined to be "safe and effective for use" in nonabsorbable surgical sutures by the FDA in 1969,[15] and has been used ever since. PROLENE sutures are manufactured by a melt spinning process (previously described in this report).[16] In addition to manufacturing PROLENE sutures, Ethicon has knitted PROLENE filaments in to mesh materials used in hernia repair, and in the treatment of pelvic organ prolapse and stress urinary incontinence.

Composition

As with many commercially available resin compounds, Ethicon's PROLENE resin is comprised of several raw material ingredients in addition to the base isotactic polypropylene. The additional formulation ingredients and corresponding loading level ranges are:[17]

- Calcium Stearate – 0.25-0.35% − lubricant to help reduce tissue drag and promote tissue passage
- Santonox R – 0.10-0.30% – primary hindered phenol antioxidant
- Dilauralthiodipropionate (DLTDP) – 0.40-0.60% − secondary thioester antioxidant
- Procol LA-10 – 0.25-0.35% – lubricant to help reduce tissue drag and promote tissue passage
- Copper Phthalocyanate (CPC) Pigment – 0.55% max – colorant to enhance visibility (in blue filaments only)

A summary of the full resin history including information on compounding, manufacturing, and formulation changes can be found in Karl's memo entitled "PROLENE Resin Manufacturing Specifications."

[15] NDA – 4.16.1969 PROLENE FDA Approval (ETH.MESH.09625731-09625737).

[16] FDA – Reclassification.pdf (ETH.MESH.10665538 – 10665565).

[17] John Karl's January 23, 2003 Memo titled PROLENE Resin Manufacturing Specifications (Eth.Mesh.02268619 – 02268621).

PROLENE Biocompatibility

The U.S. Food and Drug Administration (FDA) stipulates that a medical device "should not, either directly or through the release of their material constituents: (i) produce adverse local or systemic effects; (ii) be carcinogenic; or, (iii) produce adverse reproductive and developmental effects." The device manufacturer must follow FDA guidelines and evaluate material biocompatibility with certain tests that can vary depending on factors such as the intended application (e.g., duration and location of patient contact); alternatively, a manufacturer may not need to conduct all biocompatibility tests if its device is composed of materials that have been well characterized physically and chemically and have a long history of safe use.[18] The protocols for these tests are contained in standards established by the U.S. Pharmacopeia (USP), the International Organization for Standardization (ISO), and ASTM International.[19]

Prior to the FDA's approval of PROLENE sutures in 1969, Ethicon performed multiple animal implant studies to determine PROLENE's effect *in vivo*. These studies, performed on rats, dogs, and rabbits,[20] primarily investigated the tissue reactions caused by both colored and colorless sutures implanted in animal hosts. It was found that, the "polypropylene suture was well tolerated by tissue, evoked a reaction of the type associated with relatively non-irritation (sic) foreign bodies, was not absorbed during the test periods, did not lose appreciable tensile strength, and was not carcinogenic."

As mentioned previously, in 1969 the FDA approved PROLENE sutures as a "new drug," stating that "We have completed the review of this application as amended and have concluded that the drug is safe and effective for use as recommended in the submitted labeling."[15] Later, in 1990 the Center for Devices and Radiological Health (CDRH) of the FDA reclassified nonabsorbable polypropylene surgical sutures from class III to class II stating that "it is apparent to the FDA that a class III designation for nonabsorbable polypropylene surgical suture

[18] FDA Guidelines on Premarket Approval of Medical Devices, accessed July 25, 2015, available at: http://www.fda.gov/MedicalDevices/DeviceRegulationandGuidance/HowtoMarketYourDevice/PremarketSubmissions/PremarketApprovalPMA/ucm050490.htm#bio.

[19] FDA Guidance for the Preparation of a Premarket Notification Application for a Surgical Mesh, accessed July 25, 2015, available at: http://www.fda.gov/MedicalDevices/DeviceRegulationandGuidance/GuidanceDocuments/ucm073790.htm.

[20] PROLENE suture NDA Preclinical Studies.pdf (ETH.MESH.09626242 – 09626359).

constitutes overregulation." The FDA class II designation is used for devices for which general controls are insufficient to "assure a device's safety and effectiveness" but "sufficient information exists to establish a performance standard to provide such an assurance." The FDA concluded that the development of the performance standard necessary for class II devices was of low priority.

In addition to conducting animal studies to analyze PROLENE sutures, Ethicon also performed studies on rabbits[21] and rats[22] to analyze the tissue reaction to implanted meshes comprised of knitted PROLENE filaments. These studies showed that "[t]he tissue reaction to TVT mesh was characterized by generally mild chronic inflammation during the 28-day [rat] study, which was comparable to the tissue reaction observed for PROLENE polypropylene mesh" and that "[t]he reactions to PROLENE mesh were similar in type and extent to the response elicited by Marlex mesh implanted as a control" in the rabbit study, further supporting PROLENE's biocompatibility.

In order for PROLENE mesh to be used as a permanent tissue implant, Ethicon must comply with ISO 10993[23] and analyze the cytotoxicity, sensitization, and genotoxicity, among other tests, of the PROLENE mesh.[24] The safety of PROLENE meshes has been demonstrated through a long history of clinical use of PROLENE sutures, as well as confirmatory cytotoxicity tests. Because of the historical clinical safety of PROLENE sutures, no additional in-depth testing was considered necessary as all of the relevant biological effects listed in ISO 10993 had been previously investigated.

[21] 1973 Rabbit Study for PROLENE Mesh.pdf (ETH.MESH.10575607 – 10575613).

[22] PSE 97-0197.pdf (ETH.MESH.05315240 – 05315295).

[23] Eth Mesh 04384112 – Biocompatibility Risk Assessment for the TVT-L Device – June 6 2001.pdf (ETH.MESH.04384112 – 04284125).

[24] ISO 10993-1-2009.pdf.

Mesh as a Medical Device

Introduction to Surgical Mesh

Surgical meshes are typically implanted in the body for the repair of soft tissues, including abdominal wall defects (hernias), uro-gynecological anatomy, and cardio-thoracic defects.[25]

The design and composition of surgical mesh has evolved significantly over time. The first examples were introduced in the early 20th century, and were composed of metals like silver, tantalum, and stainless steel. All were discontinued due to complications, including corrosion, metal fragmentation, erosion, and infection. Polymeric mesh materials date back to the 1930s, when polypropylene mesh was first used to treat abdominal hernias.

Due to its decades-long success in the field of hernia management, surgical mesh has also become prevalent in the treatment of urological and gynecological conditions, such as urinary incontinence and pelvic organ prolapse. The underlying principle behind these interventions is simple: mesh structures comprised of biocompatible materials are used to reinforce existing tissue, providing both anatomic and functional results.[26]

Current Surgical Mesh Materials

The pelvic organs, which include the bladder, urethra, uterus, vagina, perineal body, and rectum, are maintained in position via the pelvis and a network of muscles and connective tissues. Pelvic organ prolapse is a condition characterized by the downward displacement of some or all pelvic organs, sometimes resulting in a bulge within the vagina. Lack of support for the urethra can also lead to stress urinary incontinence.[27]

---

[25] Pandit, A. S., Henry, J. A. "Design of Surgical Meshes – an Engineering Perspective." *Technol. Health Care*, (2004) 12(1):51–65.

[26] Dällenbach, P. "To Mesh or Not to Mesh: A Review of Pelvic Organ Reconstructive Surgery." *Int. J. Womens Health*, (2015):331.

[27] Kanagarajah, P., Ayyathurai, R., Gomez, C. "Evaluation of Current Synthetic Mesh Materials in Pelvic Organ Prolapse Repair." *Curr. Urol. Rep.*, (2012) 13(3):240–246.

The use of surgical mesh for female pelvic surgery dates back to the 1930s and 1950s, when nylon (polyamide) and Mersilene® (polyethylene terephthalate) were investigated as potential biomaterials for urinary incontinence surgery, respectively.[28,29] Today, surgical mesh used in pelvic organ prolapse repair, and in the treatment of stress urinary incontinence is predominantly manufactured from monofilament polypropylene in various weights and pore sizes.[30] The first FDA-approved synthetic mesh manufactured specifically to treat urinary incontinence was produced by Island Biosurgical, Inc., which was demonstrated to be substantially equivalent to Marlex® polypropylene in 1996.[31] That same year, Ethicon obtained approval to market modified PROLENE, a mesh constructed of knitted filaments of an extruded polypropylene based material, for repair of "hernia and other fascial deficiencies."[32]

One of the earliest FDA-approved polypropylene-based products for female pelvic reconstructive surgery was Gynemesh® (Ethicon).[33] Since then, several medical device manufacturers have obtained approval to market polypropylene meshes for similar use, including C.R. Bard,[34] American Medical Systems,[35] Mpathy Medical Devices,[36] Sofradim,[37] and Coloplast.[38] Mesh products are also marketed as kits that include not only a precut mesh,

[28] Birch, C. "The Use of Prosthetics in Pelvic Reconstructive Surgery." *Best Pract. Res. Clin. Obstet. Gynaecol.*, (2005) 19(6):979–991.

[29] DeBord, J. R. "Prostheses in Hernia Surgery: A Century of Evolution." *Abdominal Wall Hernias*. Ed. Robert Bendavid, Jack Abrahamson, Maurice E. Arregui, Jean Bernard Flament, et al. New York, NY: Springer New York, 2001.

[30] Edwards, S. L., Werkmeister, J. A., Rosamilia, A., Ramshaw, J. A. M., et al. "Characterisation of Clinical and Newly Fabricated Meshes for Pelvic Organ Prolapse Repair." *J. Mech. Behav. Biomed. Mater.*, (2013) 2353–61.

[31] Island Biosurgical, Inc. Island Biosurgical Bolster. 510(k) #K960101.

[32] Ethicon, Inc. Modified PROLENE Polypropylene Mesh Nonabsorbable Synthetic Surgical Mesh. 510(k) #962530.

[33] Ethicon, Inc. Gynemesh PROLENE Soft (Polypropylene) Mesh. 510(k) # K013718.

[34] C.R. Bard, Inc. Avaulta™ Solo Support System and Avaulta™ Plus Biosynthetic Support System. 510(k) #K063712.

[35] American Medical Systems. AMS Large Pore Polypropylene mesh. 510(k) #K033636.

[36] Mpathy Medical Devices, Ltd. Minimesh® polypropylene mesh. 510(k) #K041632.

[37] Sofradim Production. Parietene™ Duo Polypropylene mesh and Parietene™ Quadra Polypropylene mesh. 510(k) #K072951.

[38] Coloplast A/S. Restorelle™ polypropylene mesh. 510(k) #K103568.

but also tools to aid its implantation. Manufacturers of polypropylene-based mesh kits include C.R. Bard,[39] American Medical Systems,[40] Mentor,[41] MLE, [42] and Boston Scientific.[43,44]

Suture and Mesh Literature Review

As part of its analysis, Exponent has considered peer-reviewed literature that investigated the use of polypropylene sutures and mesh as medical implants. Our account and summary points of these literature papers are given below.

Clavé

Clavé[45] studied 100 explanted mesh samples that were removed due to complications. After explantation, samples were rinsed and placed in a 4% neutral buffer formalin solution. After storage in the formalin solution, samples for Fourier transform infrared spectroscopy (FTIR) were washed in a NaOCl solution for 26 hours, washed with deionized water, and then extracted with pure cyclohexane for 24 hours at room temp. Clavé did not verify that the cleaning protocol entirely removed biological material from the mesh, stating that, "FTIR absorption bands between 1,615 and 1,650 cm^{-1} could be attributed either to carboxylate carbonyl or to residual products of biological origin." Clavé further stated, "FTIR analysis neither confirmed nor excluded oxidation of PP in the *in vivo* environment."

While the use of FTIR can be very beneficial in the field of polymer science, it is important to understand the limitations. One such limitation is the precision of the sampling volume. The penetration depth of the infrared (IR) beam into the sample is typically 0.5 µm to 5 µm, depending on experimental conditions such as the wavelength of light and the angle of

[39] C.R. Bard, Inc. Bard® InnerLace™ BioUrethral Support System. 510(k) #K031295.

[40] American Medical Systems. BioArc TO™ Subfascial Hammock. 510(k) #K040538.

[41] MentorCorp. Mentor ObTape™ Trans-obdurator Surgical Kit. 510(k) #042851.

[42] MLE, Inc. Suture Fixation Device. 510(k) #K021834.

[43] Boston Scientific Corp. Pinnacle Pelvic Floor Repair Kit II. 510(k) #081048.

[44] Boston Scientific Corp. Pinnacle Lite Pelvic Floor Repair Kit. 510(k) #122459.

[45] Clavé, A., Yahi, H., Hammou, J.-C., Montanari, S., et al. "Polypropylene as a Reinforcement in Pelvic Surgery Is Not Inert: Comparative Analysis of 100 Explants." *Int. Urogynecology J.*, (2010) 21(3):261–270.

incidence.[46] According to Ethicon documents, the depth of microcracks in explanted PROLENE sutures has been measured to be 0.5 – 4.5 µm.[47] Furthermore, the spot size for sampling may range from several millimeters down to 15 µm, depending on microscope attachment.[48] Therefore, a given FTIR spectrum may consist of functional groups from neighboring materials and the underlying bulk fiber material.

Clavé also analyzed both pristine exemplar mesh and explanted polypropylene mesh materials by differential scanning calorimetry (DSC). DSC is an analysis technique used to evaluate the thermal properties of materials such as glass transition temperature, melting point and heat of fusion. His study concluded that, "no difference between DSC thermograms of pristine and degraded samples was found."

Clavé's only claimed evidence of "degradation" is the presence of a cracked outer layer on the explants, which was imaged via scanning electron microscopy (SEM). However, Clavé failed to fully remove the biological material from these samples as evidenced by the intact tissue present in the SEM images and neglected to analyze or to chemically identify the observed cracked layer. Unlike the samples that underwent FTIR that were cleaned with NaOCl, the samples that were analyzed by SEM did not undergo any cleaning prior to imaging. Instead, the samples were fixed in formalin, and then further fixed and preserved with 1% glutaradehyde and post fixed with a 1% osmium tetroxide solution. Finally, these samples were dehydrated with a series of ethanol solutions and dried using hexamethyldisilazane before being coated with gold-palladium. In short, Clavé presumes the cracked outer layer to be evidence of "degradation," however, neither generated any data that identified the chemical composition of the outermost layer nor conclusively determined whether there was any evidence of polypropylene degradation, including oxidation.

[46] ATR – Theory and Applications.pdf Pike Technologies.

[47] "Crack Depth in Explanted PROLENE Polypropylene Sutures memo (ETH.MESH.123831405 – 123831406).

[48] EAG FTIR Technique Note.

de Tayrac

A separate paper by de Tayrac *et al*. investigated Clavé's conclusion regarding a correlation between infection and polypropylene "degradation." In this study, de Tayrac *et al.* implanted polypropylene mesh materials (unspecified manufacturer) into Wistar rats along with *E. coli* bacteria for 30 days.[49] After the mesh was harvested, it was not formalin fixed, but rather it was washed in a solvent, dimethyl sulfoxide (DMSO), and ultrasonically shocked. SEM images of these samples prior to ultrasonic shock treatment showed evidence of transverse cracking, but after the ultrasonic treatment the mesh filaments appeared smooth with no persisting microscopic evidence of a cracked outer layer. Unlike Clavé *et al.*, de Tayrac concluded that the originally observed transverse cracking "appeared to concern only the biofilm, with no effect on the implant thread itself."

Costello

To evaluate the physiochemical changes that are indicative of oxidation allegedly associated with polypropylene *in vivo*, Costello *et al.* analyzed fourteen explanted polypropylene/expanded polytetrafluoroethylene (PTFE) composite hernia meshes.[50] These composite hernia meshes were not manufactured by Ethicon, none were comprised of PROLENE, and had different knit structures and pore sizes, i.e., the multi-polymer meshes analyzed were inherently different from Ethicon's PROLENE mesh and therefore the conclusions reached in this study are not directly applicable to PROLENE mesh material or design.

In this study, Costello preserved and stored the explanted meshes in a 10% v/v formalin solution before the tissue surrounding the mesh was removed in a NaOCl bath at 37 ˚C for 2 hours. Costello did not perform any chemical analysis to verify the extent to which the cleaning procedure removed bulk tissue and other biological residues from the mesh surface.

[49] De Tayrac, R., Letouzey, V. "Basic Science and Clinical Aspects of Mesh Infection in Pelvic Floor Reconstructive Surgery." *Int. Urogynecology J.*, (2011) 22(7):775–780.

[50] Costello, C. R., Bachman, S. L., Ramshaw, B. J., Grant, S. A. "Materials Characterization of Explanted Polypropylene Hernia Meshes." *J. Biomed. Mater. Res. B Appl. Biomater.*, (2007) 83B(1):44–49.

Through SEM examination, Costello observed "cracks, fissures, and increased surface roughness," as well as peeling on the surface of the explanted samples, which can be explained by the presence of buildup of foreign material on the exterior of the mesh filaments. Costello failed to perform any type of chemical characterization on this outer "peeling" material and, therefore, the chemical composition of this layer was simply undetermined in the study. Using differential scanning calorimetry (DSC) techniques, Costello claimed that a decrease in melting point was observed in the explanted samples when compared to the exemplar mesh material. Melt temperature suppression could be explained in many ways. For example, the mesh material has the potential to undergo plasticization *in vivo* as seen in a study performed by Ethicon on PROLENE sutures explanted from dogs.[51] This study found that after seven years *in vivo,* PROLENE sutures showed an increase in elongation at break and a decrease in modulus, which are consistent with plasticization.

Through a compliance test measuring the work required to "bend the mesh in half and push it through a 2.92 cm^2 slot," Costello claimed to demonstrate a decrease in compliance of the explanted mesh. Costello alleged that this decrease in compliance "is evidence of oxidation," but failed to take into account the "permanent deformation of the material while *in vivo,*" which is a result of the natural stress relaxation of the polymer. The folded geometry will artificially alter the apparent compliance (stiffness/rigidity) of the mesh. The flexural rigidity of a material is directly proportional to the modulus of elasticity and the moment of inertia, which is a geometrical term based on specimen geometry.[52] The "permanent deformation" of the explanted mesh makes a direct comparison of the rigidity of the exemplar and explants more complicated due to different moments of inertia. To truly compare the explanted and exemplar mesh materials, it is necessary to calculate the modulus of elasticity, which is independent of specimen geometry. Costello also reported that the total work required to bend the mesh and push it through the slot was greater for explanted mesh materials than for an exemplar mesh This is another example of Costello's lack of fundamental understanding of the importance of specimen geometry in mechanical testing. The work required to bend a sample is related to its stiffness, which as discussed above, is a function of both the material's modulus *and* specimen

[51] Ethicon's Seven Year Dog Study.

[52] Lubliner, J., Papadopoulos, P. *Introduction to Solid Mechanics: An Integrated Approach*. New York, NY: Springer, 2014.

geometry. Thus the increase in total work observed in this test is most likely due to the folded specimen geometry, not oxidation or degradation. Furthermore, Costello's claim of a decrease in compliance (increase in stiffness/rigidity) is contrary to the results of the Seven Year Dog study performed by Ethicon's scientists. This study found that after seven years *in vivo*, PROLENE sutures decreased in stiffness (increase in compliance) as evidenced by a reduction in modulus of PROLENE sutures after seven years *in vivo*.

Costello *et al.* also "most likely" attributed the broadening of the melting point observed in the explanted samples to *in vivo* oxidation. Their rationale is that oxidized polypropylene will result in an increase in polydispersity, which would correlate to a broader observed melting point. However, the degree to which this broadening occurred was not reported, and as such is difficult to analyze. Melting point broadening could also be due to variability in the concentration of low molecular weight species that may have been absorbed by the material while *in vivo*. Additionally, unexplained endothermic and exothermic peaks are seen in the DSC data at 230°C in the exemplar curve (Composix E/X), 275°C, 320°C and 340°C in the Subject #2 curve, and 335°C in the Subject #9 curve, which are on the order of the melting point transition, thus rendering any perceived small change in the broadening of the melting point unfounded.

Finally, Costello stated that "[o]xidized materials are expected to undergo some degree of weight loss as the material is degraded by the body. Thus oxidized materials should have less weight available to be lost during TGA." This statement shows a fundamental misunderstanding of TGA analysis. Typically, TGA data are used to report the onset of degradation or the residual (often inorganic) mass at the end of the test. Data is reported as a *percentage* of the original weight of the sample placed in the sample chamber. Assuming homogeneous mixing of any inorganic compounds within a polymer sample, the degree of weight loss determined by TGA will be the same regardless of whether or not the polymer has experienced oxidation. In the absence of any inorganic filler, 100% weight loss of the sample is expected if the TGA analysis is carried through to completion. Furthermore, Costello's data showed a shift to higher temperatures in the peak of the derivative of the mass loss with temperature curve for explanted samples (Subject #2 and Subject #9). This demonstrates the exemplar mesh degrades at a higher

rate at lower temperatures than the explanted mesh materials, which challenges, if not contradicts, Costello's hypothesis of oxidation.

Cozad

To understand tissue-material interactions occurring *in vivo*, Cozad *et al.* examined eleven explanted composite hernia meshes (not PROLENE, and not manufactured by Ethicon) that contained polypropylene and expanded polytetrafluoroethylene (ePTFE) components.[53] These composite meshes, analysis, authors, and methodology were very similar to the work previously outlined by Costello, and will not be repeated again here in complete detail. Cozad, like Costello, performed analysis (FTIR, DSC, TGA and SEM imaging) on explanted mesh materials without verifying that the samples were fully cleaned. In fact, the researchers readily admitted choosing sections to analyze which were "the most 'pristine-like' sites with no apparent tissue adsorption," strongly suggesting that they were aware that the overall samples were not adequately cleaned. Furthermore, Cozad attributed an increase in FTIR absorbance peaks at 2850 cm^{-1} to "surface hydrocarbon formation," again suggesting that the explanted mesh was not fully cleaned before analysis was performed. But instead of developing a more thorough cleaning procedure, Cozad *et al.* simply continued with their analysis without any apparent concern for the possibility of inaccurate results and without considering that the observed crust may be biologic in nature. The authors stated that the polypropylene portions of the mesh oxidized, while the ePTFE portions cross-linked *in vivo*. One of the major sources for this conclusion is the FTIR data that showed a nearly identical peak seen at 1730 cm^{-1} in both the explanted polypropylene and the ePTFE. It is unlikely that crosslinking in ePTFE and oxidation in polypropylene would show nearly identical peaks (i.e. the peaks are extremely similar in shape and location). Further, the authors give no plausible reason the ePTFE could crosslink *in vivo* as most studies, some of which are referenced in the Cozad article, require irradiation or high temperature and vacuum to crosslink PTFE.[54,55,56] Rather, a more likely

[53] Cozad, M. J., Grant, D. A., Bachman, S. L., Grant, D. N., et al. "Materials Characterization of Explanted Polypropylene, Polyethylene Terephthalate, and Expanded Polytetrafluoroethylene Composites: Spectral and Thermal Analysis." *J. Biomed. Mater. Res. B Appl. Biomater.*, (2010) 455–462.

[54] Lappan, U., Geißler, U., Lunkwitz, K. "Changes in the Chemical Structure of Polytetrafluoroethylene Induced by Electron Beam Irradiation in the Molten State." *Radiat. Phys. Chem.*, (2000) 59(3):317–322.

[55] Pugmire, D. L., Wetteland, C. J., Duncan, W. S., Lakis, R. E., et al. "Cross-Linking of Polytetrafluoroethylene during Room-Temperature Irradiation." *Polym. Degrad. Stab.*, (2009) 94(9):1533–1541.

scenario is that the 1730 cm^{-1} peak observed is actually an artifact or residue of sample handling, such as adhesive used in electron microscopy. Adhesive acrylate peaks look strikingly similar to the 1730 cm^{-1} peaks reported by Cozad *et al*.

Liebert

Liebert *et al.*[57] implanted polypropylene sutures with and without antioxidants (neither of which were PROLENE) into the backs of hamsters. They described evidence of oxidation in the sutures without antioxidants, but claimed to see no evidence of oxidation in sutures with antioxidants after 108 days of implantation. Liebert *et al.* tracked degradation by monitoring carbonyl content via FTIR, molecular weight by gel permeation chromatography (GPC) and tan δ by dynamic mechanical analysis (DMA), and found no change in the filaments with antioxidants. They concluded that the oxidation process "is retarded effectively by using an antioxidant." This finding is in concert with the historical use of antioxidant stabilizers in polypropylene formulations for implantable materials.

Mary

Comparison of PVDF (Teflene, Péters Laboratoire Pharmaceutique) and polypropylene (PROLENE, Ethicon) sutures implanted in female dogs for periods of time ranging from 4 hours to 2 years were studied by Mary *et al*.[58] Explanted samples examined via SEM and FTIR were cleaned with an enzyme incubation technique, rinsed in buffer and deionized water solutions and dried. Comparative FTIR spectra for PVDF and polypropylene enzymatically cleaned explants were tracked with time, only presenting the absorbance data at 1740 cm^{-1}, the peak assigned to carbonyl stretching. In all samples tested, Mary reported a rapid increase in carbonyl presence to a maximum value, followed by a decrease and then stabilization. This decrease in carbonyl intensity, which occurred at different times for each sample, showed absolutely no

---

[56] Lappan, U., Geißler, U., Häußler, L., Jehnichen, D., et al. "Radiation-Induced Branching and Crosslinking of Poly(tetrafluoroethylene) (PTFE)." *Nucl. Instrum. Methods Phys. Res. Sect. B Beam Interact. Mater. At.*, (2001) 185(1-4):178–183.

[57] Liebert, T. C., Chartoff, R. P., Cosgrove, S. L., McCuskey, R. S. "Subcutaneous Implants of Polypropylene Filaments." *J. Biomed. Mater. Res.*, (1976) 10(6):939–951.

[58] Mary, C., Marois, Y., King, M. W., Laroche, G., et al. "Comparison of the In Vivo Behavior of Polyvinylidene Fluoride and Polypropylene Sutures Used in Vascular Surgery:" *ASAIO J.*, (1998) 44(3):199–206.

support for Mary's theory of polypropylene *in vivo* degradation. There is no scientific basis for a claim of partial recovery of degradation, as indicated by the reduction in carbonyl intensity. Instead, this data suggests that Mary sampled a material other than the surface of the polypropylene filament, such as biologic material which changed with implantation time. The lack of testing to verify complete sample cleaning further supports this hypothesis. Alternatively, Mary may have sampled locations where there was natural variation in the concentration of any carbonyl-containing molecules within the polymer matrix. Furthermore, microscopic examination of cleaned polypropylene samples showed an absence of cracking in both sample types at 6 months, the time at which the carbonyl signal in the FTIR had already begun to stabilize, suggesting a lack of correlation between reported carbonyl functionality and observed cracking.

Wood

In order to separate out the effects of physiological variability between different patients, Wood *et al.* studied three explanted mesh samples from the same patient. The three different mesh samples were comprised of polypropylene, expanded polytetrafluoroethylene (ePTFE), and polyethylene terephthalate (PET), and were implanted to treat three separate ventral hernias.[59] The patient has a medical history of gout, morbid obesity, tobacco usage, and sleep apnea. The authors did not state why there were different materials implanted in the same patient.

After explantation, all specimens were placed in a formalin solution followed by immersion in a NaOCl solution to remove residual tissue. After the cleaning procedure, Wood *et al.* collected FTIR spectra of each of the explants and corresponding exemplar mesh materials to identify chemical changes on the surface of the mesh. FTIR revealed an increase in carbonyl functionality on each of the explanted specimens when compared to pristine exemplar meshes, "which could indicate the presence of scar tissue and/or chemical degradation." The presence of scar tissue on the cleaned specimens is further supported by photographs of the cleaned and explanted mesh which clearly show evidence of attached tissue and discoloration associated

[59] Wood, A. J., Cozad, M. J., Grant, D. A., Ostdiek, A. M., et al. "Materials Characterization and Histological Analysis of Explanted Polypropylene, PTFE, and PET Hernia Meshes from an Individual Patient." *J. Mater. Sci. Mater. Med.*, (2013) 24(4):1113–1122.

with incomplete cleaning. Additionally, the FTIR spectra of explanted ePTFE and PET show an unexplained increase of absorption bands at 3100 – 2800 cm^{-1}, which have been attributed to C-H bond stretching.[60] This increase is unexpected[61,62] in the degradation of both polypropylene and ePTFE, which further indicates Wood's lack of sufficient cleaning. Wood goes on to evaluate the cleaned mesh materials using SEM microscopy and modulated differential scanning calorimetry, but does not provide evidence of further or complete cleaning. These results cannot be relied upon to provide conclusive evidence of degradation due to the presence of tissue and/or other contaminants.

Guelcher

Guelcher studied the *in vitro* oxidation of both polypropylene pellets without antioxidants and PROLENE mesh (with antioxidants).[63] The samples were placed in a hydrogen peroxide (H_2O_2) solution containing 0.1 M $CoCl_2$ for up to five weeks. This solution was used previously by Zhao as one component of a regimen designed to mimic "the respiratory burst of adherent macrophages and foreign-body giant cells" on a poly(etherurethane) (PEU) elastomer.[64] In Zhao's study, the validation of this regimen on this particular polymer as a mimic to *in vivo* conditions was in part performed through SEM image comparison of explanted samples and *in vitro* samples. In short, the *in vitro* oxidizing environment established by Zhao was dependent on the polymer system being analyzed in the Zhao study, namely poly(etherurethane), not polypropylene. Guelcher used a similar method to induce degradation in polypropylene; however, he never validated that his method was appropriate for polypropylene. In fact, as can be seen from Guelcher's one and only SEM image of PROLENE mesh after treatment in the H_2O_2 solution for five weeks, the "pitting and flaking" seen in these samples is completely

[60] Chen, Z., Hay, J. N., Jenkins, M. J. "FTIR Spectroscopic Analysis of Poly(ethylene Terephthalate) on Crystallization." *Eur. Polym. J.*, (2012) 48(9):1586–1610.

[61] Fotopoulou, K. N., Karapanagioti, H. K. "Surface Properties of Beached Plastics." *Environ. Sci. Pollut. Res.*, (2015) 22(14):11022–11032.

[62] Atta, A., Fawzy, Y. H. A., Bek, A., Abdel-Hamid, H. M., et al. "Modulation of Structure, Morphology and Wettability of Polytetrafluoroethylene Surface by Low Energy Ion Beam Irradiation." *Nucl. Instrum. Methods Phys. Res. Sect. B Beam Interact. Mater. At.*, (2013):30046–53.

[63] Guelcher, S. A., Dunn, R. F. "Oxidative Degradation of Polypropylene Pelvic Mesh in Vitro." *Int Urogynecol J*, (2015) 26(Suppl 1):S55–S56.

[64] Zhao, Q. H., McNally, A. K., Rubin, K. R., Renier, M., et al. "Human Plasma Macroglobulin Promotesin Vitro Oxidative Stress Cracking of Pellethane 2363-80A:In Vivo Andin Vitro Correlations." *J. Biomed. Mater. Res.*, (1993) 27(3):379–388.

inconsistent with the morphology of explanted polypropylene mesh samples, thus calling into question the validity of this method with polypropylene and demonstrating that Zhao's results for poly(etherurethane) cannot be extrapolated to polypropylene.

Kurtz

Kurtz *et al.*[65] examined the tensile strength of Ethicon's ULTRAPRO mesh after six months of exposure to varied concentrations of hydrogen peroxide solution. According to Kurtz, 500µM of reactive oxygen species (ROS) have been reported in the serum of human adults. The researchers elected to use hydrogen peroxide as the representative ROS due to its "role in inflammation," and performed tensile testing on mesh samples after six months of exposure in 0M, 1mM, 0.1M, and 1M solutions. The study also included SEM of fracture surfaces of 0M and 1M exposed fibers after tensile testing. Kurtz *et al.* found that six months of exposure to 1mM and 0.1M solutions resulted in an approximately 30% decrease in tensile strength, and that samples exposed to 1M solutions exhibited qualities of "extreme embrittlement."

ULTRAPRO mesh is constructed with a different fiber composition and knit structure than PROLENE mesh. The composition of ULTRAPRO is of great significance in the interpretation of this study because the mesh is manufactured with equal parts absorbable MONOCRYL poliglecaprone-25 monofilaments and non-absorbable PROLENE polypropylene-based monofilaments.[66,67] After absorption of the MONOCRYL filaments, the PROLENE filaments remain. Kurtz *et al.* made no attempt to determine the degree to which MONOCRYL filaments were present within the mesh at the time of testing, which could have a significant effect on the tensile strength of the mesh.

In contrast to Ethicon's Seven Year Dog Study, tensile testing performed by Kurtz *et al.* showed the expected trend for an oxidized polymer. The elongation at break for samples exposed to

[65] Kurtz, J., Rael, B., Lerma, J., Wright, C., Khraishi, T., Auyang, E.D. "Effects of reactive oxygen species on the physical properties of polypropylene surgical mesh at various concentrations: a model for inflammatory reaction as a cause for mesh embrittlement and failure." *Surgical endoscopy,* (2015) : 1-6.

[66] Pott, P., Schwarz, M., Gundling, R., Nowak, K., Hohenberger, P., Roessner, E. "Mechanical properties of mesh materials used for hernia repair and soft tissue augmentation." *PloS One,* (2012) 7(10):e46978.

[67] Chowbey, Pradeep, ed. Endoscopic Repair of Abdominal Wall Hernias (2nd Edn.): Revised and Enlarged Edition. Byword Books Private Limited, 2012.

1mM and 0.1M hydrogen peroxide stayed within one standard deviation of the 0M control samples, and the samples exposed to 1M hydrogen peroxide showed a decrease in elongation at break. The PROLENE sutures examined in the Seven Year Dog Study exhibited an *increase* in elongation at break, suggesting that the polymer undergoes plasticization, rather than oxidation.

SEM was performed on samples exposed to 0M and 1M hydrogen peroxide. According to Kurtz *et al.*, only 500µM (0.5mM) of ROS was reported in the serum of human adults; therefore, the 1M samples were exposed to a more extreme environment than expected in the human body. Even so, the "cracks" observed in other studies were not observed here.[68] Rather than showing a series of images at increasing magnifications to provide context as to where the fiber failed within the knit fabric structure, the researchers elected to show only one image of a failed fiber. The fracture surface images were taken at different magnifications, 650X and 1500X for the 0M and 1M samples respectively, and are misleading. The "brittle" fiber exposed to 1M hydrogen peroxide has a diameter (75 µm) that is 20 µm smaller than the "non-brittle" fiber (95 µm) exposed to a 0M environment. By the authors' own admission, ROS concentration does not exhibit a linear relationship with changes in mechanical properties. Regardless of the numerous misgivings in the study, Kurtz *et al.* ultimately illustrated the expected tensile property trends for an oxidized polymer. All of these trends run counter to the findings in Ethicon's Seven Year Dog Study and suggest that contrived *in vitro* experiments may not accurately represent end-use, *in vivo* conditions.

Bracco

Bracco *et al.*[69] studied twenty-five explanted polypropylene and polyethylene terephthalate (PET) hernia meshes from undisclosed manufacturers. The time spent *in vivo* varied from 2 to 52 months for polypropylene meshes, and from 36 to 180 months for PET meshes. Explanted samples were stored in a 4% formalin solution, cleaned for 24 hours in a sodium hypochlorite solution, and rinsed with distilled water.

[68] Kurtz *et al.* stated that "[s]tress cracking was difficult to observe due to gold/palladium coating and limitations in resolution". This statement stands in contrast to scanning electron microscopy images taken at similar magnifications with visible "cracks" (See Clavé, de Tayrac, Cozad, Mary, Wood).

[69] Bracco, P., Brunella, V., Trossarelli, L., Coda, A., Botto-Micca, F., "Comparison of polypropylene and polyethylene terephthalate (Dacron) meshes for abdominal wall hernia repair: A chemical and morphological study." *Hernia*, (2005) 9(1):51-55.

FTIR spectra of the cleaned polypropylene explants exhibited a consistent absorption band in the carbonyl region at 1728 cm^{-1}. In contrast to other studies,[45,53,58,59] Bracco *et al.* did not assume that this peak was evidence of oxidation, and performed additional experiments to determine its origin. The researchers repeated the FTIR analysis after subjecting the explants to a 24 hour cyclohexane extraction to remove any foreign molecules which may have been adsorbed by the polypropylene material while *in vivo*. The results showed that the explants no longer exhibited the carbonyl functionality observed prior to the extraction, but the cyclohexane extraction solvent did. Gas chromatography-mass spectroscopy (GC-MS) performed on the cyclohexane extracts found evidence of squalene, palmitic acid, cholesterol, stearic acid, and other unidentified substances. Some of these substances, including palmitic and stearic acids, contain carbonyl containing functional groups that most likely contributed to the observed carbonyl functionality observed in both the explanted polypropylene meshes and the cyclohexane extracts. Based on this analysis, Bracco *et al.* concluded that carbonyl functionality in explanted polypropylene mesh "does not arise from a chemical modification of PP due to its stay in the human body," but rather from a "chemical species present in the human tissues that have been transferred to the polymer." It is worth noting that these findings are consistent with Dr. Jordi's pyrolysis mass spectrometry (PYMS) study[70] where he was able to extract similar carbonyl-containing aliphatic species from explanted meshes.

Imel

Imel *et al.*[71] studied the chemical and molecular weight characteristics of Boston Scientific (not PROLENE) meshes before and after implantation in the human body. After explantation, all meshes were stored in formalin until the study was implemented. SEM and energy dispersive X-ray spectroscopy (EDS) were performed on exemplar and uncleaned explanted meshes, while FTIR of explanted meshes was performed only after a 24 hour soak in a sodium hypochlorite cleaning solution.

[70] Jordi Wave 1 Case Report dated 2-1-16, Exhibit B, pg. 66.

[71] Imel, A., Malmgren, T., Dadmun, M., Gido, S., Mays, J. "*In vivo* oxidative degradation of polypropylene pelvic mesh." *Biomaterials*, (2015) 73:131-141.

FTIR spectra were presented for two exemplar mesh controls, as well as four explanted meshes that had been cleaned in a sodium hypochlorite solution. The study claimed that the carbonyl absorbance bands visible on the explanted samples between 1700 and 1750 cm^{-1} offered clear evidence of oxidation. However, the researchers failed to acknowledge the significance of the amide II peak at 1550 cm^{-1}, typically indicative of the presence of residual tissue, which was visible in three of the four explanted specimens. As mentioned previously, amide bonds are inherent to proteins which contain both amide and carbonyl functionality. In addition, Imel *et al.* cited observations made by Bracco *et al.* that small molecules (e.g. esterified fatty acids) with carbonyl functionality have the potential to be absorbed into the mesh material. Given the presence of residual tissue and small molecule fatty acid esters, it is impossible to attribute the presence of carbonyl functionality solely to oxidation.

Imel *et al.* also showed SEM images and EDS spectra of control and explanted mesh specimens. EDS was used to determine the elemental composition of the fiber and the fiber surface, and Imel *et al.* claimed that because nitrogen is found in proteins, the observed presence of oxygen with an absence of nitrogen on an explanted Boston Scientific mesh suggested oxidation. The problem with this logic is twofold. First, as indicated by the researchers, many of the EDS spectra for explanted mesh (both of "clean fiber" and on "biomaterial coated fiber") showed some presence of both nitrogen and oxygen. This is evidence that the tissue on the "clean fiber" region has not been fully removed and therefore the continued presence of biological material explains the oxygen detected in the EDS spectra. Secondly, Bracco *et al.* showed that small oxygen containing molecules are adsorbed into the mesh material while *in vivo*, and would be expected to contribute to the EDS spectra. In short, the presence of oxygen, either with or without nitrogen, is expected as a result of the residual tissue and small oxygen containing molecules which have been adsorbed into the mesh material.

Imel *et al.* analyzed the molecular weight and polydispersity index (PDI) of Boston Scientific Pinnacle control and explanted meshes. The researchers claimed to see a reduction in both the molecular weight and the PDI of explanted mesh when compared to control mesh. It is interesting to note that, when comparing FTIR spectra of the same explanted mesh, the presence of carbonyl functionality does not necessarily correlate with the purported reduction in

molecular weight, as would be expected if the mesh were oxidized. For example, the FTIR spectra of explant XP-7 showed minimal carbonyl functionality (even with the presence of fatty acid esters, as reported by Bracco), yet displayed an alleged reduction of 44,000 daltons in Mw and a 2.02 reduction in PDI. A reduction in molecular weight and PDI of this magnitude is expected to coincide with substantial carbonyl functionality observed by FTIR. The fact that this was not observed calls into question the validity of the controls.

Finally, it is important to restate that Imel *et al.* performed all testing on Boston Scientific explanted mesh, not on Ethicon's PROLENE mesh. Although the study reports an alleged reduction in molecular weight after implantation, similar studies performed on Ethicon's PROLENE material showed no reduction in molecular weight with implantation time.[72,73]

[72] Ethicon's Seven Year Dog Study (ETH.MESH.09888218 – 09888222) pg.146-150.

[73] Wave 1 General Expert Report of Howard Jordi Report-2-1-16.pdf., Exhibit A_Jordi Lewis Report

Artifacts in Microtome Processing

Microtoming is a known method of preparing thin cross sections of both biologic and synthetic materials.[74] The process of microtoming involves preparing a sample by embedding in paraffin or another stiff matrix, then making slices of varying thickness with a very sharp knife or blade. This process, which has been used in polymer science for decades, is often used for the purpose of preparing very thin slices of cross sections as part of a staining protocol in pathology applications to illuminate different types of cells and/or tissue that may be present within a sample.

It is important to note that not every material can be prepared by microtoming. Often, samples that are too soft cannot be sectioned effectively, resulting in a poorly prepared material slice with extraneous artifacts, including edge imperfections, which are not representative of the pre-sectioned material sample. To avoid these artifacts, biological tissue samples are often fixed, which among other effects, hardens the tissue for microtoming.

Likewise, heterogeneous samples with both hard and soft matter can be difficult to microtome without inducing artifacts. As an example, McInnes reports on artifacts caused by bone fragments in soft brain tissue. The hard fragments can be "moved by the microtome knife-edge during cutting and this causes shattering and distortion of the tissue section."[75]

During the cutting process, if the microtome knife is set at too acute of an angle or if the knife is too dull, it can compress the tissue specimen as it is being cut. This effect is exacerbated when a particularly soft material is being sectioned. In this case, the microtome knife can compress the tissue specimens and result in streaks, cracks, waviness, and other artifacts that run parallel to the edge of the microtome knife, and in some cases, rendering the sectioned tissue specimen unable to be adequately processed via microscope examination.[75,76]

[74] Bell, G. R. "Microtoming: An Emerging Tool for Analyzing Polymer Structures." *Plastics Engineering*.
[75] McInnes, E. "Artefacts in Histopathology." *Comp. Clin. Pathol.*, (2005) 13(3):100–108.
[76] Janzen, W., Ehrenstein, G. W. "Microtomy of Polymeric Materials Part 2: Application of Microtomy." *Pract. Metallogr.*, (1989): 26549–558.

Ethicon's Investigation

In the course of its investigation, Exponent has reviewed a series of internal Ethicon documents detailing experiments conducted on explanted sutures in the 1980's.

Microcrack Committee Investigation

Ethicon conducted experiments to investigate alleged cracking observed on the outer surface of explanted PROLENE sutures in the 1980s. As part of their internal investigation, Ethicon formed a "microcrack committee" of scientists that carried out multiple experiments including various forms of microscopy, mechanical testing, melting point analysis, and FTIR analysis on both explanted materials and intentionally oxidized controls to understand the composition of the observed cracked layer on the outer surface of explanted PROLENE sutures. The studies performed by this committee contain test reports, internal Ethicon memos, and correspondence among Ethicon staff, scientists, and surgeons.

Microscopy

Ethicon's scientists examined numerous uncleaned explanted PROLENE sutures by both optical microscopy[77,78,79,80,81] and SEM,[80,81] confirming an outer cracked layer on some of the explants. Further microscopic examination was performed using cross-polarized light microscopy to determine if exemplar PROLENE sutures exhibited a core/shell morphology associated with variations in crystallinity resulting from the manufacturing process. It was found that there was "no indication of a gross skin feature on PROLENE sutures."

[77] 14 – "Examination of 5/0 and 6/0 Cardiovascular PROLENE Sutures Explanted after 2 to 6 Years Implantation" memo 1983.03.25 (ETH.MESH.15958410-58432).

[78] 15 – "Human Retrieval Specimens from Dr. Roger Gregory, Norfolk Surgical Group" memo 1983.03.29 (ETH.MESH.15955440-15955442).

[79] 19 – "Examination of PROLENE (Polypropylene) Sutures from Human Cardiovascular Explants" memo 1984.05.02 (ETH.MESH.15955462-15955468).

[80] 23 – "PROLENE Microcracking" memo 1984.11.05 (ETH.MESH.15958452-15958469).

[81] 24 – "PROLENE Polypropylene Suture Explant from Dr. Drewes" memo 1984.11.07 (ETH.MESH.15958405-15958407).

Using transmission electron microscopy (TEM) in diffraction mode to examine an explanted cross-section further confirmed the presence of a semi-crystalline inner core material, and an *amorphous* cracked outer layer, suggesting the cracked outer layer was not PROLENE.

Mechanical Testing

Tensile testing was performed by Ethicon's scientists on explanted PROLENE sutures of various sizes that were "relatively free from instrument damage" and compared with exemplar sutures of similar sizes to determine the change in breaking strength. Explanted sutures exhibited breaking strengths ranging from 47%-110%[82] of the values obtained for their representative control sutures.' The elongation at break and modulus were not reported in this study and therefore it is impossible to determine if the reported reduction in breaking strength is a result of material degradation, or simply an *in vivo* plasticization effect as seen in the Seven Year Dog Study, which will be discussed in detail later.

Melting Point Analysis

In a further effort to identify the composition of the cracked outer film on explanted PROLENE sutures, Ethicon investigated the melting point of the exterior layers. Explanted sutures were heated, resulting in contraction and peeling of the outer cracked surface layer. The suture and peeled layer were further heated until the bulk PROLENE suture had melted (~165°C). In most cases, the bulk fiber melted first "but the crack (sic) layer maintains its form," indicating that the cracked layer is not degraded PROLENE, which would have a *lower* melting temperature than bulk PROLENE. Ethicon repeated these melting point experiments with protein serum coated exemplar sutures with analogous results, stating that this "protein layer has similar characteristics to the crack layer on explants in that it separates from the fiber cleanly with heating and maintains its form after the PROLENE fiber has melted."

[82] Of the 13 sutures tested, 12 exhibited breaking strengths 75% or higher of values obtained for their representative control sutures.

FTIR Analysis

FTIR is a technique used to identify particular chemical bonds present in a sample and to identify specific polymer types. Ethicon performed FTIR analysis of the cracked outer layer, bulk explanted sutures, intentionally oxidized controls, protein immersed controls, and exemplar PROLENE sutures to determine the composition of the cracked outer layer by the functional groups present in each type of sample.[80,83,84] As discussed previously, carbonyl containing functional groups are formed upon oxidation of polypropylene and are typically associated with absorption peaks between approximately 1650 cm^{-1} and 1810 cm^{-1} in the FTIR spectrum.[8,85,86] Interpreting the FTIR spectra obtained by Ethicon is non-trivial due to a multitude of factors. Characteristic functional groups in proteins, DLTDP (antioxidant), formaldehyde cross-linked proteins, fatty acid esters,[87] and oxidized polypropylene (Figure 5) include carbonyl groups, which confound the interpretation of FTIR spectra generated from explanted meshes and sutures manufactured from PROLENE.

[83] 25 – "Fourier Transform-Infrared Examination of PROLENE Microcrack and Photo-Oxidized Polypropylene" memo 1984.11.13 (ETH.MESH.15958336-15958395).

[84] 28 – "IR Microscopy of Explanted PROLENE Received from Prof. R. Guidoin" memo 1987.09.30 (ETH.MESH.12831391-12831404).

[85] Carlsson, D. J., Wiles, D. M. The Photodegradation of Polypropylene Films. III. Photolysis of Polypropylene Hydroperoxides. *Macromolecules*, (1969) 2(6):597–606.

[86] George, G. A., Celina, M., Vassallo, A. M., Cole-Clarke, P. A. Real-Time Analysis of the Thermal Oxidation of Polyolefins by FT-IR Emission. *Polym. Degrad. Stab.*, (1995) 48(2):199–210.

[87] Movasaghi, Z., Rehman, S., ur Rehman, D. I. "Fourier Transform Infrared (FTIR) Spectroscopy of Biological Tissues." *Appl. Spectrosc. Rev.*, (2008) 43(2):134–179.

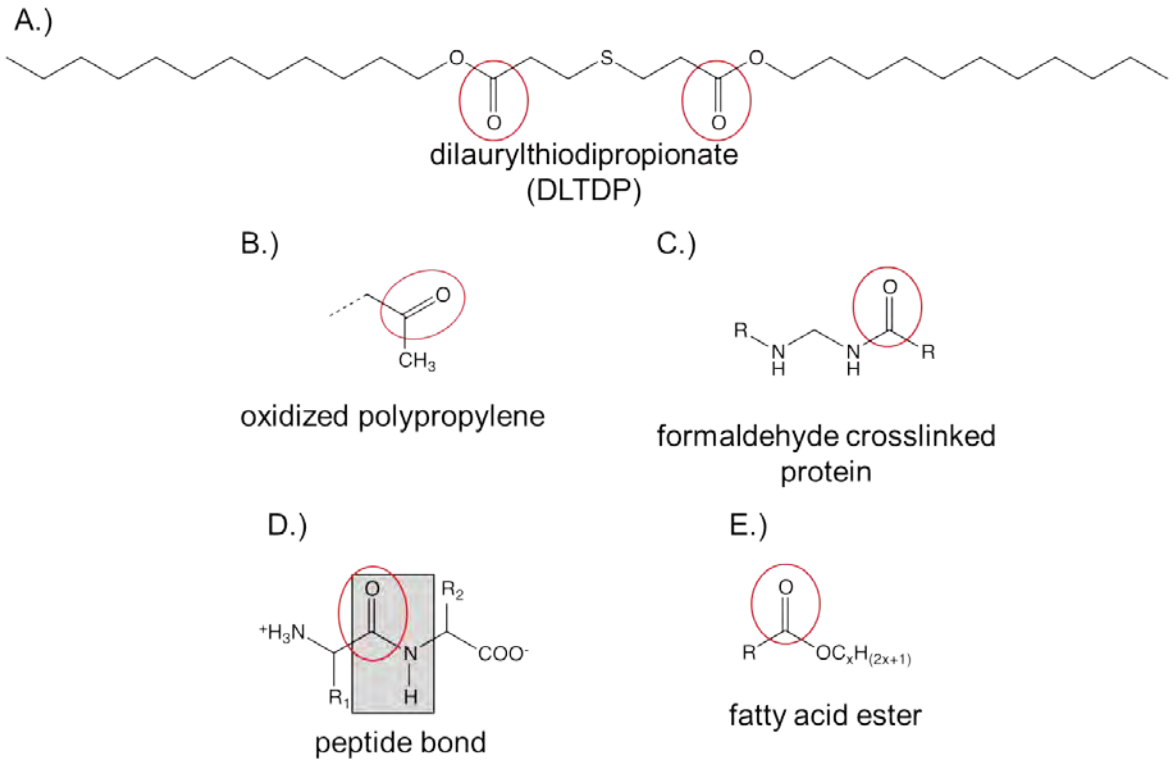

Figure 5. Chemical structure of dilaurylthiodipropionate[88] A.), oxidized polypropylene B.), formaldehyde crosslinked proteins C.), a peptide bond, which make up proteins[89] D.) and a fatty acid ester E.). All of these molecules have functional groups which contain carbonyls (circled in red).

Ethicon performed studies that included FTIR spectroscopy of intentionally oxidized polypropylene and PROLENE samples that were immersed in protein serum. Studies involving intentional oxidation, such as hot pressed samples and photo-oxidized induced samples, showed consistent carbonyl peaks in the 1720 cm^{-1} region. Explanted samples and non-explanted samples immersed in protein serum inconsistently showed peaks in the 1700 cm^{-1} to 1740 cm^{-1} region, indicating oxidation was unlikely to be the contributing factor to the peaks. Rather, carbonyl or other oxygen containing groups from the serum or *in vivo* conditions contributed to the observed peaks.

[88] Chemical Book, accessed August 23, 2015. http://www.chemicalbook.com/ChemicalProductProperty_EN_CB3712869.htm

[89] Godbey, W. T. *An Introduction to Biotechnology the Science, Technology and Medical Applications*. Woodhead Publishing, 2014.

Seven Year Dog Study

Study Protocol

As part of the microcrack committee, Ethicon initiated a comprehensive 10-year *in vivo* study commencing in 1985. One of the primary motivations of this study was to assess the long-term effects, if any, of implantation on various suture materials. Ethicon selected PROLENE (polypropylene based), PVDF (polyvinylidene fluoride), ETHILON (nylon 6 and nylon 6,6), and Novafil (polybutester) monofilament 5-0 sutures to be examined in this study. Periodic evaluations were performed after two, five, and seven years *in vivo*, with baseline testing of unimplanted sutures also performed at each period. Each periodic evaluation consisted of generating mechanical and chemical property data as well as surface morphology micrographs to capture any physical changes in the candidate suture materials. In this study, twenty-four mature female Beagle dogs served as animal models (five animals per study period, plus four replacements in case of premature death). Each animal had sutures implanted in six different locations, and each implant location received a bundle of six sutures (with each bundle containing a single type of suture). A simplified schematic of the surgery sites is shown in Figure 6.

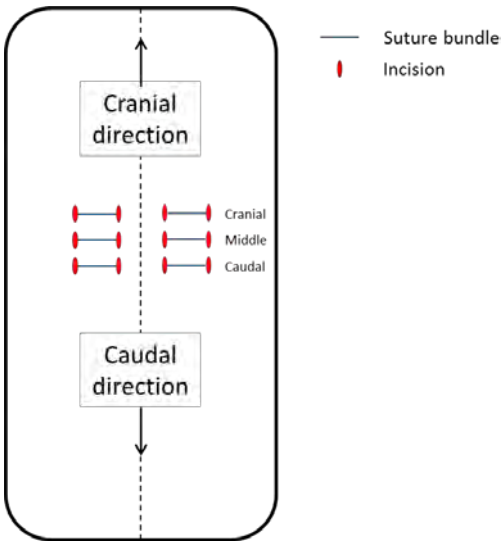

Figure 6. Simplified illustration of the ventral area of a dog torso, showing the location of the six suture implantation sites.

Five dogs were euthanized at each study period. For each suture type, one strand (selected at random) was immediately placed, without cleaning or being allowed to dry, into a test tube filled with sterilized deionized water to be examined and imaged with optical (OM), scanning electron (SEM), and infrared (IR) microscopy.

The remaining five strands were examined for surface damage, and then placed into saline-soaked towels in preparation for tensile testing, which was performed on the explanted strands of each suture type and ten non-implanted exemplars. After testing, the chemical groups present on the surfaces of the fragments were identified by FTIR, and the molecular weight was evaluated by inherent viscosity, and gel permeation chromatography (GPC).

Study Results

In this study, prior to additional testing and examination, FTIR spectra were taken on all explanted sutures to verify that they had been correctly identified during the explantation procedure.[90]

IR microscopy is a technique very similar to FTIR, albeit with smaller spatial resolution. This technique made it possible to compare the chemical groups present in cracked and non-cracked regions. After seven years *in vivo*, spectra for PROLENE sutures showed "a broadened weak absorbance at about 1650 cm^{-1}," Ethicon's scientists concluded that this was "possible evidence of slight oxidation." The absorbance peak typically assigned to carbonyl containing functional groups in oxidized polypropylene is 1650-1810 cm^{-1}.[8,85,86] However, it is important to note that these samples were not cleaned, in fact tissue was still present on the surface of the suture and "cracking of the suture was seen through the tissue."[91] The existence of tissue, including tissue that may contain lipids or fatty acids, could readily account for the observed carbonyl functionality on the cracked surface of the suture; therefore, no scientific conclusions can be drawn by IR microscopy regarding the oxidation of PROLENE sutures. The spectra from cracked areas on ETHILON and Novafil sutures were not different than spectra obtained from uncracked areas. However, it was noted that absorbance frequencies related to oxidation "would

[90] Ethicon's Seven Year Dog Study (ETH.MESH.09888187) pg.115.
[91] Ethicon's Seven Year Dog Study (ETH.MESH.09888189) pg.117.

be masked by the strong carbonyl absorbances normally observed for these sutures." Thus, no conclusions could be drawn from the IR microscopy of any of the examined explanted sutures.

Direct molecular weight measurements via GPC were performed on both unimplanted controls and PROLENE sutures after seven years *in vivo* to determine if a shift in molecular weight had occurred. It is worth mentioning that direct measurements of molecular weight reduction are the most accurate and reliable method to assess degradation in polymeric materials. Results (shown in Table 1) indicated that "there was no significant difference in molecular weight between the 4-0 PROLENE control and the seven year explant." The findings from this study are clear. Within the margins of statistical error, none of the implanted sutures suffered any meaningful losses in molecular weight and therefore, by definition, were not degraded.[92]

Table 1. Molecular weight of exemplar PROLENE compared to explanted PROLENE sutures after 7 years *in vivo*.

	M_w	M_n	PDI
Exemplar	324,000	60,000	4.67
Dog # 2007 site 1	322,000	69,000	5.13
Dog # 2007 site 6	323,000	63,000	5.54
Dog # 1995 site 3	327,000	59,000	5.17
Dog # 2019 site 3	331,000	64,000	5.82
Dog # 2019 site 2	332,000	57,000	6.08

Inherent viscosity tests of ETHILON and Novafil sutures were performed on samples from the seven year study period and compared to data from one and two year samples. The inherent viscosity of a polymer is directly related to its molecular weight. Obtained data showed no change in inherent viscosity in either type of suture after 1-2 years *in vivo* residence. However, after seven years the values ranged from 75% to 93% of those in the one and two year study period for the ETHILON sutures and 75% to 90% for the Novafil sutures.[93]

[92] This observation is also significant because it directly contradicts inferences by Plaintiff's experts that low molecular weight degradation materials from PROLENE are leaching into adjacent tissue.

[93] Ethicon's Seven Year Dog Study (ETH.MESH.09888188) pg.116.

A polymer's mechanical properties are directly influenced by its molecular weight. When a polymer experiences chemical degradation, including oxidation, its polymer chains are cleaved and reductions in molecular weight are realized. From a bulk physical property standpoint, chemical degradation/molecular weight loss generally results in embrittlement of the material. Embrittlement is best described as a decrease in a material's elongation-at-break, ductility or toughness (area under the stress-strain curve) meaning that the material's ability to stretch, prior to fracturing, has been reduced (Figure 7). Quantifiable changes or shifts in a material's ductility due to degradation are easily computed by performing tensile tests on control and degraded specimens.

In contrast, a polymer's ductility and toughness can increase as a result of plasticization. Plasticization of polymers is well documented in the scientific literature and occurs when low molecular weight compounds diffuse from an external source into the bulk polymer and physically change the intermolecular forces between polymer chains.[94] Specifically, plasticization of a polymer will result in a decreased modulus, increased elongation at break, and decreased breaking strength. Of equal importance is that plasticization is not a chemical degradation mechanism and does not, itself, result in a reduction of molecular weight.

[94] Wypych, G. *Handbook of Plasticizers*. Burlington: Elsevier Science, 2013.

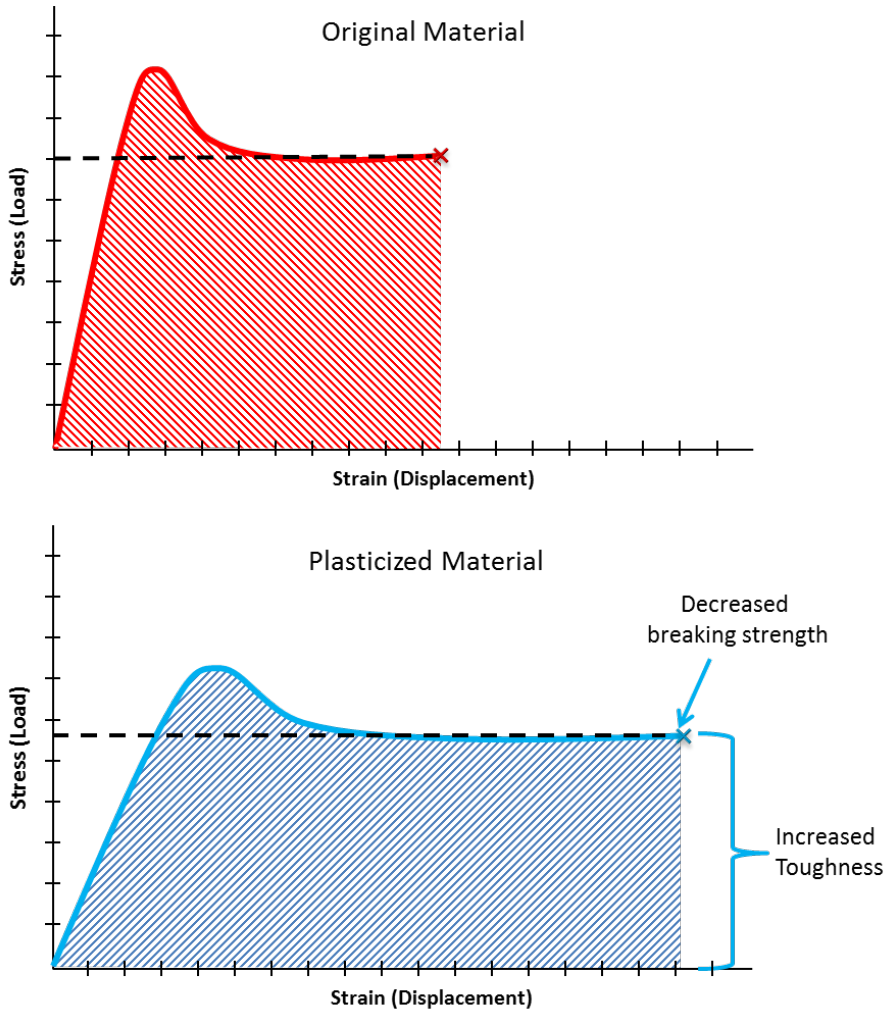

Figure 7. Schematic stress-strain curves for a non-plasticized and a plasticized material. Note the increase in toughness (area under the stress-strain curves) due to plasticization.

In addition to the molecular weight analysis, Ethicon evaluated the mechanical properties of explanted sutures from the seven year dog study to further determine if the bulk physical properties of the PROLENE material were being degraded during implantation. Tensile testing of sutures was performed on both pristine unimplanted and explanted sutures to evaluate the effect of implantation time on the mechanical properties of the suture material. The resulting breaking strength, elongation at break, and Young's modulus are summarized graphically in Figure 8. These tests revealed that ETHILON and Novafil sutures exhibited the greatest decrease in breaking strength, with a 37% and 14% decrease respectively.[95] Furthermore, the

[95] Ethicon's Seven Year Dog Study (ETH.MESH.11336183) pg.155.

physical appearance of the ETHILON sutures was reported as "fragile and worn out with spotted surface."[96] Conversely, "no significant change after seven year (sic) of implantation" in breaking strength was reported for both PROLENE and PVDF sutures.

The elongation at break reported for all explanted suture types increased after seven years and can be seen in Figure 8. The most dramatic elongation *increase* was reported in PROLENE samples, which exhibited a 111% increase over pristine, non-implanted control samples. A dramatic increase in ductility, in conjunction with a reduction in modulus (stiffness) is not indicative of degradation or oxidation, but instead confirms the PROLENE material's ductility and toughness *improve* as a function of implantation time and the improvement is most likely attributed to *in vivo* plasticization.

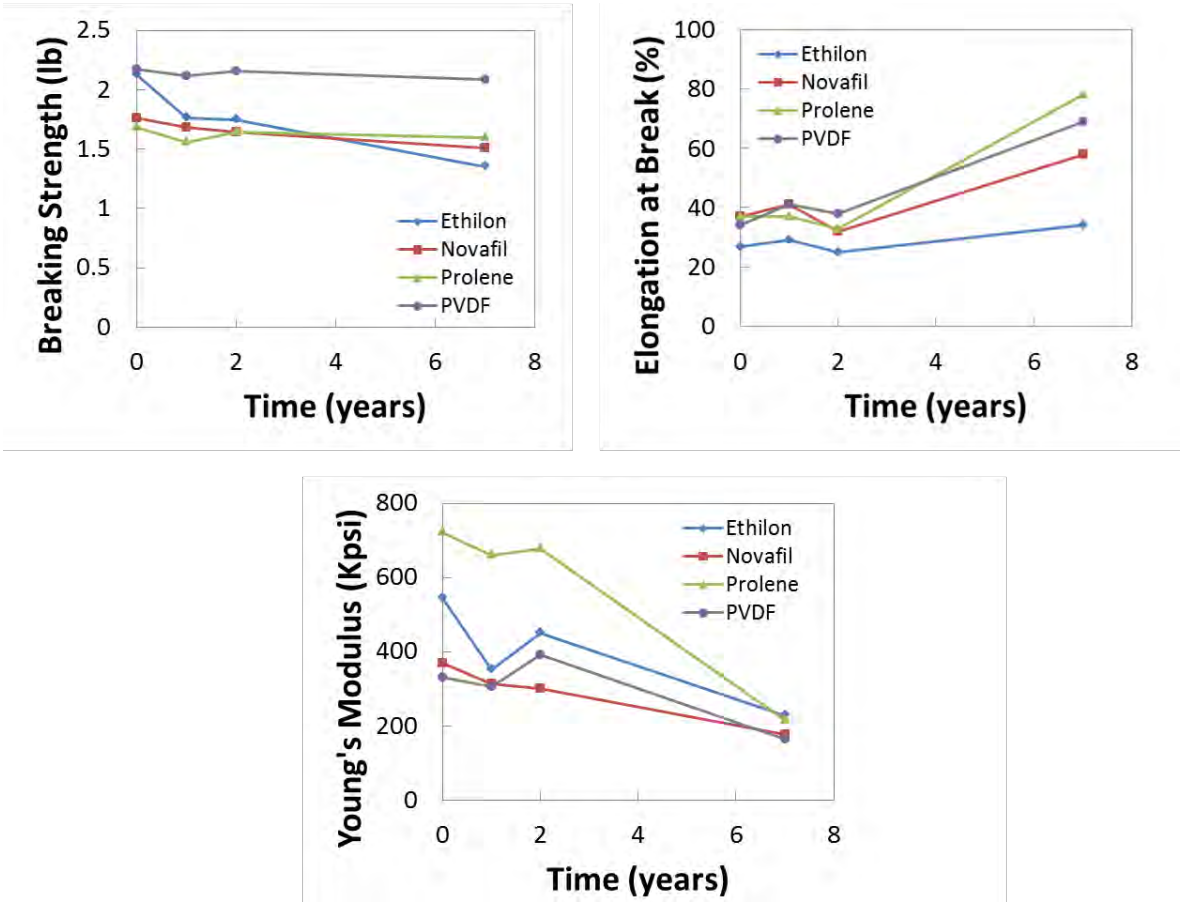

Figure 8. Summary of tensile tests performed on ETHILON, Novafil, PROLENE and PVDF sutures in Ethicon's Seven Year Dog Study.

[96] Ethicon's Seven Year Dog Study (ETH.MESH.11336181) pg.153.

Surface examinations of one suture of each type from each site were performed using both OM and SEM. Microcracking and/or damage was observed on the surface of the sutures as summarized in Table 2. Cracking was considered the most severe and widespread on ETHILON sutures, and was observed after one year *in vivo*. The presence of cracks on explanted Novafil sutures did not follow a clear trend, as seen in Table 2. After seven years *in vivo*, transverse cracking was not observed to a high degree on the Novafil sutures, although other signs of surface damage such as longitudinal scratches and a longitudinal crack were observed. Transverse cracking was not observed on the surface of PROLENE sutures after one year *in vivo;* however, after seven years the appearance of cracking was reported on the surface of 50% of the sutures. Throughout the seven year study, only one of the PVDF explanted sutures was reported to have "possible cracks" on the surface.[97]

Table 2. Summary of suture surface examinations. The number of sutures exhibiting damage (transverse cracking, longitudinal cracking, scratches, etc.) and the total number of sutures of each type after one, two, five and seven years *in vivo*.

	1 year	**2 years**	**5 years**[98]	**7 years**[99]
PROLENE	0 of 8	1 of 8	2* of 7	4 of 8
PVDF	0 of 8	1 of 8	0 of 7	1 of 7
ETHILON	7 of 7	5 of 7	8 of 8	8 of 8
Novafil	4 of 7	2 of 7	0 of 8	4 of 7

* One additional suture revealed cracking only after drying.

Conclusion

Overall, Ethicon invested substantial resources in their multi-year investigation into the composition of the cracked outer layer observed on explanted PROLENE sutures. Ethicon's Seven Year Dog Study data strongly confirms that PROLENE is not experiencing any meaningful degradation *in vivo*, in fact, the material exhibits more ductility and rupture resistance after long-term implantation.

[97] Ethicon's Seven Year Dog Study (ETH.MESH.11336081 – 11336082) pg.92-93.

[98] Ethicon's Seven Year Dog Study (ETH.MESH.11336165-11336168) pg.101-104.

[99] Ethicon's Seven Year Dog Study (ETH.MESH.09888191) pg.119.

Exponent Testing and Analysis

Introduction

Plaintiff's expert, Dr. Vladimir Iakovlev, opines that Ethicon's PROLENE mesh degrades *in vivo* based on a cracked layer observed on the outer surface of mesh fibers after explantation.[100] While this assertion has been made by other plaintiffs' experts,[101,102] Dr. Iakovlev claims that the outer degradation layer is oxidized and "differs from the non-degraded core by its ability to trap histological dyes in the nanocavities produced in polypropylene due to degradation."[103] Dr. Iakovlev bases his conclusions on flawed experiments in which he purports to show that oxidized, degraded PROLENE is stained using histological dyes such as Hematoxylin and Eosin (H&E), yet fails to perform control experiments to confirm this theory. The purpose of the following experements is to address the scientific deficiencies of Dr. Iakovlev's experiments and conclusions from a polymer science perspective. This work does not attempt address issues related to histology[104] or Dr. Iakovlev's histological analysis.

Hematoxylin and Eosin (H&E) Stain

Hematoxylin and Eosin, also referred to as H&E, is a common stain used for illuminating components of cells and tissue, many of which are long molecules (polymers). The hematoxylin dye solution itself is a mixture of hematoxylin, hematein, aluminum ions, and solvent. It is used in combination with a "mordant" compound that helps link it to the tissue. This mordant is typically a metal cation, such as aluminum. The complex is cationic (positively charged) and can react with negatively charged basophilic cell components, such as nucleic acids in the nucleus, rough endoplasmic reticulum, ribosomes, and acidic mucin. Eosin, used in combination with Hematoxylin, is negatively charged and attracts positively charged molecules. It stains

[100] Iakovlev Clowe Report dated May 23, 2015, p. 54.

[101] Expert report of Dr. Howard Jordi dated 8-24-15, p. 13.

[102] Expert report of Dr. Scott Guelcher dated 8-24-15, p. 2.

[103] Expert report of Dr. Vladimir Iakovlev dated January 29, 2016, p. 18.

[104] Histology relates to the microscopic study of tissue. Here within, I focus on the microscopic study of PROLENE polymer fibers, although the chemistry of histological staining is discussed from a background perspective.

structures with positive charges, e.g. cellular membranes, cytoplasm, connective tissue, and extracellular matrix tissue.[105,106]

Ionic bonding is the most important type of bonding that occurs during histological staining. The mechanism for H&E "staining" of tissue is simple ionic bonding between two charges: charge on the H&E staining molecules and charges on the molecules that comprise the tissue. As an example, amino acids are the molecular building blocks of proteins (which are also polymeric) and some of these amino acids contain a charge as shown in Figure 9.[107] These charged compounds will bind ionically[108] (charge-to-charge) with H&E and appear stained. The H&E staining mechanism is not physical in nature. In other words, physical voids, cracks, or crevices in PROLENE (as posited by Dr. Iakovlev)[109] or other materials do not "trap" or hold H&E stain, especially after washing and rinsing, which is part of the accepted staining protocols.

Polypropylene or PROLENE molecules are not ionically charged and are therefore not expected to stain with H&E. Furthermore, as shown previously, oxidized polypropylene does not possess a distinct ionically charged region. Therefore, in accordance with not only first principles of polymer science, but also the accepted methodology and assessment routinely reported in the literature, oxidized polypropylene is not expected to stain with H&E.

---

[105] Veuthey, T. Dyes and Stains: From Molecular Structure to Histological Application. *Front. Biosci.*, (2014) 19(1):91.

[106] Education Guide: Special Stains and H&E Second Edition, Editors: George L. Kumar and John A. Kiernan., 2010 Dako North America, Carpinteria, California.

[107] Adapted from Dan Cojocari, University of Toronto, 2011, pKa Data, *CRC Handbook of Chemistry*, 2010.

[108] A common, familiar ionically bonded material is sodium chloride, or table salt, in which Na^+ and Cl^- are bound together by ionic attraction.

[109] Expert report of Dr. Vladimir Iakovlev dated January 29, 2016, p. 18, 92, 93.

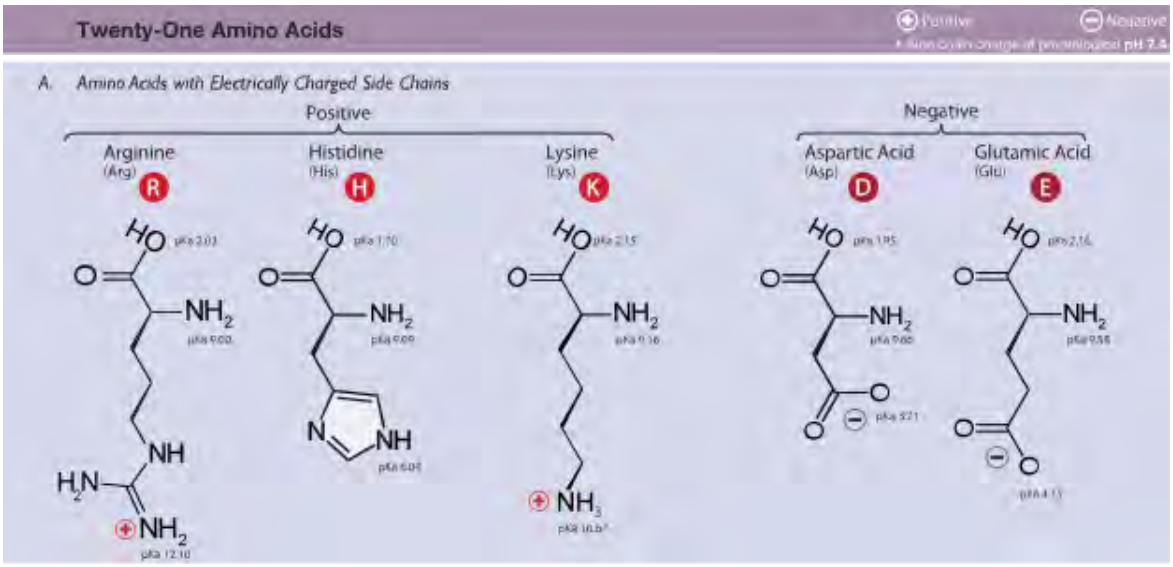

Figure 9. Amino acids that contain a net positive or negative charge.

Experimental Investigation of the Capacity of PROLENE and Oxidized PROLENE to Accept H&E Stain

In addition to my reliance on the literature and first principles of polymer science, and to further validate my assertion that H&E is not expected to stain PROLENE or oxidized PROLENE, Exponent conducted a set of laboratory experiments that serve as the control experiments Dr. Iakovlev failed to perform in his expert report. The details of these experiments are provided below.

Sample Preparation Prior to Sectioning

Exemplar PROLENE Mesh

Pristine PROLENE mesh (Ref. No. 810041B, Lot No. 3661669) was received and kept in its original packaging until use. A clean razor blade was used to cut sections for laboratory analysis.

Chemically Oxidized PROLENE Mesh

Six sections of PROLENE mesh (Ref. No. 810041B, Lot No. 3661669) were oxidized according to the protocol published by Guelcher and Dunn. Samples were incubated at 37°C for up to 5 weeks in oxidative media composed of 0.1 M $CoCl_2$ in 20 wt% H_2O_2. This solution purportedly

simulates the oxidative environment created by macrophages in response to a foreign object. The oxidative solution was changed every 2-3 days. Prior to processing, the samples were copiously rinsed in de-ionized water, air-dried, and assessed for morphological changes using scanning electron microscopy (SEM).

QUV Oxidized PROLENE Mesh

Six sections of PROLENE mesh (Ref. No. 810041B, Lot No. 3661669) were placed inside a Q-Lab QUV Accelerated Weathering Tester and irradiated with 0.98 $(\frac{W}{m^2})$ UV-A and UV-B at 60°C for 5 days. As with the chemically oxidized meshes, the samples were assessed for morphological changes using SEM prior to processing.

Sample Mounting and Sectioning

Exemplar and oxidized mesh samples were embedded in both paraffin and resin (Technovit 7200), sectioned, and stained with Hematoxylin & Eosin. All processing was performed by an independent histology lab and observed by Exponent. Detailed embedding and staining protocols can be found in Appendix A.

Paraffin-embedded samples were prepared by following the protocol submitted by Dr. Iakovlev. Samples were sequentially dehydrated in reagent alcohol and Xylene substitute using an automated tissue processor, then embedded in Leica EM400 Paraffin wax. Sections of the paraffin blocks (4-6 µm thick) were obtained using a microtome, briefly floated in a 40-45°C water bath, then mounted onto slides. Sections were air-dried for 30 minutes then baked in a 45-50°C oven overnight.

Resin-embedded samples were sequentially dehydrated in reagent alcohol using an automated tissue processor, then embedded in Technovit 7200. The polymerized resin block was trimmed, cut, and ground to a thickness of approximately 50 µm.

Paraffin and resin-embedded samples were stained with Aqueous Eosin and Harris Hematoxylin using an automated stainer. All slides were imaged by Exponent personnel using a microscope equipped with polarizing filters.

Results

SEM on Oxidized Meshes

When viewed under SEM, the QUV-oxidized mesh exhibited external cracking (Figure 10), while the chemically-oxidized mesh did not (Figure 11). This differs from the results published by Guelcher and Dunn, who reported “pitting” and “flaking” in polypropylene meshes subjected to the same treatment conditions.

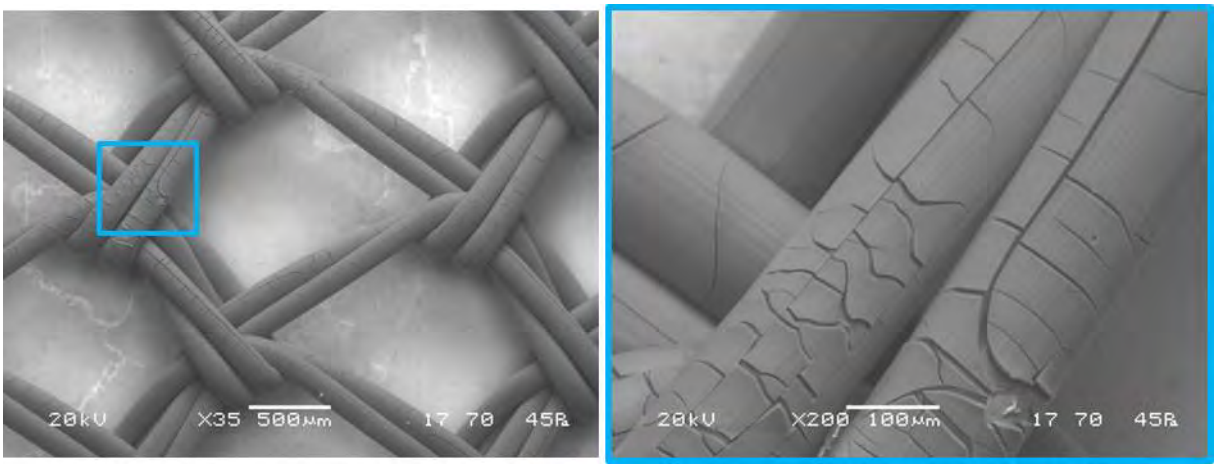

Figure 10. Scanning Electron Microscope images of QUV oxidized mesh.

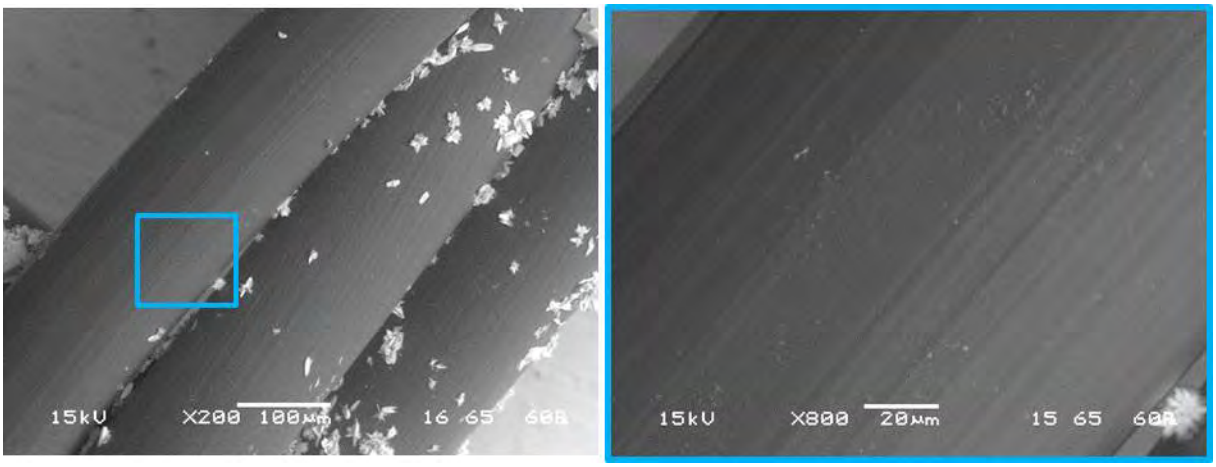

Figure 11. Scanning Electron Microscope images of mesh that was chemically-oxidized according to the Guelcher protocol.

Analysis and Experimental Validation

Six separate samples were simultaneously subjected to QUV irradiation; each contained approximately 120 individual fiber segments. While only one of these samples (Sample #2) was processed for H&E staining, it is reasonable to infer, based on SEM images of QUV-exposed samples, that a majority of the individual fibers in the treated samples were degraded, and cracked prior to being subjected to the staining process. An SEM image of Sample #4 with enumerated fiber segments used as the basis for quantifying the cracked fibers is shown below in Figure 12.

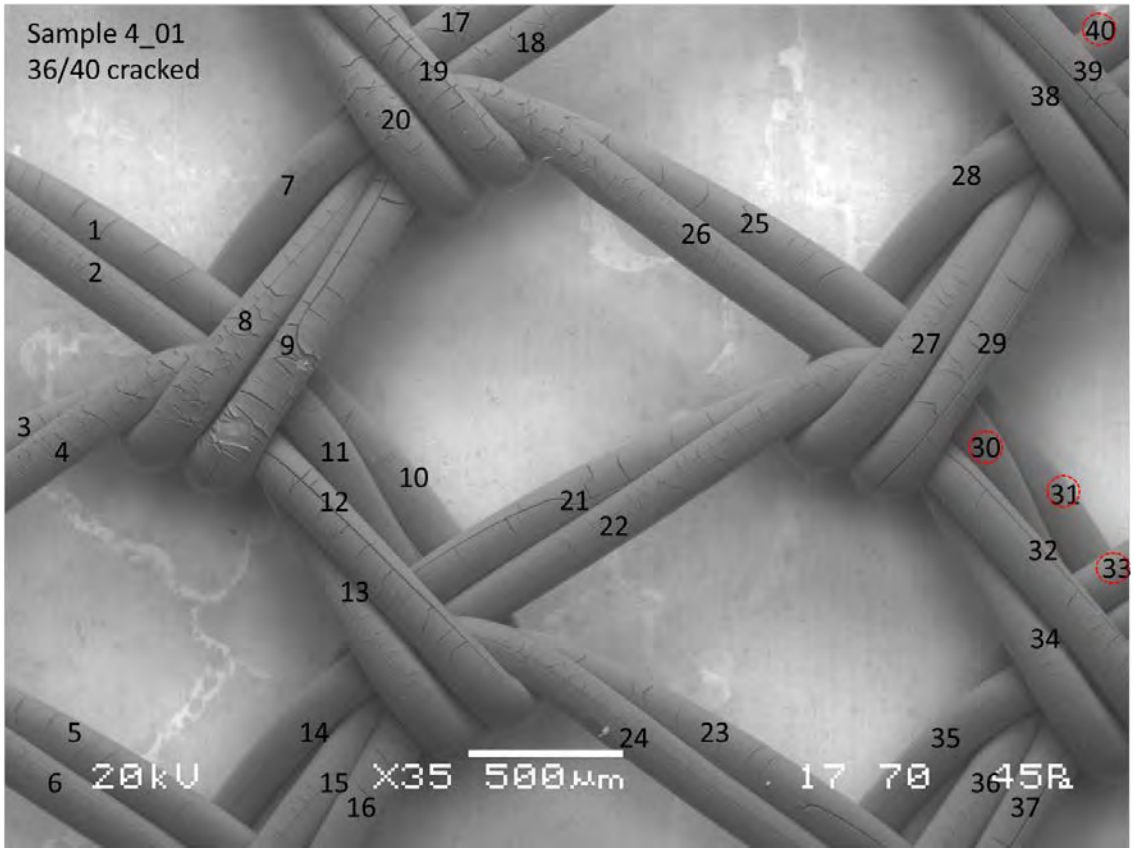

Figure 12. Scanning Electron Microscope image of QUV oxidized mesh. Numbered markings indicate individual fiber segments.

Each SEM image covers approximately one-third of the sample that was cut from the PROLENE device. The table below summarizes the findings of cracked fiber segments from portions of the three QUV-irradiated samples examined in the SEM (Samples #4, #5, and #6).

Table 3. Summary of Scanning Electron Microscope findings on QUV oxidized mesh.

Sample Number	Cracked Fiber Segments in SEM Image	Total Fiber Segments in SEM Image	% of Fiber Segments Cracked in SEM Image	95% Lower Bound on % of Cracked Fiber Segments in Sample
4	36	40	90%	80%
5	27	42	64%	52%
6	29	37	78%	66%

The rightmost column of the table presents the 95% lower confidence bound on the percentage of cracked fibers in the total sample. Although the observed percentage of cracked fiber segments varies for each of the three samples, the respective SEM images support a reliable statistical inference that, with 95% confidence, greater than half of the individual fibers in the entire sample will be cracked.

A simple conservative calculation shows that it is implausible that Sample #2 exposed to UV light and treated with histological dye contained no cracked fiber segments. Given that the treated sample contained approximately 120 fiber segments, each of which independently has a 50% probability of being cracked, the chance that none of the 120 fiber segments were cracked is only 1 in 2^{120}, or less than 1 in 10^{36} (1 followed by 36 zeroes). In other words, the probability that none of the fiber segments in Sample #2 were cracked at the time of staining is so infinitesimally small it renders the outcome, for all practical purposes, impossible.

Intentionally Oxidized PROLENE Meshes Were Not Stained by the Hematoxylin & Eosin Dyes

Positive Control – Rabbit Skin

A positive control (rabbit skin tissue) was included with the mesh samples and processed simultaneously in the automated tissue stainer to demonstrate the effectiveness of the protocol. PROLENE meshes were subjected to the staining protocol in the same batch.

The appearance of stain is evident when tissue is present and stain has been applied. Figure 13 shows the stark contrast between rabbit tissue that has not been treated with stain (left) and

rabbit tissue that has been treated with stain (right). This experiment demonstrates that our protocol is effective in staining proteinaceous materials.

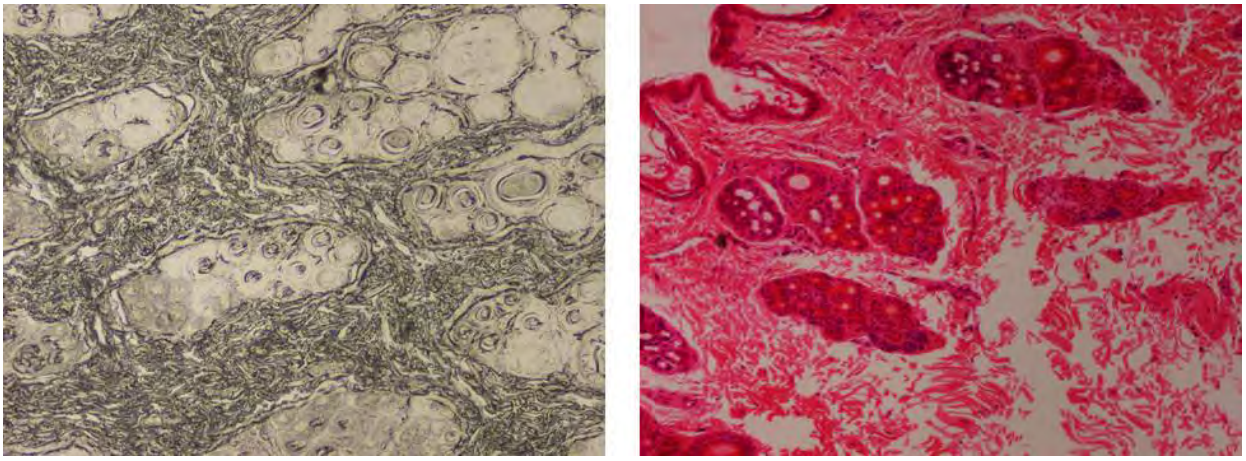

Figure 13. Processed and sectioned rabbit skin tissue not stained (left) and tissue that has been stained (right) are shown.

Non-Oxidized Control – Out-of-the-Box PROLENE Mesh

Exemplar PROLENE mesh samples with no prior exposure to laboratory UV or chemical oxidation were subjected to the Iakovlev staining protocol. As expected, the H&E stain did not bond to the PROLENE as displayed in Figure 14, confirming that the staining protocol is not effective in staining non-proteinaceous or non-ionic materials.

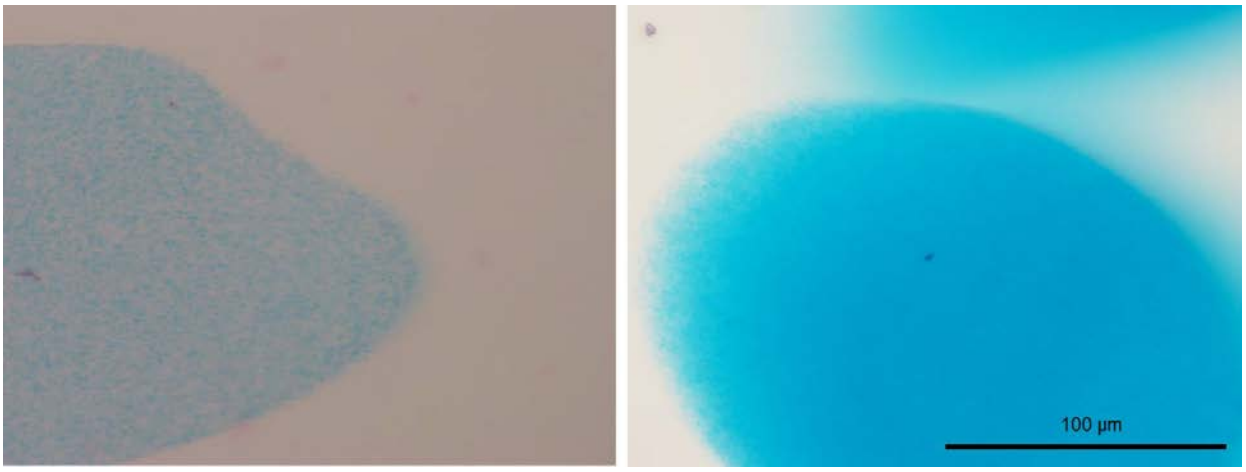

Figure 14. Pristine (exemplar) mesh embedded in paraffin (left) and resin (right), stained with H&E.

Intentionally Oxidized PROLENE – Chemical Oxidation

Exemplar PROLENE mesh samples exposed to the Guelcher chemical oxidation procedure were also subjected to the Iakovlev staining protocol. In total, twenty-two individual cross sections were examined. As shown in Figure 15, Figure 16, and Figure 17, the chemically oxidized PROLENE did not accept the H&E stain, thereby confirming the flawed methodology of Dr. Iakovlev.

Figure 15. Chemically oxidized PROLENE mesh embedded in paraffin (left) and resin (right), stained with H&E.

An additional observation made during these experiments was that manipulation of the microscope polarizers could create a "bark-like" appearance on the fiber exterior (Figure 16 and Figure 17). This effect is likely caused by the variant thickness of the fiber across its diameter as an artifact of the sectioning process. Interestingly, what Dr. Iakovlev describes as PROLENE dye particles can be seen in the false "bark."

Figure 16. PROLENE mesh chemically oxidized with the Guelcher protocol, embedded in resin, and subjected to the H&E staining protocol. Non-polarized light (left), plane-polarized light (center), cross-polarized light (right). No staining is evident.

Figure 17. PROLENE mesh chemically oxidized with the Guelcher protocol, embedded in resin, and subjected to the H&E staining protocol. Non-polarized light (left), plane-polarized light (right). No staining is evident.

Intentionally Oxidized PROLENE – UV Oxidation

Exemplar PROLENE mesh samples exposed to QUV oxidation were also subjected to the Iakovlev staining protocol. In total, over one hundred individual cross sections were examined. As shown in Figure 18, the QUV oxidized PROLENE did not accept the H&E stain. In addition, as shown in Figure 19, despite the fact that the fiber was cracked, and according to Dr. Iakovlev should have physically trapped stain, the QUV oxidized PROLENE did not accept the H&E stain, thereby again confirming Dr. Iakovlev's flawed methodology. Despite multiple observations using high and low magnifications, polarized and non-polarized light, no evidence of the stain being trapped, captured, or otherwise bound within the cracks of the damaged mesh was observed.

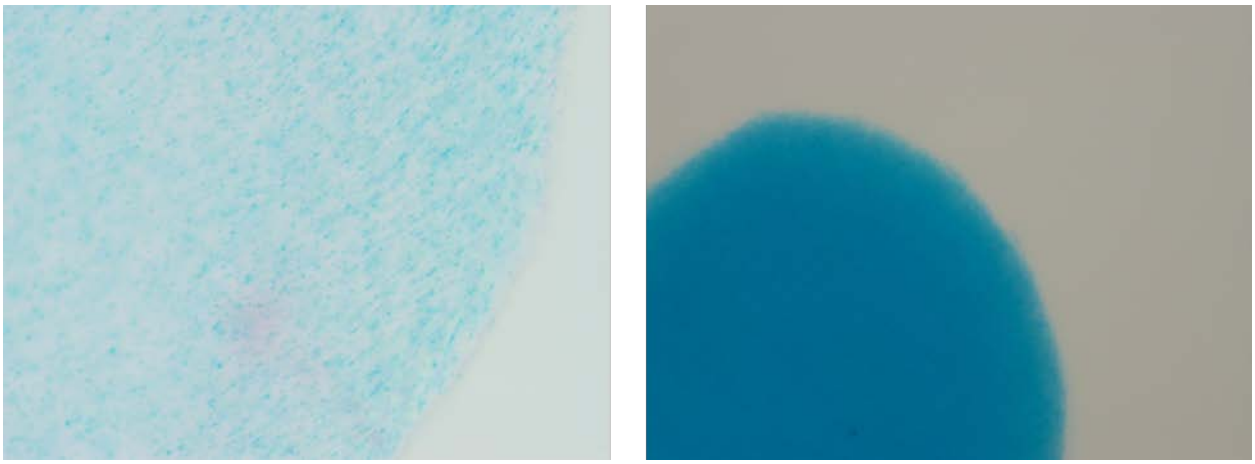

Figure 18. QUV oxidized PROLENE mesh embedded in paraffin (left) and resin (right), stained with H&E.

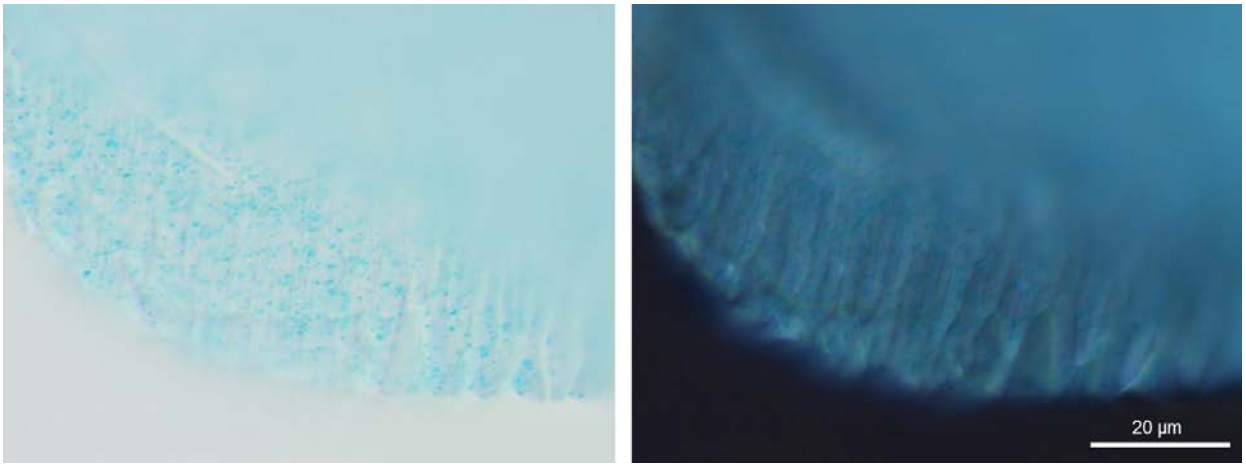

Figure 19. QUV treated mesh exhibiting several cracks but no evidence of H&E stain. Image on the left was acquired in absence of polarization, the image on the right was taken with polarization.

Statistical Significance

A statistical analysis of my control experiment was scientifically unnecessary. In the microscopy experiments conducted, intentionally oxidized PROLENE was shown to not hold stain. No variability was observed in these results, meaning none of the nearly 150 individual fiber segment cross sections prepared and examined according to Dr. Iakovlev's staining protocol were found to have stained. The lack of variability in the experimental data supports the conclusion that these observations are essentially deterministic in nature, reproducible

exactly or with negligible variability. As defined in *A Dictionary of Computing*, published by the Oxford University Press,[110] statistical methods are:

> "Methods of collecting, summarizing, analyzing, and interpreting variable numerical data. Statistical methods can be contrasted with deterministic methods, which are appropriate where observations are exactly reproducible or are assumed to be so."

In view of this definition, which distinguishes statistical from deterministic methods, the omission of a formal analysis—i.e., an application of statistical methods to the unvarying data in this experiment—is appropriate and consistent with generally accepted scientific practice.

Validation of Microscopy Experiments

To confirm the reliability of the methods and results of its microscopy experiments, Exponent repeated and expanded its work using three additional PROLENE TVT mesh devices, a PROLENE hernia mesh, PROLENE sutures, and commercially available polypropylene (not PROLENE) pellets . In addition to the examination of pristine (exemplar), and intentionally oxidized (QUV and chemical) polypropylene-based samples, sections of these PROLENE devices were coated in fetal bovine serum (a protein rich medium) as an additional positive control. Further details of these experiments and corresponding results are included in Appendix H of this report.

Imaging Artifacts

Microtome slicing of polymeric samples has been used in the field of polymer science for decades, and is a technique with which I am familiar.[111,112,113] Observation of thin-sliced polymeric specimens, including those that have been dyed, requires an understanding of potential artifacts that can exist as a result of the cutting and imaging process.

---

[110] *A Dictionary of Computing,* Oxford University Press, 2004.

[111] Wang, X., Zhou, W. Glass Transition of Microtome-Sliced Thin Films. *Macromolecules*, (2002) 35(18):6747–6750.

[112] Stiftinger, M., Buchberger, W., Klampfl, C. W. Miniaturised Method for the Quantitation of Stabilisers in Microtome Cuts of Polymer Materials by HPLC with UV, MS or MS2 Detection. *Anal. Bioanal. Chem.*, (2013) 405(10):3177–3184.

[113] Janeschitz-Kriegl, H., Krobath, G., Roth, W., Schausberger, A. On the Kinetics of Polymer Crystallization under Shear. *Eur. Polym. J.*, (1983) 19(10-11):893–898.

In some instances during this study, select images appeared to have a pink background when viewed on two separate computer monitors. An example of this is shown in Figure 20. The image on the left is the actual image file. The image on the right is a photograph of the same image file being displayed on a different monitor. A photograph was taken to capture the color difference. This perceived change in hue is one example of how optics, lighting, and related artifacts may influence visual observations.

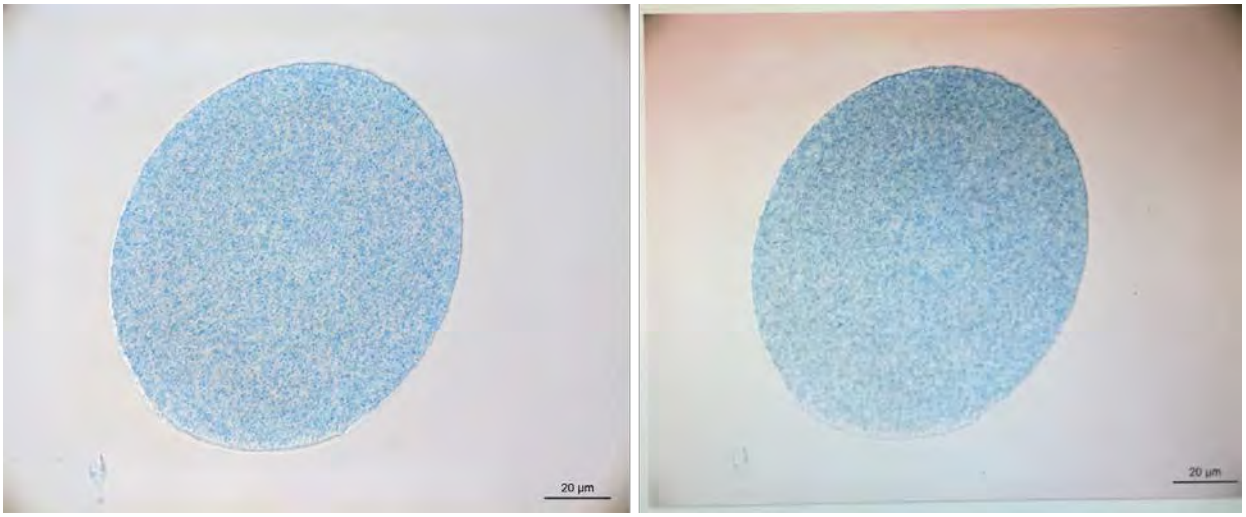

Figure 20. Same micrograph image of pristine PROLENE shown on two different computer monitors. A photograph of the image on the screen of monitor 2 was taken to preserve the observed pink coloring artifact. Sample was produced as part of the work described in Appendix H

Thickness Variation and Stain Pooling

When high aspect ratio samples (such as fibers) are sectioned with a microtome, simple geometry dictates that the thickness will be variant if the microtome knife is not orthogonal to the sample's long axis. This geometric artifact is exhibited schematically in Figure 21A-D, which illustrates that the edges of the sliced specimen are thinner when viewed under the microscope.

This same effect can result in stain pooling, which is also illustrated schematically in Figure 21E. The cylindrical fibers that compose the mesh (A) can be cut in an oval shape depending on

the angle at which the blade encounters the block (B). When the resulting section (C) is placed on a glass slide and stained, the angle between the section and the glass forms a small pocket in which stains can accumulate (D), giving the appearance, including color, of "true" staining (E) – that is, of chemical interactions between dyes and their ligands. In reality, this is merely a mechanical entrapment of the stain.

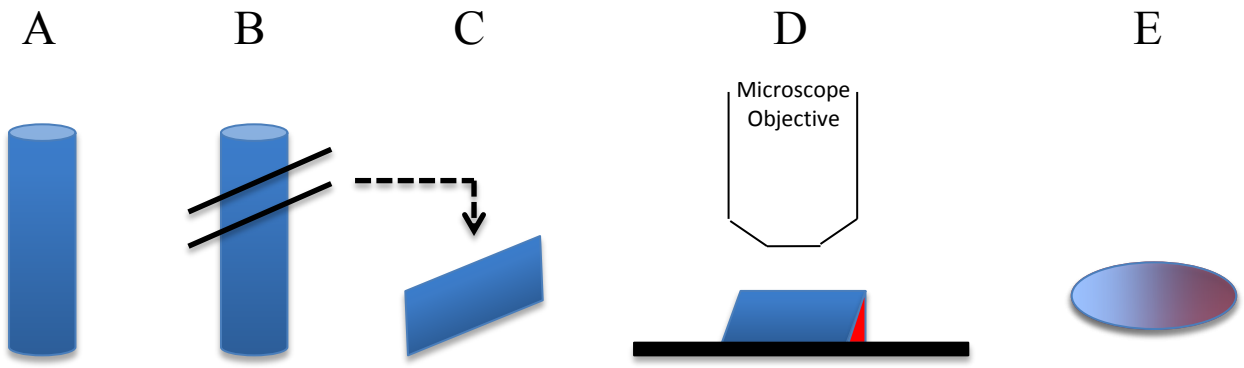

Figure 21. Potential formation mechanism of pooling artifact. A mesh fiber (A) can encounter the microtome blade at an angle (B), forming a section with an angled ledge (C), under which stain can pool (D) and give the appearance of true staining (E).

Stain pooling was observed in several fiber cross sections examined as part of this study. An example of stain pooling, as observed in a pristine TVT device not expected to stain, is given in Figure 22. Different planes of focus for the fiber cross section are given in Figure 22 that include an image of the plane of the fiber nearest the reader in focus (a) and the plane farther away from the reader, underneath the pristine fiber where the stain is pooled (b).

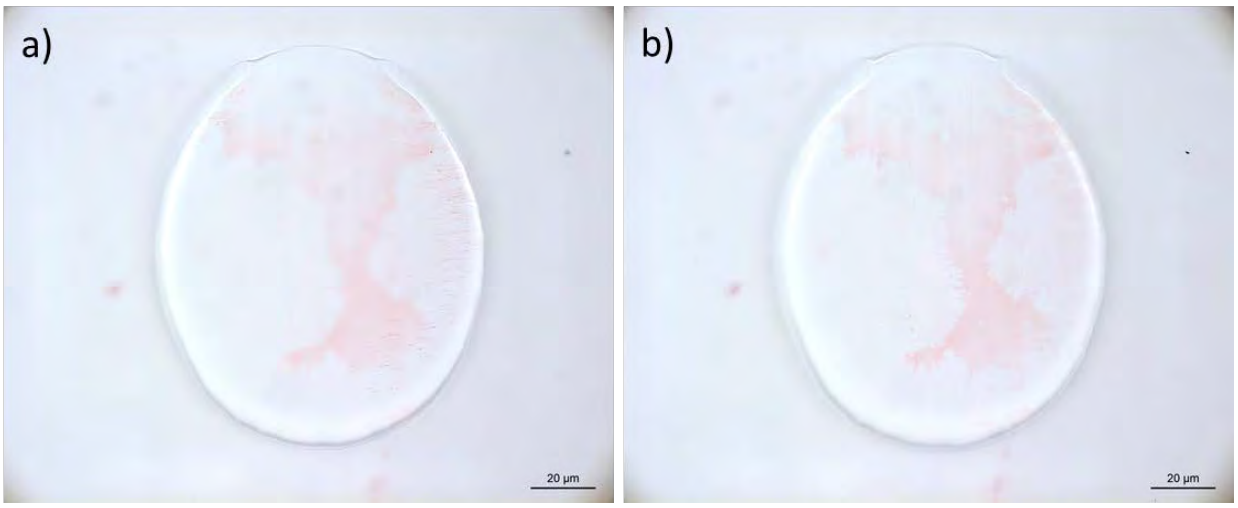

Figure 22. Example of stain pooling is shown from a sample prepared as part of the work described in Appendix H. A fiber cross section from a pristine TVT mesh, not expected to stain, is shown with different planes of focus. For image a), the plane nearest the reader is in focus. For image b), the stain pooled underneath the fiber is in focus.

Polarizing Artifact

Polarized microscopy is a powerful tool in polymer science.[114] With good optics and proper alignment, it allows for the visualization of anisotropic structures, making them appear under varying shades of brightness with a polarizing filter in the microscope's light path.[115] The brightness of the sample when imaged under polarization depends on factors such as sample alignment. The brightness is highest when the object is aligned at a 45° angle to the polarizers. On the other hand, the object can become difficult to see when aligned parallel to one of the two polarization planes.

The thickness variation resultant from microtoming, as well as the tendency of an anisotropic fiber to tear away from a surrounding matrix, can create edge artifacts under polarized light. An example of such an artifact is displayed in Figure 23, which is a micrograph of an *unoxidized* (no possible "bark") pristine PROLENE mesh fiber subjected to H&E staining. In Figure 23b

[114] Lenz, R. W. Experiments in Polymer Science, Edward A. Collins, Jan Bares, Fred W. Billmeyer, Jr., Wiley-Interscience, New York, 1973.

[115] Wolman, M. Polarized Light Microscopy as a Tool of Diagnostic Pathology. *J. Histochem. Cytochem.*, (1975) 23(1):21–50.

and Figure 23c, the fiber is shown under polarized light, and a dark ring of false "bark" is visible on a portion of the fiber exterior. The images in Figure 23 show the same region with and without the polarizer.

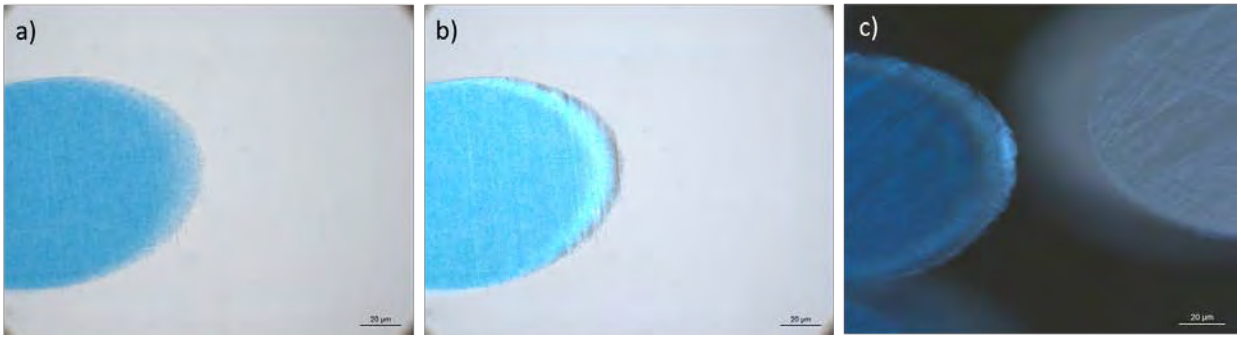

Figure 23. Pristine, unoxidized PROLENE mesh after staining with H&E produced as part of the work described in Appendix H. Image (a) was obtained without polarized light. Images (b) and (c) were acquired with polarized light.

Becke Lines

Differences in refractive indices (material density) between a transparent specimen and its surroundings can cause the appearance of light and dark parallel lines at the interface between materials. These lines are known in microscopy as Becke lines.[116] Figure 24 illustrates this imaging artifact at the edge of a QUV oxidized PROLENE mesh cross section embedded in paraffin and subjected to H&E staining. The relative location and thickness of these lines change based on the position of the focal plane with respect to the surface of the microscopy slide, with the thinnest line corresponding to the microscope being focused at the surface. These lines can be altered by changing the focus in the microscope as seen in the videos included in Appendix F.

[116] Zalevsky, Z., Sarafis, V., "Phase Imaging in Plant Cells and Tissues," *Biomedical Optical Phase Microscopy and Nanoscopy,* chapter 4. Oxford, UK: Elsevier, 2013.

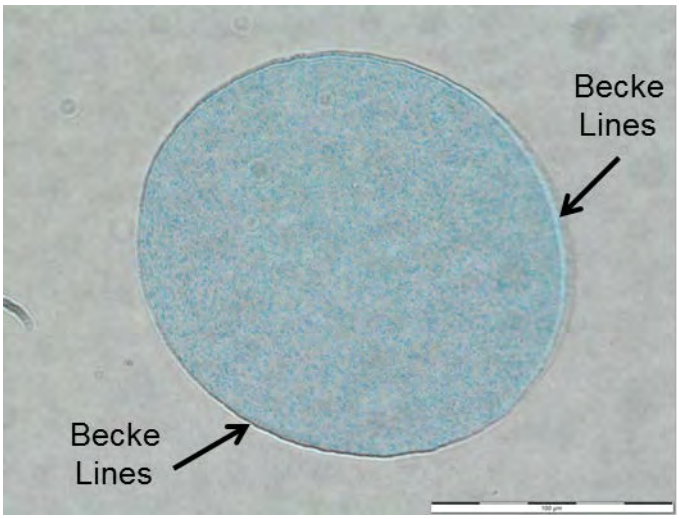

Figure 24. QUV oxidized PROLENE mesh embedded in paraffin, and subjected to the H&E staining protocol. Notice dark and light Becke lines around the fiber parameter.

Purple Hue

Additional imaging artifacts can be created due to changes in incident light. For example, the artificial faint purple hue observed in discrete locations of the specimen shown in Figure 25 (right) is the consequence of exposing the specimen to plane-polarized light. It is evident that this hue is an artifact of the imaging technique due to its absence when the same specimen is examined with the same microscope at the same magnficiation under non-polarized light (left).

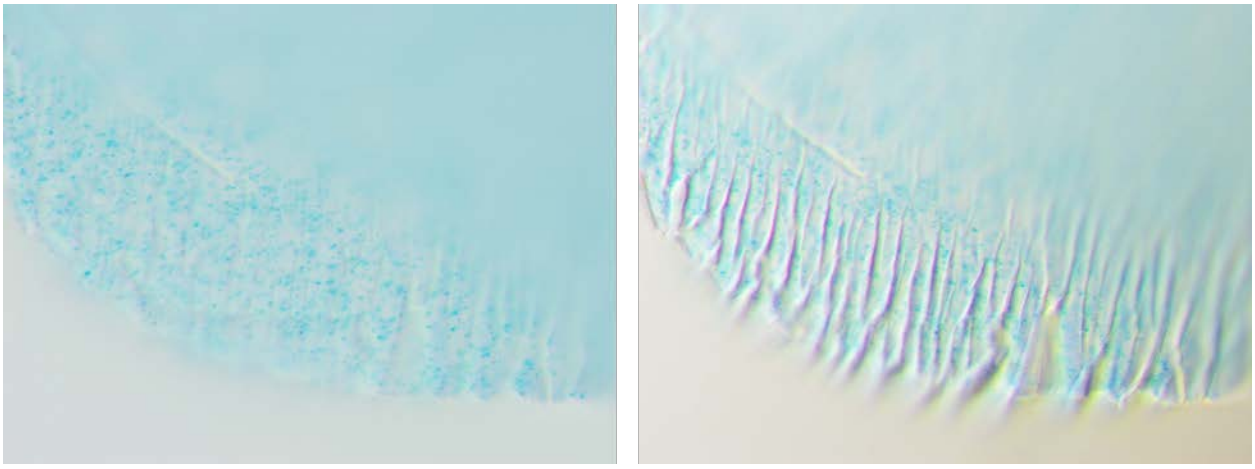

Figure 25. QUV oxidized PROLENE mesh embedded in paraffin, subjected to the H&E staining protocol, and imaged with non-polarized light (left) and plane-polarized light (right). No staining is evident. The purple hue (right) is an artifact of the imaging technique.

Blue Granules Outside Fiber Boundary

Due to the cylindrical nature of the fibers, if a cross section is not cut perfectly orthogonal to the fiber's long axis, the resulting slice will be slightly skewed as seen in Figure 26 (left). When this fiber is viewed from the top through the microscope, the blue granules beneath the top surface of the fiber cross section appear to extend beyond the fiber boundary, as shown schematically in Figure 26 (right). The Becke lines indicate the outline of the fiber at the surface of the microscope slide. An example of this artifact can be seen in Figure 27, where an unoxidized exemplar PROLENE mesh was mounted in paraffin, cross sectioned and subjected to the H&E staining protocol. When examined with the optical microscope, the fiber exhibits this artifact (i.e. has the appearance of blue granules extending beyond the fiber boundaries).

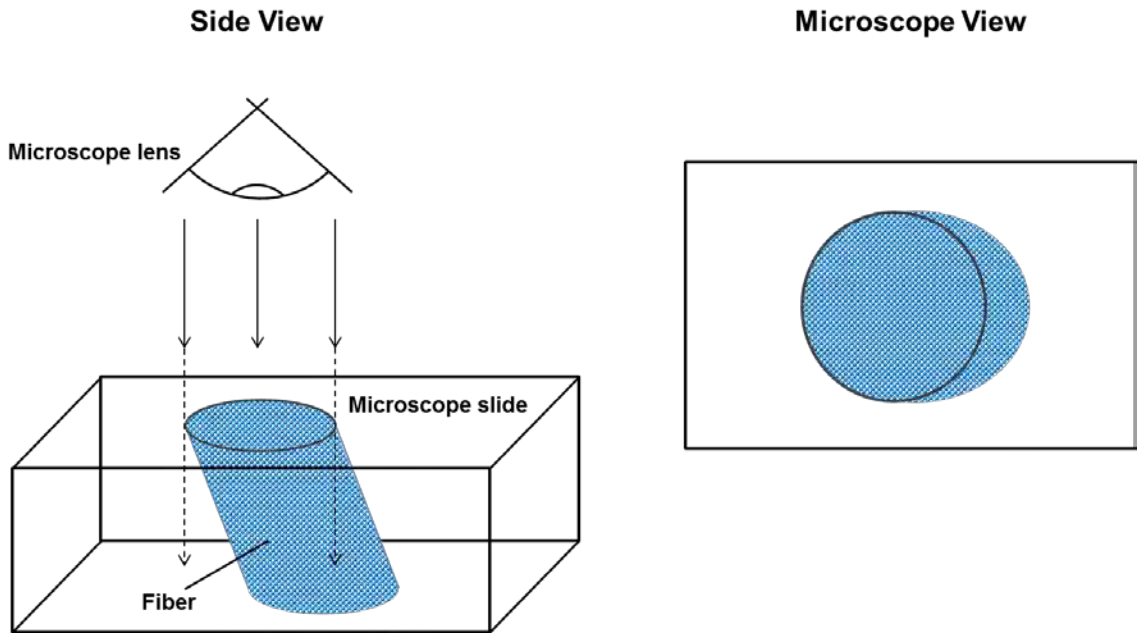

Figure 26. Schematic of potential artifact mechanism where blue granules appear outside the fiber boundary. If a fiber is cut at an angle (left) and the cross section is viewed from the top through the microscope lens (right), it can appear that the blue granules extend beyond the fiber boundary.

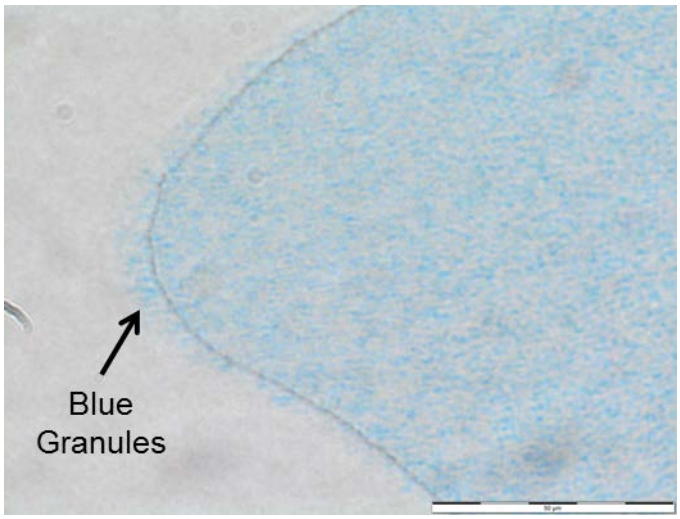

Figure 27. Unoxidized exemplar PROLENE mesh embedded in paraffin, and subjected to the H&E staining protocol. Note the appearance of blue granules beyond the exterior of the fiber.

Rebuttal of Plaintiff Experts

Iakovlev

Exponent reviewed the reports authored by Dr. Vladimir Iakovlev[117,118] and disagrees with several of his findings, opinions and methodologies. The following section summarizes the issues encountered with Dr. Iakovlev's reports.

Dr. Iakovlev stated that, "Examination reveals a polypropylene degradation layer on the outermost layer of the mesh filaments."[119] Dr. Iakovlev performed absolutely no chemical characterization of the external surface to verify his assertion that the layer is polypropylene, much less degraded polypropylene.

Dr. Iakovlev's assertion that the bark layer is comprised of PROLENE is shear speculation based on his qualitative observation that the bark illuminates when exposed to cross polarized light. Any material possessing anisotropic domains has the potential to become visible when examined under cross polarized light. In fact, Dr. Iakovlev has clearly demonstrated that stained biological material (collagen), with presumably a low degree of molecular order, has the ability to illuminate when microscopically imaged under cross polarized light. The results from his polarized light experiment, at best and at most, suggest that the bark layer contains crystalline domains (local ordering of molecules) within its structure. In short, these results do not confirm the "bark" layer is synthetic, nor does it conclusively prove the layer is PROLENE.

According to the GPC data generated during the Seven Year Dog Study (Table 1), none of the explanted PROLENE sutures exhibited any signs of degradation after seven years *in vivo*. No meaningful differences were observed in any of the molecular weight values between unimplanted control sample material and explanted sample material. Moreover, Dr. Iakovlev did not performed any testing that attempts to quantify losses in PROLENE molecular weight,

[117] Iakovlev MDL Consolidated Case Report dated 8-24-15.

[118] Iakovlev Wave 1 General Report with attachments dated 1-29-16.

[119] Iakovlev MDL Consolidated Case Report dated 8-24-15, pg 17.

which is the ultimate determination as to whether a polymer has suffered from any meaningful degree of degradation. Without having generated this data on material from PROLENE control specimens and explanted specimens, any opinions rendered by Dr. Iakovlev that are related to PROLENE degradation are baseless and, therefore unreliable.

For long-chain, linear polymeric materials such as polypropylene, which is the base material in PROLENE, the term degradation is most often ascribed to a reduction in the polymer's molecular weight, which in turn, results in measurable changes in bulk physical properties such as elongation at break. The data generated by Ethicon during its Seven Year Dog Study is both clear and overwhelming. None of the tested PROLENE sutures explanted from the subject dogs showed any signs of molecular weight loss or tensile property loss when compared to control samples.[72,95] In fact, the *in vivo* environment had a positive effect on the PROLENE's tensile properties, in particular, the elongation (also referred to as ductility or toughness) increased over the seven year testing period and ultimately achieved strain-at-break values in excess of 80% (an increase of 111% over unimplanted controls). To put this value in perspective, the PROLENE explanted specimens, on average, almost doubled (1.8x) in length prior to breaking during the tensile test. In contrast, polymeric materials that truly exhibit brittle behavior have strain-at-break values that are less than 2%, meaning they are only capable of extending by a mere 2% of their original length prior to breaking during a tensile test. When the data is viewed in totality, it is clear that the PROLENE did not suffer from material degradation and did not become embrittled.

Dr. Iakovlev also opined that PROLENE mesh becomes brittle and, as a consequence, also becomes stiffer with time spent *in vivo*. These opinions are subjective as they are based solely on Dr. Iakovlev's visual observations of the microcracking and the tactile feel of explanted, and perhaps formalin-fixed, bulk tissue and PROLENE mesh specimens. Estimating a material's "stiffness" or change in "stiffness" by manually manipulating a specimen is not an accepted scientific method within the material science community. Moreover, Dr. Iakovlev has not performed any testing to quantify any perceived increase in stiffness; therefore these assertions are both speculative and baseless. Scientifically reliable test methods exist that quantitatively assess a material's inherent stiffness, namely tensile testing, which determines the stiffness

(modulus) of a material of known dimensions based on load-deflection or stress-strain data. In fact, tensile testing on explanted PROLENE sutures was performed by Ethicon at the one year, two year, and seven year time intervals during its Seven Year Dog Study. The results of these tests were conclusive; the explanted PROLENE material not only became tougher and more ductile over time, but also became *less* stiff based on the reduction in modulus as a function of time *in vivo*. The results are also in complete contradiction to Dr. Iakovlev's assertion that the "degradation of polypropylene with resultant stiffening of the mesh is progressive over the years."[120]

Dr. Iakovlev opined in a recently published article that "[a]lthough the degraded layer is thin in relation to the fiber diameter, its circumferential distribution provides the highest mechanical effect on the mesh fibers. Degradation related stiffening of the mesh is expected to increase over time."[121] Dr. Iakovlev also noted that his alleged "bark" layer showed nanocavities (cracks) that indicate brittleness.

From a fundamental polymer science perspective, Dr. Iakovlev's above-stated opinions are flawed for a number of reasons. First, if we assume, for sake of argument, that the "bark" layer is more stiff then the underlying material, if it is filled with cracks (or nanopores and nanocavities as Dr. Iakovlev calls them), it is by definition discontinuous and therefore mechanistically cannot contribute to an increase in stiffening.[122] Dr. Iakovlev cannot have it both ways, either the material is stiff and uniform and leads to mesh stiffening, or it cracks and forms pores and traps dyes; the two are mutually exclusive. Second, if the polypropylene is actually being broken down into smaller molecules, it will tend to become less stiff, not more. Again, Dr. Iakovlev cannot have it both ways (indeed, by stating degradation into smaller molecules leads to stiffening, Dr. Iakovlev underscores the flawed nature of his reasoning).

---

[120] Iakovlev MDL Consolidated Case Report dated 8-24-15, pg 13.

[121] Iakovlev, V. V., Guelcher, S. A., Bendavid, R. Degradation of Polypropylene *in Vivo*: A Microscopic Analysis of Meshes Explanted from Patients. *J. Biomed. Mater. Res. B Appl. Biomater.*, (2015) 00B:000–000.

[122] Had he chosen to do so, with even a fundamental knowledge of mechanics, Dr. Iakovlev could have easily calculated that a continuous (without his observed pores and cracks) bark of the thickness he has measured could not meaningfully contribute to an increase in mesh stiffness.

Dr. Iakovlev presented a short-term control study to show that formalin will not cause a degraded layer to form on PROLENE mesh. His study consisted of immersing pristine PROLENE samples in formalin for four months followed by embedding in paraffin and staining. Dr. Iakovlev stated that this control showed an "absence of degradation after exposure to formalin and chemicals of tissue processing,"[123] due to the fact that a bark layer did not form when a pristine PROLENE sample was placed in formalin. This control experiment is scientifically useless as he chose to neglect the potential contribution that biological materials may have on the formation of the "bark" layer. If the "bark" were biologic in nature, it would be necessary to not only expose the fibers to formalin, but also include biological exposure/material to properly explore the experimental design space. Excluding one of the potential experimental factors that may contribute to "bark" formation invalidates the findings from his *in vitro* control experiment. In addition, even if he had included all the necessary components for this control experiment, the time period of this study was approximately an order of magnitude (10x) shorter than the length of time explanted samples are stored in formalin and therefore is inadequate.

Dr. Iakovlev used the "bark" thickness increase with time *in vivo* as further evidence that the "bark" is degraded PROLENE. In his analysis, he completely ignored the possibility that a biological material covering the PROLENE mesh could also increase in thickness with time; creating a crust that will correspond in thickness to the biological material deposited *in vivo*. Furthermore, Dr. Iakovlev did not specify his process for measuring the crust layer on his explants. Histological slides have very few, if any, completely circular fiber cross sections. Unless each measurement was taken at the exact minimum diameter location on each sample, his results are completely unreliable. The presence of a time-dependent bark thickness is simply not instructive in determining the composition of the bark.

No basis has been provided for Dr. Iakovlev's suggestion that oxidized PROLENE will stain with Hematoxylin and Eosin (H&E). He neglected to perform a simple control experiment or provide scientific rational to support his implication that his dying technique is appropriate to differentiate between the purported oxidized PROLENE bark layer and the inner core of the

[123] Iakovlev MDL Consolidated Case Report dated 8-24-15, pg 17.

same fiber, as demonstrated in the experiments described previously. This lack of a simple control shows that Dr. Iakovlev's claims are based on flawed and untested hypotheses. Furthermore, H&E stain will adhere to any material with acidic or basic functional groups, which are commonly found in biologic conditions. If anything, the staining shows that the crust layer is more likely biologic in nature than oxidized PROLENE.

Dr. Iakovlev further opined that the trapping of histological dyes in 'nanocavities' somehow indicates degradation due to a decrease in pore size farther from the outer surface of the crust layer. This experiment is wrought with faults that are contradicted by Dr. Iakovlev's own report and also suffer from a lack of controls. The basis for this experiment is that a dye of smaller size will be able to penetrate further into the bark layer due to the presence of supposed nanocavities that purportedly decrease in size as they approach the PROLENE core. Dr. Iakovlev provided no justification or reasoning that nanocavities would exist on the size scale that would be selective to the size difference of the molecules, nor does he even provide the size difference between the staining molecules. In his limited description of the experiment, which is not fully documented within the report, Dr. Iakaovlev again failed to provide any control materials with known pores or with varying conditions to show this size selectivity is even a possibility. Additionally, Dr. Iakovlev used multiple stains throughout the course of his investigations, including H&E. Assuming Dr. Iakovlev's hypothesis is correct and there were pores capable of size selecting for these stains and assuming chemical adsorption was not occurring, H&E stain would show the same size exclusion as the trichrome stain. This does not happen, indicating that the idea of pore size selection based on molecular size is not occurring.

Dr. Iakovlev opined that microcracking of the PROLENE mesh fibers occurs *in vivo*, but failed to consider the possibility that the microcracking could occur during the explantation process. To the best of Exponent's knowledge, all observations of surface microcracking by numerous researchers have been made on explanted meshes.[45,49,50,58,59] In addition, an Ethicon study determined that explanted mesh material, maintained and examined under wet conditions showed little, if any, signs of cracking while wet samples that were allowed to dry under ambient conditions developed cracks. In fact, the report states that the "[s]utures kept in the wet state do not exhibit cracks. Upon drying, cracks appear – this was actually observed happening

by drying '83-165 6 yr. wet' on the microscope stage." It is possible that the microcracking observed by Dr. Iakovlev in PROLENE mesh "immediately after explantation from the body"[124] resulted from exposure to ambient conditions, mechanical stress imposed on the mesh during explantation, or a combination of both.

Dr. Iakovlev further opined that the retention of blue particles within the "bark" material covering the blue fibers proves that the bark is degraded PROLENE. Unfortunately, he failed to consider an important aspect of the sample preparation procedure which may account for this result. These samples were microtomed, or sliced very thinly with a knife. Although microtoming is a well-utilized specimen preparation technique within the scientific community, it is essential to be aware of the well-documented artifacts associated with the procedure. It is well-known in the scientific community that microtoming can cause tearing or smearing artifacts, cutting defects, structure deformations[125] and other sometimes difficult to identify artifacts. In addition, blue granules in the "bark" can also be an artifact of a non-orthoganol cross section as demonstrated earlier in this report. The fact that the majority of the blue particles appear close to the polymer core of each image strongly suggests sample preparation artifacts opposed to the degraded "bark," as proposed by Dr. Iakovlev. If the "bark" was degraded PROLENE, the entrapped blue particles would be more uniformly present throughout the bark layer and not biased towards the inner surface.

Dr. Iakovlev stated, "[f]or nearly a half century, scientists around the world have studied polypropylene, including Ethicon's Prolene used in TVT product [sic] and have consistently found that polypropylene degrades over time after being implanted in the body."[126] Dr. Iakovlev used fifteen journal articles as references for this statement, but many of them have absolutely no relevance to *in vivo* oxidation of polypropylene. For example, the articles written by Schmidt,[127] Rosa,[128] and Blais[129] report on the *photo* oxidation of polypropylene, these

[124] Iakovlev MDL Consolidated Case Report dated 8-24-15, pg 17.

[125] Morgan, C. "Some Effects of the Microtome Knife and the Electron Beam on Methacrylate-Embedded Thin Sections." *J Biophysi Biochem Cyto*, (1956) 2(4 Suppl):21–28.

[126] Iakovlev MDL Consolidated Case Report dated 8-24-15, pg 8.

[127] Schmidt, H., Witkowska, B., Kaminska, I., Twarowska-Schmidt, K., et al. "Comparison of the Rates of Polypropylene Fibre Degradation Caused by Artificial Light and Sunlight." *Fibres Text. East. Eur.*, (2011) 19(4):53–58.

articles in no way support Dr. Iakovlev's statement that polypropylene degrades *in vivo*. The use of irrelevant references at best shows Dr. Iakovlev's lack of polymer science education, training, and experience, and at worst, displays an attempt to artificially bolster his opinion with misleading references.

In his final opinions, Dr. Iakovlev claimed that the absence of a stainable outer layer encompassing the explanted nonpolypropylene materials he examined is further proof that the outer layer is degraded polypropylene. His rationale for this statement is that biologic material supposedly does not have varying degrees of affinity for diverse polymers. There are two reasons why this hypothesis is incorrect. First, the exact makeup of the biological material comprising the outer layer is unknown. Second, numerous studies have been published showing visual differences in the surface features between different explanted mesh materials (e.g. PDVF, PET, PTFE, etc.), including many cited in Dr. Iakovlev's own report.[45,58,59,69,99] Moreover, it is well understood in the polymer science community that different polymers with different molecular structures will have different physical and chemical attributes. Two such relavent attributes are the polymers ability to permit foreign material (e.g. body proteins) to diffuse through or adsorb to its outer surface.

Jordi

Exponent reviewed the report authored by Dr. Howard Jordi[130,131] and disagrees with several of his methodologies, findings and opinions. In particular, issues were found in both Jordi's interpretation of literature as well as his own research. The following section summarizes these issues.

---

[128] Rosa, D. S., Angelini, J. M. G., Agnelli, J. A. M., Mei, L. H. I. "The Use of Optical Microscopy to Follow the Degradation of Isotactic Polypropylene (iPP) Subjected to Natural and Accelerated Ageing." *Polym. Test.*, (2005) 24(8):1022–1026.

[129] Blais, P., Carlsson, D. J., Clark, F. R. S., Sturgeon, P. Z., et al. "The Photo-Oxidation of Polypropylene Monofilaments: Part II: Physical Changes and Microstructure." *Text. Res. J.*, (1976) 46641–648.

[130] Jordi MDL Consolidated Case Report dated 8-24-15.

[131] Jordi Wave 1 Expert Report dated 2-1-16.

Dr. Jordi carried out FTIR measurements on three samples (a PROLENE mesh explant, a pristine PROLENE fiber, and human albumin) to identify the presence of specific chemical functional groups which are indicative of oxidation in the explanted sample. He claimed the explanted sample contains oxidized regions of PROLENE based on the presence of an absorbance peak at 1761 cm^{-1}, which he attributed to carbonyl functionality. However, he did not discuss the amide I and amide II peaks that are clearly present at 1650 and 1550 cm^{-1} respectively, which also appear for the human albumin sample, and are indicative of biological material. Amide bonds are inherent to proteins and are the units that link multiple polypeptides together; many biological materials would be expected to exhibit both of these amide peaks as well as a carbonyl peak. In addition, Dr. Jordi attributed a peak at 1761 cm^{-1} as evidence of oxidation; however, he did not discuss how he differentiates this peak from the peak associated with the carbonyl containing groups in fatty acid esters which Dr. Jordi claimed have "absorbed into the TVT devices."[132]

There are several instances in which Dr. Jordi failed to mention, reference or explain figures that are in his report. One such example can be seen in Figure 8, it is unknown what, if any, conclusions are intended to be drawn since the sample description, procedure used and observations are absent. If it was Dr. Jordi's intention to demonstrate the presence of oxidation in this sample from the FTIR absorbance peak observed at 1740 cm^{-1}, then this conclusion is unsupported since, as discussed previously, he did not provided a method to differentiate between other sources of carbonyl containing functional groups which may be present on or in the explanted PROLENE fibers.

Dr. Jordi used nanothermal analysis to attempt to determine the surface melting point of pristine and explanted PROLENE mesh fibers. Part of the commonly accepted procedure when using this technique, is to calibrate the temperature of the cantilever as a function of resistance. Dr. Jordi calibrated the cantilevers utilized in this experiment using the melting points of polyethylene terephthalate, polyethylene, and polycaprolactone.[133] His justification for using

[132] Jordi MDL Consolidated Case Report dated 8-24-15, pg 23.

[133] Jordi Bellew Report dated 7-7-14.

these samples as calibration standards was his reference to Nelson, *et al*.[134] However, based on their work in determining a proper calibration procedure, Nelson *et al.* state that "the use of organic melting standards is thus ineffective for temperature calibration of silicon-heated cantilevers having extremely sharp tips." Since Dr. Jordi's referenced calibration procedure directly states not to use the sample type Dr. Jordi indeed used for his calibration, the calculated melting point values cannot be relied upon as accurate. It is unclear what the offset from the reported values should be since the relationship between bulk and surface melting temperatures is nonlinear.[134]

Even if the values reported by Dr. Jordi are accurate, the conclusion drawn from them is incorrect. Dr. Jordi reported an average melting temperature of the Bellew explanted samples of 124 °C, compared to 176 °C for the pristine non-explanted control samples. According to Dr. Jordi, the over 50 °C decrease in observed melting temperature can be considered proof of sample oxidation. This is incorrect for two reasons. First, surface oxidation of a fiber would result in a decrease in molecular weight. An isotactic polypropylene sample with a melting temperature of 124 °C would correspond with a M_n of roughly 4,500.[135] A decrease in molecular weight of this magnitude of the surface material would be apparent in bulk molecular weight measurements of the explanted samples. If one assumes that the cracked region has a depth of 4 μm[117,136] and is uniformly distributed over the surface of 5-0 sutures as seen in the Seven Year Dog Study (suture diameter of 0.1 mm), then the bulk PROLENE M_n should drop from 60,000 in the pristine sample to approximately 51,000 (see Figure 28). However, from the bulk molecular measurements made in the Seven Year Dog Study, it is known that the molecular weight of explanted sutures is 61,000 ± 6,000. Since the molecular weight according to Dr. Jordi is below the statistically predicted range of values, it is unlikely that oxidation is the cause of the melting temperature drop. The second issue with his conclusion is that Dr. Jordi did not consider alternative explanations for this decrease. The decrease in melting temperature

[134] Nelson, B. A., King, W. P. "Temperature Calibration of Heated Silicon Atomic Force Microscope Cantilevers." *Sens. Actuators Phys.*, (2007) 140(1):51–59.

[135] Natta, G., Pasquon, I., Zambelli, A., Gatti, G. "Dependence of the Melting Point of Isotactic Polypropylenes on Their Molecular Weight and Degree of Stereospecificity of Different Catalytic Systems." *Makromol. Chem.*, (1964) 70(1):191–205.

[136] 11 – "Crack Depth in Explanted PROLENE Polypropylene Sutures" memo 1982.06.15 (ETH.MESH.12831405-12831406).

could also be caused by tissue or small molecule plasticizers that are preferentially on or adhered to the outside diameter surface of the fiber, but these factors were never explored by Dr. Jordi.

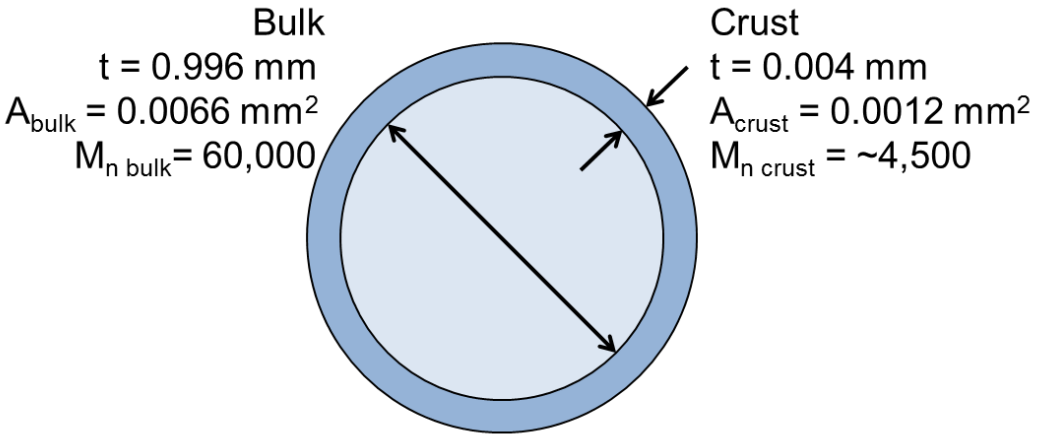

$$M_{n\ total} = \frac{(A_{crust} \times M_{n\ crust}) + (A_{bulk} \times M_{n\ bulk})}{A_{total}}$$

$$M_{n\ total} = \sim 51,000$$

Figure 28. Cross sectional schematic and calculated theoretical total molecular weight (M_n) of excised 5-0 PROLENE sutures from Ethicon's seven year dog study using Dr. Jordi's surface melting temperature to calculate M_n of the crust layer (note: dimensions are not to drawn to scale).

Dr. Jordi reviewed Ethicon's internal documents, including the Seven Year Dog Study, and concluded that PROLENE degrades *in vivo*. While these documents have already been discussed in the body of this report, several statements from Dr. Jordi were found to be in error and will be discussed herein.

In the process of summarizing Ethicon's documents, Dr. Jordi highlighted FTIR data taken by Ethicon, in which Ethicon mentioned the possibility that a weak peak at 1650 cm^{-1} could be attributed to slight oxidation. However, in the very next paragraph of Dr. Jordi's report, he contradicted his observation, stating "[t]he 1650 cm^{-1} and 1540^{-1} cm bands are typically indicative of what are known as the amide-I and amide-II bands respectively of the

polyamides."[137] These bands, as discussed above, in this context, are suggestive of proteins or other biological materials.

Dr. Jordi believed that a "polypropylene mesh placed in the pelvic region of a woman's body will undergo greater degradation than polypropylene placed in the heart of a dog." His basis for this opinion is several articles discussing the bacterial concentrations typically found in this part of the body. In order to make such a statement, Dr. Jordi would need to compare this environment with that of the heart of a dog. He makes no such comparison and his opinion is not based on scientific facts.

Dr. Jordi analyzed the cracked regions of explanted PROLENE mesh devices through SEM imaging to demonstrate that fibers had undergone oxidative degradation. However, Dr. Jordi did not remove the biological material from his samples, which can clearly be seen in Figures 11, 12, and 14 of his report. As such, he did not account for the fact that the cracked surface may in fact be biological in nature. Furthermore, Dr. Jordi did not present data that identifies the composition of the cracked regions (EDS, FTIR, GPC, or nanothermal analysis). Therefore, while visual observations can be made from these images, no definitive conclusions regarding the composition of the cracked material can be drawn.

Dr. Jordi further opined that the antioxidant DLTDP leaches with time, his sole evidence for this presented in his report dated August 17, 2015, is from intensity differences in FTIR measurements conducted by Ethicon. As discussed in detail in the Microcrack Committee Investigation section, an independent analysis of the FTIR spectra would lead to the conclusion that it is impossible to isolate spectral contributions from DLTDP since the carbonyl peak could also be due to proteins. In addition, the FTIR data generated by Ethicon cannot be used to reliably quantify functional group concentrations in a sample material in the absence of a calibration study with corresponding calibration curves. No such calibration study was noted in the reviewed Ethicon documents and no such study was independently performed by Dr. Jordi. Therefore, Dr. Jordi's opinion regarding the in vivo leaching of DLTDP is scientifically baseless and, in turn, unreliable.

[137] Jordi MDL Consolidated Case Report dated 8-24-15, pg 14.

Dr. Jordi maked the unsubstantiated claim that "a vast majority of scientists who have studied polypropylene for degradation have consistently concluded that polypropylene (including PROLENE) undergoes *in vivo* degradation"[138] by failing to cite the documents with which he maked this conclusion.

Dr. Jordi stated in his opinions that *in vivo* degradation causes PROLENE to become brittle. However, he never once discussed the topic of embrittlement in the main text of his report, nor did he perform or cite any mechanical testing to support his opinion, which left it unclear as to how this conclusion is reached. Furthermore, this opinion is completely contradictory to the results of the tensile testing experiments presented in Ethicon's Seven Year Dog Study.

Another of Dr. Jordi's opinions is that somehow, the manufacturing process leaves PROLENE susceptible to environmental stress cracking (ESC). It is unknown on what Dr. Jordi based this statement, since there is no mention of the manufacturing process in the text of his report, and thus this opinion is completely unsupported.

In Dr. Jordi's final opinion, he stated that cholesterols and fatty acids absorbed by the PROLENE mesh leave it susceptible to ESC. His entire basis for this claim is his reference to Clavé's conclusion that "the diffusion of organic molecules into the polymer (especially esterified fatty acids or cholesterol) *may* (emphasis added) be a cause of the polymer structure degradation."[45] Dr. Jordi failed to realize that a polymer suffering from ESC will be embrittled,[139] resulting in a decrease in elongation at break, which directly contradicts the results of Ethicon's Seven Year Dog Study. Additionally Dr. Jordi neglected to perform any original research or literature review on this topic and relies solely on conjecture and hypothesizing to form his opinions and therefore his opinion should not be considered scientifically valid.

[138] Jordi MDL Consolidated Case Report dated 8-24-15, pg 23.

[139] Wright, D. C., Rapra Technology Limited. *Environmental Stress Cracking of Plastics*. Shrewsbury: Rapra Technology, 1996. 3.

Mays

Exponent reviewed the report authored by Dr. Jimmy Mays[140] and disagrees with several of his findings, and opinions. Dr. Mays did not perform any experiments, but relied on the previously discussed works of Liebert, Mary, Costello, Bracco, Clavé, Imel, Iakovlev,[141] and various Ethicon documents.[142]

Dr. Mays discussed the "cracked" layer observed on the exterior of explanted PROLENE fibers in both reference literature and Ethicon-produced documents, and inferred degradation, failing to recognize that cracking and degradation should not be treated as synonymous. In doing so, he ignores the possibility that the cracked layer is composed of something other than oxidized PROLENE.

Dr. Mays repeatedly emphasized the decrease in mechanical properties expected to accompany PROLENE degradation, including stiffening and embrittlement, but failed to perform any mechanical testing, or rely on any published testing of explanted PROLENE material to support his claim. While Dr. Mays acknowledged that plasticization can be caused by "esterified fatty acids," and that Bracco *et al.*[69] confirmed the presence of such molecules on explants, he failed to link *in vivo* plasticization of the mesh with the mechanical properties associated with this well documented and understood polymer phenomenon.[143] In fact, the changes in mechanical properties observed during Ethicon's Seven Year Dog Study (decrease in stiffness, increase in elongation at break, decrease in breaking strength)[144] are consistent with plasticization of the PROLENE suture, and completely contradict Dr. May's theory of degradation.[143]

---

[140] Mays Wave 1 Report dated 1-12-16.

[141] Iakovlev, V. V., Guelcher, S. A., Bendavid, R. Degradation of Polypropylene in Vivo : A Microscopic Analysis of Meshes Explanted from Patients. J. Biomed. Mater. Res. B Appl. Biomater., (2015) 000–000.

[142] EthMesh12831405, EthMesh 15955438-15955473, EthMesh 15958452, EthMesh 15406978, EthMesh 15958470, EthMesh 1595843, EthMesh 15958336, EthMesh 15958445, EthMesh 00000367, EthMesh 12831391-1404, EthMesh 12831407, EthMesh 09888220, EthMesh 05439518, EthMesh 12006257, EthMesh 12009027, EthMesh 00865322.

[143] Wypych, G. *Handbook of Plasticizers*. Burlington: Elsevier Science, 2013.

[144] Ethicon's Seven Year Dog Study (ETH.MESH.11336183) pg.155.

Dr. Mays' claim that PROLENE mesh undergoes a reduction in molecular weight while *in vivo* is not supported by literature or PROLENE testing results. Dr. Mays ignored the two molecular weight studies performed on explanted PROLENE by the Plaintiffs' expert, Dr. Jordi, and by Ethicon in the Seven Year Dog Study (Table 1), both of which directly contradict his claim of *in vivo* molecular weight reduction. Instead, Dr. Mays relied on the previously discussed work by Imel *et al.*[71] on explanted Boston Scientific mesh (not PROLENE). This study is not applicable to the current matter due to likely formulation differences in mesh materials between the two manufacturers.

Priddy

Exponent reviewed the report authored by Dr. Duane Priddy[145] and disagrees with several of his methodologies, findings and opinions. In particular, issues were found in both Dr. Priddy's interpretation of established testing standards, as well as his own research.

Dr. Priddy performed DSC experiments on ten PROLENE exemplar meshes in an attempt to illustrate variability in oxidation resistance between mesh lots. In doing so, he claimed that oxidation induction time (OIT) varied by 150% between the samples, which he attributed to variability in antioxidant concentration. Exponent found several flaws in his methods, analysis, and conclusions. Dr. Priddy claimed that his DSC testing followed the procedure detailed in ASTM D3895,[146] and specifically stated that the testing did "not deviate from the protocol listed in this testing procedure."[147] However, Dr. Priddy's report indicates that there were deviations taken from the protocol, and it is possible that these deviations contributed to the variability in Dr. Priddy's test results, and not necessarily the samples themselves.

The standard recommends preparing samples by melting the material into a solid disk of consistent size and weight prior to testing. Presumably, this is to facilitate uniform thermal and atmospheric conditions to the sample, as well as to provide consistency between samples.

---

[145] Priddy Wave 1 Report.

[146] ASTM D3895-14, Standard Test Method for Oxidative-Induction Time of Polyolefins by Differential Scanning Calorimetry, ASTM International, West Conshohocken, PA, 2014, www.astm.org.

[147] Priddy Wave 1 Report, pg 3.

Instead, Dr. Priddy stated that he placed "a small (~10 milligrams) fiber of the mesh inside a very sensitive instrument called a differential scanning calorimeter (DSC)." This implies that the sample geometry did not meet the ASTM standard recommendation. A deviation from the standard of this nature could lead to variability in OIT. Dr. Priddy's DSC data analysis method also differed from the ASTM standard in ways that may statistically alter the OIT values obtained. The exothermic peaks in his data likely come from two types of thermal events. The large exotherm at the end of each scan can likely be attributed to degradation of polypropylene. The smaller, intermittent peaks are likely the result of antioxidants and other additives present in the PROLENE sample being consumed, as stated in Note 12 of ASTM D3895.[146] Dr. Priddy does not consider this possibility during his analysis, as evidenced by the statement, "[a]s long as the antioxidants are present in the sample protecting the PP against oxidation, no exotherm is detected."[145]

In accordance with ASTM D3895, Dr. Priddy correctly defined OIT as the intersection of the baseline and a line drawn from the steepest linear slope of the exotherm. However, as described in Note 12 of the ASTM standard, when additives are used, the slope of the polypropylene exotherm may not be smooth. This is the case for the majority of Dr. Priddy's reported data (samples 3, 5, 6, 7, 8, 9 and 10). To that end, Note 12 of the ASTM standard recommends resampling and retesting to "ensure that the testing is representative of the oxidation process." Note 13 of the ASTM standard also states that "[i]f multiple slopes result from the oxidation process, OIT needs to be defined to accurately reflect the oxidation of the polymer." None of these recommendations were correctly applied by Dr. Priddy. An illustration of these shortcomings in Dr. Priddy's work can be seen in his analysis of samples 9 and 10. These samples were taken from the same model and lot number, and can be reasonably expected to have a similar additive content. However, the tangent lines used to determine OIT correspond to different features of the curves, meaning that comparison of Dr. Priddy's obtained OIT values will likely lead to false conclusions.

Dr. Priddy also used the value of "Incipient Oxidation Time" or "Incipient Surface Oxidation Temperature" (ISOT) to compare his DSC data. There are several issues with both his determination and use of these values. First, it is unknown what this value physically represents

since it was (1) not referenced, (2) absent in any literature that I have encountered on this topic, (3) not included in the ASTM standard, and (4) similarly defined to OIT according to the ASTM standard. Regarding the last point, the ASTM standard defines OIT as the "onset of the exothermic oxidation of a material." This is remarkably similar to Dr. Priddy's definition of ISOT, "the point at which the surface of the mesh shows evidence of incipient oxidation."

Secondly, even if this value had some meaningful significance, his determination of the value is incorrect. Assuming the material being oxidized at the smaller initial peaks is polypropylene, his determination of that time point is incorrect for his data. As previously discussed, additives included in the sample can result in multiple peaks and slopes in the DSC curve. Dr. Priddy mistakenly assigns these features to the oxidation of polypropylene.

Lastly, even with the assumption that the initial exothermic peaks correspond to the oxidation of polypropylene, Dr. Priddy does not employ a consistent analysis method in his determination of ISOT values. For example, there are exothermic peaks in his curves for samples 4, 5, 6, and 9 at time points earlier than his determined ISOT, while ISOT values obtained for samples 2, 3, 7 and 8 are taken from the first observed peak. The inconsistency of this analytical procedure will likely lead to variable values and unreliable conclusions.

In addition to the issues with Dr. Priddy's DSC data analysis, he made several unfounded conclusions based on that data. These conclusions stem from his misapplication of the purpose and scope of any results obtained following ASTM D3895. The standard explicitly states in multiple instances that "OIT is a qualitative assessment of the level (or degree) of stabilization of the material tested." Additionally, the standard states that no "definitive relationships [have] been established for comparing OIT values on field samples to those on unused products, hence the use of such values for determining life expectancy is uncertain and subjective." A possible reason for this limitation may be because the testing environment (i.e. pure oxygen) is expected to be different from the end-use environmental. Furthermore, accelerated aging tests of

polypropylene do not follow a linear trend[148,149] and cannot be applied in the manner implemented by Dr. Priddy.

In particular, Dr. Priddy attempted to use OIT values obtained using the ASTM standard to predict approximate times to oxidative degradation. In doing so, he made several scientifically invalid statements about the validity of PROLENE as a permanently implantable medical material.

Dr. Priddy attempted to correlate the levels of antioxidant present in exemplar samples with his OIT measurements. He claimed that the variation in antioxidant concentration was "significant and correlated with the variation in the OIT of the same mesh samples." However, contrary to standard practices in the scientific and engineering fields, Dr. Priddy does not present any data related to these experiments,. As such, his statements cannot be critically assessed.

Additionally, Dr. Priddy's extraction method is neither referenced nor experimentally validated, which could explain why he was unable to find DLTDP in any of the samples tested. Another Plaintiffs' expert, Dr. Jordi, was able to identify DLTDP in all of the exemplar and explanted samples tested. Dr. Priddy's dubious extraction technique, combined with the shortcomings of his OIT testing, render any conclusions related to the variability of antioxidant loading levels and the efficiacy of said additives under *in vivo* conditions, scientifically unreliable.

Dr. Priddy supported his opinion regarding the alleged invalidity of PROLENE as a permanently implantable material by claiming that "the antioxidants are themselves degraded over time." His basis for this statement is a study he co-authored, in which various antioxidants are intentionally oxidized using UV-light or *N*-bromo, *N*'-chloro-hydantoin in methylene

[148] Woo, L., Khare, A.R., Sanford, C.L., Ling, M.T.K., and Ding, S.Y., 2001, Relevance of High Temperature Oxidative Stability Testing to Long Term Polymer Durability: *Journal of Thermal Analysis and Calorimetry*, v. 64, no. 2, p. 539–548.

[149] Woo, L., Ling, M., Khare, A.R., and Ding, Y.S., 2001, Polypropylene Degradation and Durability Estimates Based on the Master Curve Concept, *in* Ageing Studies and Lifetime Extension of Materials, Springer US, p. 499–506.

chloride.[150] Neither of these oxidizing media are found *in vivo*, and therefore his statement is unfounded.

In claiming that PROLENE mesh surfaces rapidly degrade and become brittle due to oxidation, Dr. Priddy referenced work published by Leibert, which was discussed earlier in this report.[57] However, Liebert concluded the opposite of what Dr. Priddy stated, "[i]nfrared spectra and mechanical testing of implanted and non-implanted filaments containing an antioxidant show no changes in chemical or physical properties as a result of implantation."

Dr. Priddy's report contained numerous statements that either lack the specificity required to conclude that it applies to PROLENE mesh, were unfounded based on the scientific literature or lack thereof, or both. For example, his opinion that PROLENE cannot withstand decades-long exposure to a hypothetical situation containing four criteria is both generalized and unfounded. He failed to specify both how large the surface area of the mesh needs to be, and how much oxygen content is needed in the medium for degradation to occur. In addition, he failed to provide critical stress levels that PROLENE mesh may experience, while also failing to provide any literature supporting his accusation that this negatively impacts PROLENE's *in vivo* performance.

In his conclusion, Dr. Priddy made the unfounded statement that PROLENE "mesh will rapidly lose its strength as the polymer chains disentangle when the mesh is placed under mechanical stress." Nowhere did he specify the applied *in vivo* stress on the mesh, the failure stress for PROLENE mesh, nor did he cite any instances of failure occurring with any mesh, let alone PROLENE.

Guelcher

Exponent reviewed the report authored by Dr. Scott Guelcher[151,152] and disagrees with several of his opinions. In this report, Dr. Guelcher did not perform any experiments, but instead relied

[150] Bell, B., Beyer, D.E., Maecker, N.L., Papenfus, R.R., and Priddy, D.B., 1994, Permanence of polymer stabilizers in hostile environments: *Journal of Applied Polymer Science*, v. 54, no. 11, p. 1605–1612.
[151] Guelcher Wave 1 Report.

on a small-scale study he previously conducted, and others' studies to form his opinions. In particular, he relies on the works of Liebert, Fayolle,[153] and Oswald.[154]

Dr. Guelcher equated the observed cracked layer covering the exterior of the explanted PROLENE mesh fibers with embrittlement and degradation. In fact, when referencing Ethicon's internal documents he stated, "[t]hese documents report evidence of chronic inflammation, oxidation, and degradation (referred to as micro-cracking in the Ethicon documents) of Prolene sutures,"[155] when in fact, micro-cracking and degradation should not be treated as synonyms. In doing so, he ignored the possibility that the cracked outer layer is something other than oxidized PROLENE without demonstrating any chemical or physical data supporting his accusation of *in vivo* embrittlement.

Dr. Guelcher correctly pointed out that in a study by Fayolle on thermal oxidation of polypropylene films, a reduction in the elongation at break was observed after only 150 hours of aging while an increase in carbonyl and hydroxyl concentration was detected after 250 hours (induction time). It was also shown that the polypropylene films demonstrated reduced molecular weight after approximately 150 hours. These results demonstrate that when polypropylene is subjected to oxidative degradation the polymer's elongation at break and molecular weight should both decrease and be detectable prior to the detection of any increase in carbonyl or hydroxyl groups by FTIR. In contrast, in Ethicon's Seven Year Dog Study, Ethicon's scientists demonstrated that there was no significant difference in molecular weight of PROLENE sutures implanted for seven years compared with controls, and that the sutures demonstrated increases in elongation at break after seven years *in vivo*. These results suggest the PROLENE is undergoing plasticization, not degradation. Dr. Guelcher presented no evidence that conclusively demonstrates that the observed cracking is degraded PROLENE, or that the "degradation" is detrimental to the bulk physical properties of the mesh.

---

[152] Guelcher MDL Consolidated Case Report dated 8-24-15.

[153] Fayolle, B., Audouin, L., Verdu, J. "Oxidation Induced Embrittlement in Polypropylene — a Tensile Testing Study." *Polym. Degrad. Stab.*, (2000) 70(3):333–340.

[154] Oswald, H. J., Turi, E. "The Deterioration of Polypropylene by Oxidative Degradation." *Polym. Eng. Sci.*, (1965) 5(3):152–158.

[155] Guelcher MDL Consolidated Case dated 8-24-15, pg 9.

Dr. Guelcher's example of the degradation of poly(ether urethane)s (PEU) used as pacemaker lead insulation is not relevant to the discussion of alleged PROLENE oxidation *in vivo*. PEU and PROLENE are completely different polymers; PEU is a segmented elastomer and PROLENE is a polyolefin. Their chemical composition, polarity, polymerization chemistry, mechanical properties and likely their antioxidant packages are all dissimilar. Hence, there is no reason to believe they would behave similarly or encounter the same failure mechanism *in vivo*. This is supported by Dr. Guelcher's own results. As mentioned previously, Dr. Guelcher attempted to simulate oxidative degradation of PROLENE using an H_2O_2 solution enriched with $CoCl_2$; however, the resulting morphology of the fiber looked nothing like PROLENE mesh explants, further emphasizing the fact that conclusions cannot be extrapolated from PEU to PROLENE.

Likewise, Dr. Guelcher included a reproduced plot from an article written by Oswald, of the intrinsic viscosity of *unstabilized* polypropylene at room temperature. The viscosity remains constant until approximately 500 days, where it starts to drop off. This plot is not relevant to PROLENE mesh because as mentioned previously, PROLENE has two different antioxidants (Santonox R and dilauralthiodipropionate) added to prevent this type of degradation behavior.

Dr. Guelcher opined that "the presence of antioxidants does not permanently protect the TVT mesh against degradation, and thus it is not possible to guarantee that it will perform its intended function after implantation,"[156] yet he failed to produce or cite any literature or testing that supports his opinion that the overall intended "function" of the mesh has been compromised or that it is suffering from a depletion of antioxidants. This statement ignored Dr. Jordi's finding in his expert report on the Bellew v. Ethicon matter that antioxidants remain in explanted PROLENE mesh even after storage in formalin, which was shown to extract Santonox R from PROLENE.[157]

Dr. Guelcher went on to claim that the "effects of oxidation on the stability of PROLENE were known to Ethicon prior to launching TVT, but the company did not consider the risks associated

[156] Guelcher MDL Consolidated Case Report dated 8-24-15, pg 8.

[157] Jordi Bellew Report dated 7-7-14, pg 73-74.

with polypropylene oxidation on the stability of the TVT mesh." This statement completely ignored the years of research conducted at Ethicon into the safety and efficacy of PROLENE. In fact, the development of the TVT device leveraged work on the raw material, PROLENE resin, which began as early as the mid-1960s. Ethicon was very active in "considering" the risks involved in this device and after consideration of these risks Ethicon (and the FDA) determined it was sufficiently safe and effective to market.

Finally, Dr. Guelcher stated that Costello[50,158] reported polypropylene mesh oxidation and embrittlement; the conclusions were drawn by comparing pristine and explanted meshes via molecular weight, SEM imaging and compliance testing. This is simply incorrect; Costello never reported the molecular weight of either pristine material or explanted material in either of the two articles cited by Dr. Guelcher. As discussed previously, Costello's pseudo-compliance testing methodology is flawed and contradicts Ethicon's testing results in the Seven Year Dog study. Furthermore, while the SEM images presented by Costello show the presence of transverse cracking, no work was done to identify the elemental composition of the layer, thereby not confirming the cracked surface is indeed oxidatively degraded PROLENE instead of remnant biological material.

Klinge

Exponent reviewed the report authored by Dr. Uwe Klinge[159,160,161] and disagrees with several of his opinions. In this report, Dr. Klinge did not perform any experiments to support his claims of *in vivo* degradation of PROLENE, but instead relied on others' studies to form his opinions. In particular, he relies on the works of Liebert, Costello, Cozad, and Clavé as well as Ethicon's Seven Year Dog Study, all of which have been previously discussed in detail.

[158] Costello, C. R., Bachman, S. L., Grant, S. A., Cleveland, D. S., et al. "Characterization of Heavyweight and Lightweight Polypropylene Prosthetic Mesh Explants From a Single Patient." *Surg. Innov.*, (2007) 14(3):168–176.

[159] Klinge Wave 1 POP Report dated 11-17-15.

[160] Klinge Wave 1 SUI Report dated 11-16-15.

[161] Klinge ETH MDL Consolidated Case Report dated 8-24-15.

Dr. Klinge opined that antioxidants, DLTDP and Santonox R, leach from PROLENE with time *in vivo*, but failed to perform his own experiments and instead relied on a study presented in an expert report authored by Dr. Jordi in 2013.[162] In this study, Dr. Jordi used liquid chromatography-mass spectrometry (LC-MS) to attempt to show that antioxidants can leach from PROLENE. LC-MS is an experimental technique that, when correctly employed, can be utilized to determine the concentration of various extractable components in a polymer. Dr. Jordi performed this analysis on explants as well as on various control samples in an attempt to determine the concentrations of DLTDP and Santonox R in each specimen. In this study, during sample preparation, Dr. Jordi attempted to mechanically remove attached biological material using forceps, however, complete tissue removal was never confirmed prior to his LC-MS analysis. Dr. Jordi then maked *quantitative* conclusions on the amount of antioxidants in the explanted mesh based on the original mass of the specimen. Without verifying that the measured mass is solely from the mesh and not in part from residual biologic material, any conclusions regarding the levels of antioxidants DLTDP and Santonox R present are erroneous. Furthermore, Dr. Jordi's control experiments leave much to be desired. His formalin treated mesh controls were only exposed for a fraction of the length of time the explants were exposed to formalin. As a result, this control is invalid and it is impossible to eliminate the possibility that Santonox R and DLTDP were drawn out of the explants during their extended storage in formalin. In fact, Dr. Jordi showed in his analysis that Santonox R is easily extracted from PROLENE after exposure to formalin for only 48 hours at 60°C. Therefore, any conclusions relating to the concentration of antioxidants in explanted mesh while *in vivo* based on Dr. Jordi's LCMS data are unfounded.

[162] Jordi Lewis Report dated 10-12-13.

Conclusion and Opinions

Based on my analysis, as well as my education, training, and experience in mechanics of materials, polymer science, materials chemistry, and mechanical engineering, I have formed the following opinions to a reasonable degree of engineering and scientific certainty. If additional information becomes available, I reserve the right to supplement or amend any or all of these opinions.

- Based on the tensile testing performed by Ethicon during its Seven Year Dog Study, it has been conclusively determined that the PROLENE material becomes more ductile, tougher, and less stiff while implanted.

- Based on the molecular weight analyses performed by Ethicon during the seven year dog study, the PROLENE material is not suffering from any quantifiable degradation while *in vivo*.

- Based on its historical use, long-term testing performed by Ethicon, and retention of bulk physical properties while *in vivo*, PROLENE is a suitable material for implanted mesh devices.

- No reliable scientific evidence has been presented to decisively determine that the "bark layer" is comprised of PROLENE. H&E staining, polarized light microscopy, and melting point analysis are not accepted methods used in the conclusive chemical identification of polypropylene-based materials.

- Plaintiffs' experts' assertion that the PROLENE mesh material has degraded *in vivo* is based solely on an observed reduction in melting point as well as visual and microscopic observations of "bark micro-cracking," which is contrary to scientific principles.

- Plaintiffs' experts' assertion that the PROLENE mesh material has become brittle is also solely based on visual and microscopic observations of "bark micro-cracking," not on mechanical testing, and is contrary to the scientific findings from Ethicon's Seven Year Dog Study.

- Plaintiffs' experts' assertion that PROLENE becomes stiffer (less pliable) and resists tissue contraction causing inflammation/pain is based on observed "bark micro-cracking" and tactile feel (a highly subjective assessment). No standardized mechanical testing has been performed to support this subjective assertion. This assertion is contradicted by the mechanical property testing performed by Ethicon, and the fundamental principles of mechanics of materials.

- The images presented in the Plaintiffs' expert report[163] of "freshly excised" cracked PROLENE mesh that has reportedly never been exposed to formalin need to be tempered with Ethicon's findings that exposure to air alone can cause a saline-preserved "wet" explanted fiber to crack in a relatively short period of time. Moreover, the possibility cannot be excluded that mechanical forces applied to the mesh during explantation did not contribute, and/or cause the observed cracking.

- There has been no testing performed or scientific literature cited to support the belief that degraded PROLENE is capable of being histologically stained with H&E stain. Therefore, any related conclusions, are scientifically unreliable.

- Dr. Iakovlev has not used any reliable scientific methods to conclusively determine that an outer oxidized PROLENE layer stains when exposed to H&E. Dr. Iakovlev's assertion that the PROLENE mesh material has degraded *in vivo* is based solely on visual and microscopic observations of "bark" microcracking. He has conducted no quantitative experiments to confirm his visually based allegation that the mesh material is degraded or oxidized.

[163] Iakovlev MDL Consolidated Case Report dated 8-24-15, pg 83-84.

- Dr. Iakovlev has not performed any control experiments nor cited any scientific studies that support his belief that degraded PROLENE is capable of being histologically stained with H&E stains, and for these reasons, his conclusions are flawed and suspect.

- Through a series of controlled oxidation, microtoming, and microscopy experiments, Exponent demonstrated that oxidized PROLENE mesh fibers and sutures do not become stained with H&E dyes. This fact is supported by polymer science first principles, given that PROLENE does not possess chemical groups amenable to binding with the H&E stain molecules.

- Artifacts can be easily introduced during sample preparation, sectioning, staining, and imaging, giving the appearance of darkened outer layers.

- A brittle outer layer will not contribute to the stiffness of the mesh if it is thin, cracked, and discontinuous. Dr. Iakovlev's opinion that a thin, cracked, porous outer layer causes an increase in mesh stiffness is not consistent with first principles of polymer science and contradicted by the measured modulus data from Ethicon's seven year dog study.

If you have any questions or require additional information, please do not hesitate to contact me.

Steven MacLean, Ph.D., P.E.
Principal Engineer

Appendix H

Experimental Reproducibility Validation

To confirm the reliability of the original microscopy experiments outlined in this report, this work was repeated and expanded by examining pristine (i.e., out-of-the-box, never implanted in the body), serum-coated, and purposefully oxidized PROLENE mesh and suture products which were processed and subjected to histological dyes (Hematoxylin & Eosin) in accordance with Dr. Iakovlev's protocols which were outlined in a trial exhibit during the *Bellew v Ethicon* matter.[164] In an effort to demonstrate that the original microscopy findings were not limited to PROLENE TVT mesh, additional PROLENE devices were evaluated. Those additional devices included:

- Ethicon PROLENE GYNECARE TVT™ Trans-Vaginal Tape Mesh Devices from two different lots
- Ethicon PHSE PROLENE Hernia System Extended Mesh Device
- Ethicon PROLENE 6-0 Blue Monofilament Suture

Rabbit tissue was included as a positive control for histological staining and polypropylene pellets that do not contain the same additive package (e.g., antioxidants, processing aids, or lubricants) as PROLENE in our analysis.

The above PROLENE devices and polypropylene pellets were subjected to the following preconditioning treatments prior to treating them with Dr. Iakovlev's staining protocol:

1. Photo-oxidation treatment by UV light[165]
2. Chemical oxidation solution treatment that reportedly degrades polypropylene[166]

[164] None of Dr. Iakovlev's expert reports related to Ethicon mesh products describe or detail the microtoming, embedding or staining protocols used on any of his stained specimens.

[165] QUV conditions employed here are the same UV conditions used in my microscopy report dated September 10, 2015.

[166] Guelcher, S. A., & Dunn, R. F. (2015, June). Oxidative degradation of polypropylene pelvic mesh in vitro. International. Urogynecology Journal. 26 (Suppl 1): S55–S56.

3. Fetal bovine serum treatment as a protein-rich matrix

Pristine mesh was also included as a control. Preconditioning treatments are described in greater detail in later sections of this study. It is important to note that none of the materials included and examined here have been implanted in the body.

Sample Preparation Prior to Sectioning

Exemplar PROLENE Samples

Pristine PROLENE TVT mesh (Ethicon TVT Devices—Ref. No. 810041B, two devices from Lot Number 3859228 and one device from Lot Number 3832826), PHSE hernia mesh (Lot No. 27770-20), 6-0 suture, and polypropylene resin pellets were received and kept in their original packaging until use. A clean razor blade was used to cut ~ 1 cm long sections of each sample for laboratory analysis (Table AH.4). Polypropylene pellets (Sigma-Aldrich, isotactic, average M_w ~340,000, average M_n~ 97,000) were used as received.

Chemically Oxidized PROLENE Samples

Sections of PROLENE TVT meshes, PHSE hernia mesh, 6-0 suture, and polypropylene resin pellets were oxidized according to the protocol published by Guelcher and Dunn (Exponent protocol "Chemical Oxidation Protocol per Guelcher," 1504469.000-5191).[167] Samples were incubated at 37°C for 5 weeks in oxidative media composed of 0.1 M $CoCl_2$ in 20 wt% H_2O_2. This solution purportedly simulates the oxidative environment created by macrophages in response to a foreign object.[168] The oxidative solution was changed every two to three days. Prior to processing, the samples were rinsed copiously in deionized water, then immersed in an ultrasonic bath (Exponent protocol "Rinsing Samples After Chemical Oxidation," 1504469.000-7542). Samples were subsequently air-dried and the visual and microscopic appearance was assessed using optical microscopy and scanning electron microscopy (SEM).

[167] Ibid.

[168] Ibid.

QUV-Oxidized PROLENE Samples

Sections of PROLENE TVT meshes, PHSE hernia mesh, and 6-0 sutures were placed inside a Q-Lab QUV Accelerated Weathering Tester and irradiated with 0.98 ($\frac{W}{m^2}$) UV light at 60°C (Exponent protocol "QUV Oxidation Protocol for PROLENE," 1504469.000-4837). Samples were imaged by SEM periodically and QUV exposure was stopped after extensive cracking was observed over the entire UV-exposed surface of the samples (5–12 days). Prior to being sent to a third-party lab for histological processing, the visual and microscopic appearance was assessed using SEM and optical microscopy.

Fetal Bovine Serum (FBS) Coated PROLENE Samples

Sections of PROLENE TVT meshes, PHSE hernia mesh, 6-0 sutures, and polypropylene resin pellets were incubated in solutions of fetal bovine serum (FBS) at 37°C for six days (Exponent protocol "Serum Coated PROLENE Protocol," 1504469.000-1151). After six days, the samples were removed from the serum, air-dried, assessed with optical microscopy and SEM, and immersed in a 10% formalin buffer solution for storage. Prior to being sent to a third-party lab for histological processing, samples were removed from formalin, air-dried, and then visually and microscopically inspected using optical microscopy and SEM.

Table AH.4. PROLENE Samples for Sectioning

	QUV Oxidized (Paraffin)[169]	QUV Oxidized (Resin)	Chemically Treated (Paraffin)	Chemically Treated (Resin)	Serum-coated (Paraffin)	Serum-coated (Resin)	Pristine (Out-of-the-box) Control (Paraffin)	Pristine (Out-of-the-box) Control (Resin)
PROLENE TVT mesh Lot 3859228 #1	ID: 157162 TVT Device Lot 3859228 #1 QUV-P	ID: 157163 TVT Device Lot 3859228 #1 QUV-R	ID: 157164 TVT Device Lot 3859228 #1 ChemOx-P	ID: 157165 TVT Device Lot 3859228 #1 ChemOx-R	ID: 157166 TVT Device Lot 3859228 #1 Serum-P	ID: 157167 TVT Device Lot 3859228 # 1 Serum-R	ID: 157880 TVT Device Lot 3859228 #1 Control-P	ID: 157169 TVT Device Lot 3859228 #1 Control-R
PROLENE TVT mesh Lot 3859228 #2	ID: 157170 TVT Device Lot 3859228 #2 QUV-P	ID: 157171 TVT Device Lot 3859228 #2 QUV-R	ID: 157172 TVT Device Lot 3859228 #2 ChemOx-P	ID: 157173 TVT Device Lot 3859228 #2 ChemOx-R	ID: 157174 TVT Device Lot 3859228 #2 Serum-P	ID: 157175 TVT Device Lot 3859228 #2 Serum-R	ID: 157884 TVT Device Lot 3859228 #2 Control-P	ID: 157177 TVT Device Lot 3859228 #2 Control-R
PROLENE TVT mesh Lot 3832826	ID: 157178 TVT Device Lot 3832826 QUV-P	ID: 157179 TVT Device Lot 3832826 QUV-R	ID: 157180 TVT Device Lot 3832826 ChemOx-P	ID: 157181 TVT Device Lot 3832826 ChemOx-R	ID: 157182 TVT Device Lot 3832826 Serum-P	ID: 157183 TVT Device Lot 3832826 Serum-R	ID: 157895 TVT Device Lot 3832826 Control-P	ID: 157185 TVT Device Lot 3832826 Control-R
PROLENE hernia mesh	ID: 157186 Hernia Mesh Lot 27770-20 QUV-P	ID: 157187 Hernia Mesh Lot 27770-20 QUV-R	ID: 157188 Hernia Mesh Lot 27770-20 ChemOx-P	ID: 157189 Hernia Mesh Lot 27770-20 ChemOx-R	ID: 157190 Hernia Mesh Lot 27770-20 Serum-P	ID: 157191 Hernia Mesh Lot 27770-20 Serum-R	ID: 157899 Hernia Mesh Lot 27770-20 Control-P	ID: 157193 Hernia Mesh Lot 27770-20 Control-R
PROLENE 6-0 suture	ID: 157194 PROLENE 6-0 Suture QUV-P	ID: 157195 PROLENE 6-0 Suture QUV-R	ID: 159703 PROLENE 6-0 Suture ChemOx-P	ID: 159704 PROLENE 6-0 Suture ChemOx-R	ID: 157198 PROLENE 6-0 Suture Serum-P	ID: 157199 PROLENE 6-0 Suture Serum-R	ID: 157903 PROLENE 6-0 Suture Control-P	ID: 157201 PROLENE 6-0 Suture Control-R
Polypropylene Pellet	--	--	ID: 157232 Polypropylene pellet Sample #1	ID: 157233 Polypropylene pellet Sample #2	ID: 157234 Polypropylene pellet Sample #3	ID: 157235 Polypropylene pellet Sample #4	ID: 157236 Polypropylene pellet Sample #5	ID: 157237 Polypropylene pellet Sample #6

[169] The embedding material is listed parenthetically.

Histology Sample Preparation

Exemplar, oxidized, and serum-coated mesh samples were embedded in both paraffin and resin (Technovit 7200), sectioned, and stained with H&E. All processing was performed by an independent GLP-compliant[170] histology lab with more than 25 years of experience in histological processing of samples. Detailed embedding and staining protocols can be found at the end of this study.

Paraffin-embedded samples were prepared by following the protocol submitted by Dr. Iakovlev. Samples were sequentially dehydrated in reagent alcohol and xylene substitute using an automated tissue processor, and then embedded in Leica EM400 paraffin wax. Sections of the paraffin blocks (4–6 µm thick) were obtained using a microtome, briefly floated in a 40–45^{o}C water bath, and mounted onto slides. Sections were air-dried for 30 minutes, and then baked in a 45–50^{o}C oven overnight.

Resin-embedded samples were sequentially dehydrated in reagent alcohol using an automated tissue processor and embedded in Technovit 7200. The polymerized resin block was trimmed. Then sections were cut and ground to a thickness of 10–61µm with a mean thickness of approximately 30 µm.

Paraffin and resin-embedded samples were subjected to staining with H&E. All slides were imaged by Exponent personnel using a microscope equipped with polarizing filters.

[170] Per 21 CFR Part 58 – Good Laboratory Practice for Nonclinical Laboratory Studies.

Results

Scanning Electron Microscopy of PROLENE and Polypropylene Samples

All samples listed in Table AH.4 were imaged with SEM prior to histological processing and microscopy evaluation (Figure AH.1). To observe surface features clearly, images of mesh samples were obtained at 100× magnification. Representative images of 6-0 suture samples were obtained at 200× magnification (Figure AH.2).

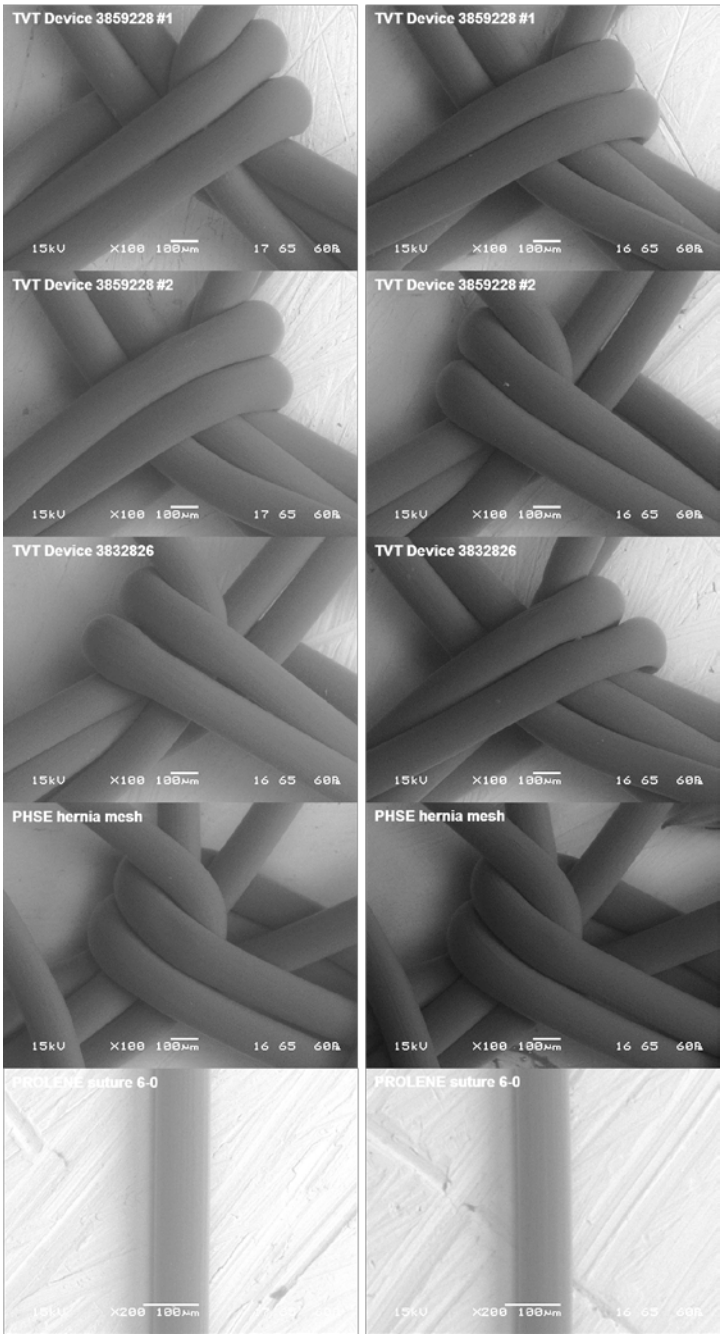

Figure AH.1. SEM images of pristine untreated samples. Left column: samples intended for paraffin mounting, sectioning, and staining as part of following Dr. Iakovlev's protocol. Right column: samples intended for resin mounting, sectioning, and staining.[171]

[171] The images were brightened during post-processing to enhance contrast.

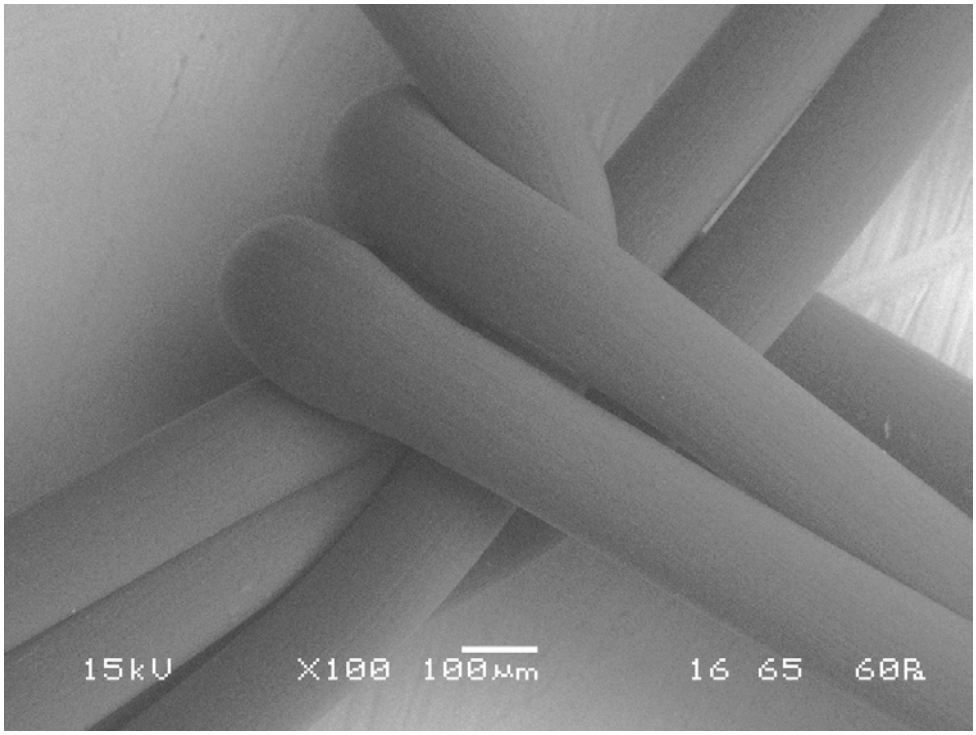

Figure AH.2. SEM image of a representative pristine TVT mesh sample prior to being subjected to Dr. Iakovlev's histological processing protocol.[172]

As expected, the sample surfaces of pristine untreated PROLENE TVT devices, PHSE hernia mesh, and 6-0 suture appeared smooth and uniform, with no apparent defects or cracking. The surface of the polypropylene pellet, as imaged by SEM, was similarly smooth and uniform, with no apparent defects (Figure AH.9a).

The surfaces of chemically oxidized samples were similarly smooth and uncracked (Figure AH.3). However, several crystals, likely inorganic cobalt-based, were observed to be well-adhered to the surface of the PROLENE samples after exposure to the chemical treatment protocol as shown in Figure AH.4.

[172] Ibid.

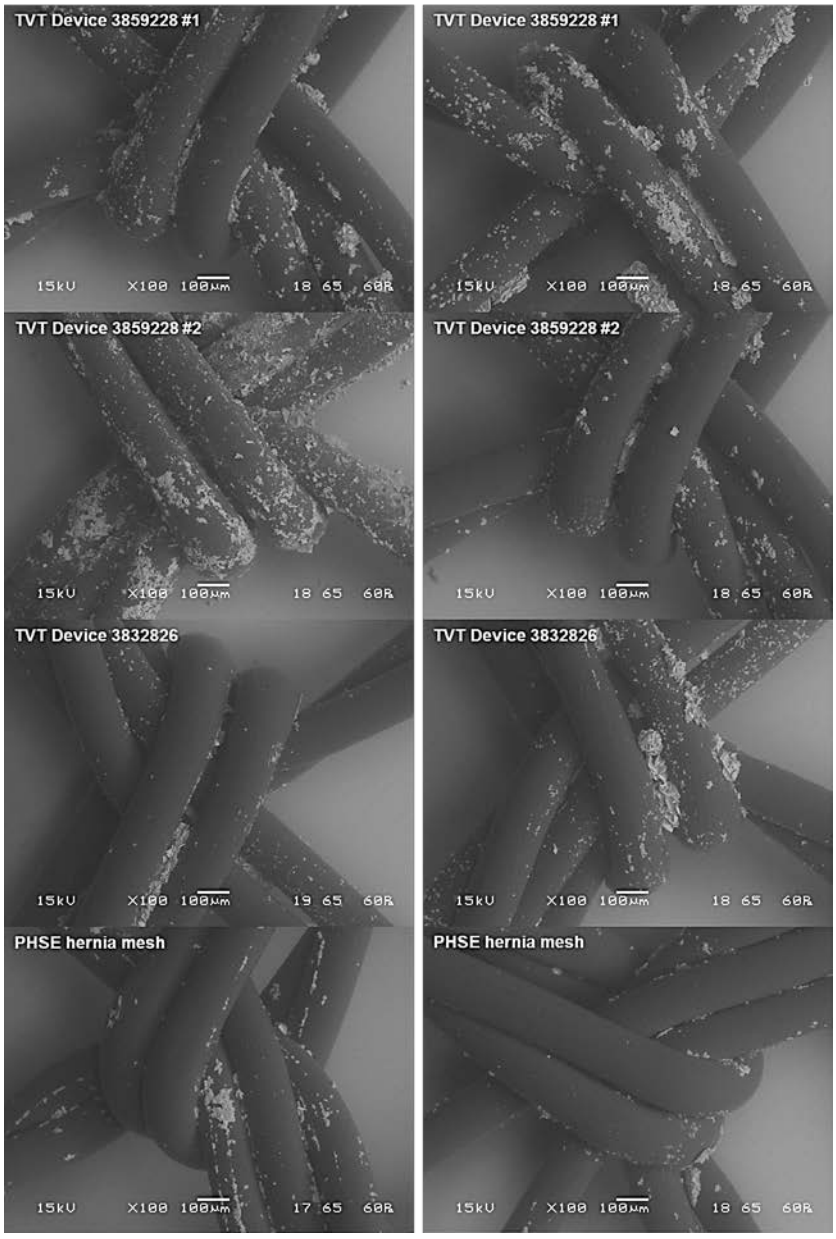

Figure AH.3. SEM images of chemically treated samples. Left column: samples intended for paraffin mounting, sectioning, and staining per Dr. Iakovlev's protocol. Right column: samples intended for resin mounting followed by staining with H&E.

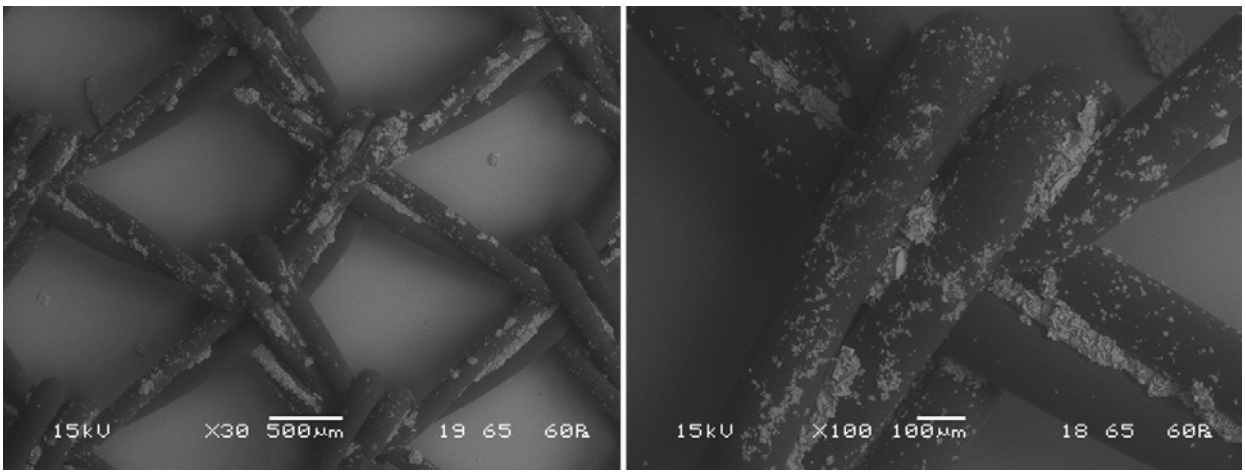

Figure AH.4. SEM images of an area of a TVT device after exposure to chemical treatment.

These observations differ from the results published by Guelcher and Dunn, who reported "pitting" and "flaking" in polypropylene meshes subjected to the same treatment conditions.[14] The light-colored crystallite material not removed during the rinsing procedure (Exponent protocol "Rinsing Samples After Chemical Oxidation," 1504469.000-7542) and observed on the surface of the samples is consistent with cobalt-based crystallite deposits according to energy dispersive X-ray spectroscopy (EDS) analysis. EDS was performed on two areas of a representative mesh sample (TVT Device 3859228 #1) after chemical oxidation treatment. EDS measurements revealed that the PROLENE surface was composed predominantly of carbon, and that the light-colored crystals were predominantly composed of cobalt (Figure AH.5).

In contrast to the pristine (untreated control) and chemically treated samples, QUV-oxidized samples exhibited extensive cracking covering most of the mesh and suture surfaces. A representative image illustrating the extensive cracking observed over most of the surface is shown in Figure AH.6. Longitudinal cracks with length scales of several hundreds of microns were observed traversing the length of the mesh fibers. Accompanying radial cracks, with length scales on the order of 100 microns or less, were observed perpendicularly to the longitudinal cracks. The extent of cracking was uniform across the five different PROLENE devices examined (Figure AH.7).

Prior to embedding, cross-sectioning, and staining per Dr. Iakovlev's protocol, the serum-coated samples were also imaged with SEM. The proteinaceous coating deposited on the surface of PROLENE mesh samples treated with FBS can be seen clearly with SEM (Figure AH.8). The coating had a sheet-like appearance concentrated predominantly in the areas between the mesh fibers. However, the PROLENE surfaces themselves were uncracked and smooth, and similar to pristine untreated samples. A thin layer of the proteinaceous coating was also observed on the surface of 6-0 suture samples and polypropylene pellet samples (Figure AH.9c and Figure AH.10c).

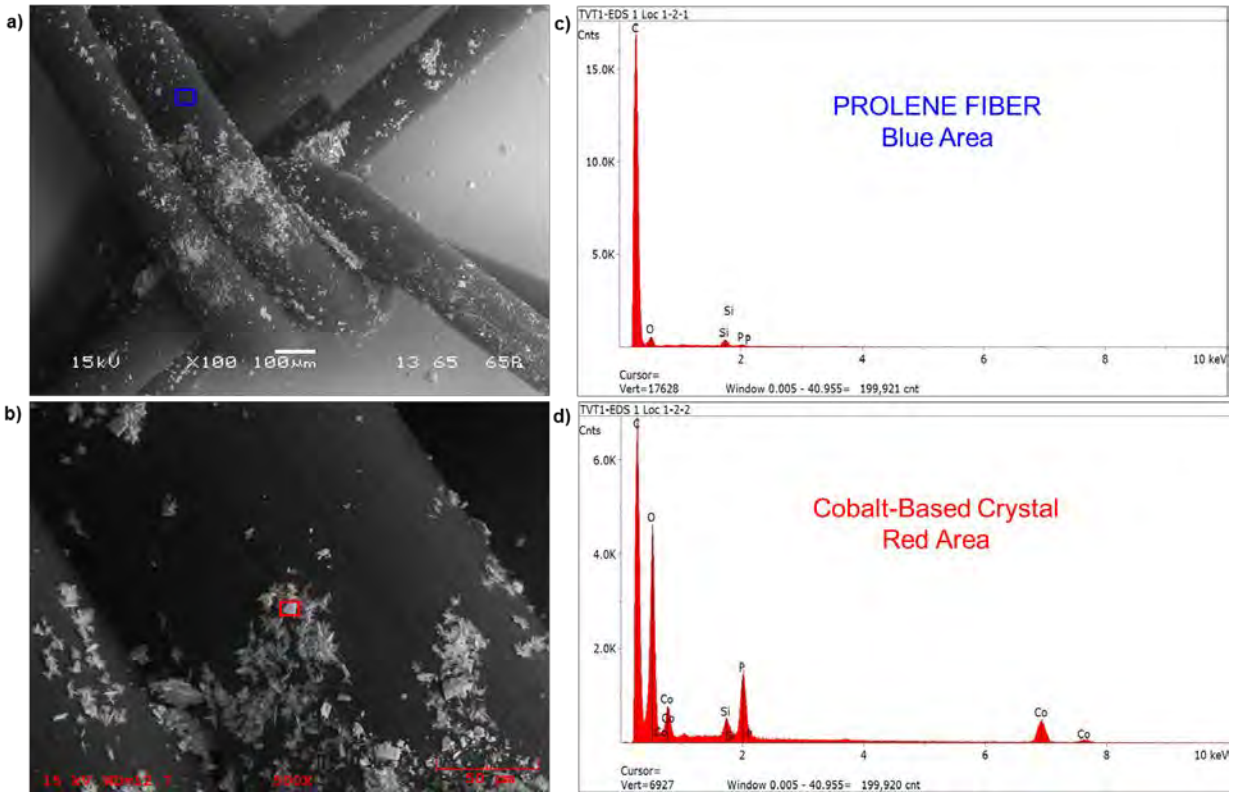

Figure AH.5. SEM images with corresponding EDS analysis areas performed on TVT Device 3859228 #1 after chemical treatment.[173,174,175] (a) SEM image of mesh, (b) 500×

[173] Guelcher, S. A., & Dunn, R. F. (2015 June). Oxidative degradation of polypropylene pelvic mesh in vitro. International Urogynecology Journal 26 (Suppl 1): S55-S56.

[174] Exponent protocol "Chemical Oxidation Protocol per Guelcher," 1504469.000-5191.

[175] Exponent protocol "Rinsing Samples After Chemical Oxidation," 1504469.000-7542.

magnification of mesh fiber, (c) EDS elemental profile of mesh fiber surface, (d) EDS elemental profile of light-colored crystals.

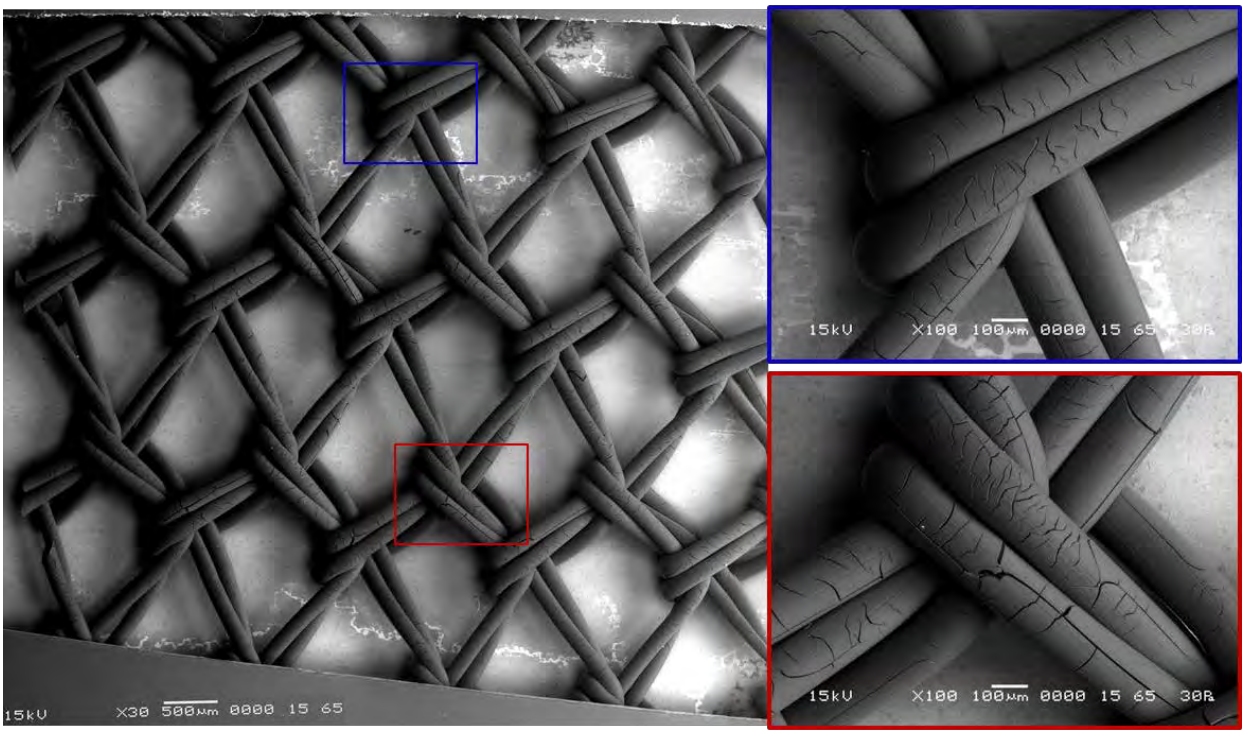

Figure AH.6. SEM images of QUV-oxidized TVT Device 3859228 #1 resin sample. Left: representative overall image at 30× magnification. Right: representative images at 100× magnification.

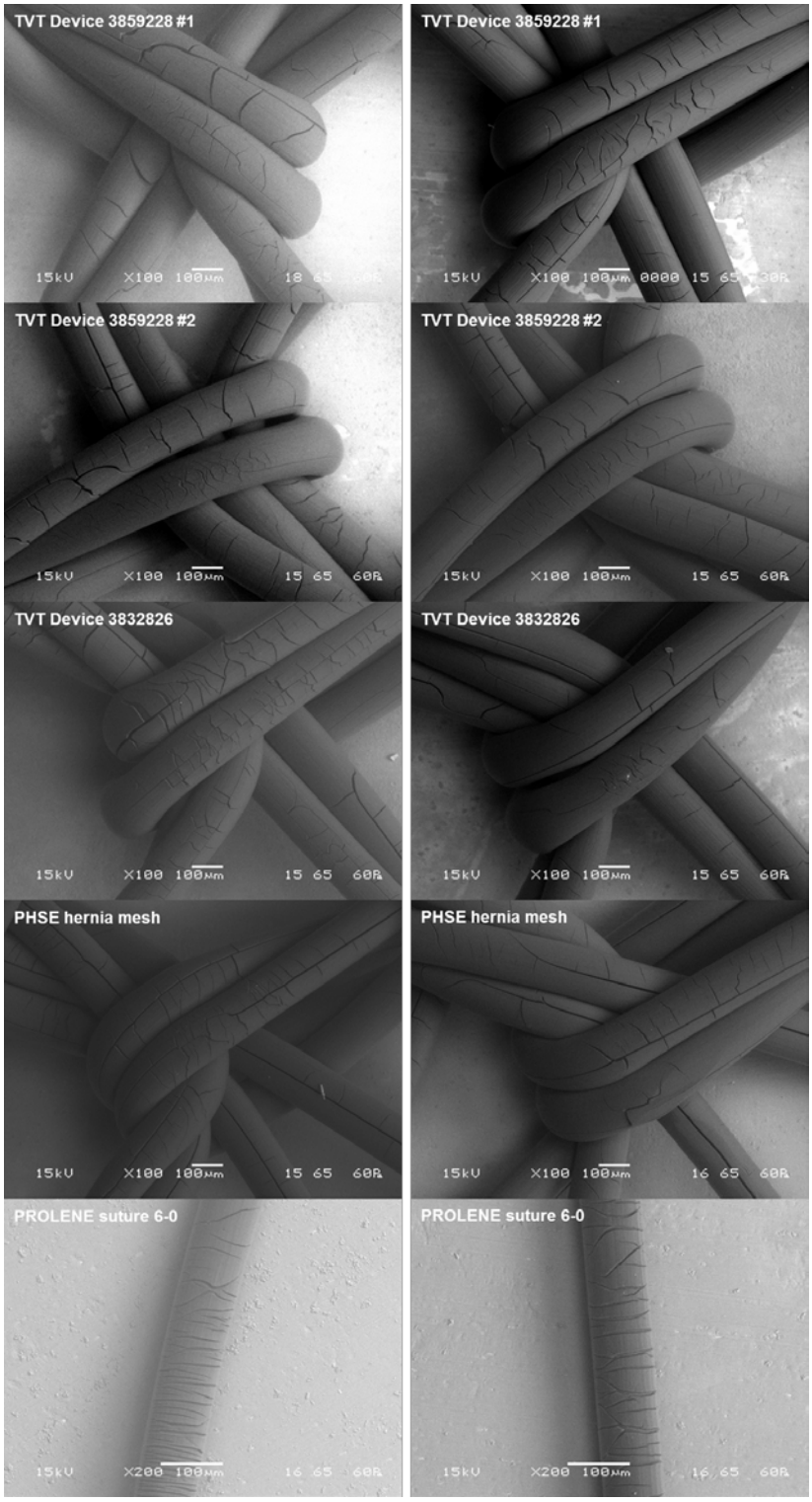

Figure AH.7. SEM images of representative areas of QUV-oxidized samples. Left column: samples intended for paraffin mounting, sectioning, and staining according to Dr.

Iakovlev's protocol. Right column: samples intended for resin mounting. Longitudinal and radial cracks are observed over the entire surface.

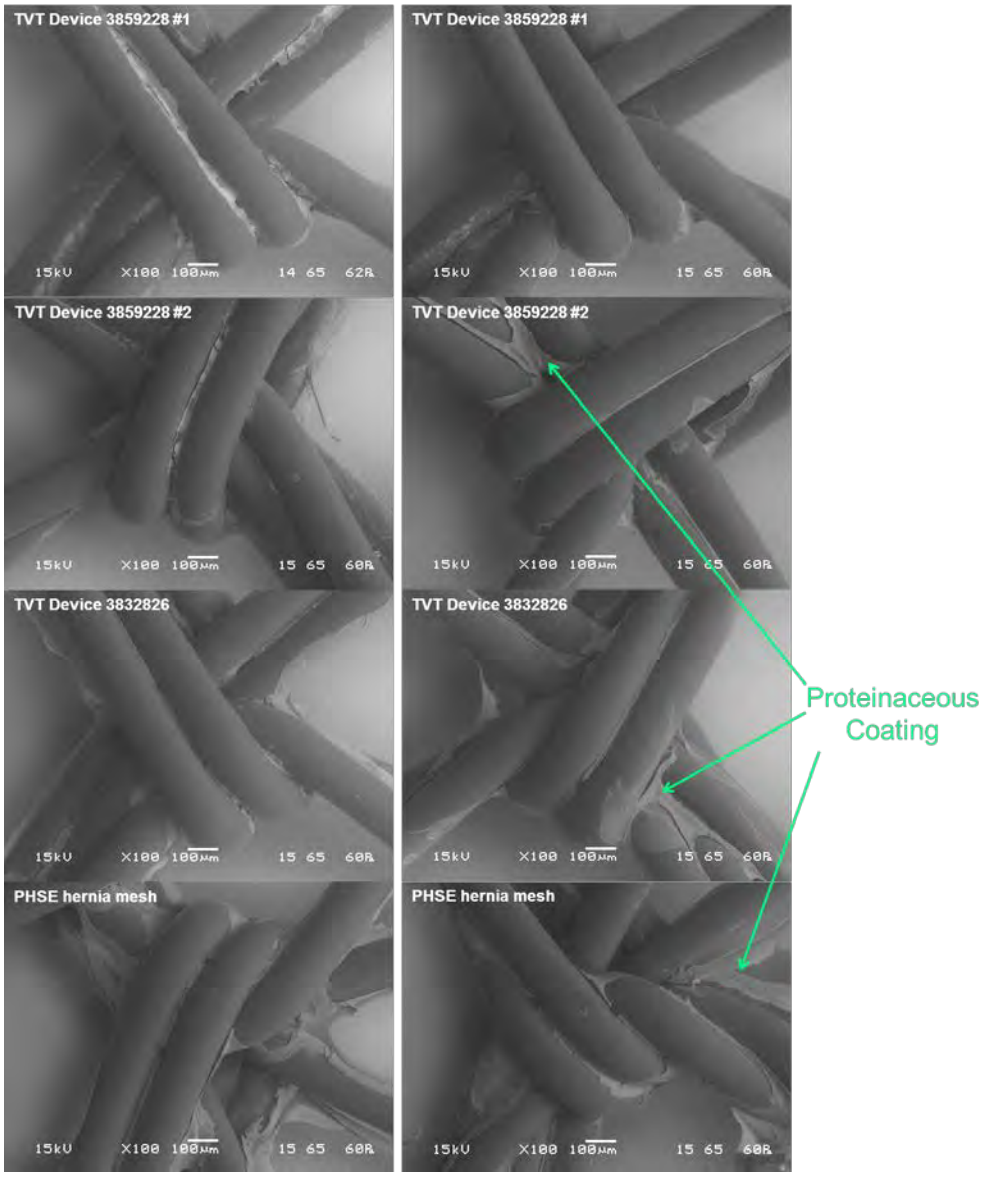

Figure AH.8. SEM images of serum-coated samples. Left column: samples intended for paraffin mounting, cross-sectioning, and staining according to Dr. Iakovlev's protocol. Right column: samples intended for resin embedding. Green arrows indicate examples of proteinaceous coating and cracks within the coating.[176]

[176] The images were brightened during post-processing to enhance contrast.

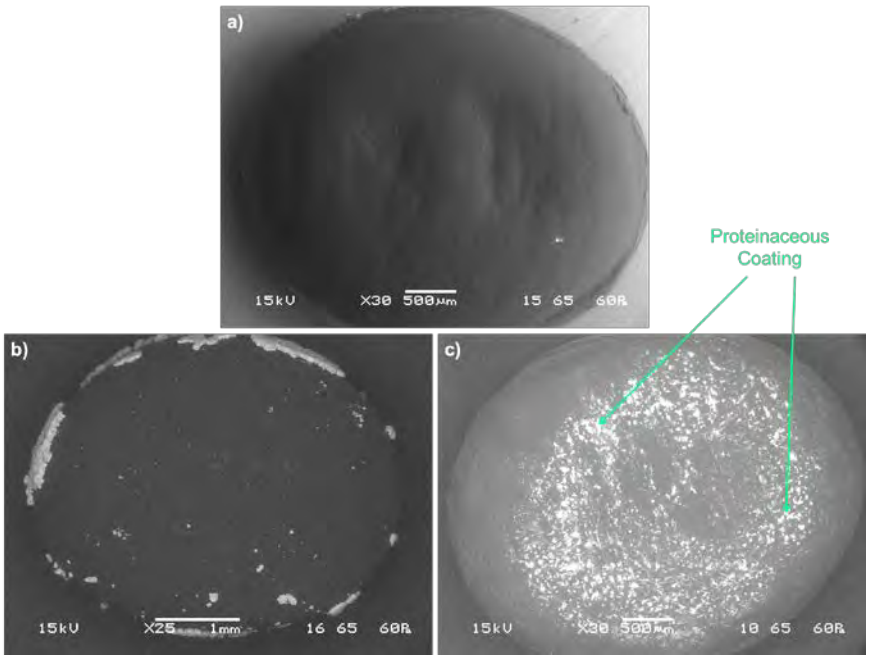

Figure AH.9. SEM images of polypropylene pellets intended for paraffin mounting. (a) Pristine sample, (b) chemically oxidized sample, and (c) serum-coated sample.[177]

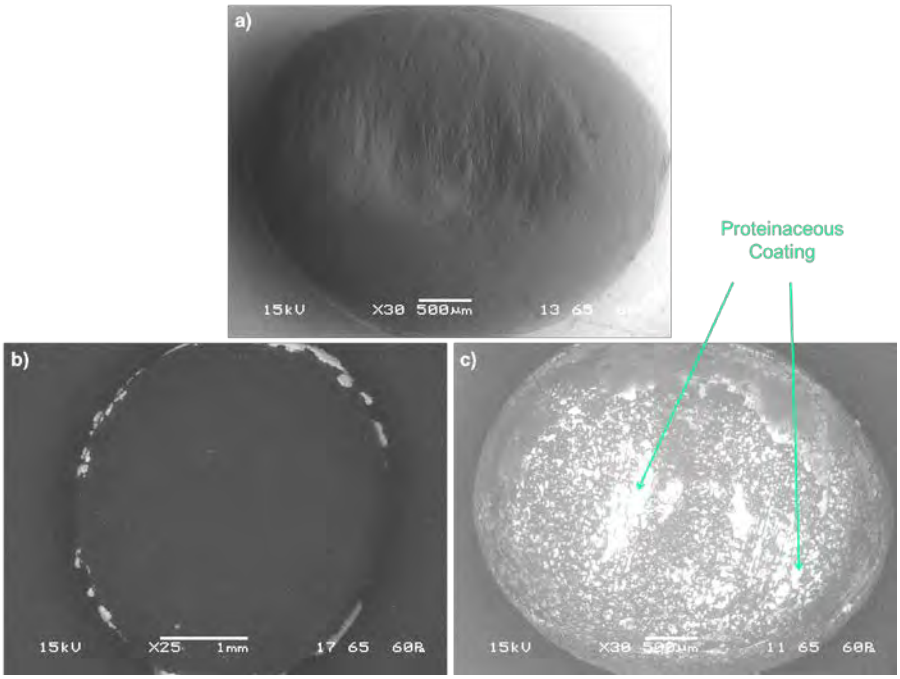

[177] The images were brightened during post-processing to enhance contrast.

Figure AH.10. SEM images of polypropylene pellets intended for resin mounting. (a) Pristine sample, (b) chemically oxidized sample, and (c) serum-coated sample. Samples intended in for resin mounting.

Fourier Transform Infrared Spectroscopy (FTIR) Analysis of Intentionally Oxidized Samples

Small segments of the chemically treated and UV-oxidized samples listed in Table AH.4 were analyzed by Fourier transform infrared spectroscopy (FTIR) to potentially identify functional groups consistent with oxidation. FTIR spectra were acquired on a pristine PROLENE sample for comparison. In the UV-treated and chemically treated samples, we observed bands consistent with hydroxyl (OH) bands and carbonyl (C=O) bands that can be indicative of oxidation. These bands were not observed in the pristine samples. Representative spectra are shown in Figure AH.11.

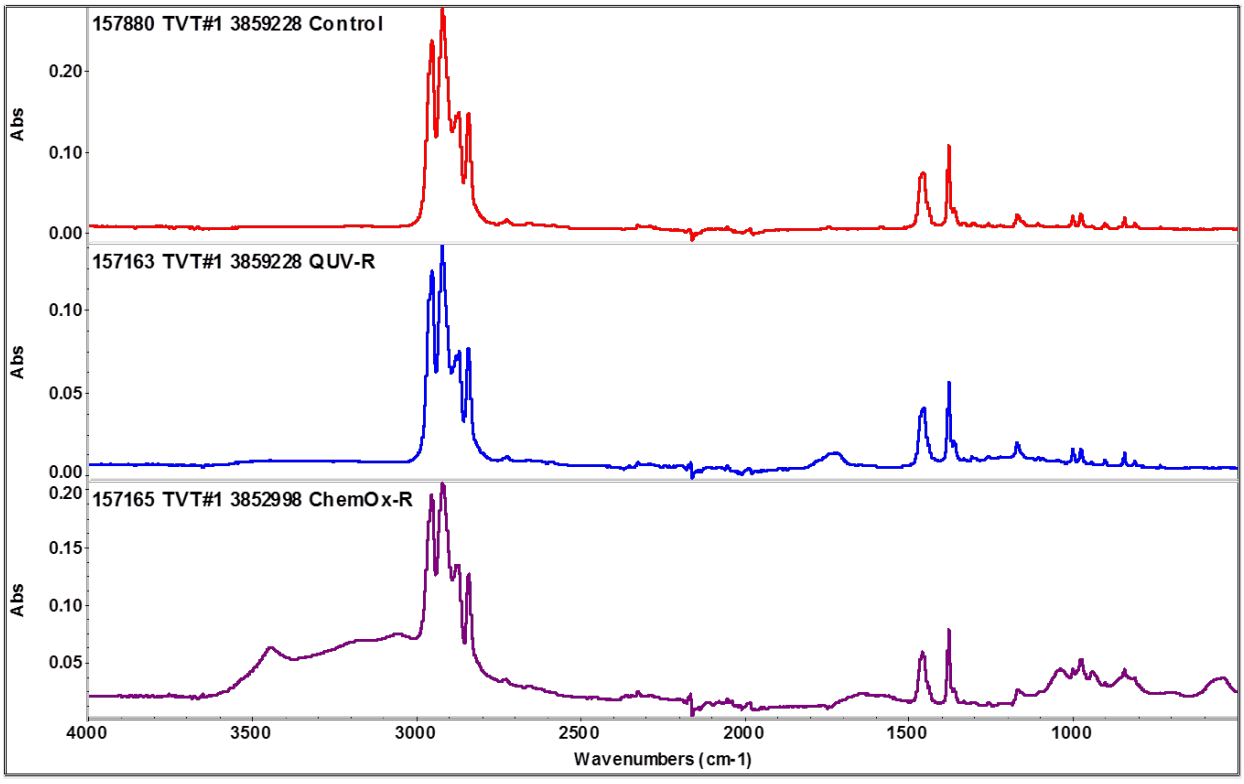

Figure AH.11. FTIR spectra of a pristine (untreated control) TVT mesh sample, QUV-treated sample, and chemically treated sample. Bands consistent with –OH groups

(~3000 cm^{-1} – 3500 cm^{-1}) and C = O groups (1600 cm^{-1} – 1760 cm^{-1}) are observed in the treated samples but not in the pristine samples.

Intentionally Oxidized PROLENE TVT and Hernia Mesh Devices, Sutures, and Polypropylene Pellets Were Not Stained by the Hematoxylin & Eosin Dyes

Positive Control: Rabbit Skin Tissue

A positive control (rabbit skin tissue) was processed to demonstrate the effectiveness of the processing and staining protocol. PROLENE meshes and sutures, treated and untreated, along with the polypropylene pellets, were subjected to the staining protocol at the same time.

The appearance of stain is evident when tissue is present and stain has been applied. Figure AH.12 shows rabbit tissue that has been treated with stain, evident by the coloration within the tissue. These results confirm that the staining protocol employed in these experiments is effective in staining proteinaceous materials.

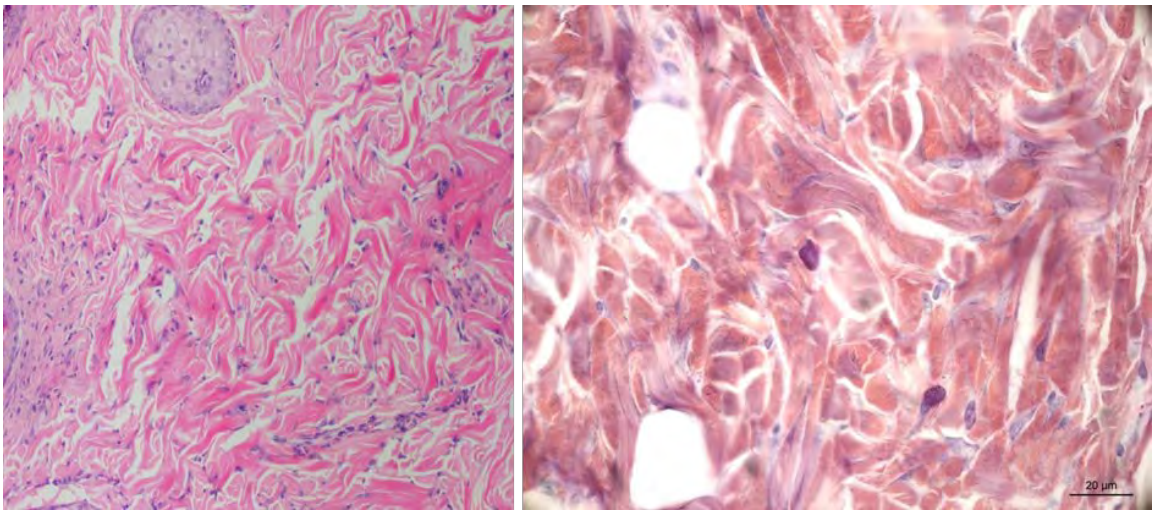

Figure AH.12. Processed and sectioned tissue that has been subjected to the staining protocol and is modified by the H&E stain. Representative images of rabbit tissue embedded in paraffin (left) and resin (right) are shown.[178]

[178] All images collected as part of our experiments are given at the end of this study.

Serum-Coated PROLENE—PROLENE with Protein-Rich Coating

PROLENE coated with FBS and stored in formalin was also subjected to the staining protocol. The protein-rich serum coating around the pristine PROLENE mesh was found to stain, as expected, while the PROLENE fiber itself did not stain. The color of the stain on the serum coating is similar to that of the positive control of rabbit skin. Representative images of serum-coated TVT and hernia mesh are shown in Figure AH.13. In Figure AH.13b, a segment of serum is observed adjacent to the bottom of the PROLENE fiber in the top half of the image. Upon closer inspection, blue granules are visible within the serum coating, creating an illusion that blue granules are present in the exterior coating, when really they are separate, distinct materials. The illusion is created by both the fiber and serum segment being partially in focus. Additional examples that demonstrate this effect are given in Figure AH.14. Figure AH.14a shows the fiber in focus; the serum segment overlaid with the fiber is not. However, blue granules from a PROLENE fiber are visible within the protein-rich serum coating or "bark" as Dr. Iakovlev asserts, giving the illusion of stained PROLENE.[179]

[179] Expert report of Dr. Vladimir Iakovlev dated January 29, 2016, p. 88, 94.

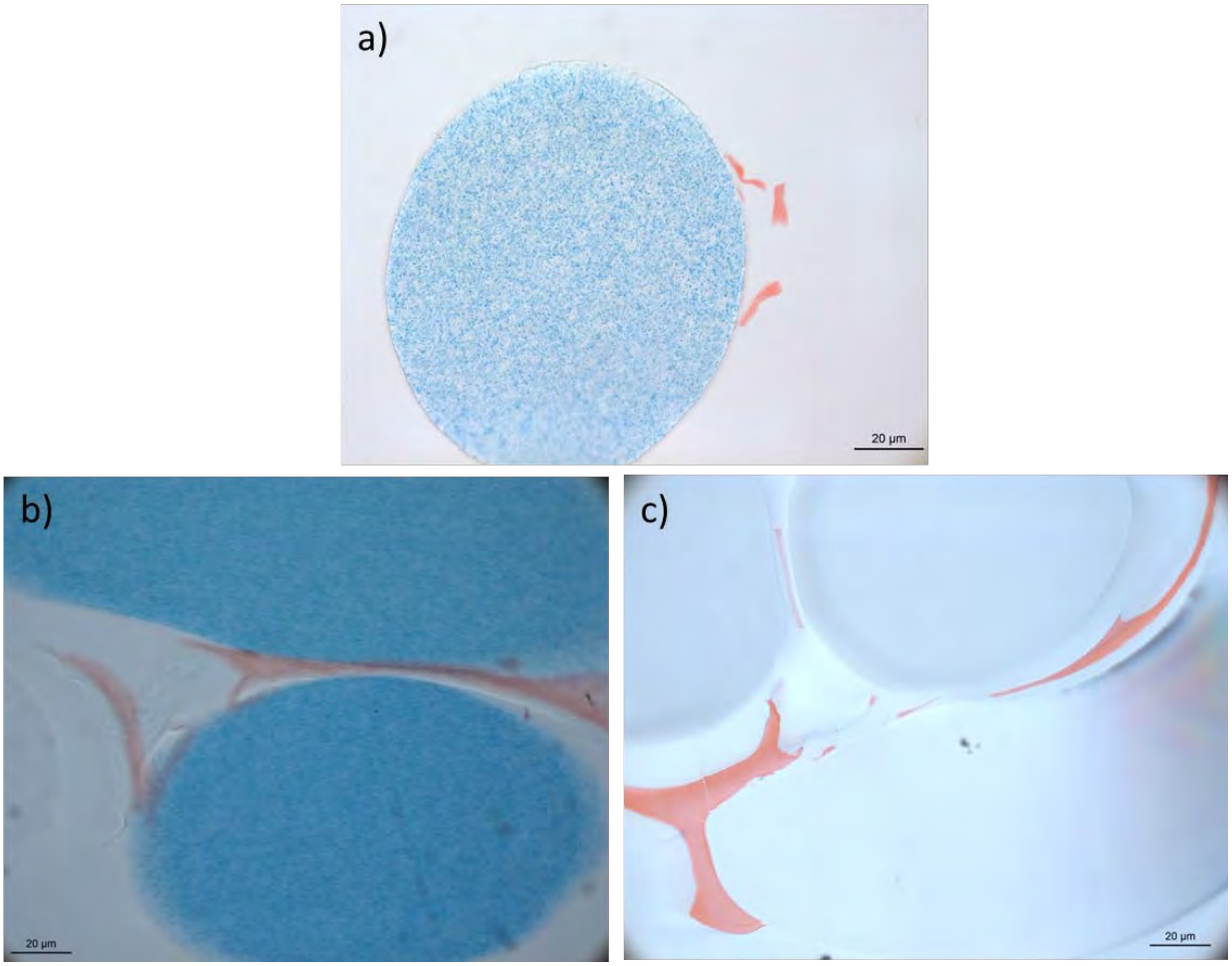

Figure AH.13. Serum-coated PROLENE fibers. (a) Paraffin embedded and (b) resin embedded are from TVT devices. (c) Resin embedded is from a hernia device. All samples were subjected to the staining protocol.

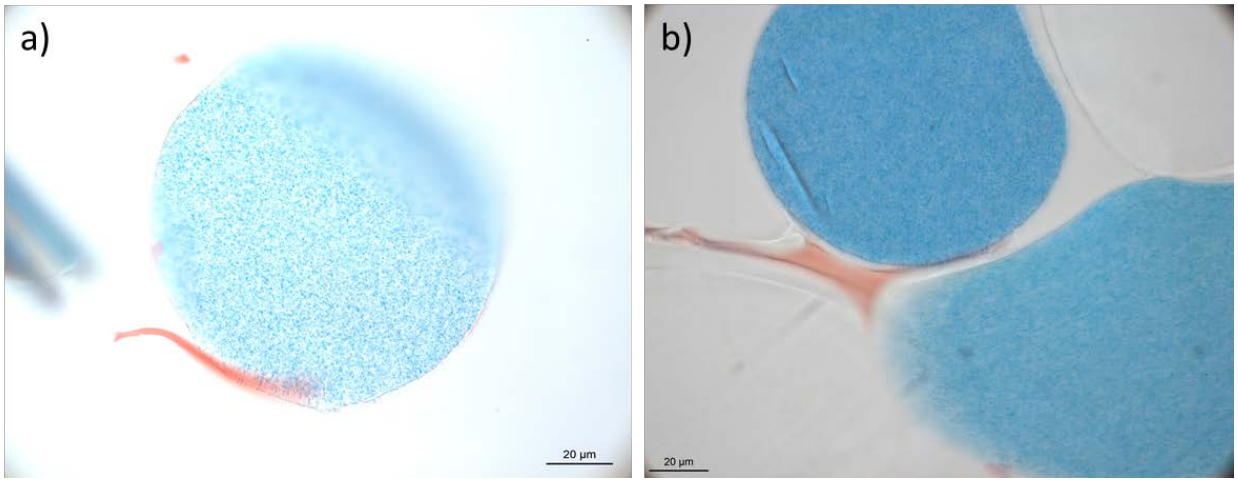

Figure AH.14. Blue granules from a PROLENE fiber are visible within the protein-rich serum coating, giving the illusion of stained PROLENE.

Non-oxidized Control—Out-of-the-Box PROLENE Mesh

In contrast, pristine PROLENE material processed using the same protocol and subjected to H&E staining protocol did not stain. The absence of staining is indicated by the absence of any pink coloration of the mesh fibers in samples embedded in either paraffin or resin (Figure AH.15).

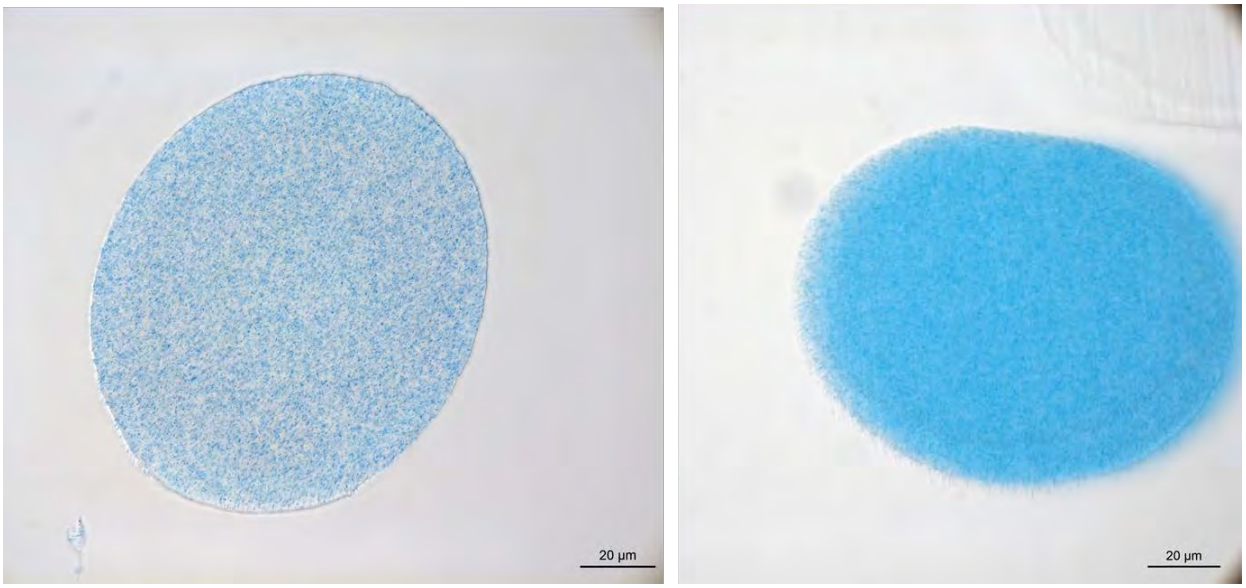

Figure AH.15. Pristine mesh fiber embedded in paraffin and subjected to Dr. Iakovlev's protocol (left). Pristine mesh fiber embedded in Technovit resin and subjected to staining (right). Both samples show an absence of H&E dye being absorbed.

Intentionally Oxidized PROLENE—Chemical Oxidation

The chemically treated PROLENE was not modified by the H&E stain in any of the five PROLENE devices examined, thereby confirming the flawed methodology of Dr. Iakovlev. The cobalt-based crystallites observed to cover the fiber surface when imaged with SEM appeared to be preserved in the cross-sections. The crystals that coat the surface of the PROLENE fibers appear pink. They also appear pink/purple in micrographs taken after the samples were embedded in paraffin and sectioned, but before they were subjected to the staining protocol, as shown in Figure AH.16. The pink color appears enriched in the image of the stained fiber, likely because cobalt chloride is an ionic compound and therefore susceptible to accepting H&E stain.

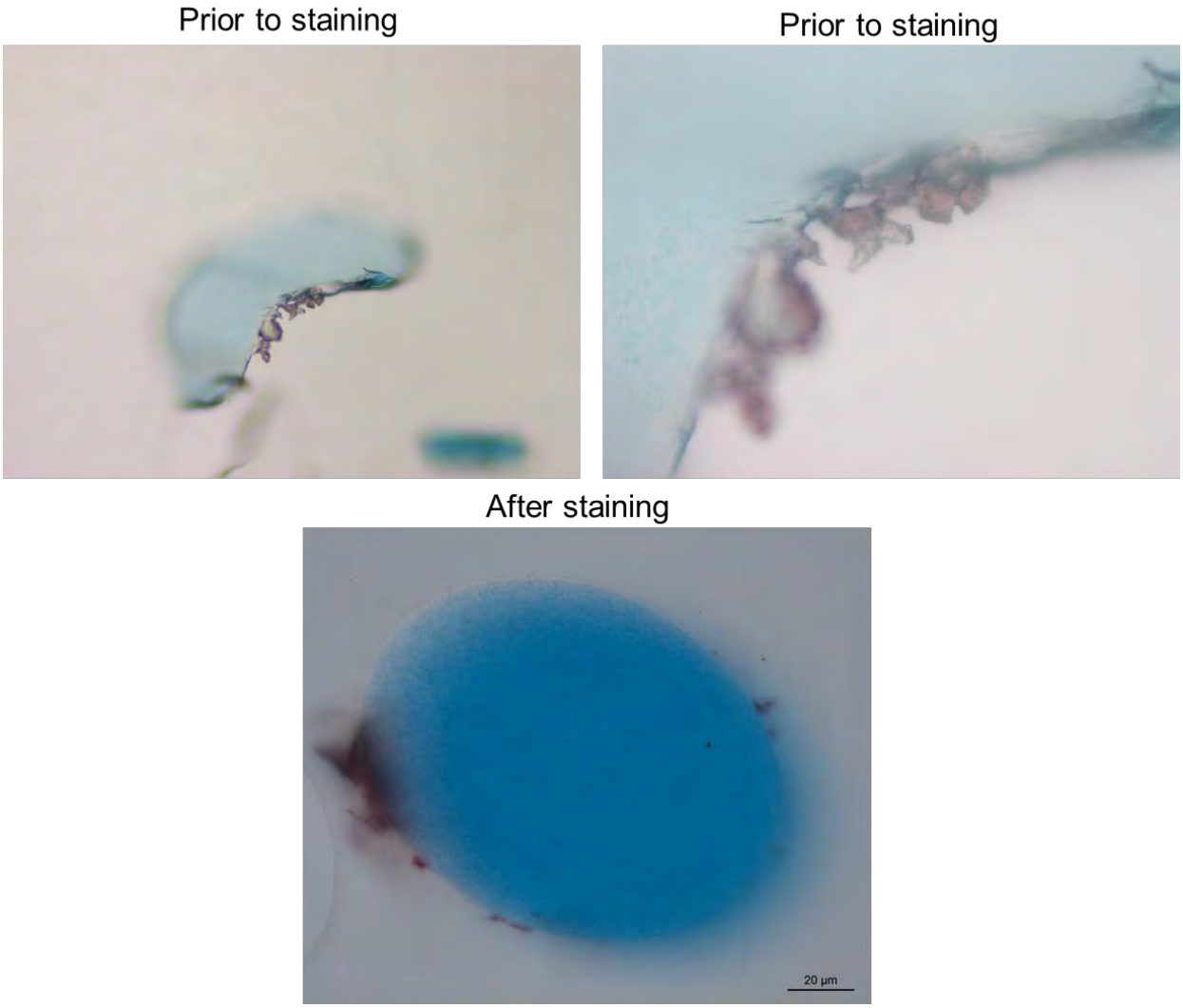

Figure AH.16. Cobalt-based crystallites adhered to the fiber surface are observed to be pink prior to being exposed to stain and after being stained.

Furthermore, cobalt-based crystallites appeared to be easily lodged between mesh fibers embedded in resin. An example is shown in Figure AH.17. An image of the fibers illuminated under cross-polarized light is also shown.

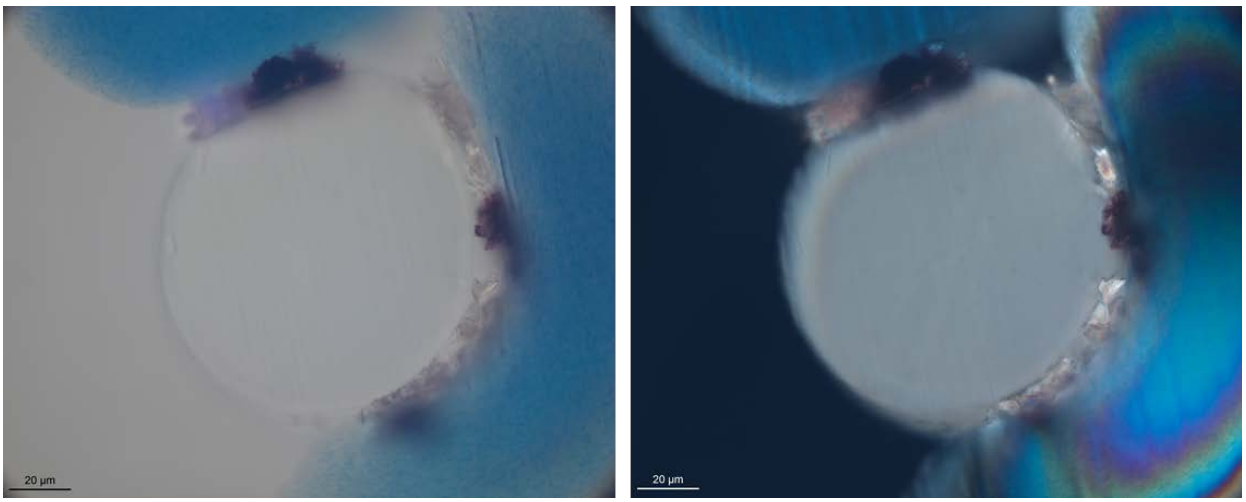

Figure AH.17. Cobalt-based crystallites are lodged between fibers. A bright field image is shown (left) as well as an image of the same fibers under cross-polarized light (right).

Intentionally Oxidized PROLENE—UV Oxidation

Exemplar PROLENE mesh samples exposed to QUV oxidation were also subjected to the Iakovlev staining protocol. As shown in Figure AH.18, despite the fact that fibers are extensively cracked and should have trapped stain according to Dr. Iakovlev, the QUV-oxidized PROLENE did not accept the H&E stain. This finding further supports the conclusion that Dr. Iakovlev's methodology is flawed. Despite multiple observations, using high and low magnifications, polarized and nonpolarized light, no evidence of the stain being trapped, captured, or otherwise bound within the cracks of the damaged mesh was observed in any of the five different PROLENE devices examined.

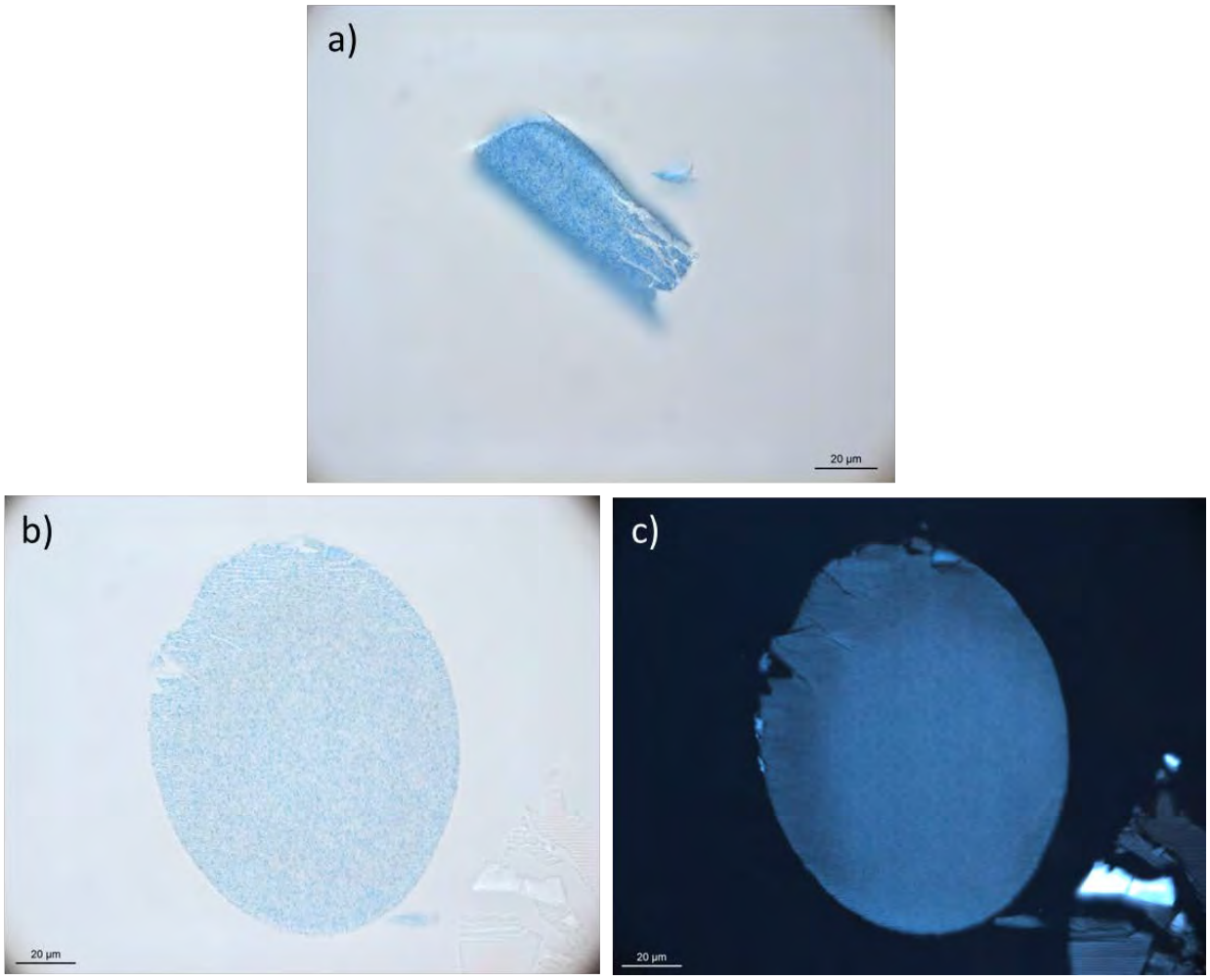

Figure AH.18. QUV-oxidized PROLENE fibers with several cracks embedded in paraffin. No staining is evident. Mesh fibers are shown under bright field light (a) and (b) and illuminated under cross-polarized light (c).

Histology Protocols

Paraffin-embedded samples

1. Samples were processed and embedded in an automated tissue processor according to the following schedule:

Processing Step	Incubating Solution	Number of Changes	Duration of Each Incubation Step
1	70% Reagent Alcohol	2	1 hour each
2	80% Reagent Alcohol	1	1 hour
3	95% Reagent Alcohol	1	1 hour
4	100% Reagent Alcohol	3	1.5 hours each
5	Xylene substitute (ProPar, Manufacturer)	3	1.5 hours each
6	Leica EM400 Paraffin wax	2	2 hours each

2. Tissues were embedded in paraffin blocks using Leica EM400 wax
3. The paraffin blocks were trimmed as necessary and cut at 4-6 µm-thick sections
4. The paraffin sections were briefly floated in a water bath set to 40-45^{o}C to remove wrinkles and allow them to flatten
5. The sections were mounted onto adhesive-coated glass slides, then air-dried for 30 minutes and baked in a 45-50^{o}C oven overnight

6. Paraffin-embedded samples were stained by hand using the following protocol:

Processing Step	Incubating Solution	Duration of Each Incubation Step
1	65°C	10 min
2	Xylene	3 min
3	Xylene	2 min
4	Xylene	2 min
5	100% Alcohol	1 min
6	100% Alcohol	1 min
7	95% Alcohol	1 min
8	Water	1 min
9	Harris Hematoxylin	10 min
10	Wash station	1 min
11	Acid Alcohol	30 sec
12	Water	2 min
13	Ammonia Water	1 min
14	Water	1 min
15	Eosin	2 min
16	Water	20 sec
17	100% Alcohol	1 min
18	100% Alcohol	1 min
19	100% Alcohol	1 min
20	Xylene	1 min
21	Xylene	1 min

Resin-embedded samples

1. Samples were processed and embedded according to the following schedule:

Processing Step	Incubating Solution	Number of Changes	Duration of Each Incubation Step
1	70% Reagent Alcohol	2	1 hour each
2	80% Reagent Alcohol	1	1 hour
3	95% Reagent Alcohol	1	1 hour
4	100% Reagent Alcohol	3	1.5 hours each
5	Technovit 7200	3	3 hours each

2. The resin samples were polymerize using a visible light polymerization unit
3. The blocks were trimmed as necessary, cut using a diamond saw blade, then ground and polished to 10 – 61 μm with a mean thickness of approximately 30 μm.

4. Resin-embedded samples were stained by hand using the following protocol:

Processing Step	Incubating Solution	Duration of Each Incubation Step
1	Water	1 min
2	Harris Hematoxylin	4 hours[180]
3	Water	1 min
4	Acid Alcohol	30 sec
5	Water	1 min
6	Ammonia water	1 min
7	Water	1 min
8	Eosin	1 min
9	Water	30 sec

[180] The intensity of the stain was monitored microscopically every 15 minutes until the positive control, rabbit skin, was dark enough.

Study Images

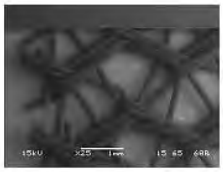

HerniaMeshR_01

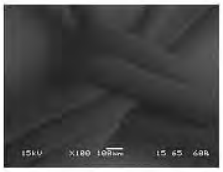

HerniaMeshR_02

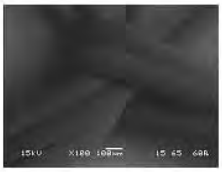

HerniaMeshR_03

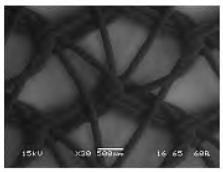
HerniaP-01

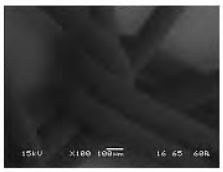
HerniaP-02

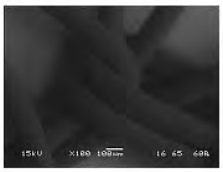
HerniaP-03


HerniaR-01

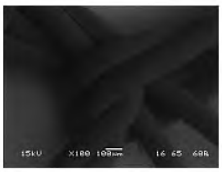
HerniaR-02

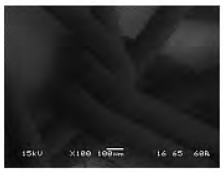
HerniaR-03

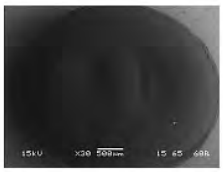
PelletP-01


PelletP-02


PelletP-03

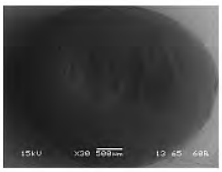
PelletR-01

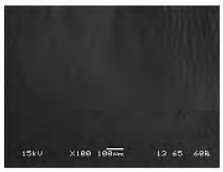
PelletR-02


PelletR-03

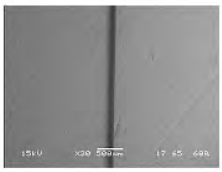
SutureP-01

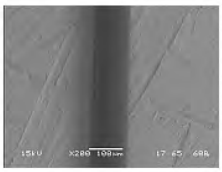
SutureP-02

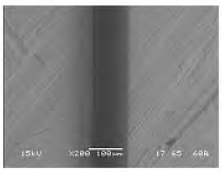
SutureP-03

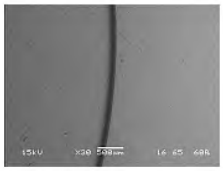
SutureR-01

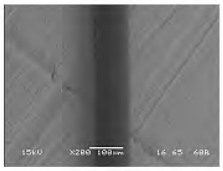
SutureR-02

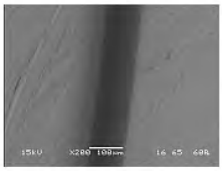
SutureR-03

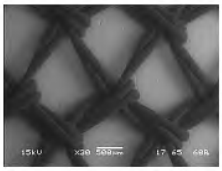
TVT1P-01

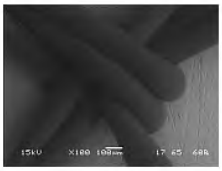
TVT1P-02


TVT1P-03

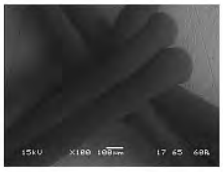
TVT1P-04

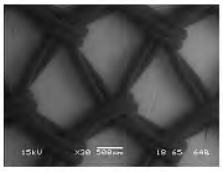
TVT1R-01

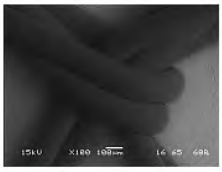
TVT1R-02


TVT1R-03

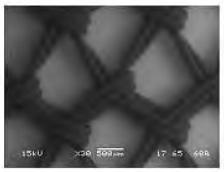
TVT2P-01

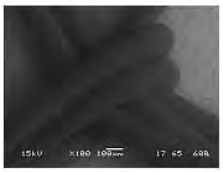
TVT2P-02

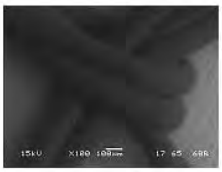
TVT2P-03

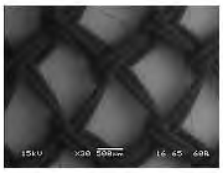
TVT2R-01

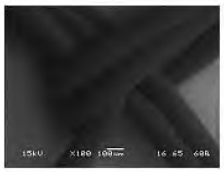
TVT2R-02

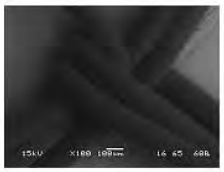
TVT2R-03

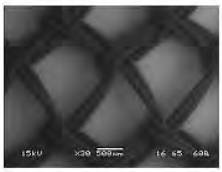
TVT3P-01

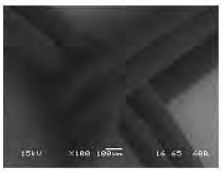
TVT3P-02


TVT3P-03

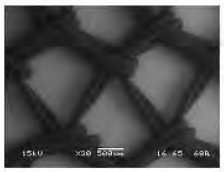
TVT3R-01


TVT3R-02


TVT3R-03


DSC_5380


DSC_5381


DSC_5388


DSC_5389


DSC_5398


DSC_5399


DSC_5410


DSC_5411


DSC_5421


DSC_5422


DSC_5423


DSC_5432


DSC_5433


DSC_5384


DSC_5385


DSC_5402


DSC_5403


DSC_5414


DSC_5415


DSC_5426


DSC_5427


DSC_5436


DSC_5437


DSC_5443


DSC_5444


DSC_5473


DSC_5474


DSC_5475


DSC_5386


DSC_5387


DSC_5404


DSC_5405


DSC_5416


DSC_5417


DSC_5428


DSC_5429


DSC_5438


DSC_5439


DSC_5445


DSC_5446


DSC_5382


DSC_5383


DSC_5400


DSC_5401


DSC_5412


DSC_5413


DSC_5424


DSC_5425


DSC_5434


DSC_5435


DSC_5441


DSC_5442


DSC_5462


DSC_5463


DSC_5464


DSC_5465


DSC_5466


DSC_5467

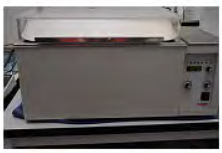
DSC_5468


DSC_5469


DSC_5470


DSC_5471

DSC_5476

DSC_5477

DSC_5478

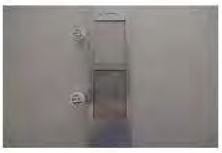

DSC_5479

DSC_5480

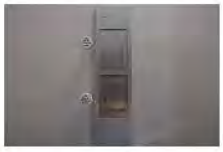

DSC_5481

DSC_5482

DSC_5483

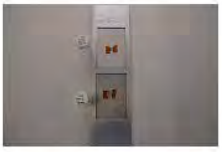

DSC_5484

DSC_5485

DSC_5486

DSC_5487

DSC_5488

DSC_5489

DSC_5490

DSC_5491

DSC_5492


DSC_5493


DSC_5494

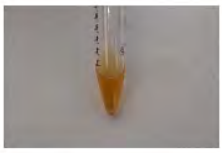
DSC_5495


DSC_5496


DSC_5497


DSC_5498


DSC_5499


DSC_5500


DSC_5501


DSC_5502


DSC_5503


DSC_5504


DSC_5505


DSC_5506


DSC_5507

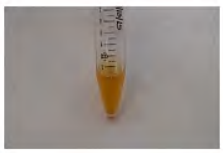
DSC_5508


DSC_5509


DSC_5510


DSC_5511

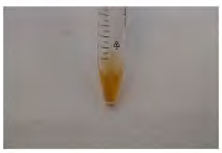
DSC_5512


DSC_5513


DSC_5514

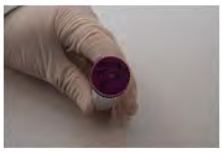
DSC_5515

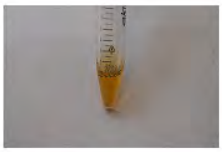
DSC_5516


DSC_5517


DSC_5518

DSC_7023

DSC_7024

DSC_7025

DSC_7026

DSC_7027

DSC_7028

DSC_7029

DSC_7030

DSC_7031

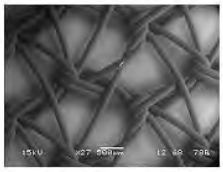

Hernia_mesh_P-01

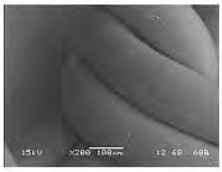

Hernia_mesh_P-02

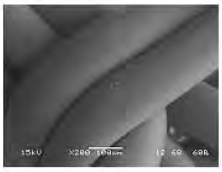

Hernia_mesh_P-03

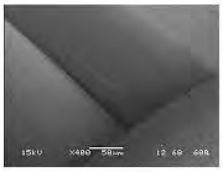

Hernia_mesh_P-04

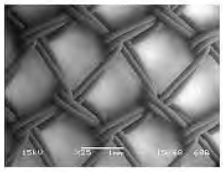

TVT_mesh3_P-01

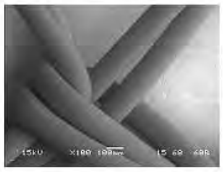

TVT_mesh3_P-02

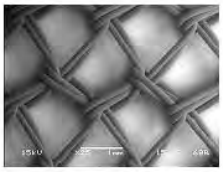

TVT_mesh3_P-03

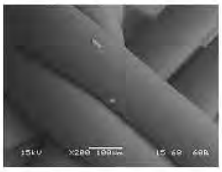

TVT_mesh3_P-04

TVT_mesh3_P-05

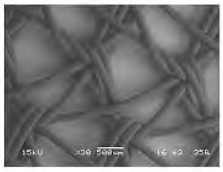

Hernia Mesh_48 hrs-01

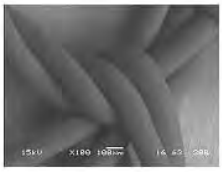

Hernia Mesh_48 hrs-02

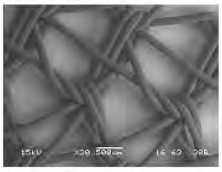

Hernia Mesh_48 hrs-03

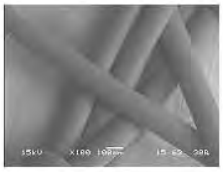

Hernia Mesh_48 hrs-04

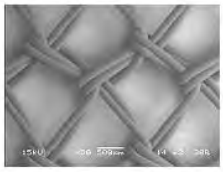

TVT Mesh 3_48 hrs-01

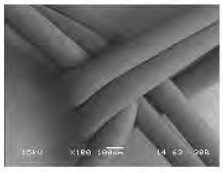

TVT Mesh 3_48 hrs-02

TVT Mesh 3_48 hrs-03

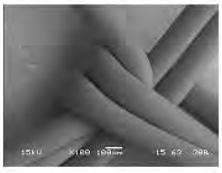

TVT Mesh 3_48 hrs-04

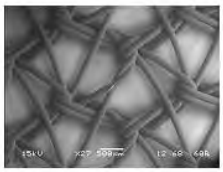

Hernia_mesh_P-01

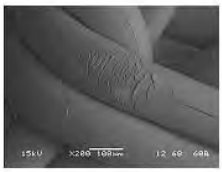

Hernia_mesh_P-02

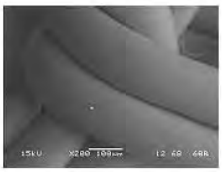

Hernia_mesh_P-03

Hernia_mesh_P-04

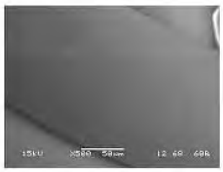

Hernia_mesh_P-05

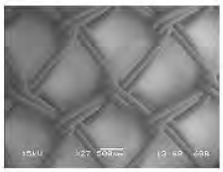

TVT3_mesh-01

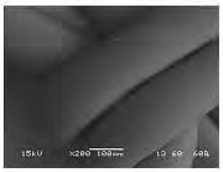

TVT3_mesh-02

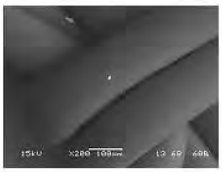

TVT3_mesh-03

TVT3_mesh-04

IMG_2077

IMG_2078

IMG_2079

IMG_2080

IMG_2081

IMG_2082

IMG_2083

IMG_2084

IMG_2085

IMG_2086

IMG_2087


157164_TVT#1_Paraffin_01


157164_TVT#1_Paraffin_02

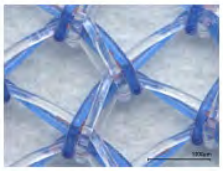
157164_TVT#1_Paraffin_03


157165_TVT#1_Resin_01

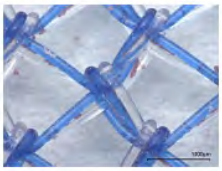
157165_TVT#1_Resin_02


157165_TVT#1_Resin_03

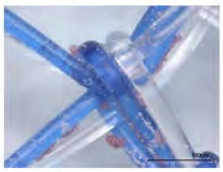
157165_TVT#1_Resin_04


157172_TVT#2_Paraffin_01

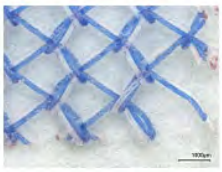
157172_TVT#2_Paraffin_02

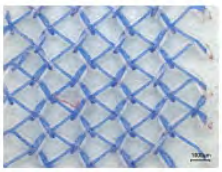
157172_TVT#2_Paraffin_03

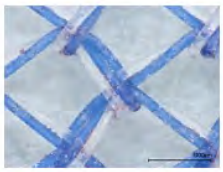
157172_TVT#2_Paraffin_04


157173_TVT#2_Resin_01

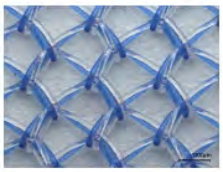
157173_TVT#2_Resin_02

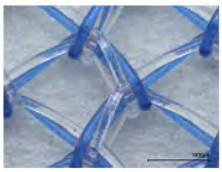
157173_TVT#2_Resin_03

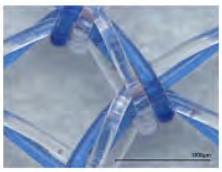
157173_TVT#2_Resin_04


157180_TVT#3_Paraffin_01

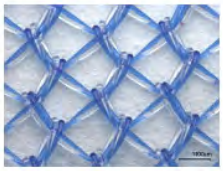
157180_TVT#3_Paraffin_02

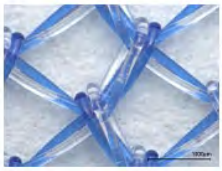
157180_TVT#3_Paraffin_03


157181_TVT#3_Resin_01

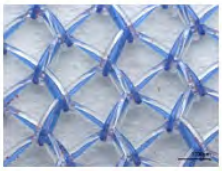
157181_TVT#3_Resin_02

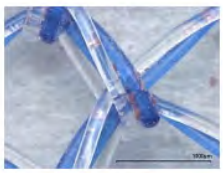
157181_TVT#3_Resin_03


57188_HerniaMesh_Paraffin_0

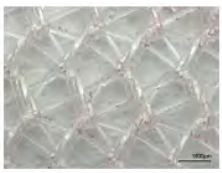
57188_HerniaMesh_Paraffin_0

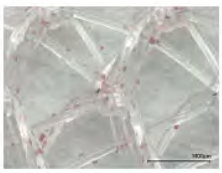
57188_HerniaMesh_Paraffin_0


157189_HerniaMesh_Resin_01


157189_HerniaMesh_Resin_02

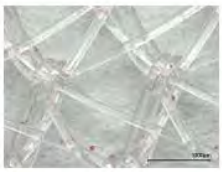
157189_HerniaMesh_Resin_03


57196_Suture_Paraffin-Resin_C


57196_Suture_Paraffin-Resin_C


57196_Suture_Paraffin-Resin_C


157232_pellet_Paraffin_01

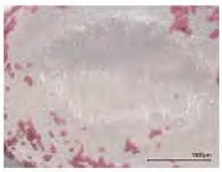
157232_pellet_Paraffin_02

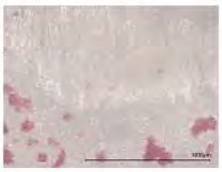
157232_pellet_Paraffin_03


157233_pellet_Resin_01

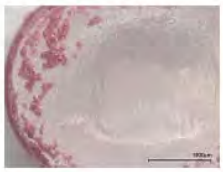
157233_pellet_Resin_02

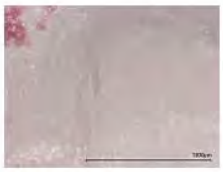
157233_pellet_Resin_03


157164_TVT#1_Paraffin_01

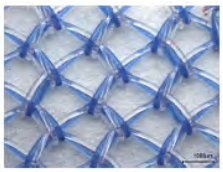
157164_TVT#1_Paraffin_02

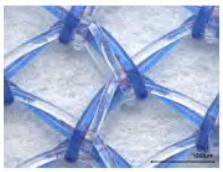
157164_TVT#1_Paraffin_03

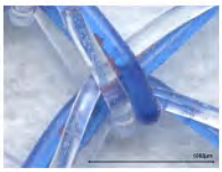
157164_TVT#1_Paraffin_04


157165_TVT#1_Resin_01


157165_TVT#1_Resin_02

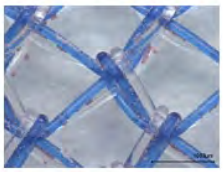
157165_TVT#1_Resin_03

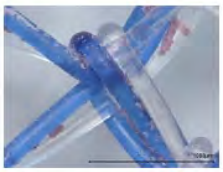
157165_TVT#1_Resin_04

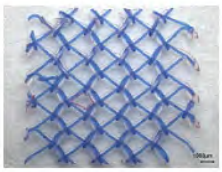
157172_TVT#2_Paraffin_01

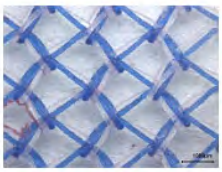
157172_TVT#2_Paraffin_02

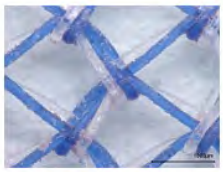
157172_TVT#2_Paraffin_03

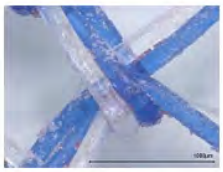
157172_TVT#2_Paraffin_04


157173_TVT#2_Resin_01

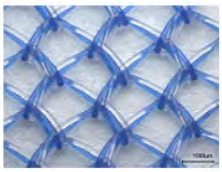
157173_TVT#2_Resin_02

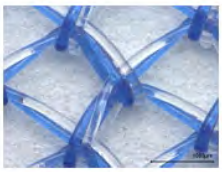
157173_TVT#2_Resin_03

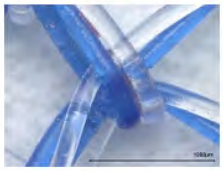
157173_TVT#2_Resin_04


157180_TVT#3_Paraffin_01

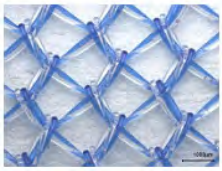
157180_TVT#3_Paraffin_02


157180_TVT#3_Paraffin_03


157180_TVT#3_Paraffin_04


157181_TVT#3_Resin_01

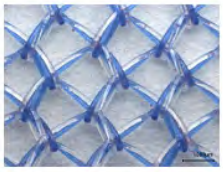
157181_TVT#3_Resin_02


157181_TVT#3_Resin_03

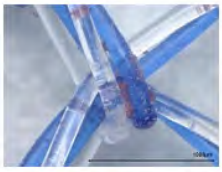
157181_TVT#3_Resin_04


57188_HerniaMesh_Paraffin_0


57188_HerniaMesh_Paraffin_0


57188_HerniaMesh_Paraffin_0


57188_HerniaMesh_Paraffin_0


157189_HerniaMesh_Resin_01


157189_HerniaMesh_Resin_02

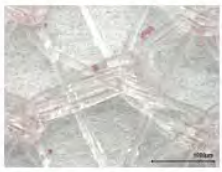
157189_HerniaMesh_Resin_03


157189_HerniaMesh_Resin_04


57196_Suture_Paraffin-Resin_C


57196_Suture_Paraffin-Resin_C


57196_Suture_Paraffin-Resin_C

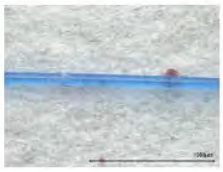
57196_Suture_Paraffin-Resin_C


157232_pellet_Paraffin_01


157232_pellet_Paraffin_02

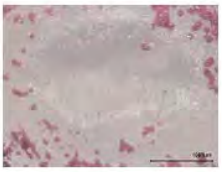
157232_pellet_Paraffin_03


157233_pellet_Resin_01


157233_pellet_Resin_02


157233_pellet_Resin_03


IMG_2153


IMG_2154


IMG_2155


IMG_2156


IMG_2157


IMG_2158


157166_TVT1_Serum-P_01

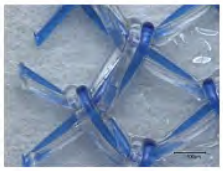
57166_TVT1_Serum-P_100x_0


57166_TVT1_Serum-P_150x_0

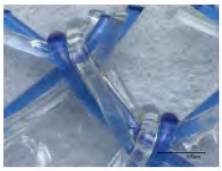
57166_TVT1_Serum-P_150x_0


57166_TVT1_Serum-P_150x_0

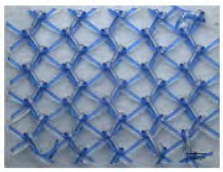
57167_TVT1_Serum-R_030x_0

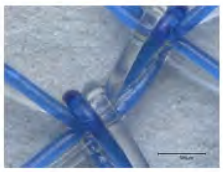
57167_TVT1_Serum-R_150x_0


57167_TVT1_Serum-R_150x_0

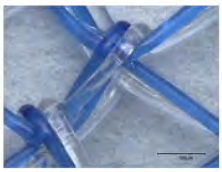
57167_TVT1_Serum-R_150x_0


57167_TVT1_Serum-R_150x_0

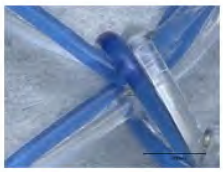
57167_TVT1_Serum-R_200x_0


57174_TVT2_Serum-P_030x_0


I74_TVT2_Serum-P_030x_stitch

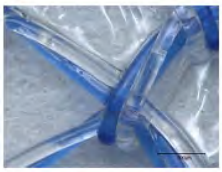
57174_TVT2_Serum-P_150x_0


57174_TVT2_Serum-P_150x_0


57175_TVT2_Serum-R_030x_0


I75_TVT2_Serum-R_030x_stitch


57175_TVT2_Serum-R_150x_0


57175_TVT2_Serum-R_150x_0


57175_TVT2_Serum-R_150x_0


57182_TVT3_Serum-P_030x_0

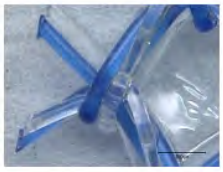
57182_TVT3_Serum-P_150x_0


57182_TVT3_Serum-P_150x_0


57182_TVT3_Serum-P_150x_0


57182_TVT3_Serum-P_150x_0


57183_TVT3_Serum-R_030x_0

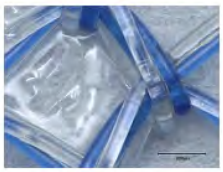
57183_TVT3_Serum-R_150x_0

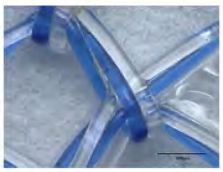
57183_TVT3_Serum-R_150x_0

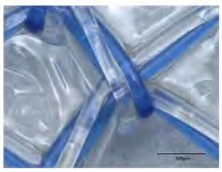
57183_TVT3_Serum-R_150x_0


57190_Hernia_Serum-P_030x_(


57190_Hernia_Serum-P_150x_(


57190_Hernia_Serum-P_150x_(

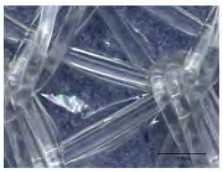
57190_Hernia_Serum-P_150x_(


57191_Hernia_Serum-R_030x_(

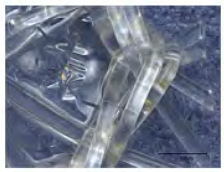
57191_Hernia_Serum-R_150x_(


57191_Hernia_Serum-R_150x_(

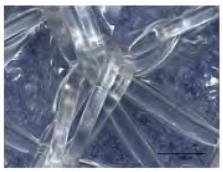
57191_Hernia_Serum-R_150x_(


57198_Suture_Serum-P_030x_(


57198_Suture_Serum-P_200x_(


57198_Suture_Serum-P_200x_(


57198_Suture_Serum-P_200x_(


57198_Suture_Serum-P_200x_(


57199_Suture_Serum-R_030x_(


57199_Suture_Serum-R_200x_(


57199_Suture_Serum-R_200x_(


57199_Suture_Serum-R_200x_(


157234_Pellet 3_050x_01

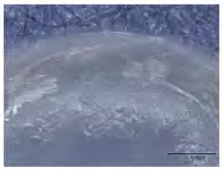
157234_Pellet 3_150x_02

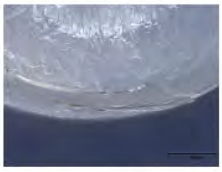
157234_Pellet 3_150x_03


157234_Pellet 3_150x_04


157235_Pellet 4_050x_01

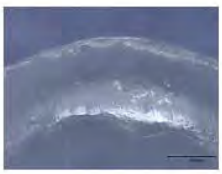
157235_Pellet 4_150x_02

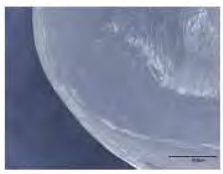
157235_Pellet 4_150x_03

IMG_1022

IMG_1023

IMG_1024

IMG_1025

IMG_1026

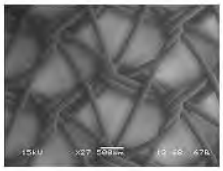

Hernia_mesh_P-01

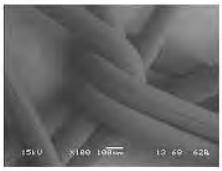

Hernia_mesh_P-02

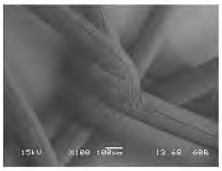

Hernia_mesh_P-03

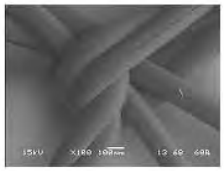

Hernia_mesh_P-04

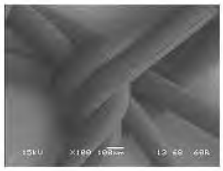

Hernia_mesh_P-05

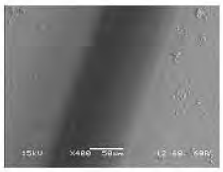

Suture_P-01

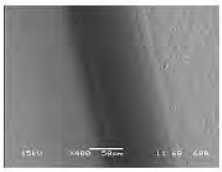

Suture_R-01

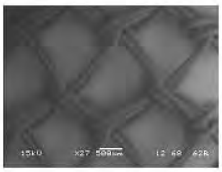

TVT3_mesh-01

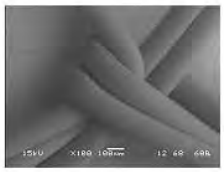

TVT3_mesh-02

TVT3_mesh-03

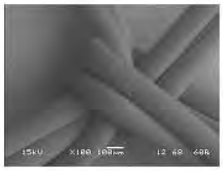

TVT3_mesh-04

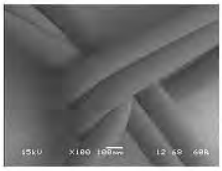

TVT3_mesh-05

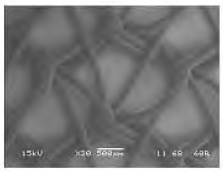
Hernia_mesh_P-01

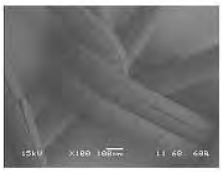
Hernia_mesh_P-02

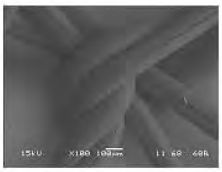
Hernia_mesh_P-03


Suture_P-01

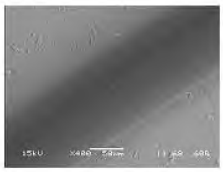
Suture_P-02


Suture_P-03


Suture_P-04

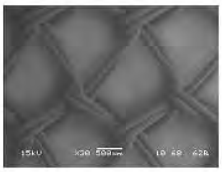
TVT3_mesh-01

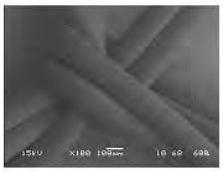
TVT3_mesh-02

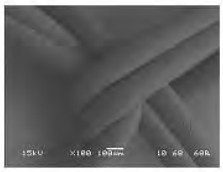
TVT3_mesh-03

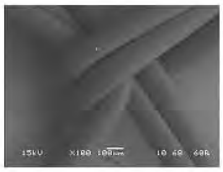
TVT3_mesh-04

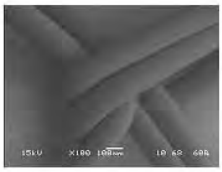
TVT3_mesh-05

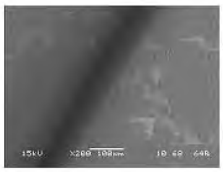
Suture_P-01

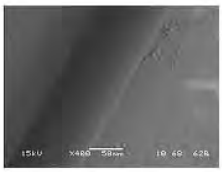
Suture_P-02

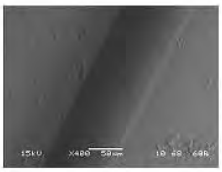
Suture_P-03

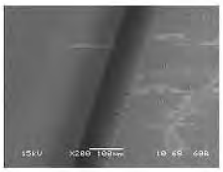
Suture_P-04

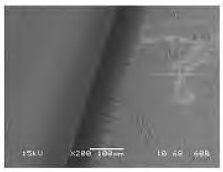
Suture_P-05

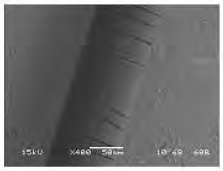
Suture_P-06

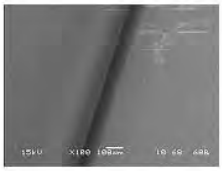
Suture_P-07

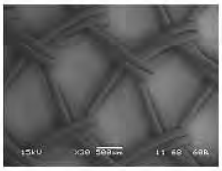
TVT2_mesh-P-01


TVT2_mesh-P-02

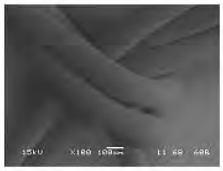
TVT2_mesh-P-03

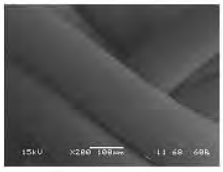
TVT2_mesh-P-04


TVT3_mesh-P-01

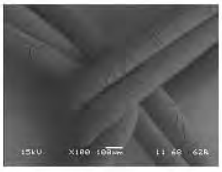
TVT3_mesh-P-02

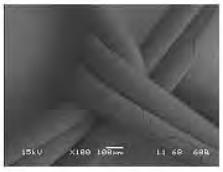
TVT3_mesh-P-03

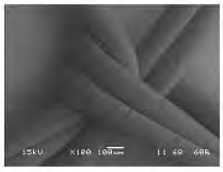
TVT3_mesh-P-04

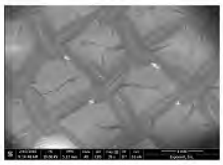
157166_TVT1-P_001

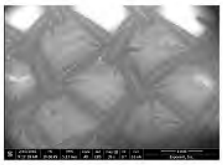
157166_TVT1-P_002

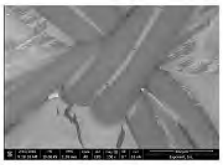
157166_TVT1-P_003

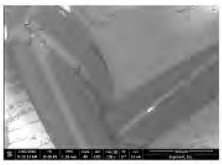
157166_TVT1-P_004

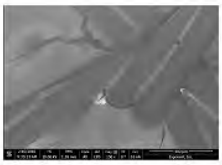
157166_TVT1-P_005

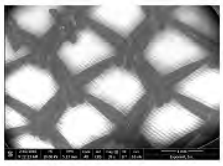
157167_TVT1-R_001

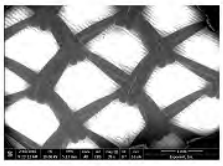
157167_TVT1-R_002

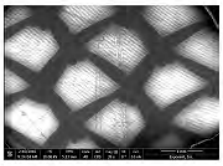
157167_TVT1-R_003

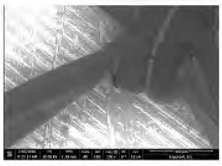
157167_TVT1-R_004

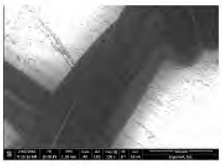
157167_TVT1-R_005


157167_TVT1-R_006

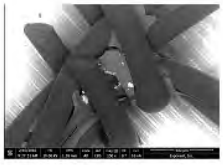
157167_TVT1-R_007

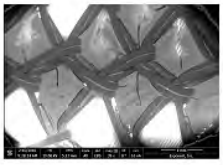
157174_TVT2-P_001

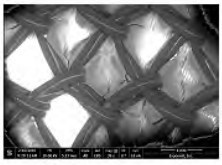
157174_TVT2-P_002


157174_TVT2-P_003

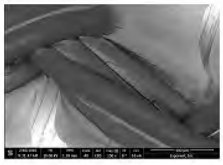
157174_TVT2-P_004

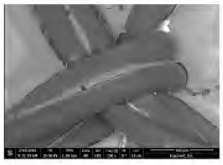
157174_TVT2-P_005

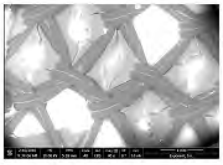
157175_TVT2-R_001

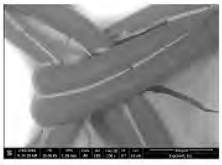
157175_TVT2-R_002

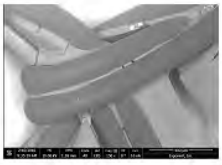
157175_TVT2-R_003

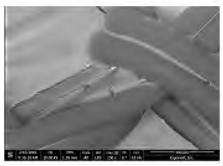
157175_TVT2-R_004


157182_TVT3-P_001

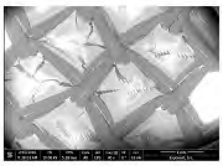
157182_TVT3-P_002


157182_TVT3-P_003

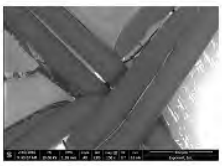
157182_TVT3-P_004


157182_TVT3-P_005

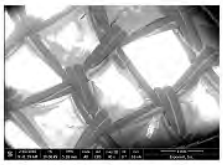
157183_TVT3-R_001

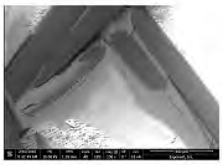
157183_TVT3-R_002


157183_TVT3-R_003


157183_TVT3-R_004

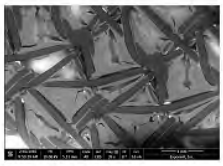
157190_Hernia-P_001

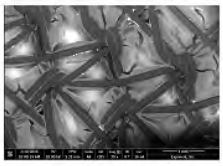
157190_Hernia-P_002


157190_Hernia-P_003

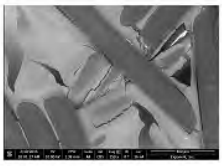
157190_Hernia-P_004

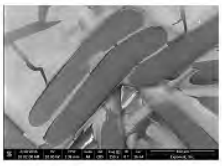
157190_Hernia-P_005

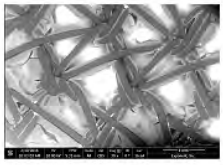
157191_Hernia-R_001


157191_Hernia-R_002

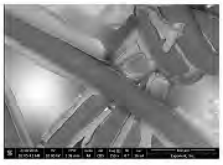
157191_Hernia-R_003


157191_Hernia-R_004

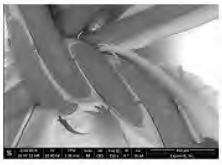
157191_Hernia-R_005

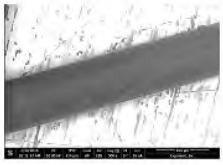
157198_Suture-P_001

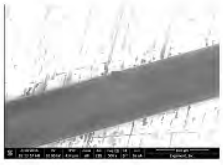
157198_Suture-P_002

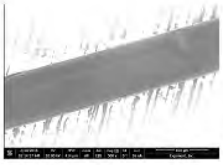
157198_Suture-P_003

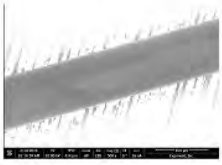
157198_Suture-P_004

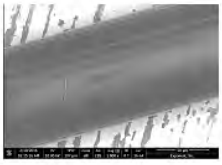
157198_Suture-P_005

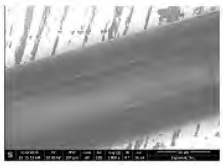
157198_Suture-P_006

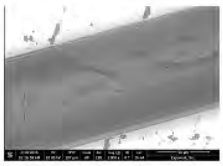
157198_Suture-P_007

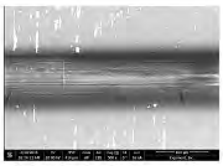
157199_Suture-R_001


157199_Suture-R_002

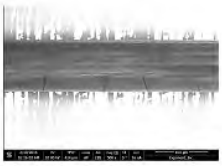
157199_Suture-R_003

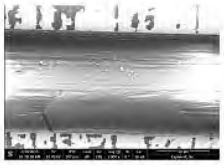

157199_Suture-R_004

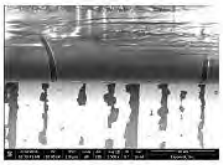

157199_Suture-R_005

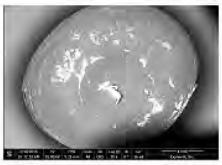

157234_Pellet3_001

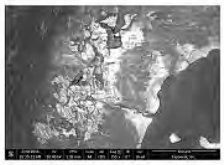

157234_Pellet3_002

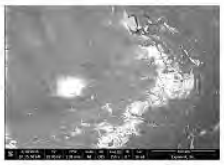

157234_Pellet3_003

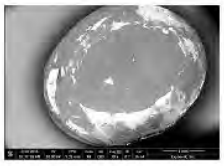

157235_Pellet4_001

157235_Pellet4_002

157235_Pellet4_003

DSC_7052

DSC_7053

DSC_7054

DSC_7055

DSC_7056

DSC_7057

DSC_7058

DSC_7059

IMG_1008

IMG_1009

IMG_1010

IMG_1011

IMG_1012

IMG_1013

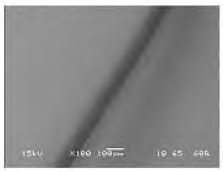
Suture_P_01

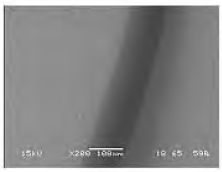
Suture_P_02

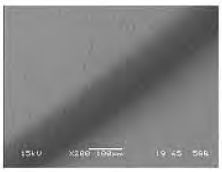
Suture_P_03

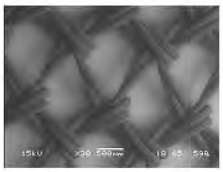
TVT1_Mesh_P_01


TVT1_Mesh_P_02

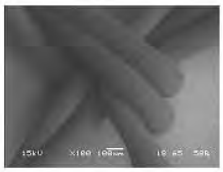
TVT1_Mesh_P_03

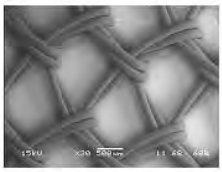
TVT2_mesh-P-01


TVT2_mesh-P-02

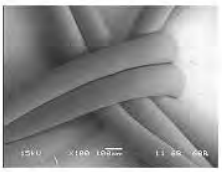
TVT2_mesh-P-03

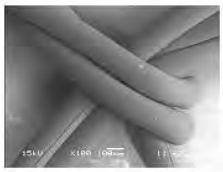
TVT2_mesh-P-04


TVT3_Mesh_P_01

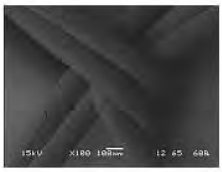
TVT3_Mesh_P_02

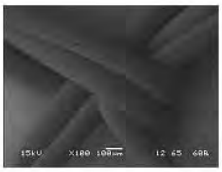
TVT3_Mesh_P_03

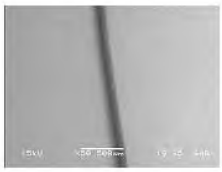
SutureR_01

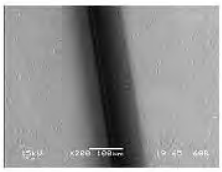
SutureR_02

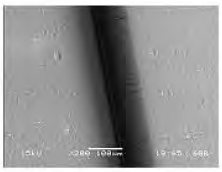
SutureR_03

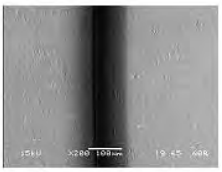
SutureR_04

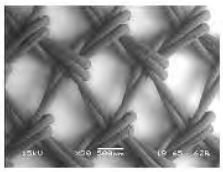
TVT1P_01


TVT1P_02


TVT1P_03

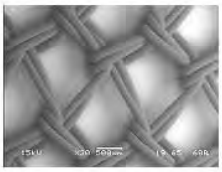
TVT1R_01


TVT1R_02

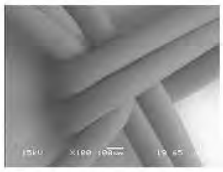
TVT1R_03

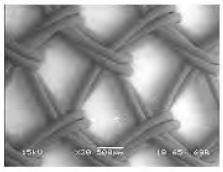
TVT2P_01


TVT2P_02


TVT2P_03

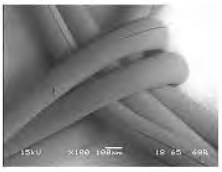
TVT2P_04

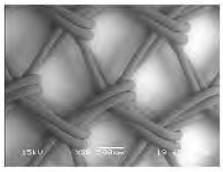
TVT2R_01

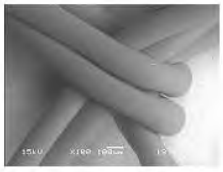
TVT2R_02


TVT2R_03

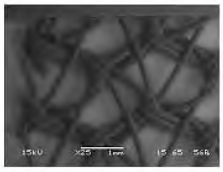
HerniaMeshP_01


HerniaMeshP_02

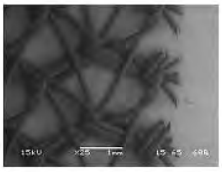
HerniaMeshP_03

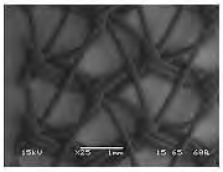
HerniaMeshP_04

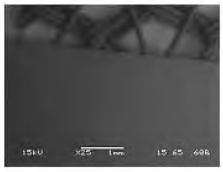
HerniaMeshP_05

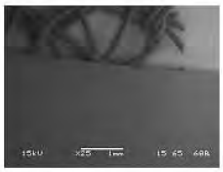
HerniaMeshP_06

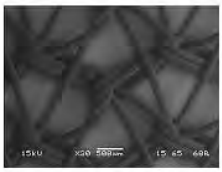
HerniaMeshP_07


HerniaMeshP_08


HerniaMeshP_09

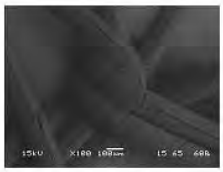
HerniaMeshP_10

TVT3P_01

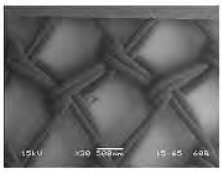

TVT3P_02

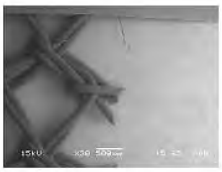

TVT3P_03

TVT3P_04

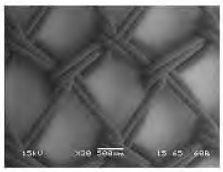

TVT3P_05

TVT3P_06

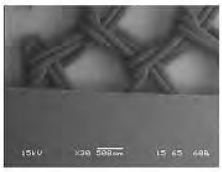

TVT3P_07

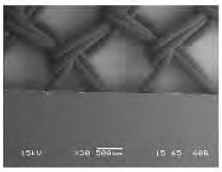

TVT3P_08

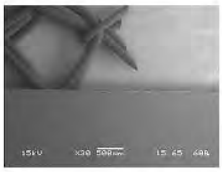

TVT3P_09

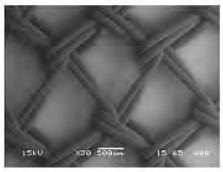

TVT3P_10

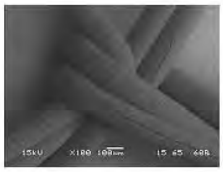

TVT3P_11

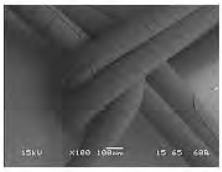

TVT3P_12

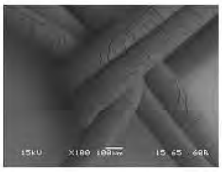

TVT3P_13

IMG_2314

IMG_2315

IMG_2316

IMG_2317

IMG_2318

IMG_2319

IMG_2320

IMG_2321

IMG_2322

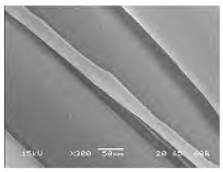
157166_TVT1_P_01

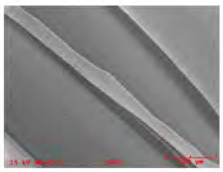
157166_TVT1_P_EDS

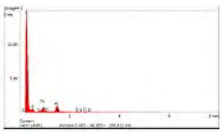
157166_TVT1_P_EDS_Loc1


157166_TVT1_P_EDS_Loc1-2

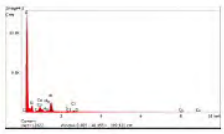
157166_TVT1_P_EDS_Loc2

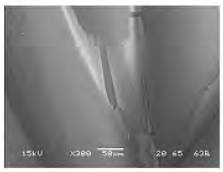
157173_TVT2_P_01

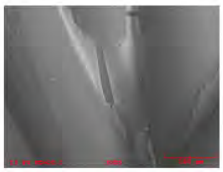
157173_TVT2_P_EDS

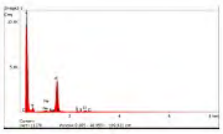
157173_TVT2_P_EDS_Loc1

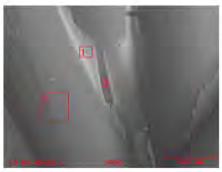
157173_TVT2_P_EDS_Loc1-3

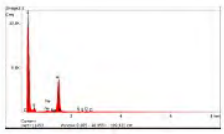
157173_TVT2_P_EDS_Loc2

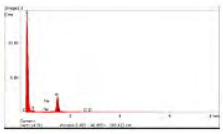
157173_TVT2_P_EDS_Loc3

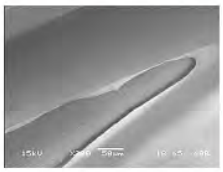
157182_TVT3_P_01

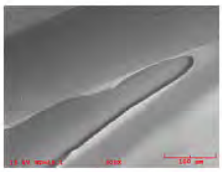
157182_TVT3_P_EDS

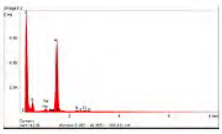
157182_TVT3_P_EDS_Loc1

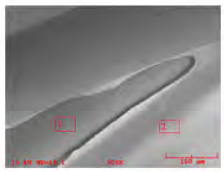
157182_TVT3_P_EDS_Loc1-2

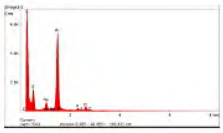
157182_TVT3_P_EDS_Loc2

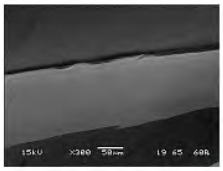
157190_Hernia_P_01

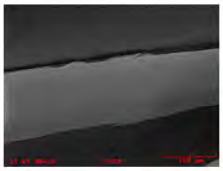
157190_Hernia_P_EDS

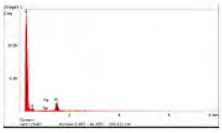
157190_Hernia_P_EDS_Loc1

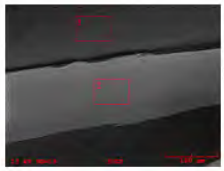
157190_Hernia_P_EDS_Loc1-2

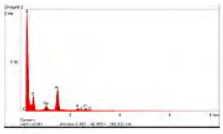
157190_Hernia_P_EDS_Loc2

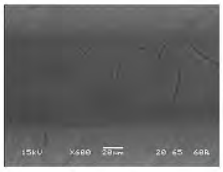
157198_Suture_01


157198_Suture_EDS

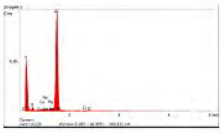
157198_Suture_EDS_Loc1


157198_Suture_EDS_Loc1-2

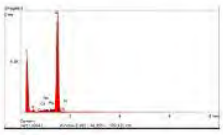

157198_Suture_EDS_Loc2

157234_Pellet3_P_01

157234_Pellet3_P_EDS

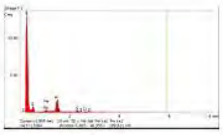

157234_Pellet3_P_EDS_Loc1

157234_Pellet3_P_EDS_Loc1-2

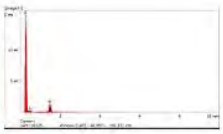

157234_Pellet3_P_EDS_Loc2

SutureP_01

SutureP_02

SutureP_03

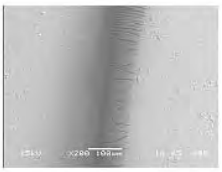

SutureP_04

SutureP_05

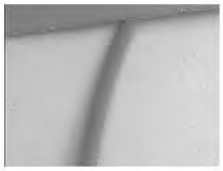

SutureP_06

SutureP_07

SutureP_08

SutureP_09

SutureP_10

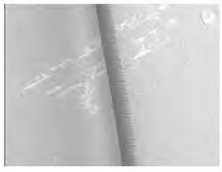

SutureP_11

SutureP_12

SutureP_13

SutureP_14

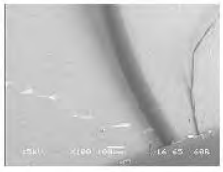

SutureP_15

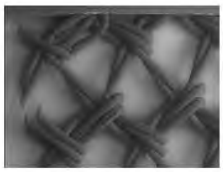
TVT1P_01


TVT1P_02


TVT1P_03

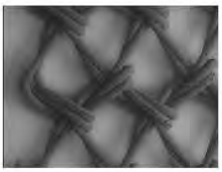
TVT1P_04


TVT1P_05


TVT1P_06


TVT1P_07

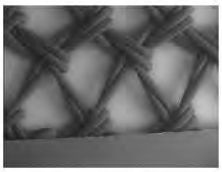
TVT1P_08


TVT1P_09

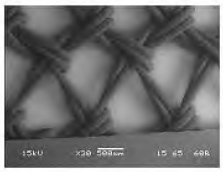
TVT1P_10


TVT1P_11


TVT1P_12


TVT1P_stitch

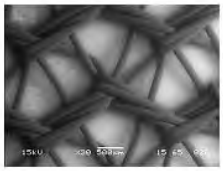
HerniaR_01

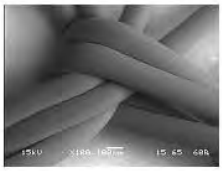
HerniaR_02


HerniaR_03

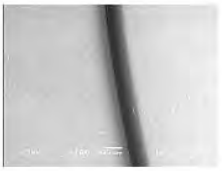
SutureR_01

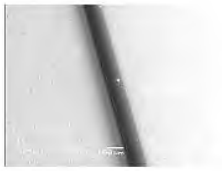
SutureR_02


SutureR_03

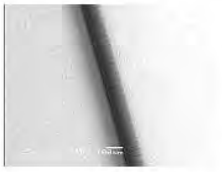
SutureR_04


TVT1R_01

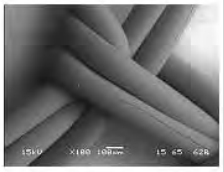
TVT1R_02

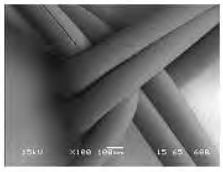
TVT1R_03

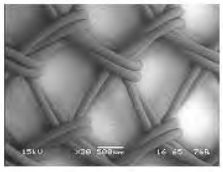
TVT2R_01


TVT2R_02

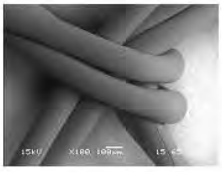
TVT2R_03

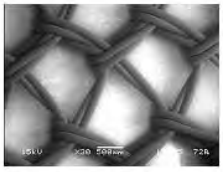
TVT3R_01


TVT3R_02

TVT2P_01

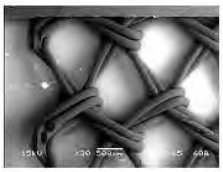

TVT2P_02

TVT2P_03

TVT2P_04

TVT2P_05

TVT2P_06

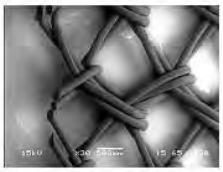

TVT2P_07

TVT2P_08

TVT2P_09

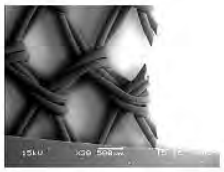

TVT2P_10

TVT2P_11

TVT2P_12

DSC_7105

DSC_7106

DSC_7107

DSC_7108

DSC_7109

DSC_7110

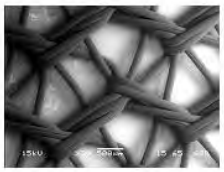
HerniaR_01


HerniaR_02


HerniaR_03


HerniaR_04


SutureR_01


SutureR_02


SutureR_03


TVT1R_01

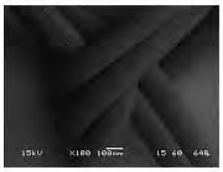
TVT1R_02

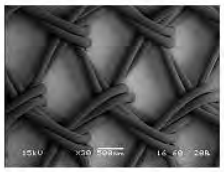
TVT2R_01


TVT2R_02


TVT2R_03


TVT2R_04

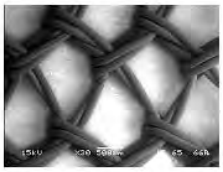
TVT3R_01

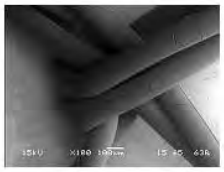
TVT3R_02


TVT3R_03


TVT3R_04


TVT2R_01


TVT2R_02


TVT2R_03


TVT2R_04

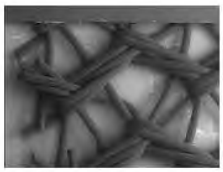
HerniaR_01

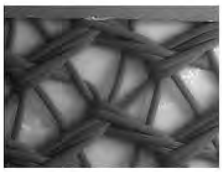
HerniaR_02


HerniaR_03

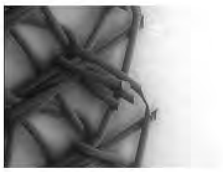
HerniaR_04

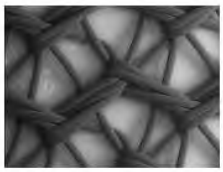
HerniaR_05

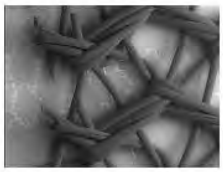
HerniaR_06

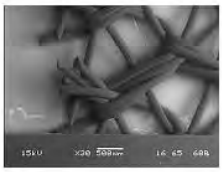
HerniaR_07


HerniaR_08


HerniaR_09

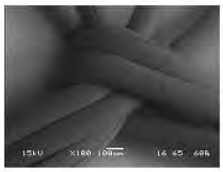
HerniaR_10

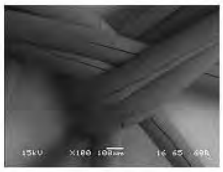
HerniaR_11


SutureR_01


SutureR_02


SutureR_03


SutureR_04


SutureR_05


SutureR_06


SutureR_07


SutureR_08

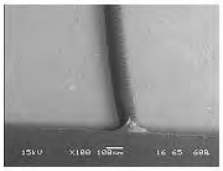
SutureR_09

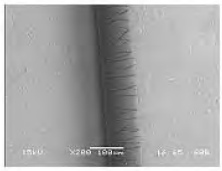
SutureR_10

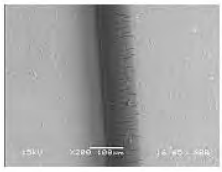
SutureR_11


TVT1R_01


TVT1R_02


TVT1R_03


TVT1R_04

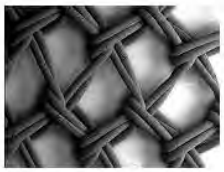
TVT1R_05

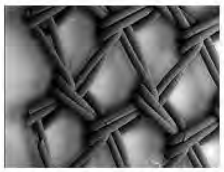
TVT1R_06


TVT1R_07


TVT1R_08


TVT1R_09


TVT1R_10


TVT1R_11


TVT1R_stitch


TVT2R_01

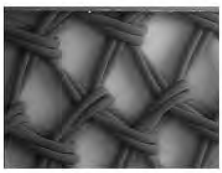
TVT2R_02


TVT2R_03


TVT2R_04

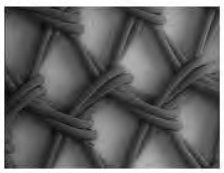
TVT2R_05


TVT2R_06

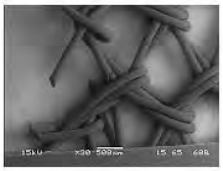
TVT2R_07

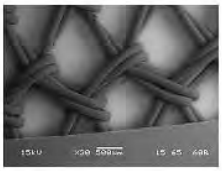
TVT2R_08


TVT2R_09

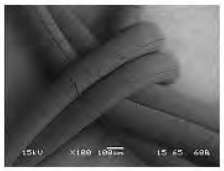
TVT2R_10


TVT2R_11

TVT3R_01

TVT3R_02

TVT3R_03

TVT3R_04

TVT3R_05

TVT3R_06

TVT3R_07

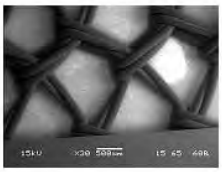

TVT3R_08

TVT3R_09

TVT3R_10

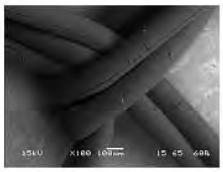

TVT3R_11

DSC_9597

DSC_9598

DSC_9599

DSC_9600

DSC_9601

DSC_9683

DSC_9684

DSC_9685

DSC_9686

DSC_9687

DSC_9688

DSC_9689

IMG_1054

IMG_1055

IMG_1056

IMG_1057

IMG_1058

DSC_9696

DSC_9697

DSC_9698

DSC_9699

DSC_9700

DSC_9701

DSC_9702

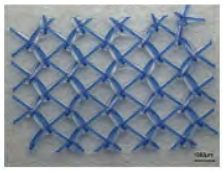
157166_TVT#1_Paraffin_01


157166_TVT#1_Paraffin_02

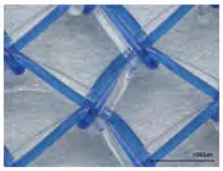
157166_TVT#1_Paraffin_03


157166_TVT#1_Paraffin_04


157166_TVT#1_Paraffin_05


157167_TVT#1_Resin_01


157167_TVT#1_Resin_02

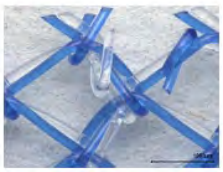
157167_TVT#1_Resin_03

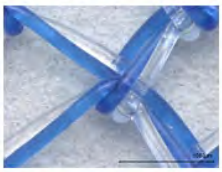
157167_TVT#1_Resin_04

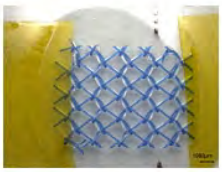
157167_TVT#1_Resin_05

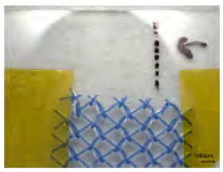
157167_TVT#1_Resin_06


157174_TVT#2_Paraffin_01


157174_TVT#2_Paraffin_02

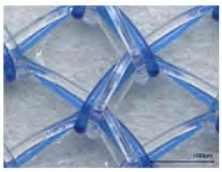
157174_TVT#2_Paraffin_03

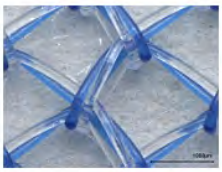
157174_TVT#2_Paraffin_04


157174_TVT#2_Paraffin_05


157174_TVT#2_Paraffin_06


157175_TVT#2_Resin_01


157175_TVT#2_Resin_02

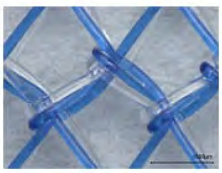
157175_TVT#2_Resin_03


157175_TVT#2_Resin_04


157175_TVT#2_Resin_05


157175_TVT#2_Resin_06

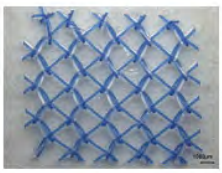
157182_TVT#3_Paraffin_01


157182_TVT#3_Paraffin_02

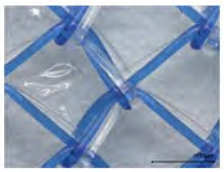
157182_TVT#3_Paraffin_03

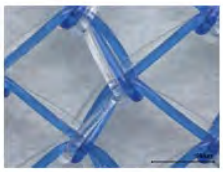
157182_TVT#3_Paraffin_04


157182_TVT#3_Paraffin_05


157182_TVT#3_Paraffin_06


157183_TVT#3_Resin_01


157183_TVT#3_Resin_02

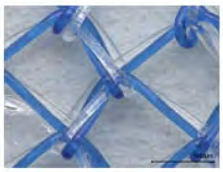
157183_TVT#3_Resin_03

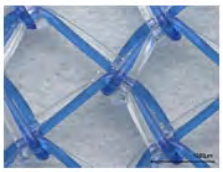
157183_TVT#3_Resin_04


157183_TVT#3_Resin_05


157183_TVT#3_Resin_06


57190_HerniaMesh_Paraffin_0


57190_HerniaMesh_Paraffin_0


57190_HerniaMesh_Paraffin_0


57190_HerniaMesh_Paraffin_0


57190_HerniaMesh_Paraffin_0


57190_HerniaMesh_Paraffin_0


157191_HerniaMesh_Resin_01


157191_HerniaMesh_Resin_02


157191_HerniaMesh_Resin_03


157191_HerniaMesh_Resin_04


157191_HerniaMesh_Resin_05


157191_HerniaMesh_Resin_06


157198_Suture_Paraffin_01


157198_Suture_Paraffin_02


157198_Suture_Paraffin_03


157198_Suture_Paraffin_04


157198_Suture_Paraffin_05


157198_Suture_Paraffin_06


157199_Suture_Resin_01


157199_Suture_Resin_02


157199_Suture_Resin_03


157199_Suture_Resin_04


157199_Suture_Resin_05


157199_Suture_Resin_06


157199_Suture_Resin_07


157234_pellet_Paraffin_01


157234_pellet_Paraffin_02


157234_pellet_Paraffin_03

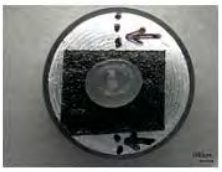
157234_pellet_Paraffin_04


157235_pellet_Resin_01


157235_pellet_Resin_02


157235_pellet_Resin_03

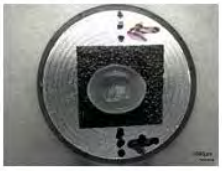
157235_pellet_Resin_04


DSC_4479


DSC_4480


DSC_4481


DSC_4482


DSC_4483

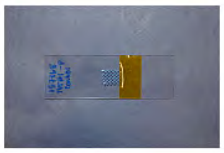

DSC_4483

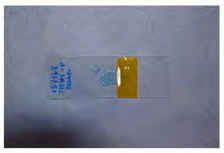

DSC_4484

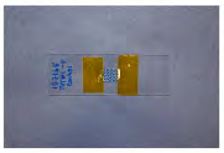

DSC_4485

DSC_4486

DSC_4512

DSC_4513

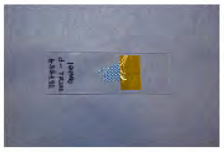

DSC_4514

DSC_4515

DSC_4516

DSC_4517

DSC_4518

DSC_4519

DSC_4520

DSC_4521

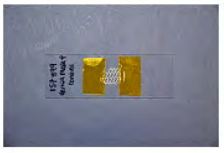

DSC_4522

DSC_4523

DSC_4524

DSC_4525

DSC_4526

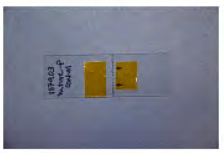

DSC_4527

DSC_4528

DSC_4529

DSC_4530

DSC_4531

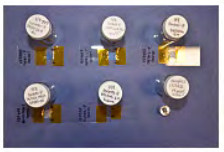

DSC_4532

DSC_4533

DSC_4465

DSC_4466

DSC_4467

DSC_4468

DSC_4469

DSC_4470

DSC_4471

DSC_4472

DSC_4473

DSC_4474

DSC_4475

DSC_4476

DSC_4477

DSC_4478

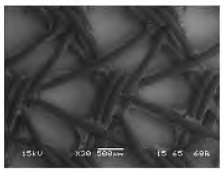
HerniaP-01


HerniaP-02

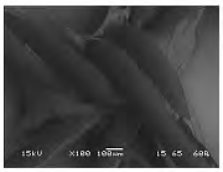
HerniaP-03


HerniaR-01

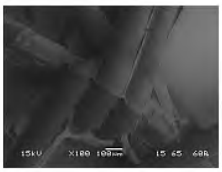
HerniaR-02

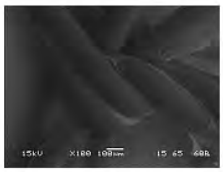
HerniaR-03

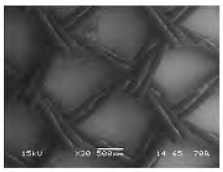
TVT1P-01

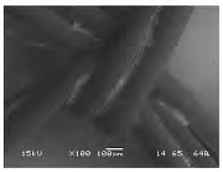
TVT1P-02

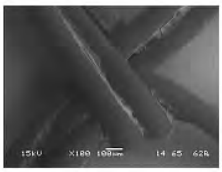
TVT1P-03

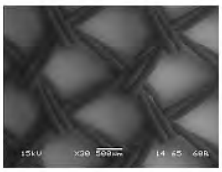
TVT1R-01

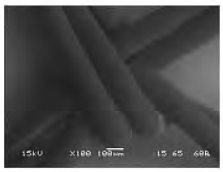
TVT1R-02

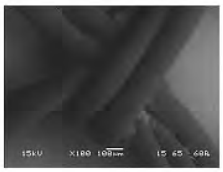
TVT1R-03

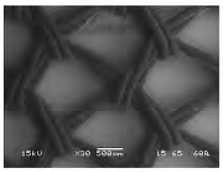
TVT2P-01

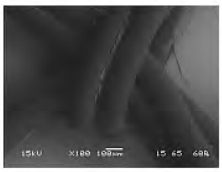
TVT2P-02


TVT2P-03

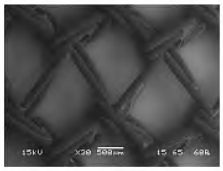
TVT2R-01

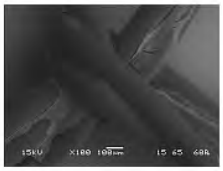
TVT2R-02

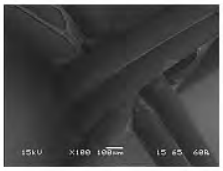
TVT2R-03

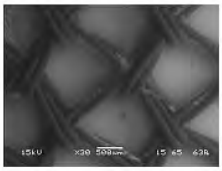
TVT3P-01

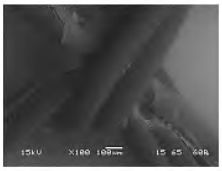
TVT3P-02

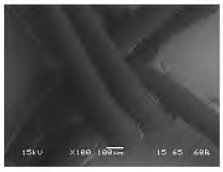
TVT3P-03

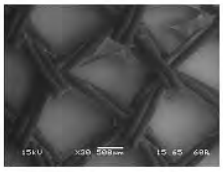
TVT3R-01

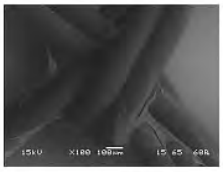
TVT3R-02

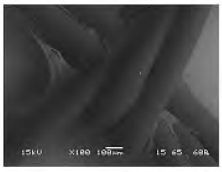
TVT3R-03

DSC_4487

DSC_4488

DSC_4489

DSC_4490

DSC_4491

DSC_4492

DSC_4493

DSC_4494

DSC_4495

DSC_4496

DSC_4497

DSC_4498

DSC_4499

DSC_4500

DSC_4501

DSC_4502

DSC_4503

DSC_4504

DSC_4505

DSC_4506

DSC_4507

DSC_4508

DSC_4509

DSC_4510

DSC_4511

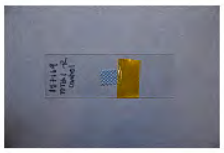
DSC_4534

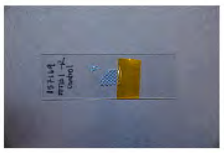
DSC_4535


DSC_4536


DSC_4537


DSC_4538


DSC_4539


DSC_4540


DSC_4541


DSC_4542


DSC_4543


DSC_4544


DSC_4545


DSC_4547


DSC_4548


DSC_4549


DSC_4550


DSC_4551

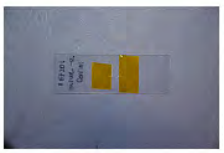
DSC_4552


DSC_4553


DSC_4554


DSC_4555


DSC_4556


DSC_4557

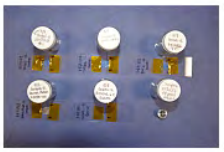
DSC_4558

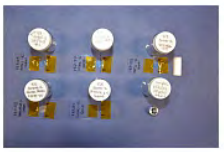
DSC_4559


DSC_4560


DSC_4561


DSC_4562

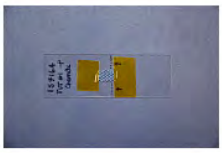
DSC_4563


DSC_4564


DSC_4565


DSC_4566


DSC_4567


DSC_4568


DSC_4569

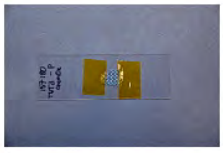
DSC_4570


DSC_4571

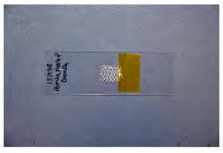
DSC_4572

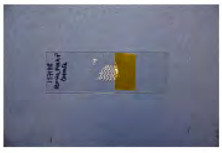
DSC_4573

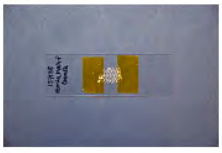
DSC_4574

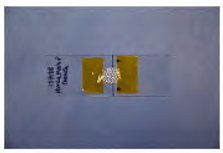
DSC_4575


DSC_4576


DSC_4577


DSC_4578


DSC_4579


DSC_4580


DSC_4581


DSC_4582


DSC_4583


DSC_4584


DSC_4585


DSC_4586


DSC_4587


DSC_4588

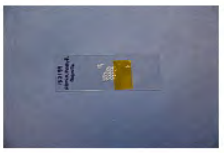
DSC_4589


DSC_4590


DSC_4591


DSC_4592


DSC_4593


DSC_4594


DSC_4595


DSC_4596


DSC_4597


DSC_4598


DSC_4599


DSC_4600


DSC_4601


DSC_4602

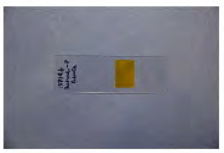
DSC_4603


DSC_4604


DSC_4605

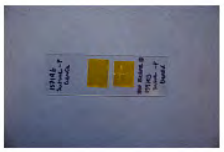
DSC_4606


DSC_4607


DSC_4608


DSC_4609


IMG_3190


PP Pellet-P-01

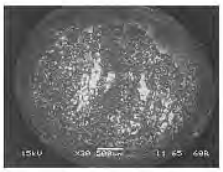
PP Pellet-R-01

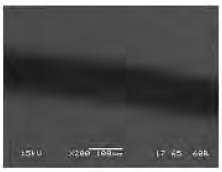
Suture-P-01

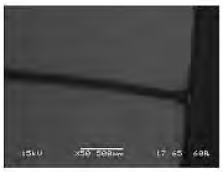
Suture-P-02

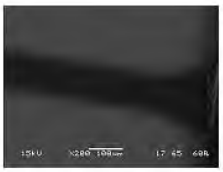
Suture-P-03

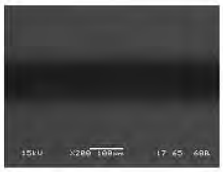
Suture-P-04

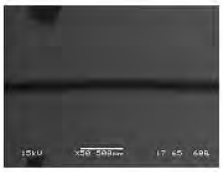
Suture-P-05

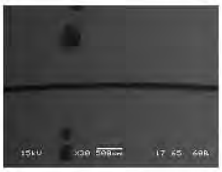
Suture-P-06


Suture-P-07

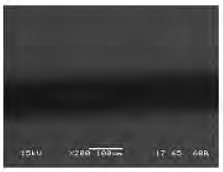
Suture-P-08

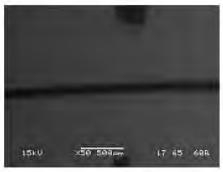
Suture-P-09

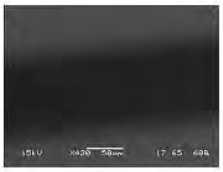
Suture-R-01

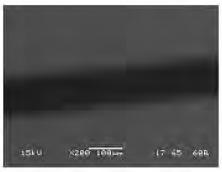
Suture-R-02

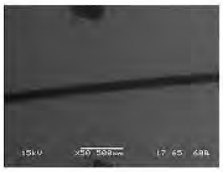
Suture-R-03


Suture-R-04

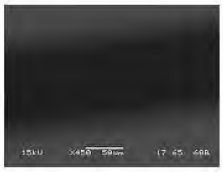
Suture-R-05


Suture-R-06

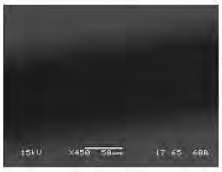
Suture-R-07

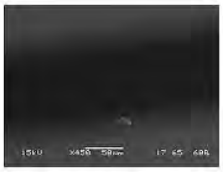
Suture-R-08


Suture-R-09

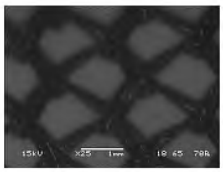
157164-TVT1-Chem Ox-P-01

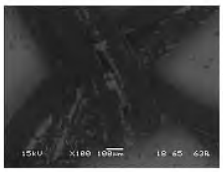
157164-TVT1-Chem Ox-P-02


157164-TVT1-Chem Ox-P-03

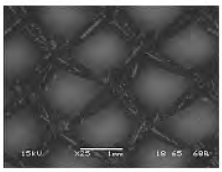
157165-TVT1-Chem Ox-R-01

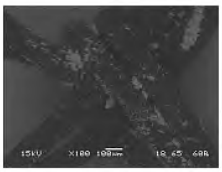
157165-TVT1-Chem Ox-R-02

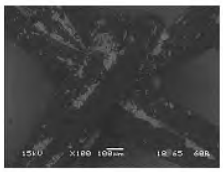
157165-TVT1-Chem Ox-R-03

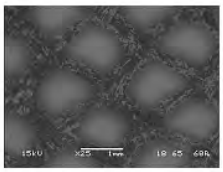
157172-TVT2-Chem Ox P-01

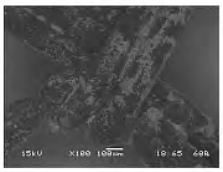
157172-TVT2-Chem Ox P-02

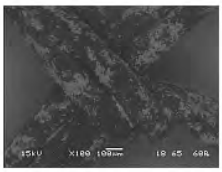
157172-TVT2-Chem Ox P-03

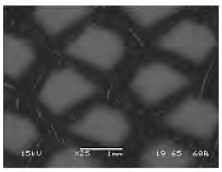
157173-TVT2-Chem Ox R-01

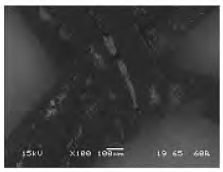
157173-TVT2-Chem Ox R-02

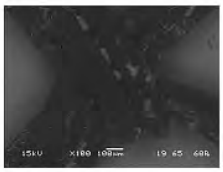
157173-TVT2-Chem Ox R-03

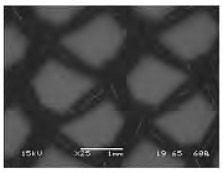
157180-TVT3-Chem Ox-P-01


157180-TVT3-Chem Ox-P-02

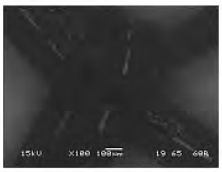
157180-TVT3-Chem Ox-P-03

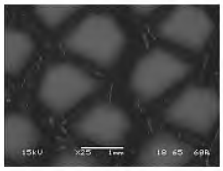
157181-TVT3-Chem Ox-R-01

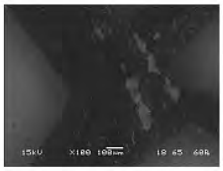
157181-TVT3-Chem Ox-R-02

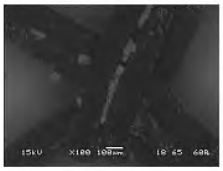
157181-TVT3-Chem Ox-R-03

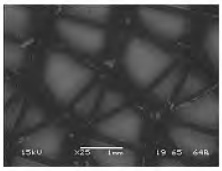
157188-Hernia Chem Ox-P-01

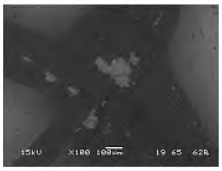
157188-Hernia Chem Ox-P-02

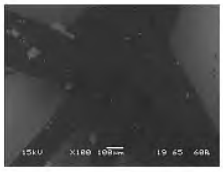
157188-Hernia Chem Ox-P-03

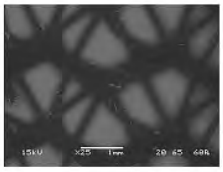
157189-Hernia Chem Ox-R-01

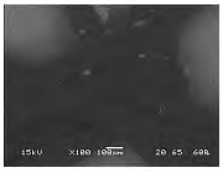
157189-Hernia Chem Ox-R-02

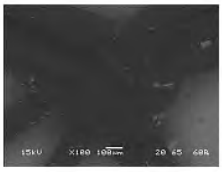
157189-Hernia Chem Ox-R-03

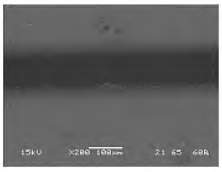
157196-Suture-Chem Ox-01

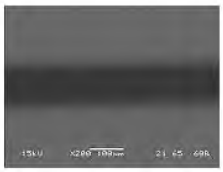

157196-Suture-Chem Ox-02

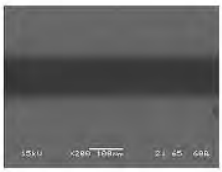

157196-Suture-Chem Ox-03

157196-Suture-Chem Ox-04

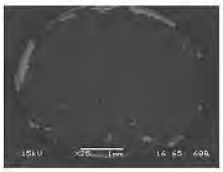

157232-PP Pellet-P-01

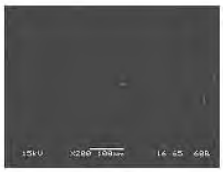

157232-PP Pellet-P-02

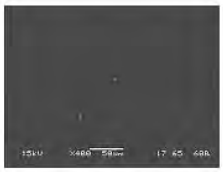

157232-PP Pellet-P-03

157232-PP Pellet-P-04

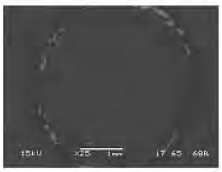

157233-PP Pellet-R-01

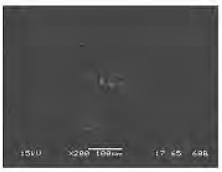

157233-PP Pellet-R-02

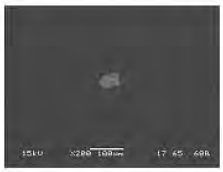

157233-PP Pellet-R-03

157233-PP Pellet-R-04

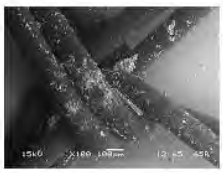

TVT1-01

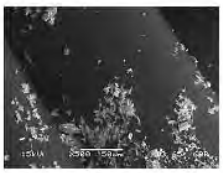

TVT1-02

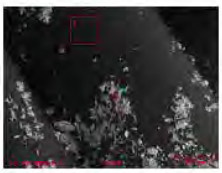

TVT1-EDS 1 Loc 1-2

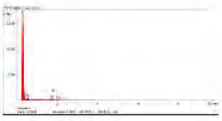

TVT1-EDS 1 Loc 1-2-1

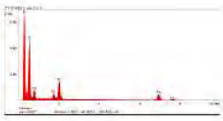

TVT1-EDS 1 Loc 1-2-2

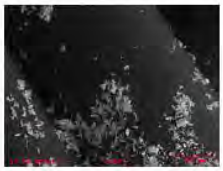

TVT1-EDS 1


157178_QUV_P_63x_H&E_ana_01-Image Export-01

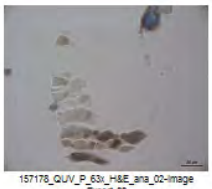
157178_QUV_P_63x_H&E_ana_02-Image Export-02


157178_QUV_P_63x_H&E_ana_03-Image Export-03


157178_QUV_P_63x_H&E_BF_01-Image Export-04


157178_QUV_P_63x_H&E_BF_02-Image Export-05


157178_QUV_P_63x_H&E_BF_03-Image Export-06


157178_QUV_P_63x_H&E_xpol_01-Image Export-07


157178_QUV_P_63x_H&E_xpol_02-Image Export-08

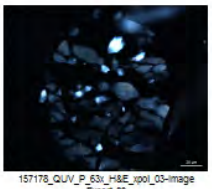
157178_QUV_P_63x_H&E_xpol_03-Image Export-09

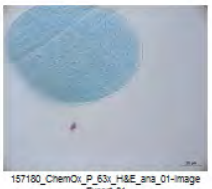
157180_ChemOx_P_63x_H&E_ana_01-Image Export-01

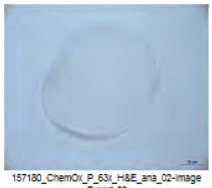
157180_ChemOx_P_63x_H&E_ana_02-Image Export-02


157180_ChemOx_P_63x_H&E_ana_03-Image Export-03


157180_ChemOx_P_63x_H&E_ana_04-Image Export-04

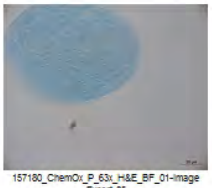
157180_ChemOx_P_63x_H&E_BF_01-Image Export-05


157180_ChemOx_P_63x_H&E_BF_02-Image Export-06


157180_ChemOx_P_63x_H&E_BF_03-Image Export-07


157180_ChemOx_P_63x_H&E_BF_04-Image Export-08

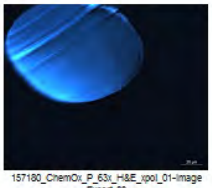
157180_ChemOx_P_63x_H&E_xpol_01-Image Export-09

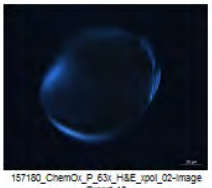
157180_ChemOx_P_63x_H&E_xpol_02-Image Export-10

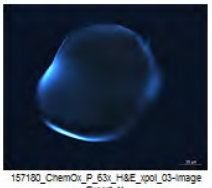
157180_ChemOx_P_63x_H&E_xpol_03-Image Export-11


157180_ChemOx_P_63x_H&E_xpol_04-Image Export-12

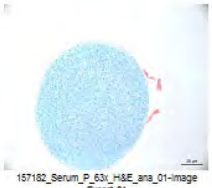
157182_Serum_P_63x_H&E_ana_01-Image Export-01

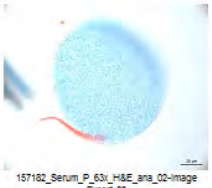
157182_Serum_P_63x_H&E_ana_02-Image Export-02

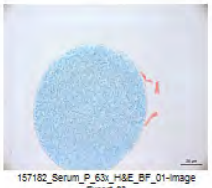
157182_Serum_P_63x_H&E_BF_01-Image Export-03

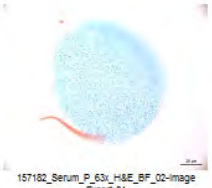
157182_Serum_P_63x_H&E_BF_02-Image Export-04

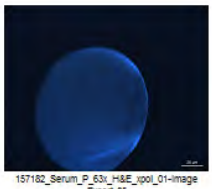
157182_Serum_P_63x_H&E_xpol_01-image Export-05

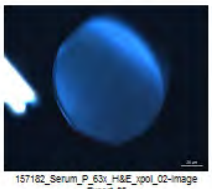
157182_Serum_P_63x_H&E_xpol_02-image Export-06

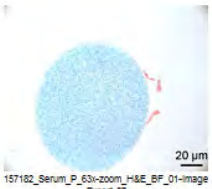

157182_Serum_P_63x-zoom_H&E_BF_01-image Export-07

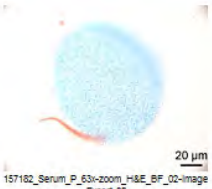

157182_Serum_P_63x-zoom_H&E_BF_02-image Export-08


157186_Hernia_QUV_P_63x_H&E_ana_01-image Export-01

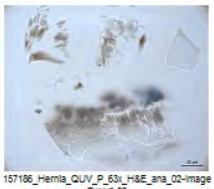
157186_Hernia_QUV_P_63x_H&E_ana_02-image Export-02


157186_Hernia_QUV_P_63x_H&E_BF_01-image Export-03


157186_Hernia_QUV_P_63x_H&E_BF_02-image Export-04


157186_Hernia_QUV_P_63x_H&E_xpol_01-image Export-05

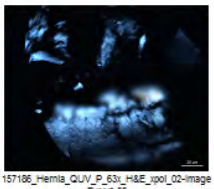
157186_Hernia_QUV_P_63x_H&E_xpol_02-image Export-06


157188_Hernia_ChemOx_P_63x_H&E_ana_01-image Export-01


157188_Hernia_ChemOx_P_63x_H&E_ana_02-image Export-02


157188_Hernia_ChemOx_P_63x_H&E_ana_03-image Export-03


157188_Hernia_ChemOx_P_63x_H&E_BF_01-image Export-04


157188_Hernia_ChemOx_P_63x_H&E_BF_02-image Export-05


157188_Hernia_ChemOx_P_63x_H&E_BF_03-image Export-06

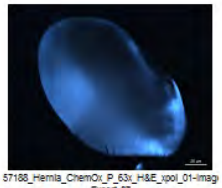
157188_Hernia_ChemOx_P_63x_H&E_xpol_01-image Export-07

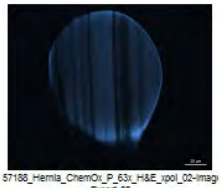
157188_Hernia_ChemOx_P_63x_H&E_xpol_02-image Export-08

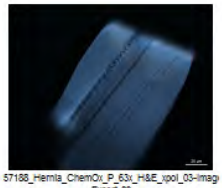
157188_Hernia_ChemOx_P_63x_H&E_xpol_03-image Export-09


157190_Hernia_Serum_P_63x_H&E_ana_01-image Export-01


157190_Hernia_Serum_P_63x_H&E_ana_02-image Export-02


157190_Hernia_Serum_P_63x_H&E_BF_01-image Export-03


157190_Hernia_Serum_P_63x_H&E_BF_02-image Export-04

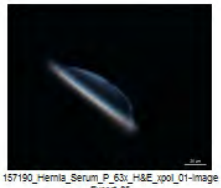
157190_Hernia_Serum_P_63x_H&E_xpol_01-image Export-05

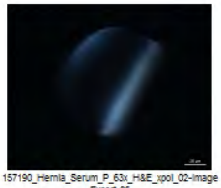
157190_Hernia_Serum_P_63x_H&E_xpol_02-image Export-06


157194_Suture_QUV_P_63x_H&E_ana_01-Image Export-07


157194_Suture_QUV_P_63x_H&E_ana_05-Image Export-08


157194_Suture_QUV_P_63x_H&E_BF_01-Image Export-09


157194_Suture_QUV_P_63x_H&E_BF_02-Image Export-10


157194_Suture_QUV_P_63x_H&E_BF_03-Image Export-11


157194_Suture_QUV_P_63x_H&E_BF_04-Image Export-12


157194_Suture_QUV_P_63x_H&E_BF_05-Image Export-13


157194_Suture_QUV_P_63x_H&E_xpol_01-Image Export-14


157194_Suture_QUV_P_63x_H&E_xpol_05-Image Export-15


157198_Suture_Serum_P_63x_H&E_ana_04-Image Export-01


157198_Suture_Serum_P_63x_H&E_BF_01-Image Export-02


157198_Suture_Serum_P_63x_H&E_BF_02-Image Export-03


157198_Suture_Serum_P_63x_H&E_BF_03-Image Export-04


157198_Suture_Serum_P_63x_H&E_BF_04-Image Export-05


157198_Suture_Serum_P_63x_H&E_xpol_04-Image Export-06


157880_Control_P_63x_H&E_ana_01-Image Export-01


157880_Control_P_63x_H&E_ana_02-Image Export-02


157880_Control_P_63x_H&E_ana_03-Image Export-03


157880_Control_P_63x_H&E_ana_06-Image Export-04


157880_Control_P_63x_H&E_BF_01-Image Export-05


157880_Control_P_63x_H&E_BF_02-Image Export-06


157880_Control_P_63x_H&E_BF_03-Image Export-07


157880_Control_P_63x_H&E_BF_04-Image Export-08


157880_Control_P_63x_H&E_BF_05-Image Export-09


157880_Control_P_63x_H&E_BF_06-Image Export-10


157880_Control_P_63x_H&E_xpol_01-image Export-11


157880_Control_P_63x_H&E_xpol_02-image Export-12

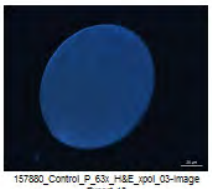
157880_Control_P_63x_H&E_xpol_03-image Export-13

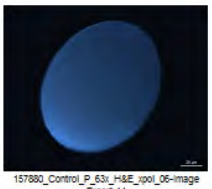
157880_Control_P_63x_H&E_xpol_06-image Export-14


157884_Control_P_63x_H&E_ana_01-image Export-01


157884_Control_P_63x_H&E_ana_04-image Export-02

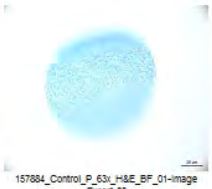
157884_Control_P_63x_H&E_BF_01-image Export-03


157884_Control_P_63x_H&E_BF_02-image Export-04


157884_Control_P_63x_H&E_BF_03-image Export-05


157884_Control_P_63x_H&E_BF_04-image Export-06

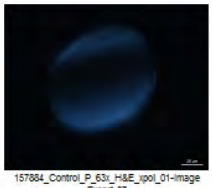
157884_Control_P_63x_H&E_xpol_01-image Export-07


157884_Control_P_63x_H&E_xpol_04-image Export-08

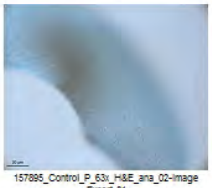
157895_Control_P_63x_H&E_ana_02-image Export-01


157895_Control_P_63x_H&E_ana_05-image Export-02

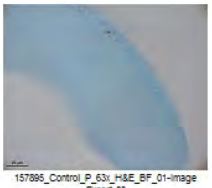
157895_Control_P_63x_H&E_BF_01-image Export-03

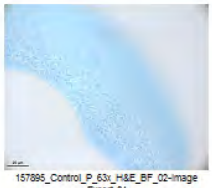
157895_Control_P_63x_H&E_BF_02-image Export-04


157895_Control_P_63x_H&E_BF_03-image Export-05


157895_Control_P_63x_H&E_BF_04-image Export-06


157895_Control_P_63x_H&E_BF_05-image Export-07

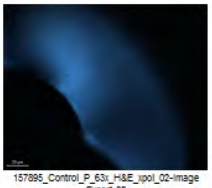
157895_Control_P_63x_H&E_xpol_02-image Export-08

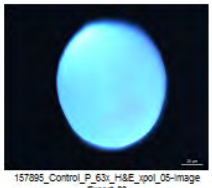
157895_Control_P_63x_H&E_xpol_05-image Export-09


157899_Hernia_Control_P_63x_H&E_ana_01-image Export-01


157899_Hernia_Control_P_63x_H&E_ana_02-image Export-02


157899_Hernia_Control_P_63x_H&E_BF_01-image Export-03


157899_Hernia_Control_P_63x_H&E_BF_02-image Export-04

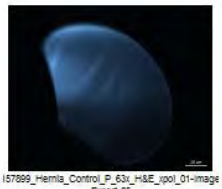
157899_Hernia_Control_P_63x_H&E_ypol_01-image Export-05


157899_Hernia_Control_P_63x_H&E_ypol_02-image Export-06

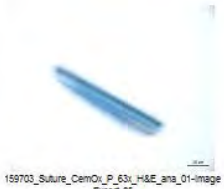
159703_Suture_CemOx_P_63x_H&E_ana_01-image Export-05


159703_Suture_CemOx_P_63x_H&E_ana_05-image Export-08


159703_Suture_CemOx_P_63x_H&E_BF_01-image Export-01


159703_Suture_CemOx_P_63x_H&E_BF_02-image Export-02


159703_Suture_CemOx_P_63x_H&E_BF_03-image Export-03


159703_Suture_CemOx_P_63x_H&E_BF_04-image Export-04


159703_Suture_CemOx_P_63x_H&E_BF_05-image Export-07

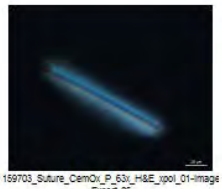
159703_Suture_CemOx_P_63x_H&E_ypol_01-image Export-06


159703_Suture_CemOx_P_63x_H&E_ypol_05-image Export-09

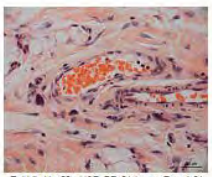
Rabbit skin_63x_H&E_BF_01-image Export-01

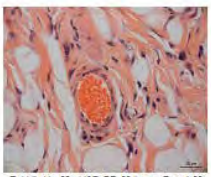
Rabbit skin_63x_H&E_BF_02-image Export-02

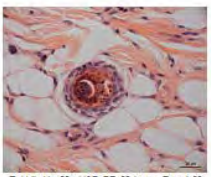
Rabbit skin_63x_H&E_BF_03-image Export-03

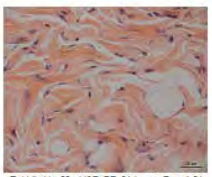
Rabbit skin_63x_H&E_BF_04-image Export-01

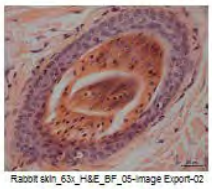
Rabbit skin_63x_H&E_BF_05-image Export-02

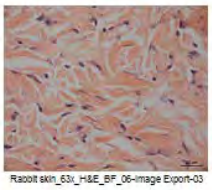
Rabbit skin_63x_H&E_BF_06-image Export-03

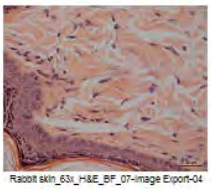
Rabbit skin_63x_H&E_BF_07-image Export-04


162_QUV-P_40x_Unstained_BF

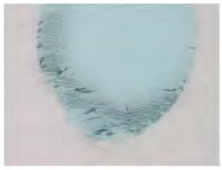
162_QUV-P_40x_Unstained_BF


4_ChemOx-P_10x_Unstained_I


4_ChemOx-P_10x_Unstained_I


4_ChemOx-P_10x_Unstained_I

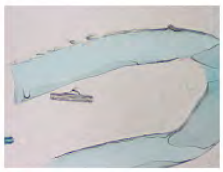
66_Serum-P_10x_Unstained_B


66_Serum-P_40x_Unstained_B


66_Serum-P_40x_Unstained_B


170_QUV-P_10x_Unstained_BF


170_QUV-P_10x_Unstained_BF

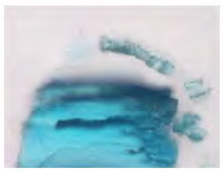
170_QUV-P_40x_Unstained_BF


2_ChemOx-P_10x_Unstained_I


2_ChemOx-P_40x_Unstained_I


2_ChemOx-P_40x_Unstained_I


74_Serum-P_40x_Unstained_B

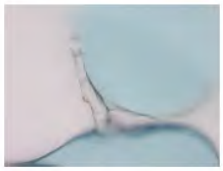
74_Serum-P_40x_Unstained_B


178_QUV-P_10x_Unstained_BF


178_QUV-P_40x_Unstained_BF

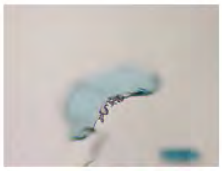
0_ChemOx-P_10x_Unstained_I


0_ChemOx-P_10x_Unstained_I


0_ChemOx-P_10x_Unstained_I


0_ChemOx-P_10x_Unstained_I


0_ChemOx-P_40x_Unstained_I


0_ChemOx-P_40x_Unstained_I


0_ChemOx-P_40x_Unstained_I

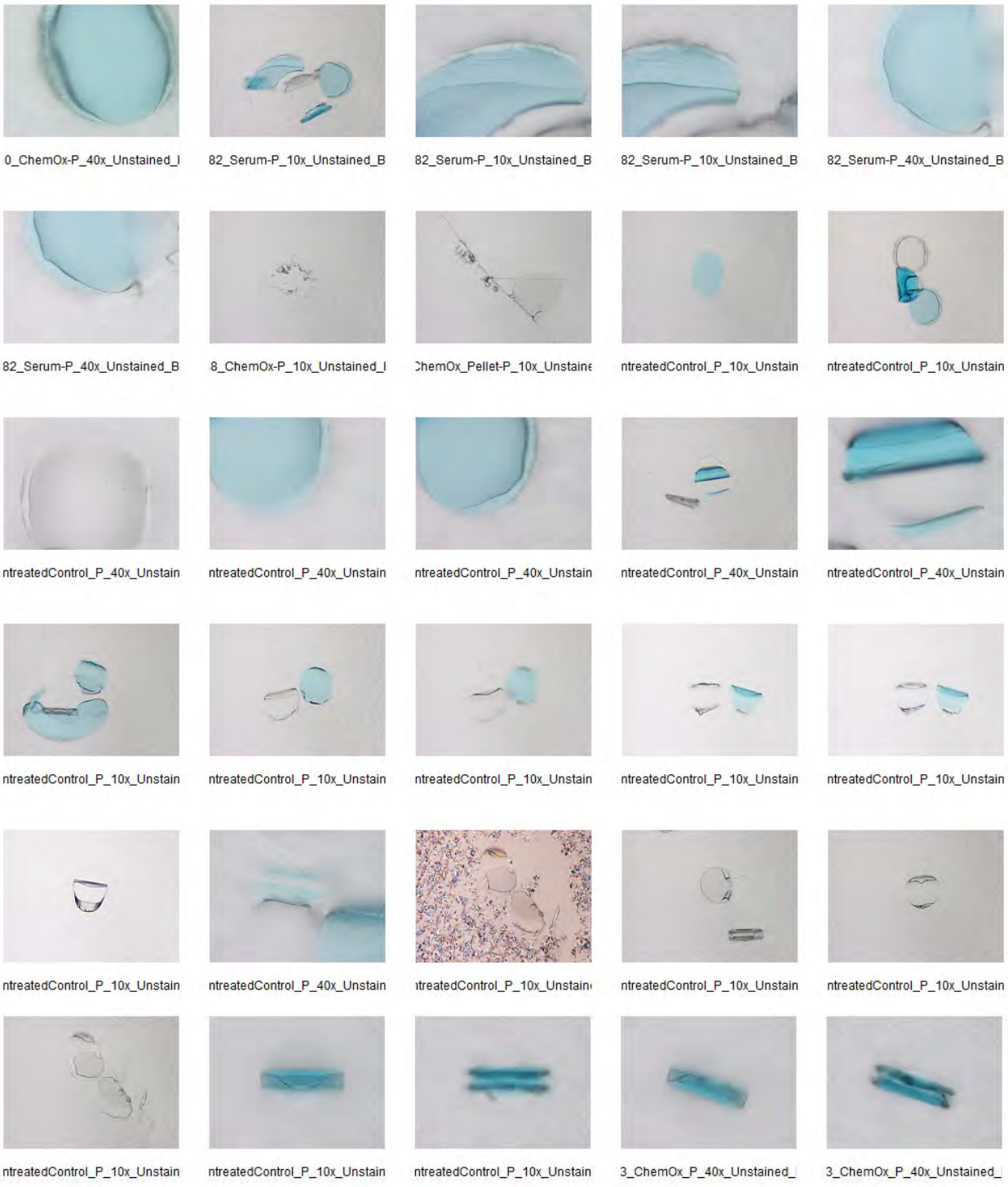
0_ChemOx-P_40x_Unstained_I
82_Serum-P_10x_Unstained_B
82_Serum-P_10x_Unstained_B
82_Serum-P_10x_Unstained_B
82_Serum-P_40x_Unstained_B
82_Serum-P_40x_Unstained_B
8_ChemOx-P_10x_Unstained_I
ChemOx_Pellet-P_10x_Unstaine
ntreatedControl_P_10x_Unstain
ntreatedControl_P_10x_Unstain
ntreatedControl_P_40x_Unstain
ntreatedControl_P_40x_Unstain
ntreatedControl_P_40x_Unstain
ntreatedControl_P_40x_Unstain
ntreatedControl_P_40x_Unstain
ntreatedControl_P_10x_Unstain
ntreatedControl_P_10x_Unstain
ntreatedControl_P_10x_Unstain
ntreatedControl_P_10x_Unstain
ntreatedControl_P_10x_Unstain
ntreatedControl_P_10x_Unstain
ntreatedControl_P_40x_Unstain
ntreatedControl_P_10x_Unstain
ntreatedControl_P_10x_Unstain
ntreatedControl_P_10x_Unstain
ntreatedControl_P_10x_Unstain
ntreatedControl_P_10x_Unstain
3_ChemOx_P_40x_Unstained_
3_ChemOx_P_40x_Unstained_


157164_ChemOx_P_63x_H&E_ana_01-image Export-15


157164_ChemOx_P_63x_H&E_BF_01-image Export-16


157164_ChemOx_P_63x_H&E_BF_02-image Export-17

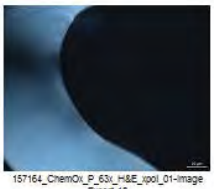
157164_ChemOx_P_63x_H&E_xpol_01-image Export-18

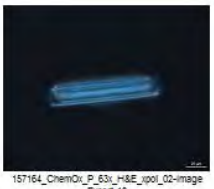
157164_ChemOx_P_63x_H&E_xpol_02-image Export-19

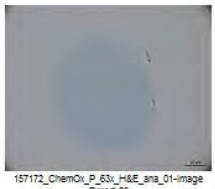
157172_ChemOx_P_63x_H&E_ana_01-image Export-29


157172_ChemOx_P_63x_H&E_ana_02-image Export-30


157172_ChemOx_P_63x_H&E_BF_01-image Export-31

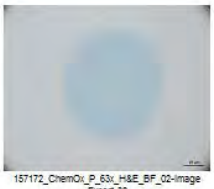
157172_ChemOx_P_63x_H&E_BF_02-image Export-32

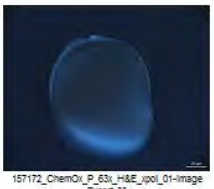
157172_ChemOx_P_63x_H&E_xpol_01-image Export-33

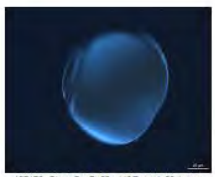
157172_ChemOx_P_63x_H&E_xpol_02-image Export-34

157172_ChemOx_P_63xzoom_H&E_BF_02-image Export-35

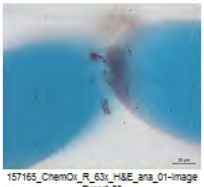
157165_ChemOx_R_63x_H&E_ana_01-image Export-82

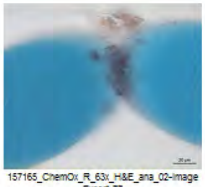
157165_ChemOx_R_63x_H&E_ana_02-image Export-77

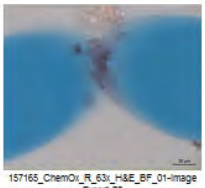
157165_ChemOx_R_63x_H&E_BF_01-image Export-78

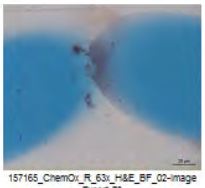
157165_ChemOx_R_63x_H&E_BF_02-image Export-79

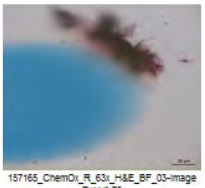
157165_ChemOx_R_63x_H&E_BF_03-image Export-73

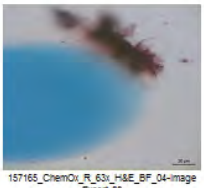
157165_ChemOx_R_63x_H&E_BF_04-image Export-80

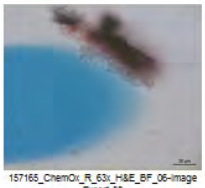
157165_ChemOx_R_63x_H&E_BF_06-image Export-50

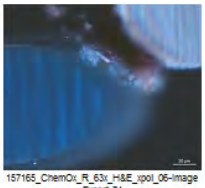
157165_ChemOx_R_63x_H&E_xpol_06-image Export-74

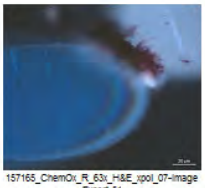
157165_ChemOx_R_63x_H&E_xpol_07-image Export-51

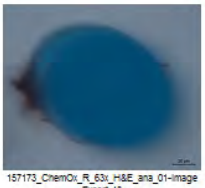
157173_ChemOx_R_63x_H&E_ana_01-image Export-43

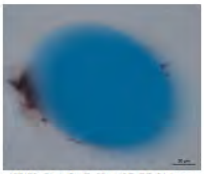
157173_ChemOx_R_63x_H&E_BF_01-image Export-44

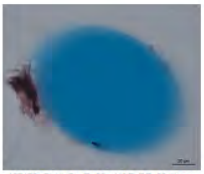
157173_ChemOx_R_63x_H&E_BF_02-image Export-45


157173_ChemOx_R_63x_H&E_xpol_01-image Export-48


157181_ChemOx_R_63x_H&E_ana_01-image Export-34

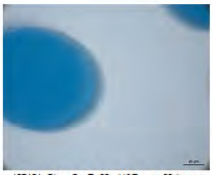
157181_ChemOx_R_63x_H&E_ana_03-image Export-13


157181_ChemOx_R_63x_H&E_BF_01-image Export-39

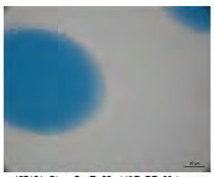
157181_ChemOx_R_63x_H&E_BF_02-image Export-14


157181_ChemOx_R_63x_H&E_xpol_01-image Export-35


157181_ChemOx_R_63x_H&E_xpol_03-image Export-15

157181_ChemOx_R_63xzoom_H&E_BF_02-image Export-01


157189_ChemOx_R_63x_H&E_ana_01-image Export-17


157189_ChemOx_R_63x_H&E_ana_02-image Export-18


157189_ChemOx_R_63x_H&E_BF_01-image Export-19


157189_ChemOx_R_63x_H&E_BF_02-image Export-20

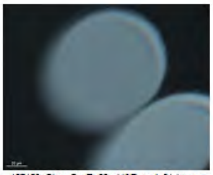
157189_ChemOx_R_63x_H&E_xpol_01-image Export-09

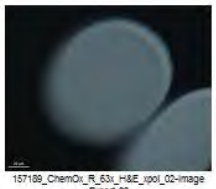
157189_ChemOx_R_63x_H&E_xpol_02-Image Export-22


157233_Pellet_ChemOx_R_63x_H&E_ana_01-Image Export-45


157233_Pellet_ChemOx_R_63x_H&E_BF_01-Image Export-26

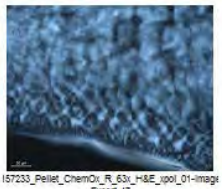
157233_Pellet_ChemOx_R_63x_H&E_xpol_01-Image Export-47


159704_ChemOx_R_10x_H&E_BF_01-Draw Scale Bar Annotation-01-Image Export-07


159704_ChemOx_R_10x_H&E_BF_01-Image Export-56


159704_ChemOx_R_20x_H&E_ana_01-Image Export-58


159704_ChemOx_R_63x_H&E_ana_01-Image Export-59

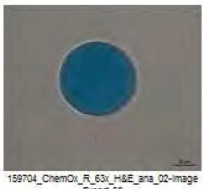
159704_ChemOx_R_63x_H&E_ana_02-Image Export-60

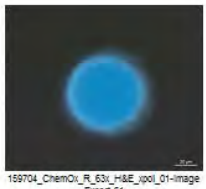
159704_ChemOx_R_63x_H&E_xpol_01-Image Export-61

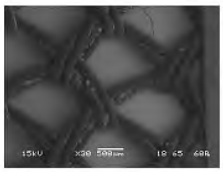
157164-TVT1-Chem Ox-P_01

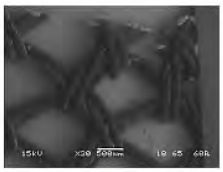
157164-TVT1-Chem Ox-P_02

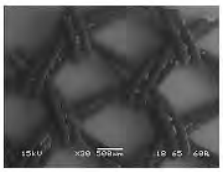
157164-TVT1-Chem Ox-P_03

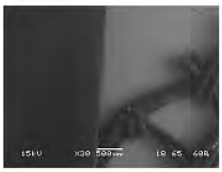
157164-TVT1-Chem Ox-P_04

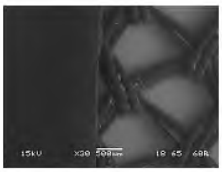
157164-TVT1-Chem Ox-P_05

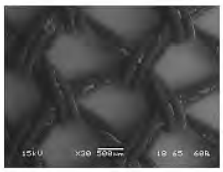
157164-TVT1-Chem Ox-P_06

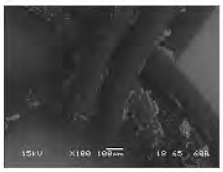
157164-TVT1-Chem Ox-P_07

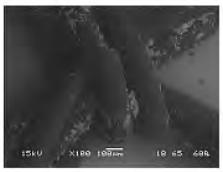
157164-TVT1-Chem Ox-P_08

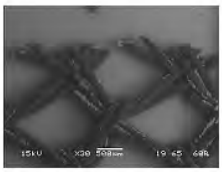
157165-TVT1-Chem Ox-R_01


157165-TVT1-Chem Ox-R_02

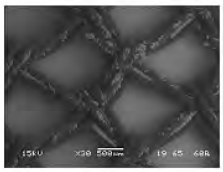
157165-TVT1-Chem Ox-R_03

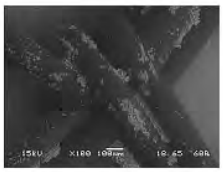
157165-TVT1-Chem Ox-R_04

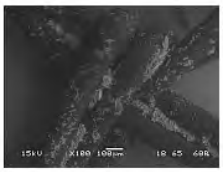
157165-TVT1-Chem Ox-R_05


157172-TVT2-Chem Ox P_01

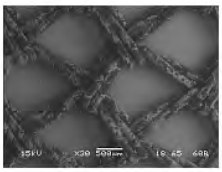
157172-TVT2-Chem Ox P_02

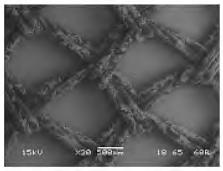
157172-TVT2-Chem Ox P_03

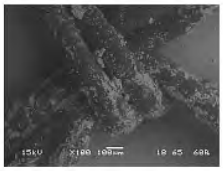
157172-TVT2-Chem Ox P_04

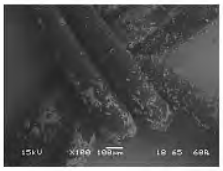
157172-TVT2-Chem Ox P_05

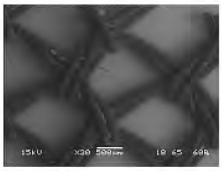
157173-TVT2-Chem Ox R_01

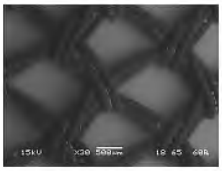
157173-TVT2-Chem Ox R_02

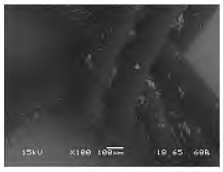
157173-TVT2-Chem Ox R_03

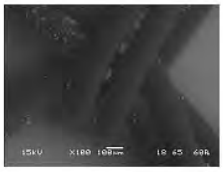
157173-TVT2-Chem Ox R_04

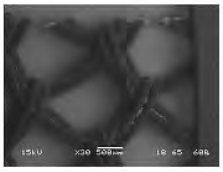
157180-TVT3-Chem Ox-P_01

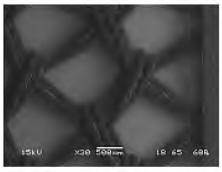
157180-TVT3-Chem Ox-P_02

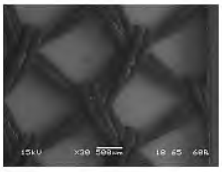
157180-TVT3-Chem Ox-P_03

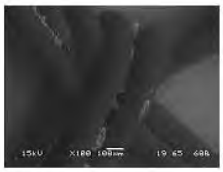
157180-TVT3-Chem Ox-P_04

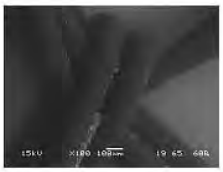
157180-TVT3-Chem Ox-P_05

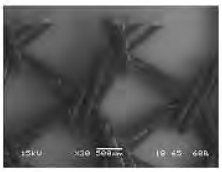
157181-TVT3-Chem Ox-R_01

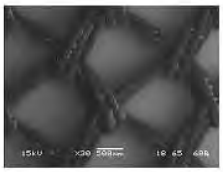
157181-TVT3-Chem Ox-R_02

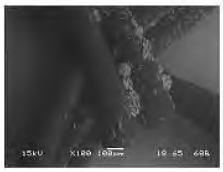
157181-TVT3-Chem Ox-R_03

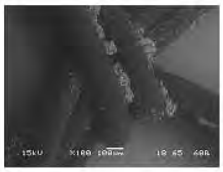
157181-TVT3-Chem Ox-R_04


157188-Hernia Chem Ox-P_01

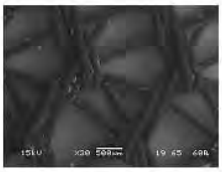
157188-Hernia Chem Ox-P_02


157188-Hernia Chem Ox-P_03

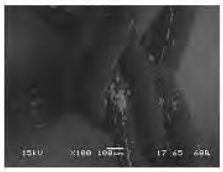
157188-Hernia Chem Ox-P_04

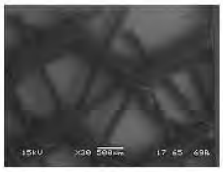
157189-Hernia Chem Ox-R_01

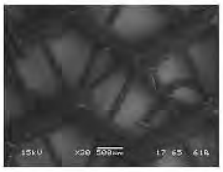
157189-Hernia Chem Ox-R_02

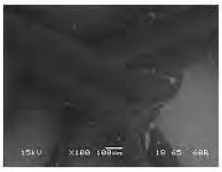
157189-Hernia Chem Ox-R_03


157189-Hernia Chem Ox-R_04

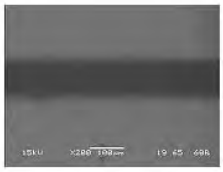
159703-Suture-Chem Ox-P_01

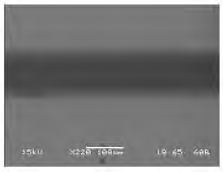
159703-Suture-Chem Ox-P02

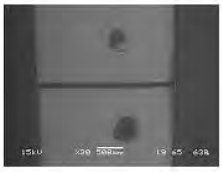
159704-Suture-Chem Ox-R_01

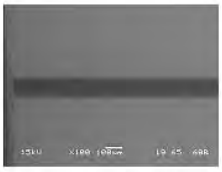
159704-Suture-Chem Ox-R_02

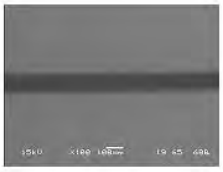
159704-Suture-Chem Ox-R_03

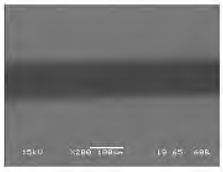
159704-Suture-Chem Ox-R_04


157185_Pristine_R_63x_H&E_BF_01-Image Export-36


157187_QUV_R_63x_H&E_ana_01-Image Export-21


157187_QUV_R_63x_H&E_ana_04-Image Export-22


157187_QUV_R_63x_H&E_BF_02-Image Export-23


157187_QUV_R_63x_H&E_BF_05-Image Export-12


157187_QUV_R_63x_H&E_xpol_02-Image Export-24

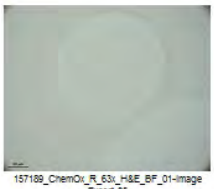
157189_ChemOx_R_63x_H&E_BF_01-Image Export-25

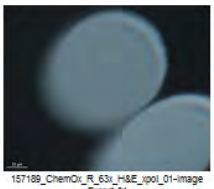
157189_ChemOx_R_63x_H&E_xpol_01-Image Export-21


157193_Pristine_R_63x_H&E_BF_01-Image Export-32

157195_QUV_R_63x-zoom_H&E_ana_01-Image Export-37


157199_Serum_R_63x_H&E_BF_01-Image Export-39


157233_Pellet_ChemOx_R_63x_H&E_BF_01-Image Export-46

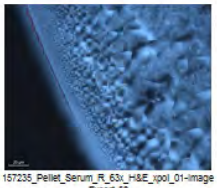
157235_Pellet_Serum_R_63x_H&E_xpol_01-Image Export-52


157237_Pellet_Pristine_R_63x_H&E_BF_01-Image Export-54

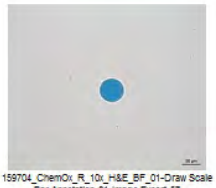
159704_ChemOx_R_10x_H&E_BF_01-Draw Scale Bar Annotation-01-Image Export-57


159704_ChemOx_R_10x_H&E_BF_01-Image Export-85

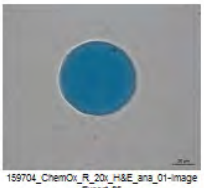
159704_ChemOx_R_20x_H&E_ana_01-Image Export-86

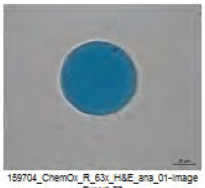
159704_ChemOx_R_63x_H&E_ana_01-Image Export-87

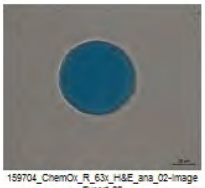
159704_ChemOx_R_63x_H&E_ana_02-Image Export-88

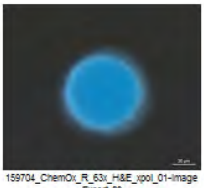
159704_ChemOx_R_63x_H&E_xpol_01-Image Export-89

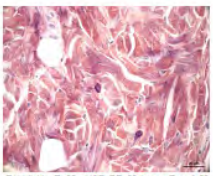
Rabbitskin_R_63x_H&E_BF_02-Image Export-63


DSC_9609

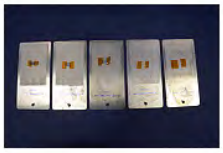
DSC_9610

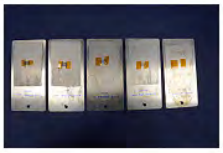
DSC_9611


DSC_9612


DSC_9613


DSC_9614


DSC_9615


DSC_9616


DSC_9617


DSC_9618


DSC_9619


DSC_9620


DSC_9621


DSC_9622


DSC_9623


DSC_9624

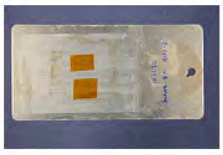
DSC_9625


DSC_9626


DSC_9627


DSC_9628

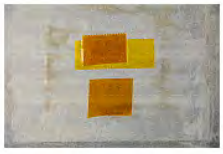
DSC_9629


DSC_9630


DSC_9631


DSC_9632


DSC_9633


DSC_9634


DSC_9635


DSC_9636


DSC_9637


DSC_9638


DSC_9639


DSC_9640

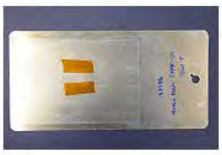
DSC_9641


DSC_9642

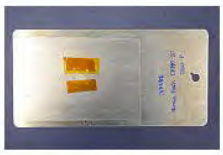
DSC_9643


DSC_9644


DSC_9645


DSC_9646


DSC_9647


DSC_9648


DSC_9649

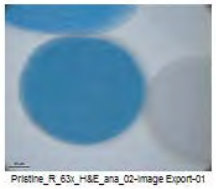
Pristine_R_63x_H&E_ana_02-Image Export-01

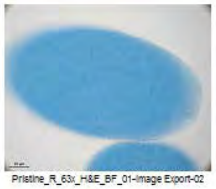
Pristine_R_63x_H&E_BF_01-Image Export-02

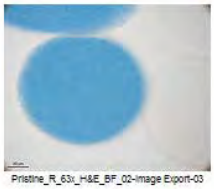
Pristine_R_63x_H&E_BF_02-Image Export-03


Pristine_R_63x_H&E_pol_02-Image Export-04

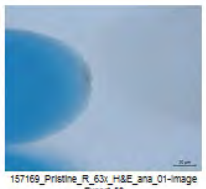
157169_Pristine_R_63x_H&E_ana_01-image Export-59

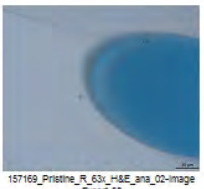
157169_Pristine_R_63x_H&E_ana_02-image Export-60


157169_Pristine_R_63x_H&E_BF_01-image Export-61

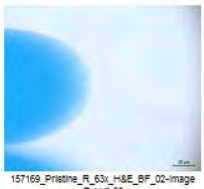
157169_Pristine_R_63x_H&E_BF_02-image Export-62

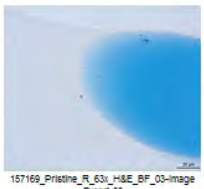
157169_Pristine_R_63x_H&E_BF_03-image Export-63

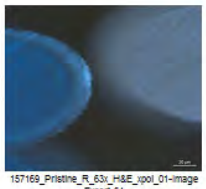
157169_Pristine_R_63x_H&E_xpol_01-image Export-64

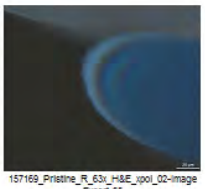
157169_Pristine_R_63x_H&E_xpol_02-image Export-65

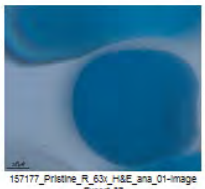
157177_Pristine_R_63x_H&E_ana_01-image Export-37


157177_Pristine_R_63x_H&E_ana_02-image Export-33


157177_Pristine_R_63x_H&E_BF_01-image Export-46


157177_Pristine_R_63x_H&E_BF_02-image Export-38

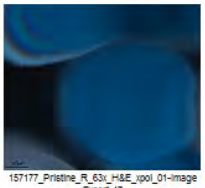
157177_Pristine_R_63x_H&E_xpol_01-image Export-47


157177_Pristine_R_63x_H&E_xpol_02-image Export-31

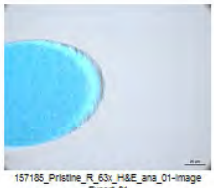
157185_Pristine_R_63x_H&E_ana_01-image Export-01


157185_Pristine_R_63x_H&E_BF_01-image Export-02

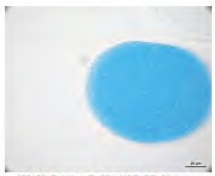
157185_Pristine_R_63x_H&E_BF_02-image Export-03

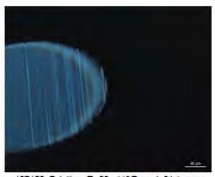
157185_Pristine_R_63x_H&E_xpol_01-image Export-04


157193_Pristine_R_63x_H&E_BF_01-image Export-30


157193_Pristine_R_63x_H&E_xpol_01-image Export-33


157201_Pristine_R_63x_H&E_ana_01-image Export-41


157201_Pristine_R_63x_H&E_BF_01-image Export-42


157201_Pristine_R_63x_H&E_xana_01-image Export-43


157201_Pristine_R_63x_H&E_xpol_01-image Export-44


157237_Pellet_Pristine_R_63x_H&E_ana_01-image Export-53


157237_Pellet_Pristine_R_63x_H&E_BF_01-image Export-28


157237_Pellet_Pristine_R_63x_H&E_xpol_01-image Export-55


157162_QUV_P_63x_H&E_ana_01-Image Export-01


157162_QUV_P_63x_H&E_ana_02-Image Export-02


157162_QUV_P_63x_H&E_ana_03-Image Export-03


157162_QUV_P_63x_H&E_ana_04-Image Export-04


157162_QUV_P_63x_H&E_BF_01-Image Export-05


157162_QUV_P_63x_H&E_BF_02-Image Export-06


157162_QUV_P_63x_H&E_BF_03-Image Export-07

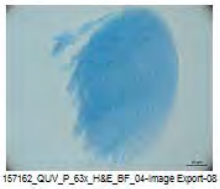
157162_QUV_P_63x_H&E_BF_04-Image Export-08

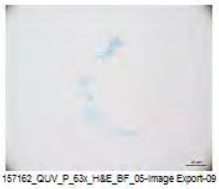
157162_QUV_P_63x_H&E_BF_05-Image Export-09

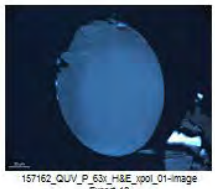
157162_QUV_P_63x_H&E_xpol_01-Image Export-10


157162_QUV_P_63x_H&E_xpol_02-Image Export-11


157162_QUV_P_63x_H&E_xpol_03-Image Export-12


157162_QUV_P_63x_H&E_xpol_04-Image Export-13


157162_QUV_xpol_1-Image Export-14


157170_QUV_P_63x_H&E_ana_01-Image Export-23


157170_QUV_P_63x_H&E_ana_02-Image Export-24


157170_QUV_P_63x_H&E_BF_01-Image Export-25


157170_QUV_P_63x_H&E_BF_02-Image Export-26

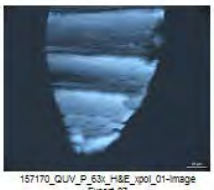
157170_QUV_P_63x_H&E_xpol_01-Image Export-27

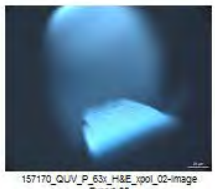
157170_QUV_P_63x_H&E_xpol_02-Image Export-28

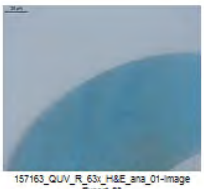
157163_QUV_R_63x_H&E_ana_01-image Export-83

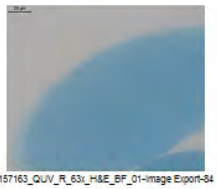
157163_QUV_R_63x_H&E_BF_01-image Export-84

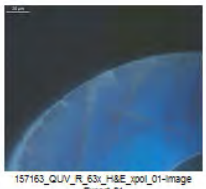
157163_QUV_R_63x_H&E_xpol_01-image Export-81

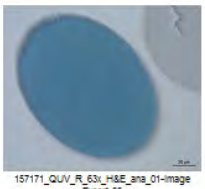
157171_QUV_R_63x_H&E_ana_01-image Export-66


157171_QUV_R_63x_H&E_ana_02-image Export-67

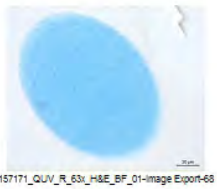
157171_QUV_R_63x_H&E_BF_01-image Export-68


157171_QUV_R_63x_H&E_BF_02-image Export-69

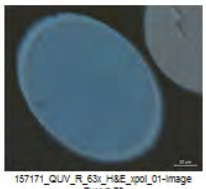
157171_QUV_R_63x_H&E_xpol_01-image Export-70

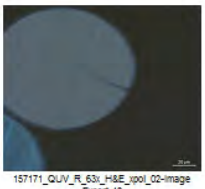
157171_QUV_R_63x_H&E_xpol_02-image Export-42


157179_QUV_R_63x_H&E_ana_01-image Export-32


157179_QUV_R_63x_H&E_BF_01-image Export-11

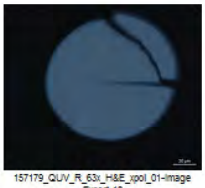
157179_QUV_R_63x_H&E_xpol_01-image Export-12


157187_QUV_R_63x_H&E_ana_01-image Export-05


157187_QUV_R_63x_H&E_ana_02-image Export-06

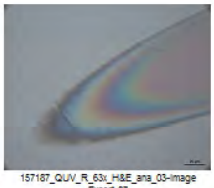
157187_QUV_R_63x_H&E_ana_03-image Export-07


157187_QUV_R_63x_H&E_ana_04-image Export-08


157187_QUV_R_63x_H&E_BF_01-image Export-09


157187_QUV_R_63x_H&E_BF_02-image Export-10


157187_QUV_R_63x_H&E_BF_04-image Export-11


157187_QUV_R_63x_H&E_BF_05-image Export-08

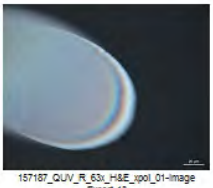
157187_QUV_R_63x_H&E_xpol_01-image Export-13


157187_QUV_R_63x_H&E_xpol_02-image Export-14

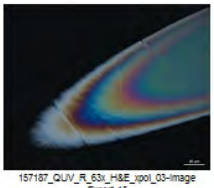
157187_QUV_R_63x_H&E_xpol_03-image Export-15

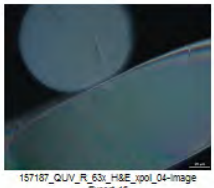
157187_QUV_R_63x_H&E_xpol_04-image Export-16


157195_QUV_R_63x_H&E_ana_01-image Export-34


157195_QUV_R_63x_H&E_BF_01-image Export-35


157195_QUV_R_63x_H&E_xpol_01-image Export-36

157195_QUV_R_63x-zoom_H&E_ana_01-image Export-06

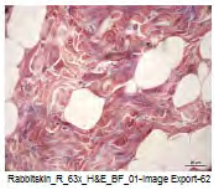
Rabbitskin_R_63x_H&E_BF_01-Image Export-62


Rabbitskin_R_63x_H&E_BF_02-Draw Scale Bar Annotation-02-Image Export-64


Rabbitskin_R_63x_H&E_BF_02-Draw Scale Bar Annotation-03-Image Export-65

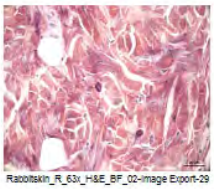
Rabbitskin_R_63x_H&E_BF_02-Image Export-29


Rabbitskin_R_63x_H&E_xpol_01-Image Export-66


Rabbitskin_R_63x_H&E_xpol_02-Draw Scale Bar Annotation-01-Image Export-68

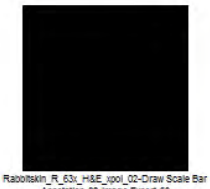
Rabbitskin_R_63x_H&E_xpol_02-Draw Scale Bar Annotation-02-Image Export-69


Rabbitskin_R_63x_H&E_xpol_02-Image Export-67

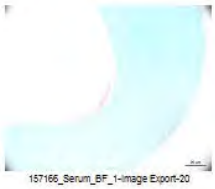
157166_Serum_BF_1-Image Export-20


157166_Serum_BF_2-Image Export-21


157166_Serum_xpol_2-Image Export-22

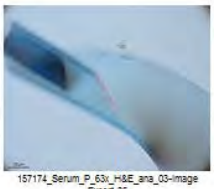
157174_Serum_P_63x_H&E_ana_03-Image Export-36

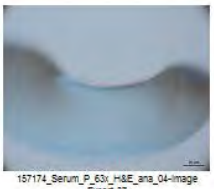
157174_Serum_P_63x_H&E_ana_04-Image Export-37


157174_Serum_P_63x_H&E_BF_01-Image Export-38


157174_Serum_P_63x_H&E_BF_02-Image Export-39


157174_Serum_P_63x_H&E_BF_03-Image Export-40


157174_Serum_P_63x_H&E_BF_04-Image Export-41


157174_Serum_P_63x_H&E_xpol_01-Image Export-42

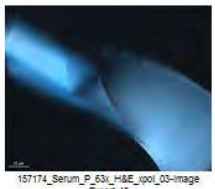
157174_Serum_P_63x_H&E_xpol_03-Image Export-43

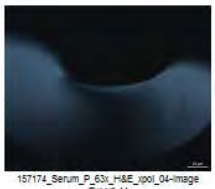
157174_Serum_P_63x_H&E_xpol_04-Image Export-44

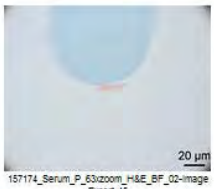

157174_Serum_P_63xzoom_H&E_BF_02-Image Export-45


157235_Pellet_Serum_R_63x_H&E_ana_01-Image Export-46

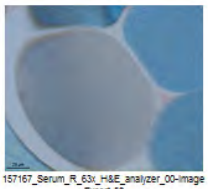
157167_Serum_R_63x_H&E_analyzer_00-Image Export-52

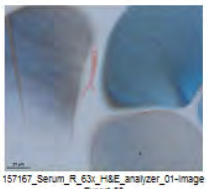
157167_Serum_R_63x_H&E_analyzer_01-Image Export-53

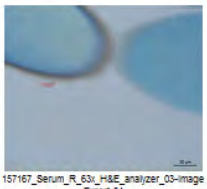
157167_Serum_R_63x_H&E_analyzer_03-Image Export-54

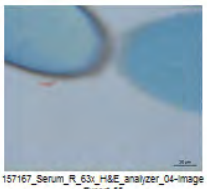
157167_Serum_R_63x_H&E_analyzer_04-Image Export-55

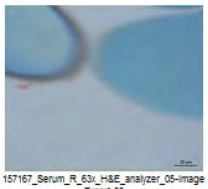
157167_Serum_R_63x_H&E_analyzer_05-Image Export-56

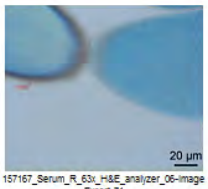

157167_Serum_R_63x_H&E_analyzer_06-Image Export-71

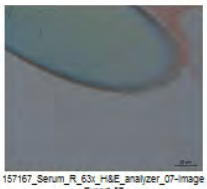
157167_Serum_R_63x_H&E_analyzer_07-Image Export-57

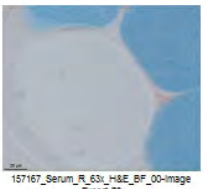
157167_Serum_R_63x_H&E_BF_00-Image Export-72

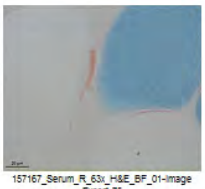
157167_Serum_R_63x_H&E_BF_01-Image Export-75

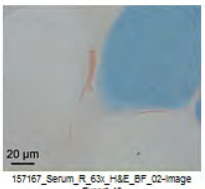

157167_Serum_R_63x_H&E_BF_02-Image Export-49

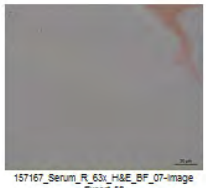
157167_Serum_R_63x_H&E_BF_07-Image Export-58

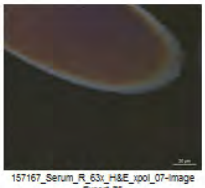
157167_Serum_R_63x_H&E_xpol_07-Image Export-76

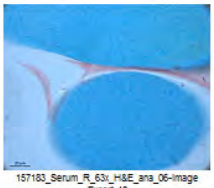
157183_Serum_R_63x_H&E_ana_06-Image Export-40

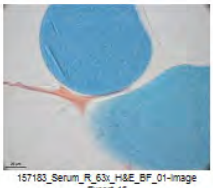
157183_Serum_R_63x_H&E_BF_01-Image Export-16

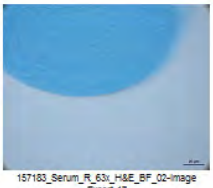
157183_Serum_R_63x_H&E_BF_02-Image Export-17

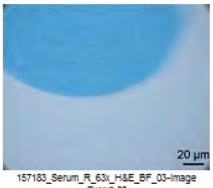

157183_Serum_R_63x_H&E_BF_03-Image Export-02

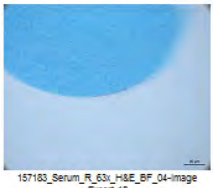
157183_Serum_R_63x_H&E_BF_04-Image Export-18

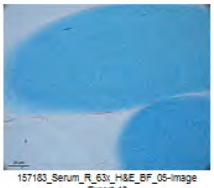
157183_Serum_R_63x_H&E_BF_05-Image Export-19

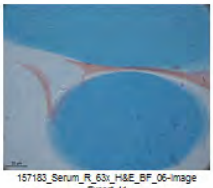
157183_Serum_R_63x_H&E_BF_06-Image Export-41

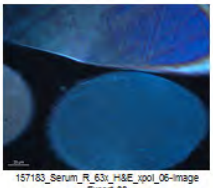
157183_Serum_R_63x_H&E_xpol_06-Image Export-20

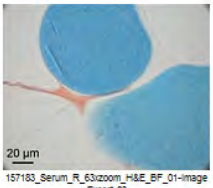

157183_Serum_R_63xzoom_H&E_BF_01-Image Export-03

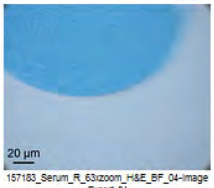

157183_Serum_R_63xzoom_H&E_BF_04-Image Export-04

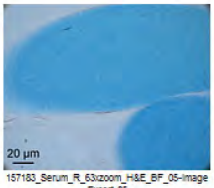

157183_Serum_R_63xzoom_H&E_BF_05-Image Export-05


157191_Serum_R_63x_H&E_ana_01-Image Export-23

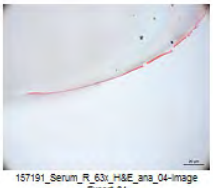
157191_Serum_R_63x_H&E_ana_04-Image Export-24


157191_Serum_R_63x_H&E_BF_01-Image Export-25

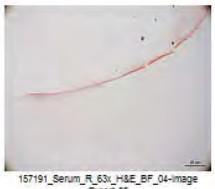
157191_Serum_R_63x_H&E_BF_04-Image Export-26

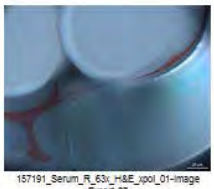
157191_Serum_R_63x_H&E_xpol_01-Image Export-27

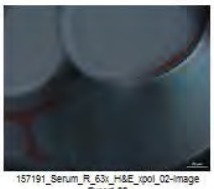
157191_Serum_R_63x_H&E_xpol_02-Image Export-28

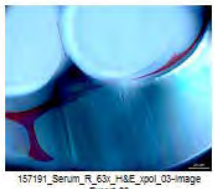
157191_Serum_R_63x_H&E_xpol_03-Image Export-29


157191_Serum_R_63x_H&E_xpol_04-Image Export-30

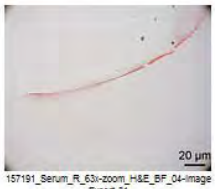

157191_Serum_R_63x-zoom_H&E_BF_04-Image Export-31

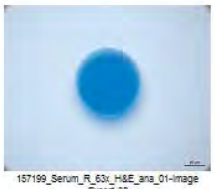
157199_Serum_R_63x_H&E_ana_01-Image Export-38


157199_Serum_R_63x_H&E_BF_01-Image Export-10

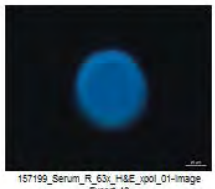
157199_Serum_R_63x_H&E_xpol_01-Image Export-40


157235_Pellet_Serum_R_63x_H&E_ana_01-Draw Scale Bar Annotation-02-Image Export-49


157235_Pellet_Serum_R_63x_H&E_ana_01-Image Export-48


157235_Pellet_Serum_R_63x_H&E_BF_01-Draw Scale Bar Annotation-01-Image Export-51


157235_Pellet_Serum_R_63x_H&E_BF_01-Image Export-50

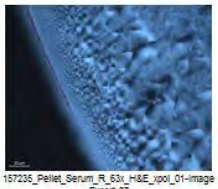
157235_Pellet_Serum_R_63x_H&E_xpol_01-Image Export-27


157162_QUV_P_10x_H&E_BF_1


157162_QUV_P_10x_H&E_BF_5


157162_QUV_P_40x_H&E_BF_1


157162_QUV_P_40x_H&E_BF_2


157162_QUV_P_40x_H&E_BF_3


157162_QUV_P_40x_H&E_BF_4


157162_QUV_P_40x_H&E_xpol_1


157164_ChemOx_P_10x_H&E_BF_1


157164_ChemOx_P_10x_H&E_BF_2


157164_ChemOx_P_40x_H&E_BF_1

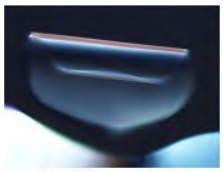
157164_ChemOx_P_40x_H&E_xpol_1


157164_ChemOx_P_100x_H&E_BF_1

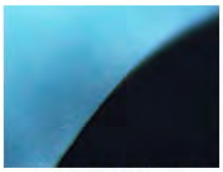
157164_ChemOx_P_100x_H&E_xpol_1


157166_Serum_P_10x_H&E_BF_01


157166_Serum_P_10x_H&E_xpol_01


157166_Serum_P_40x_H&E_BF_01


157166_Serum_P_40x_H&E_xpol_01


157170_QUV_P_10x_H&E_BF_1


157170_QUV_P_40x_H&E_ana_1


157170_QUV_P_40x_H&E_BF_1


157170_QUV_P_40x_H&E_xpol_1


157172_ChemOx_P_10x_H&E_BF_1


157172_ChemOx_P_40x_H&E_BF_1


157172_ChemOx_P_40x_H&E_BF_2

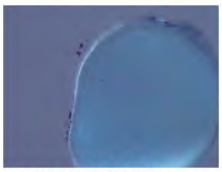
157172_ChemOx_P_40x_H&E_xpol_1


157174_Serum_P_10x_H&E_BF_1


157174_Serum_P_40x_H&E_BF_1


157174_Serum_P_40x_H&E_BF_2


157174_Serum_P_40x_H&E_BF_3


157174_Serum_P_40x_H&E_ypol_1


157174_Serum_P_100x_H&E_BF_1

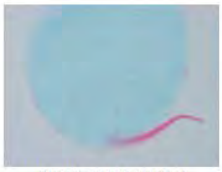
157182_Serum_P_40x_H&E_BF_01


157182_Serum_P_40x_H&E_BF_02


157182_Serum_P_40x_H&E_BF_03

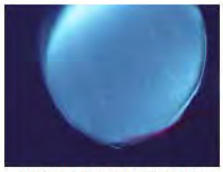
157182_Serum_P_40x_H&E_Cross-Polar_03

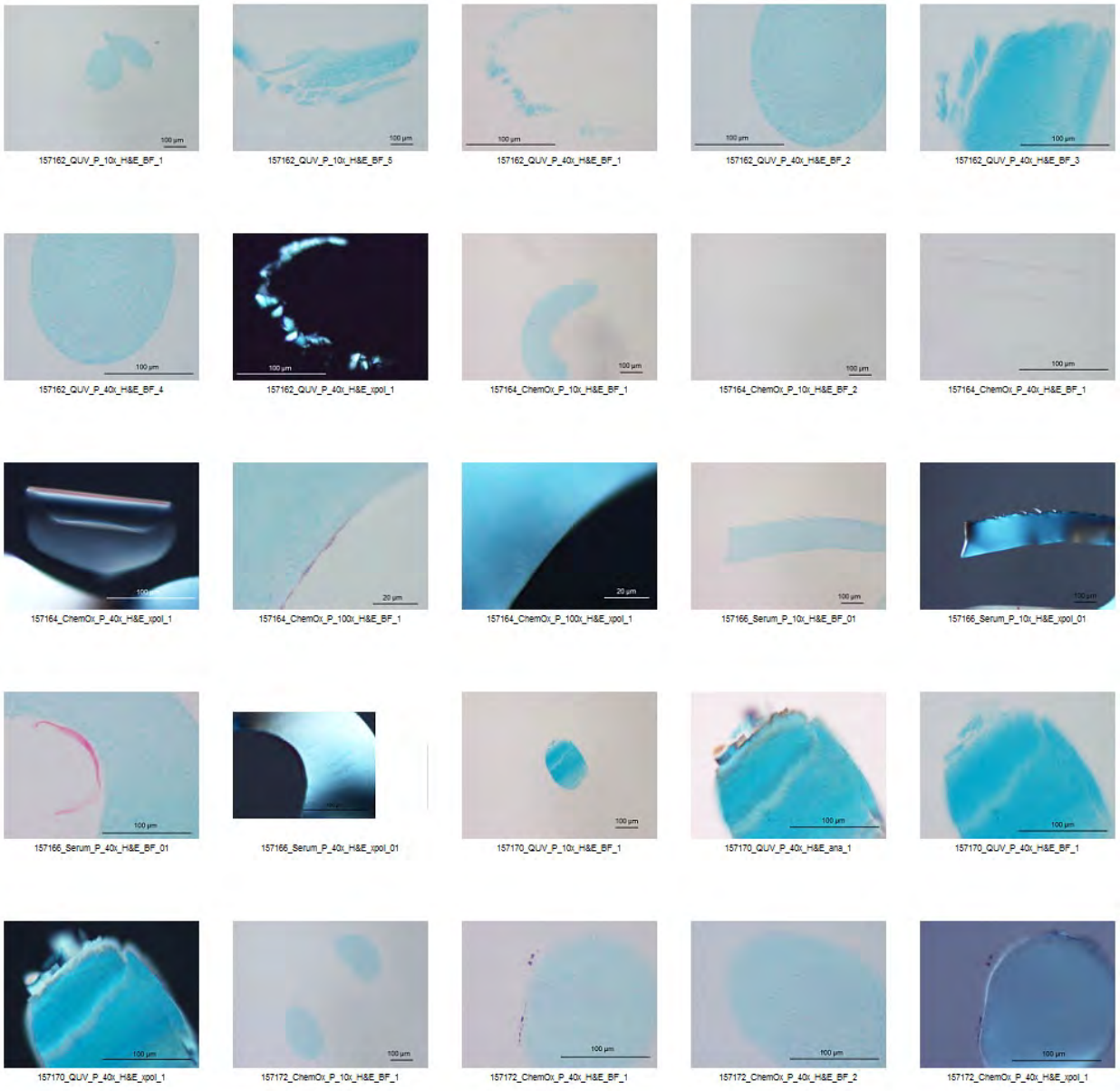
157162_QUV_P_10x_H&E_BF_1
157162_QUV_P_10x_H&E_BF_5
157162_QUV_P_40x_H&E_BF_1
157162_QUV_P_40x_H&E_BF_2
157162_QUV_P_40x_H&E_BF_3
157162_QUV_P_40x_H&E_BF_4
157162_QUV_P_40x_H&E_xpol_1
157164_ChemOx_P_10x_H&E_BF_1
157164_ChemOx_P_10x_H&E_BF_2
157164_ChemOx_P_40x_H&E_BF_1
157164_ChemOx_P_40x_H&E_xpol_1
157164_ChemOx_P_100x_H&E_BF_1
157164_ChemOx_P_100x_H&E_xpol_1
157166_Serum_P_10x_H&E_BF_01
157166_Serum_P_10x_H&E_xpol_01
157166_Serum_P_40x_H&E_BF_01
157166_Serum_P_40x_H&E_xpol_01
157170_QUV_P_10x_H&E_BF_1
157170_QUV_P_40x_H&E_ana_1
157170_QUV_P_40x_H&E_BF_1
157170_QUV_P_40x_H&E_xpol_1
157172_ChemOx_P_10x_H&E_BF_1
157172_ChemOx_P_40x_H&E_BF_1
157172_ChemOx_P_40x_H&E_BF_2
157172_ChemOx_P_40x_H&E_xpol_1

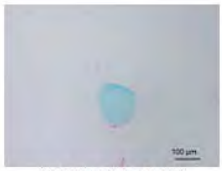
157174_Serum_P_10x_H&E_BF_1

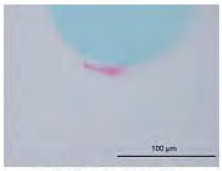
157174_Serum_P_40x_H&E_BF_1

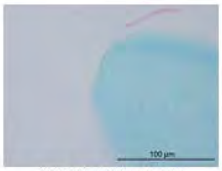
157174_Serum_P_40x_H&E_BF_2

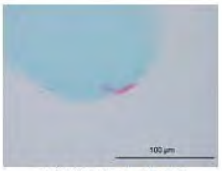
157174_Serum_P_40x_H&E_BF_3

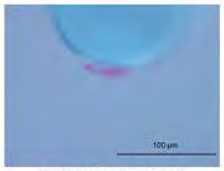
157174_Serum_P_40x_H&E_ypol_1

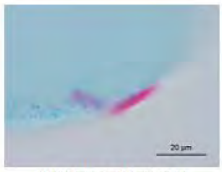
157174_Serum_P_100x_H&E_BF_1

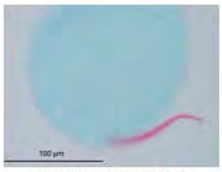
157182_Serum_P_40x_H&E_BF_01

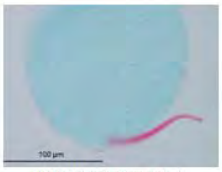
157182_Serum_P_40x_H&E_BF_02


157182_Serum_P_40x_H&E_BF_03

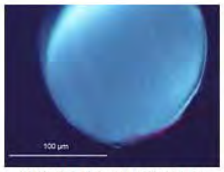
157182_Serum_P_40x_H&E_Cross-Polar_03

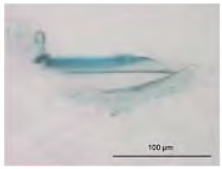
162_QUV-P_40x_Unstained_BF

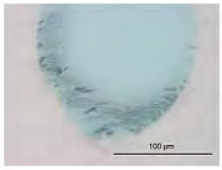
162_QUV-P_40x_Unstained_BF

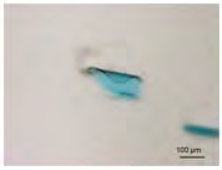
4_ChemOx-P_10x_Unstained_I


4_ChemOx-P_10x_Unstained_I

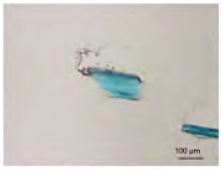
4_ChemOx-P_10x_Unstained_I


66_Serum-P_10x_Unstained_B

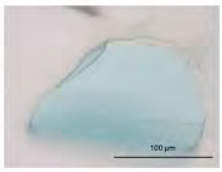
66_Serum-P_40x_Unstained_B

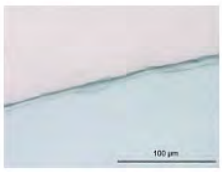
66_Serum-P_40x_Unstained_B


170_QUV-P_10x_Unstained_BF

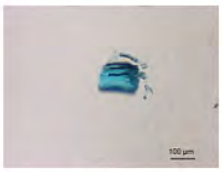
170_QUV-P_10x_Unstained_BF

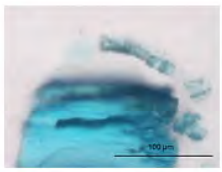
170_QUV-P_40x_Unstained_BF

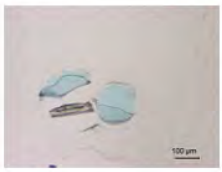
2_ChemOx-P_10x_Unstained_I

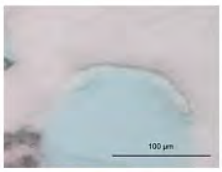
2_ChemOx-P_40x_Unstained_I


2_ChemOx-P_40x_Unstained_I

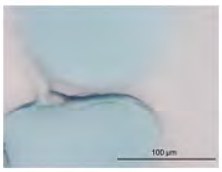
74_Serum-P_40x_Unstained_B

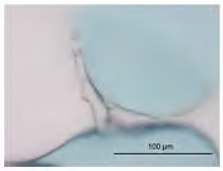
74_Serum-P_40x_Unstained_B


178_QUV-P_10x_Unstained_BF

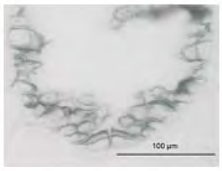
178_QUV-P_40x_Unstained_BF

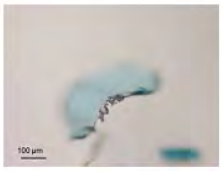
0_ChemOx-P_10x_Unstained_I

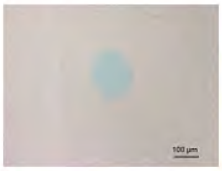
0_ChemOx-P_10x_Unstained_I


0_ChemOx-P_10x_Unstained_I


0_ChemOx-P_10x_Unstained_I

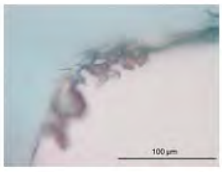
0_ChemOx-P_40x_Unstained_I

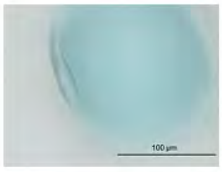
0_ChemOx-P_40x_Unstained_I

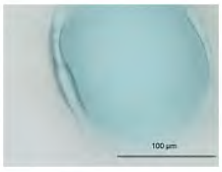
0_ChemOx-P_40x_Unstained_I

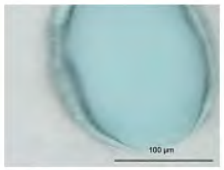
0_ChemOx-P_40x_Unstained_I


82_Serum-P_10x_Unstained_B

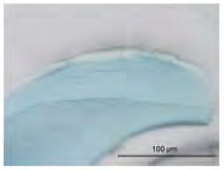
82_Serum-P_10x_Unstained_B

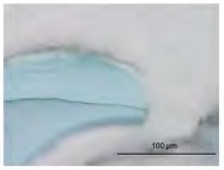
82_Serum-P_10x_Unstained_B

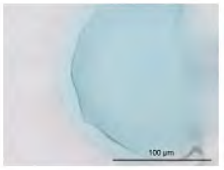
82_Serum-P_40x_Unstained_B

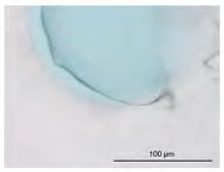
82_Serum-P_40x_Unstained_B

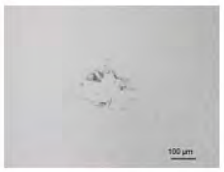
8_ChemOx-P_10x_Unstained_I


ChemOx_Pellet-P_10x_Unstaine

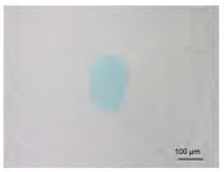
ntreatedControl_P_10x_Unstain


ntreatedControl_P_10x_Unstain

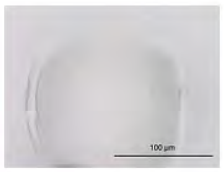
ntreatedControl_P_40x_Unstain

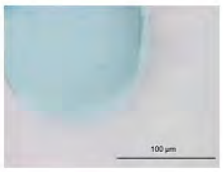
ntreatedControl_P_40x_Unstain

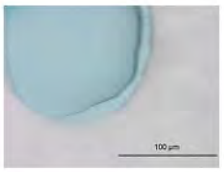
ntreatedControl_P_40x_Unstain

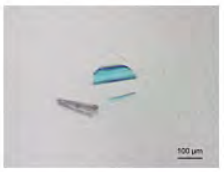
ntreatedControl_P_40x_Unstain

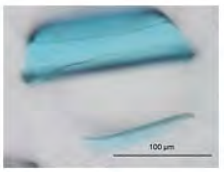
ntreatedControl_P_40x_Unstain


ntreatedControl_P_10x_Unstain


ntreatedControl_P_10x_Unstain


ntreatedControl_P_10x_Unstain


ntreatedControl_P_10x_Unstain


ntreatedControl_P_10x_Unstain


ntreatedControl_P_10x_Unstain

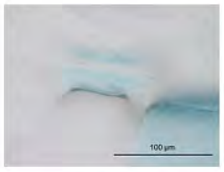
ntreatedControl_P_40x_Unstain

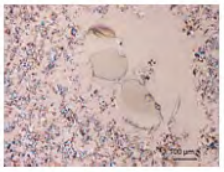
ıtreatedControl_P_10x_Unstain


ntreatedControl_P_10x_Unstain


ntreatedControl_P_10x_Unstain


ntreatedControl_P_10x_Unstain

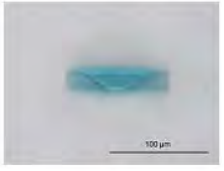
ntreatedControl_P_10x_Unstain

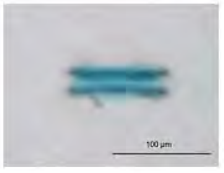
ntreatedControl_P_10x_Unstain

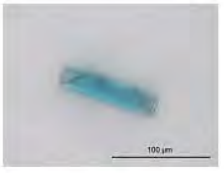
3_ChemOx_P_40x_Unstained_

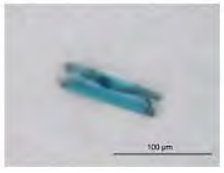
3_ChemOx_P_40x_Unstained_

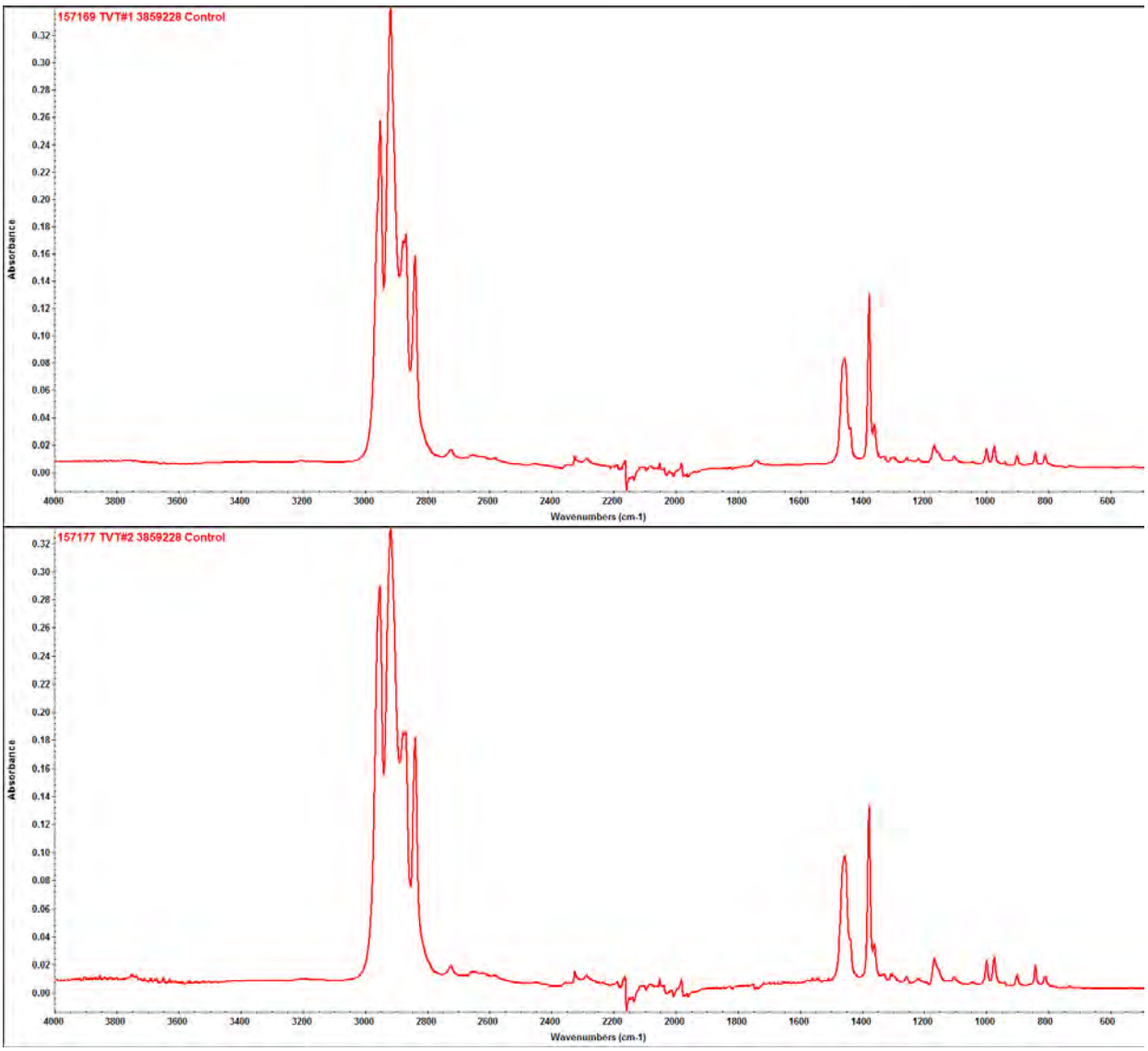
157169 TVT#1 3859228 Control
Absorbance
Wavenumbers (cm-1)
157177 TVT#2 3859228 Control
Absorbance
Wavenumbers (cm-1)

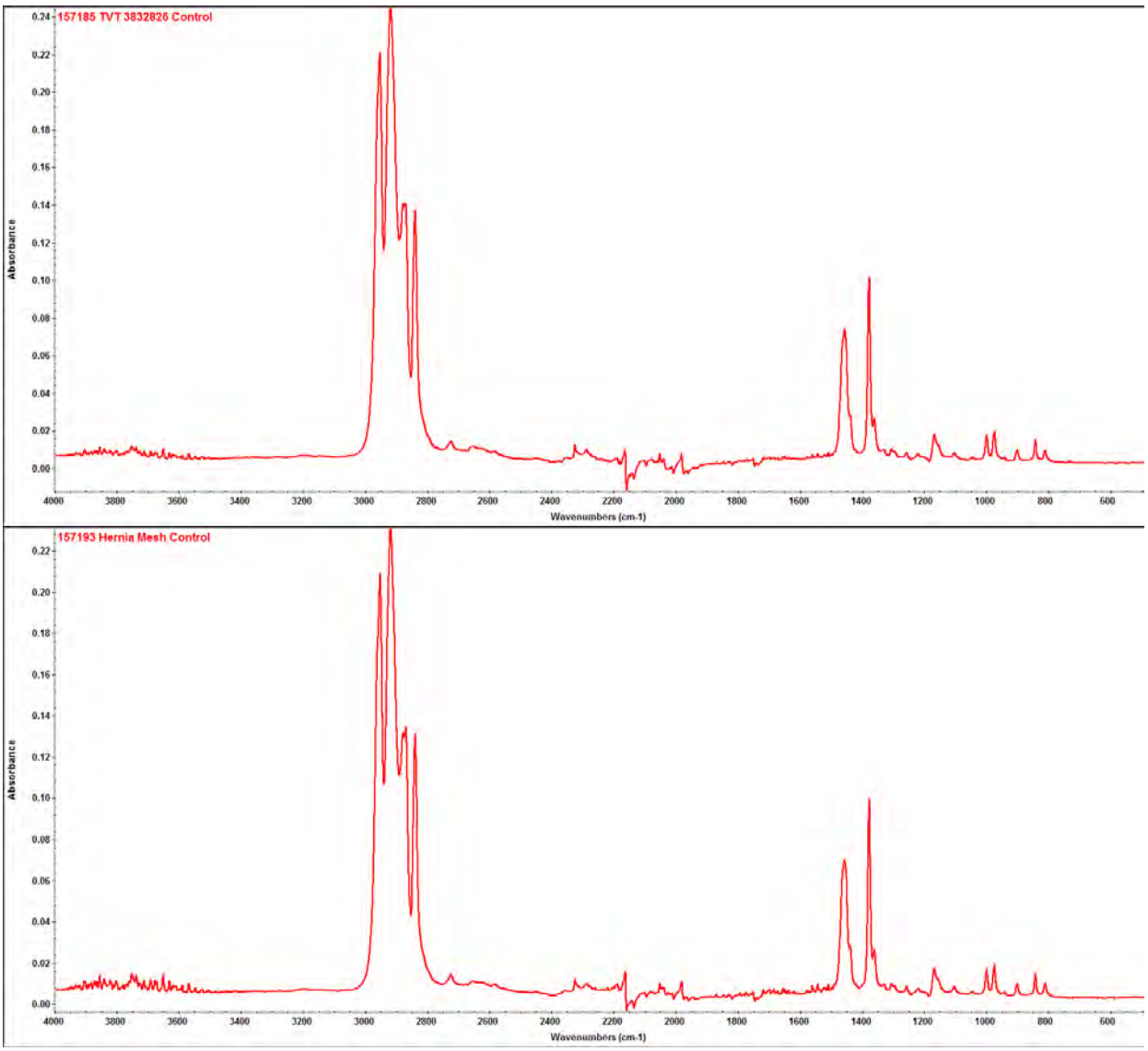
157185 TVT 3832826 Control
Absorbance
Wavenumbers (cm-1)
157193 Hernia Mesh Control
Absorbance
Wavenumbers (cm-1)

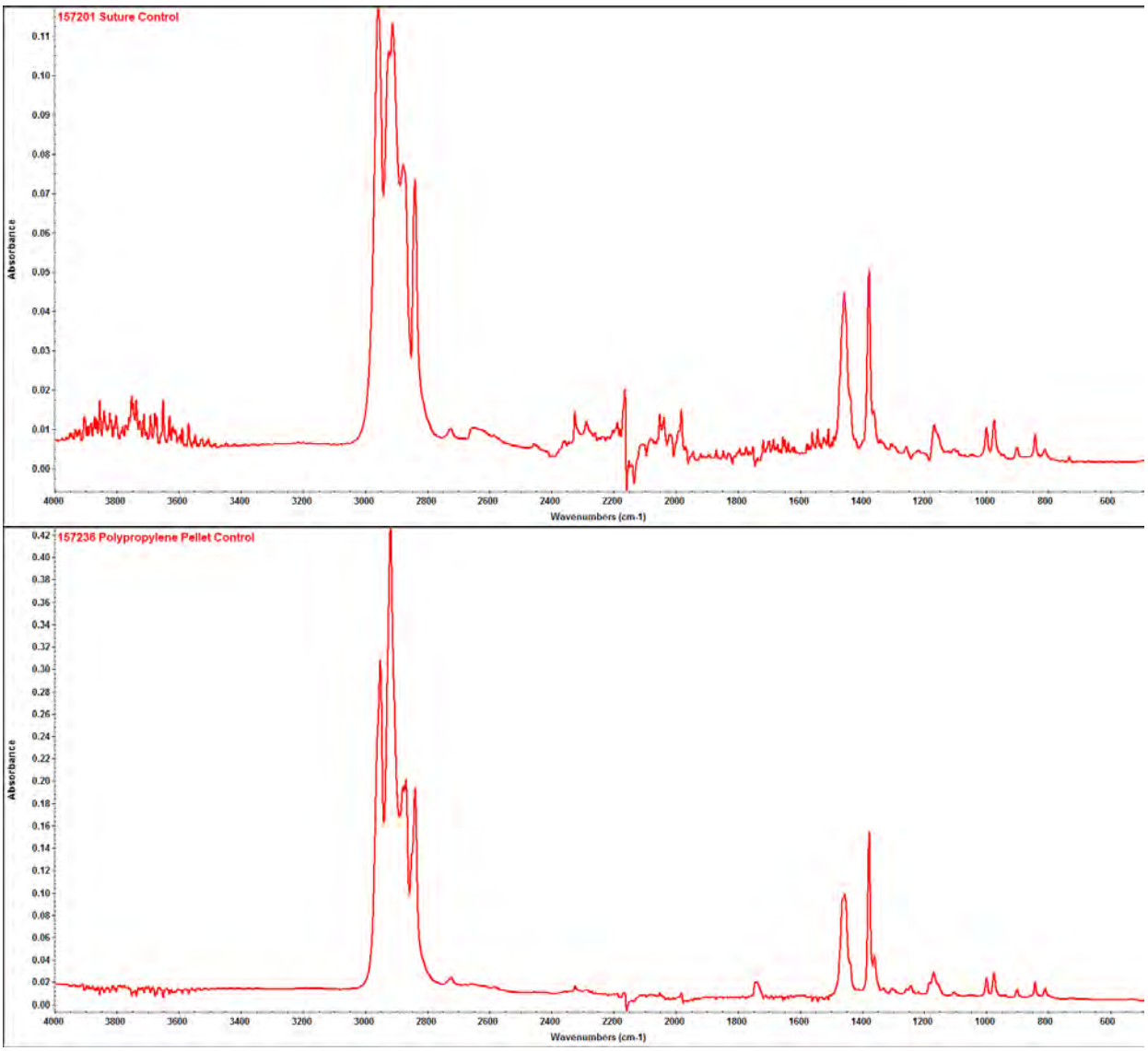
157201 Suture Control
Absorbance
Wavenumbers (cm-1)
157236 Polypropylene Pellet Control
Absorbance
Wavenumbers (cm-1)

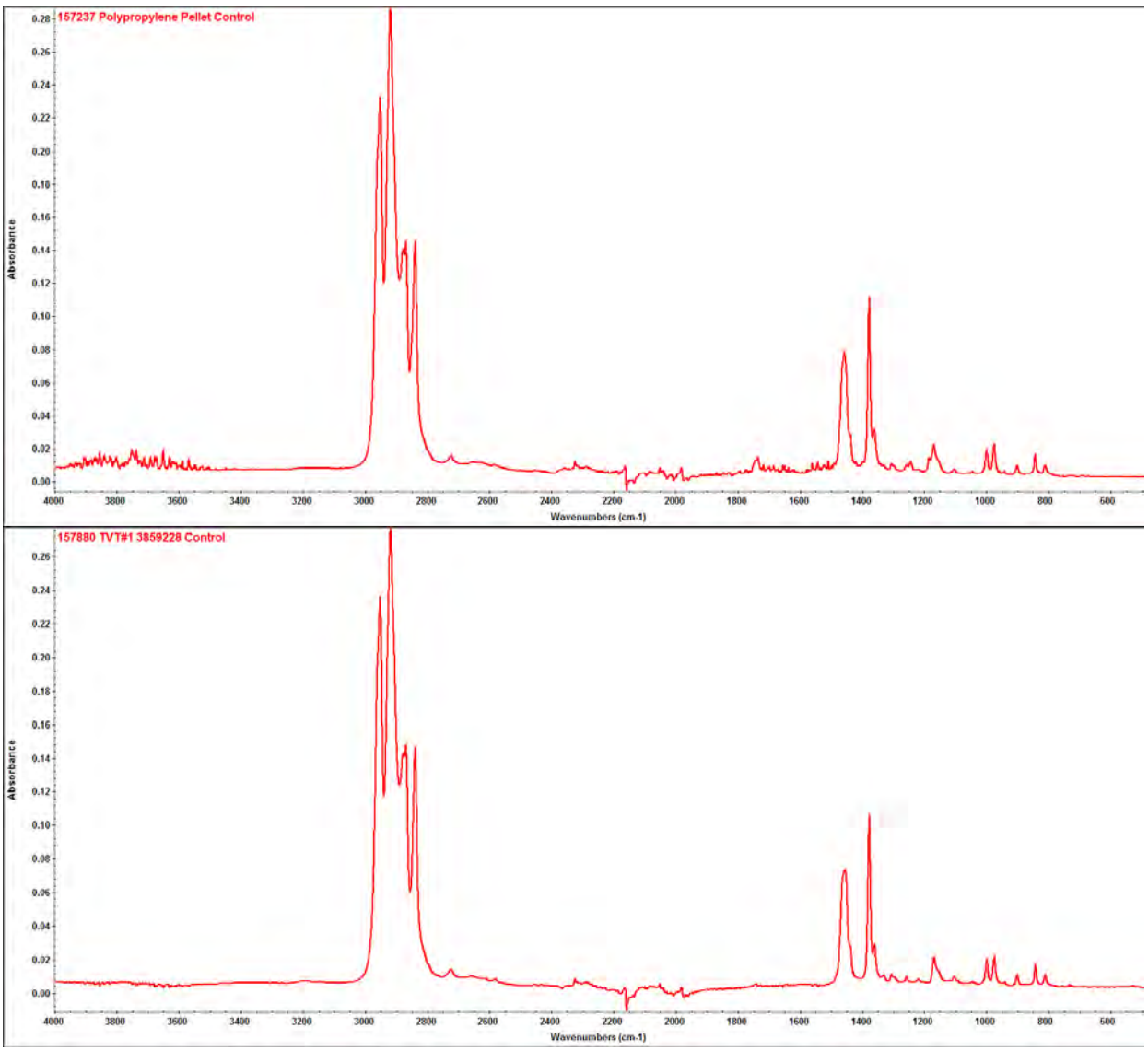
157237 Polypropylene Pellet Control
Absorbance
Wavenumbers (cm-1)
157880 TVT#1 3859228 Control
Absorbance
Wavenumbers (cm-1)

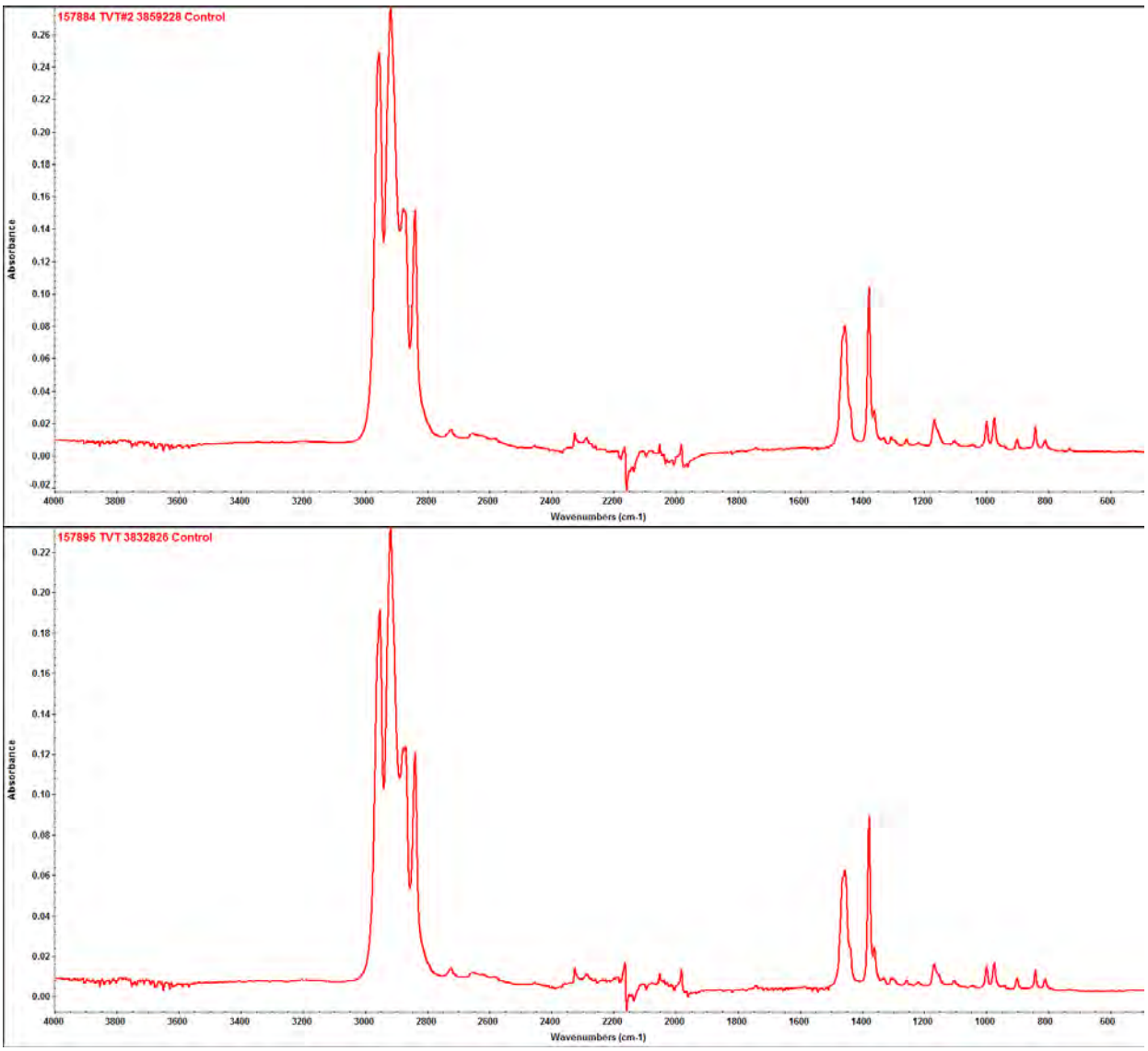
157884 TVT#2 3859228 Control
Absorbance
Wavenumbers (cm-1)
157895 TVT 3832826 Control
Absorbance
Wavenumbers (cm-1)

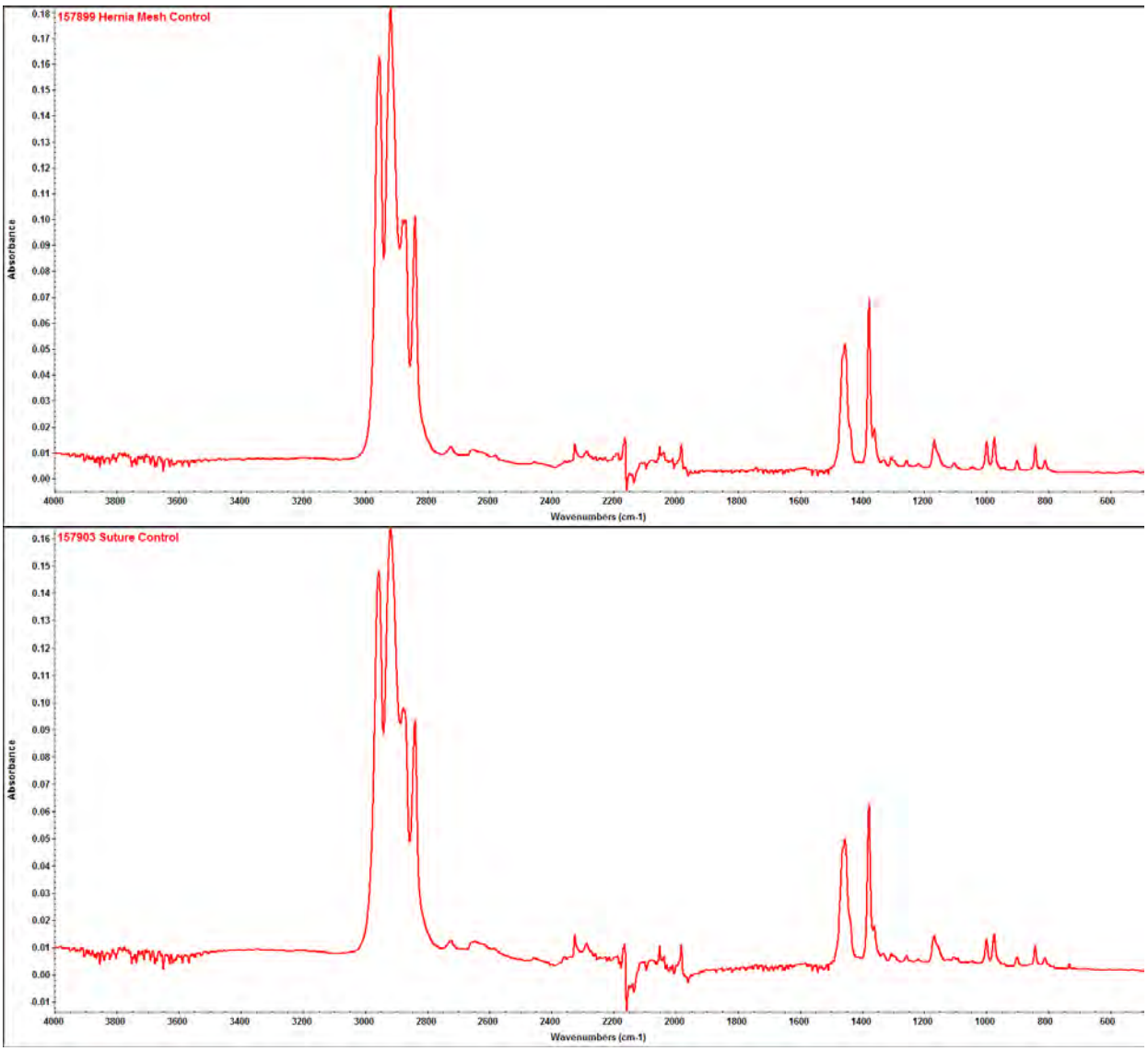
157899 Hernia Mesh Control
Absorbance
Wavenumbers (cm-1)
157903 Suture Control
Absorbance
Wavenumbers (cm-1)

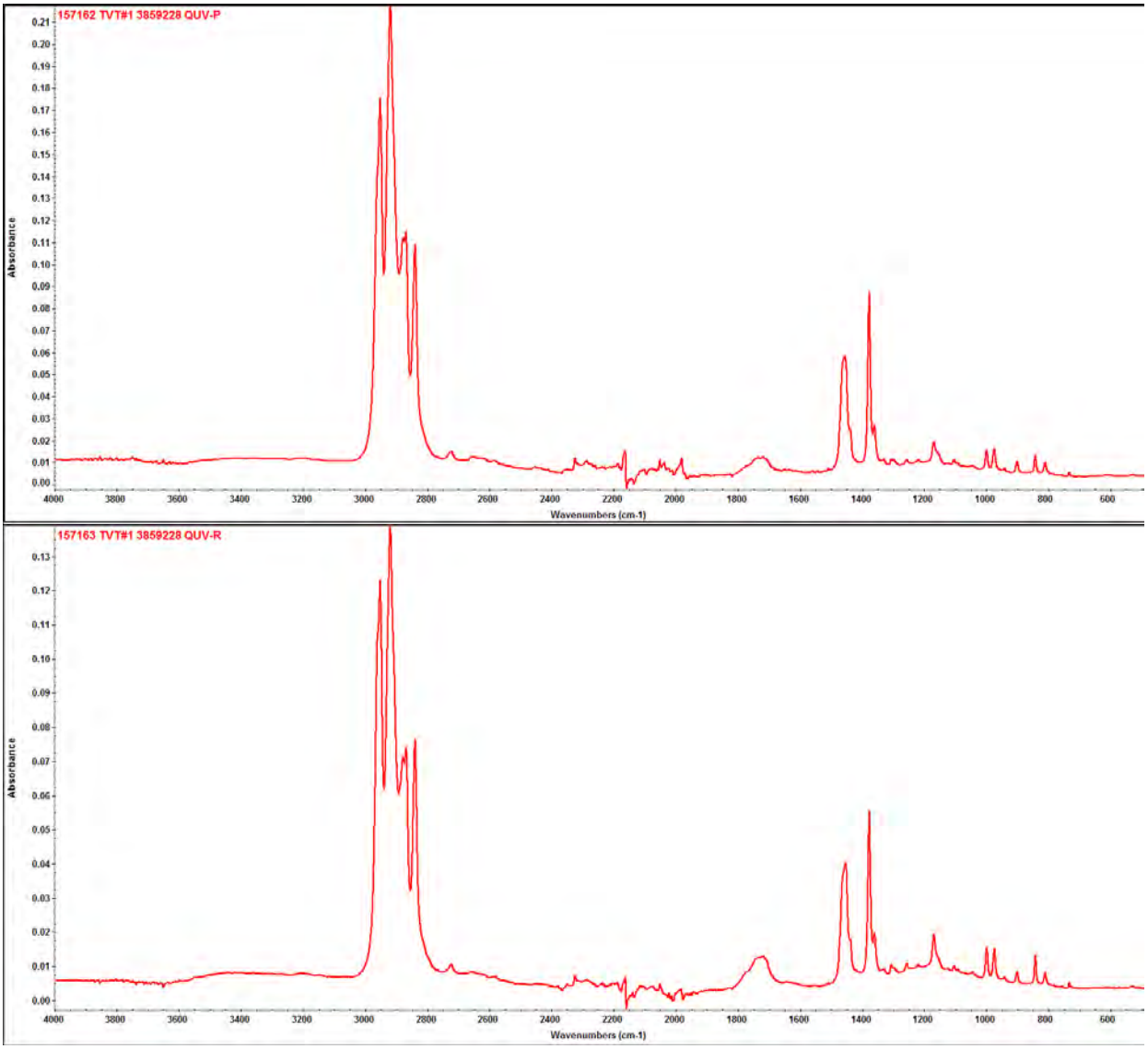
157162 TVT#1 3859228 QUV-P
Absorbance
Wavenumbers (cm-1)
157163 TVT#1 3859228 QUV-R
Absorbance
Wavenumbers (cm-1)

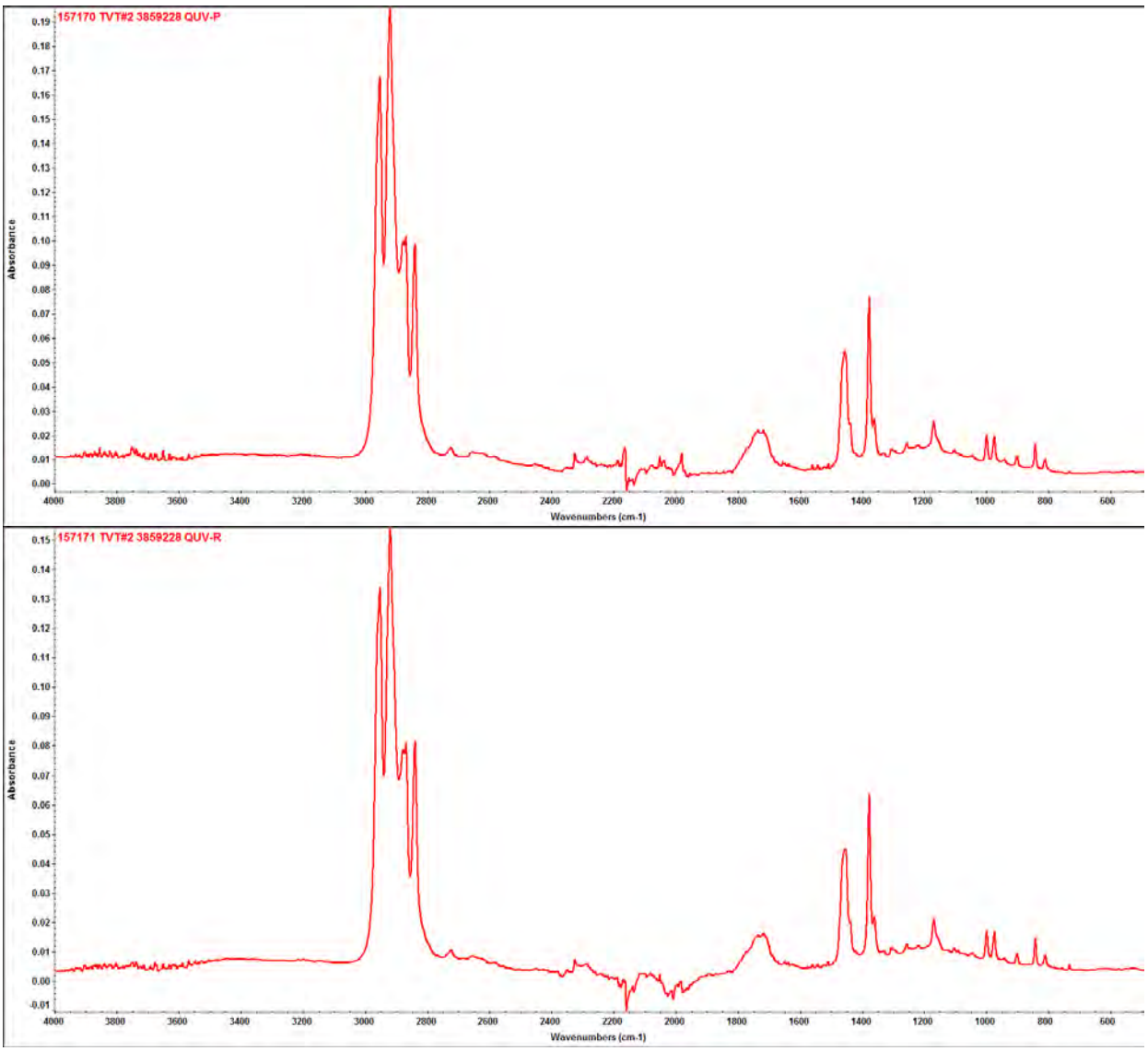
157170 TVT#2 3859228 QUV-P
Absorbance
Wavenumbers (cm-1)
157171 TVT#2 3859228 QUV-R
Absorbance
Wavenumbers (cm-1)

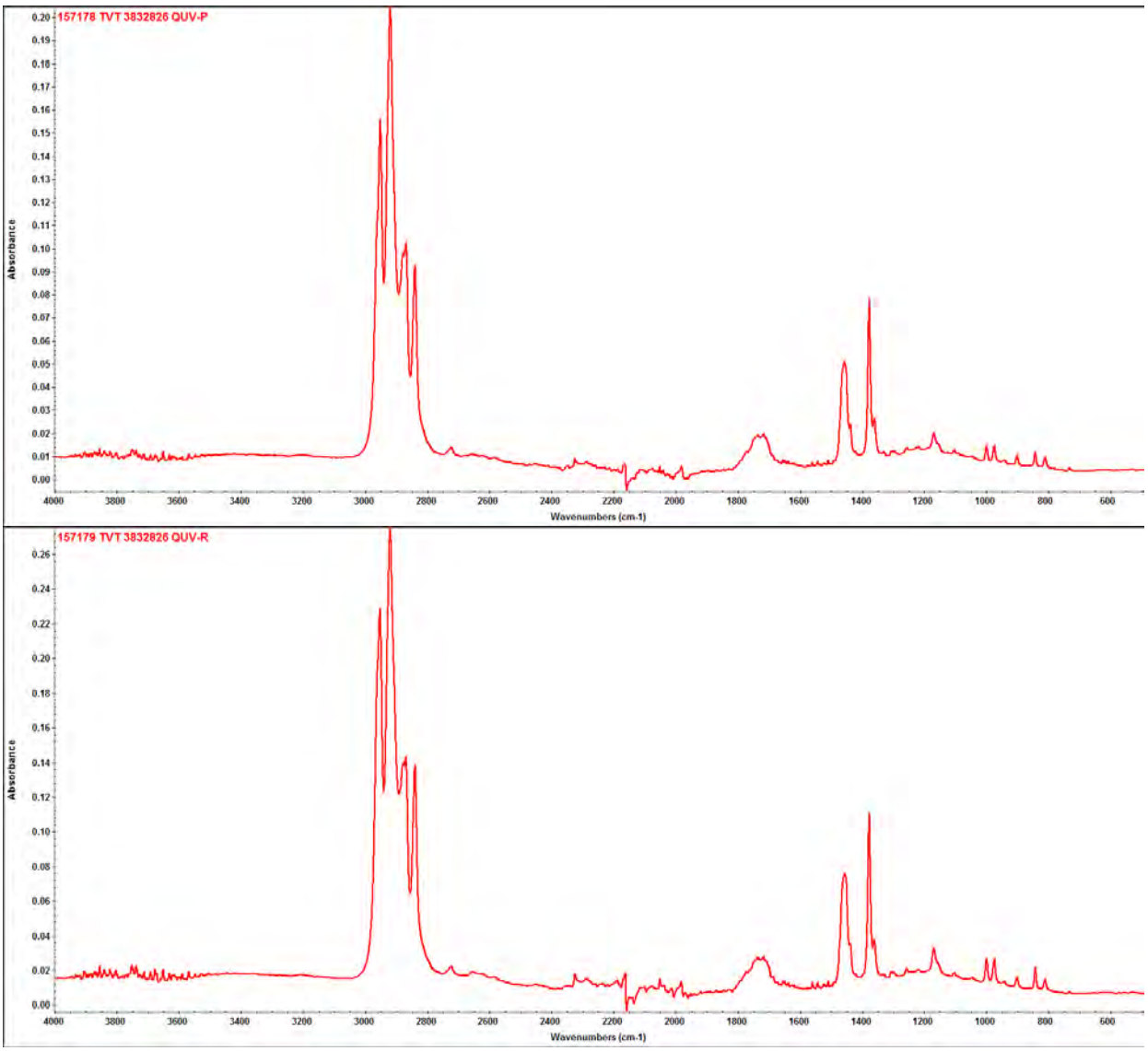
157178 TVT 3832826 QUV-P
Absorbance
Wavenumbers (cm-1)
157179 TVT 3832826 QUV-R
Absorbance
Wavenumbers (cm-1)

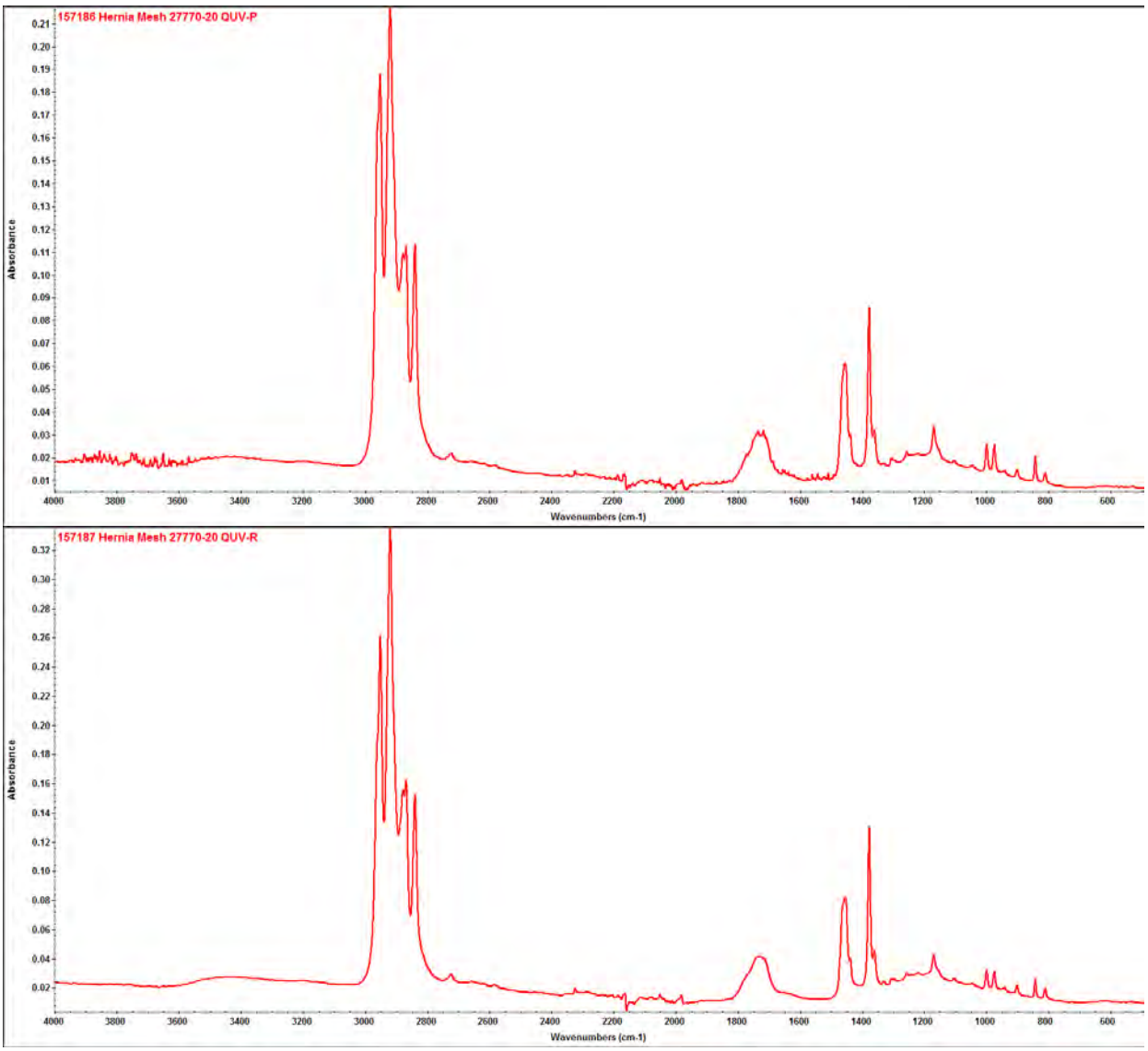
157186 Hernia Mesh 27770-20 QUV-P
Absorbance
Wavenumbers (cm-1)
157187 Hernia Mesh 27770-20 QUV-R
Absorbance
Wavenumbers (cm-1)

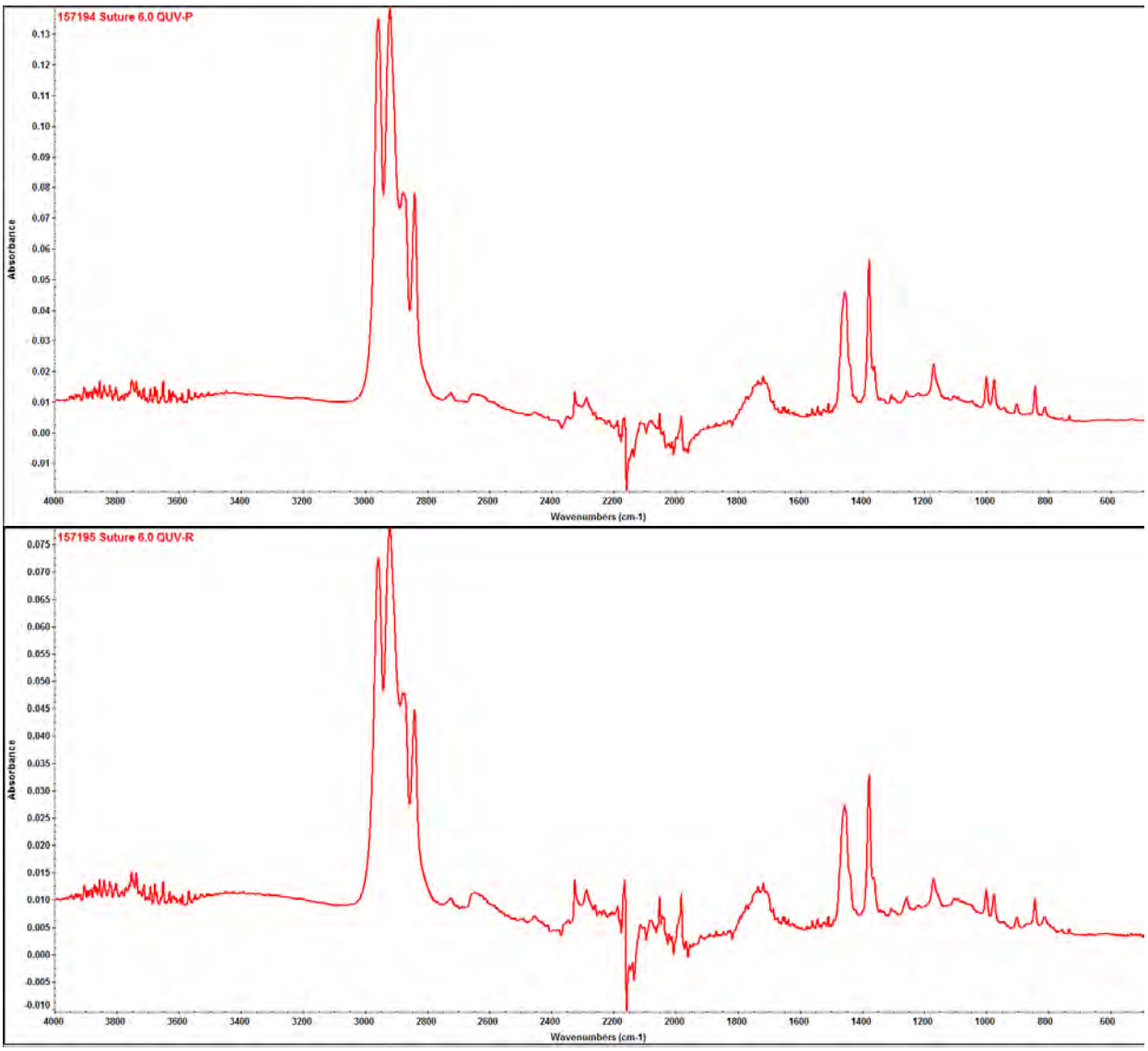
157194 Suture 6.0 QUV-P
Absorbance
Wavenumbers (cm-1)
157195 Suture 6.0 QUV-R
Absorbance
Wavenumbers (cm-1)

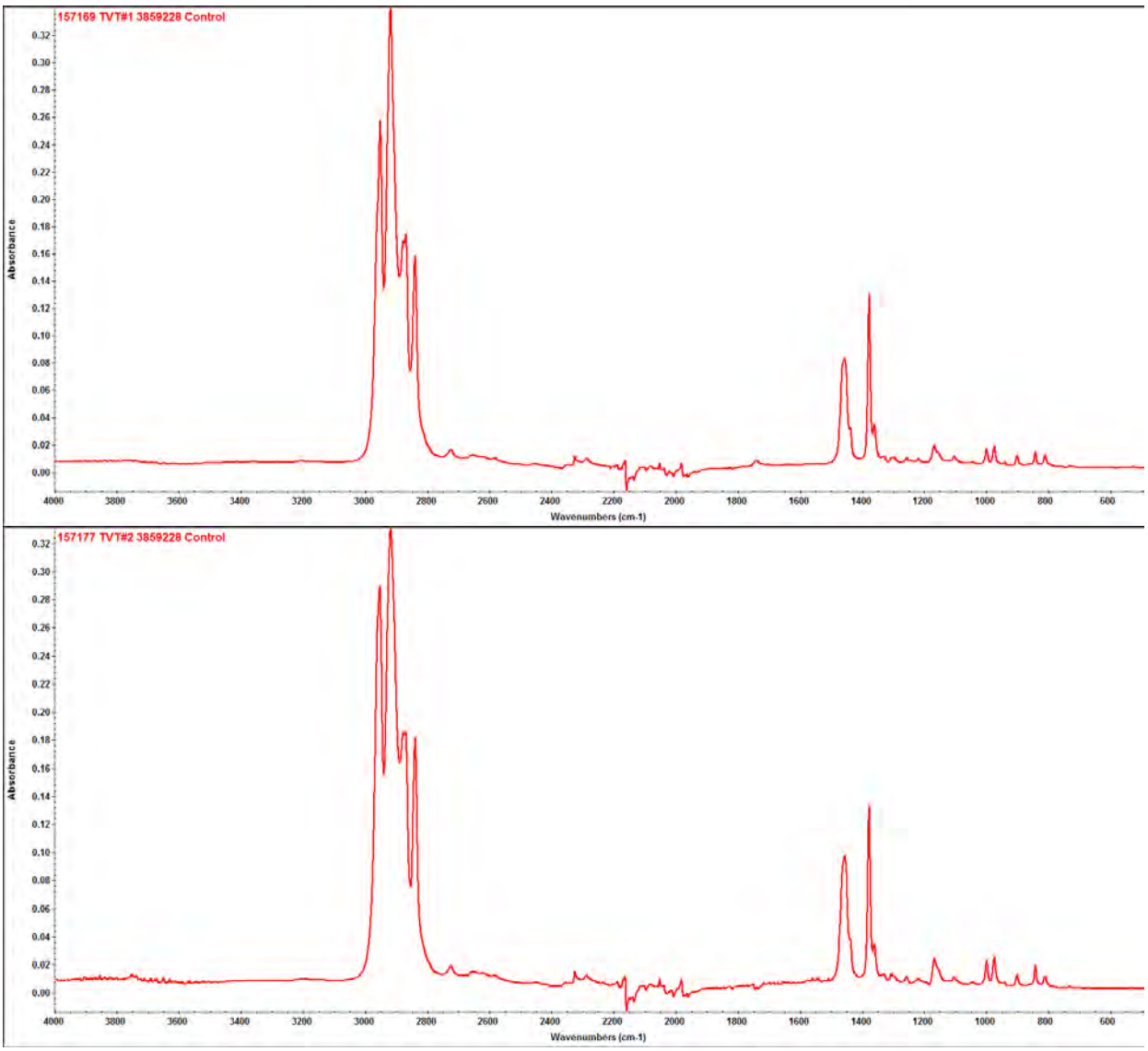
157169 TVT#1 3859228 Control
Absorbance
Wavenumbers (cm-1)
157177 TVT#2 3859228 Control
Absorbance
Wavenumbers (cm-1)

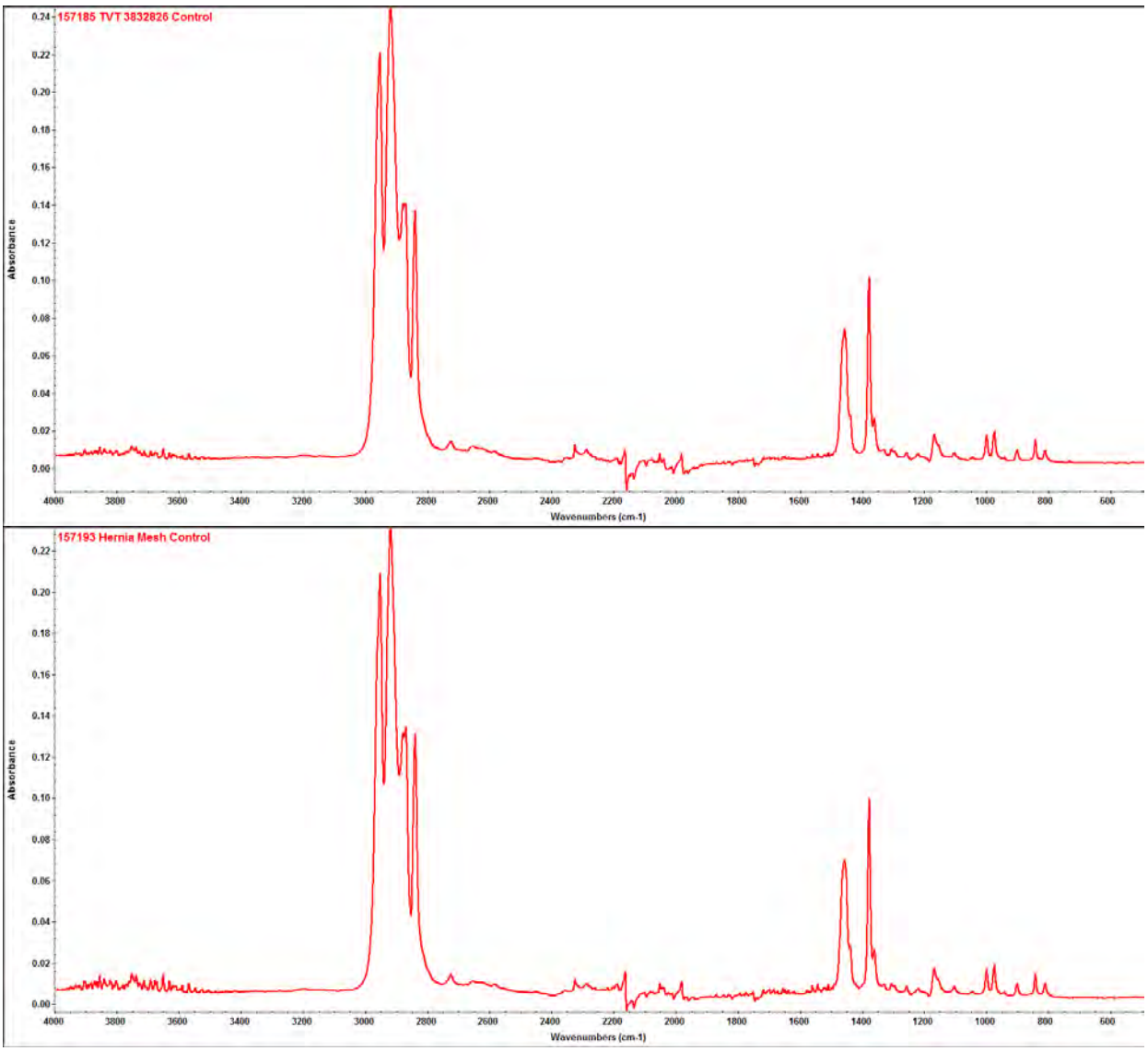
157185 TVT 3832826 Control
Absorbance
Wavenumbers (cm-1)
157193 Hernia Mesh Control
Absorbance
Wavenumbers (cm-1)

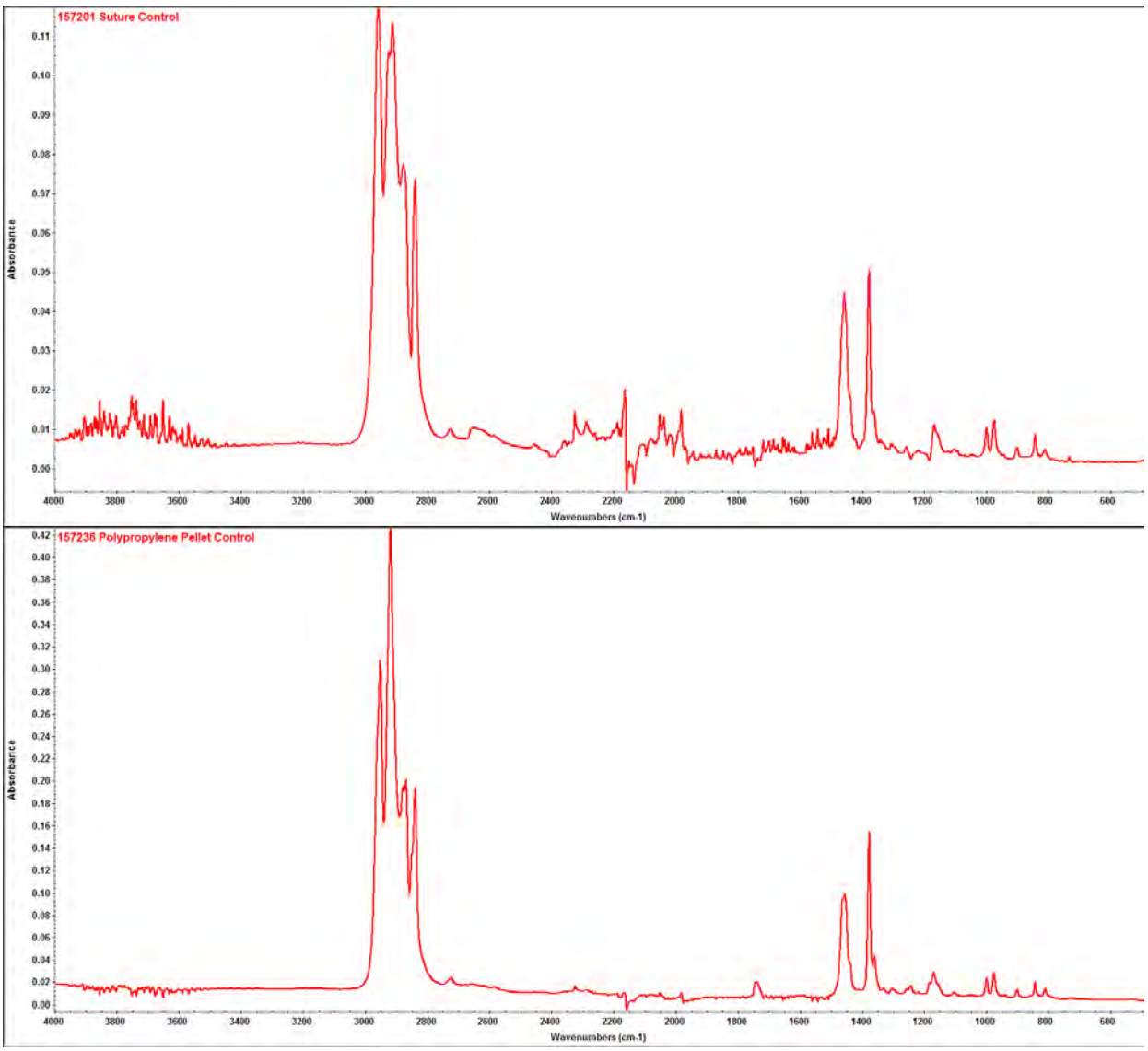
157201 Suture Control
Absorbance
Wavenumbers (cm-1)
157236 Polypropylene Pellet Control
Absorbance
Wavenumbers (cm-1)

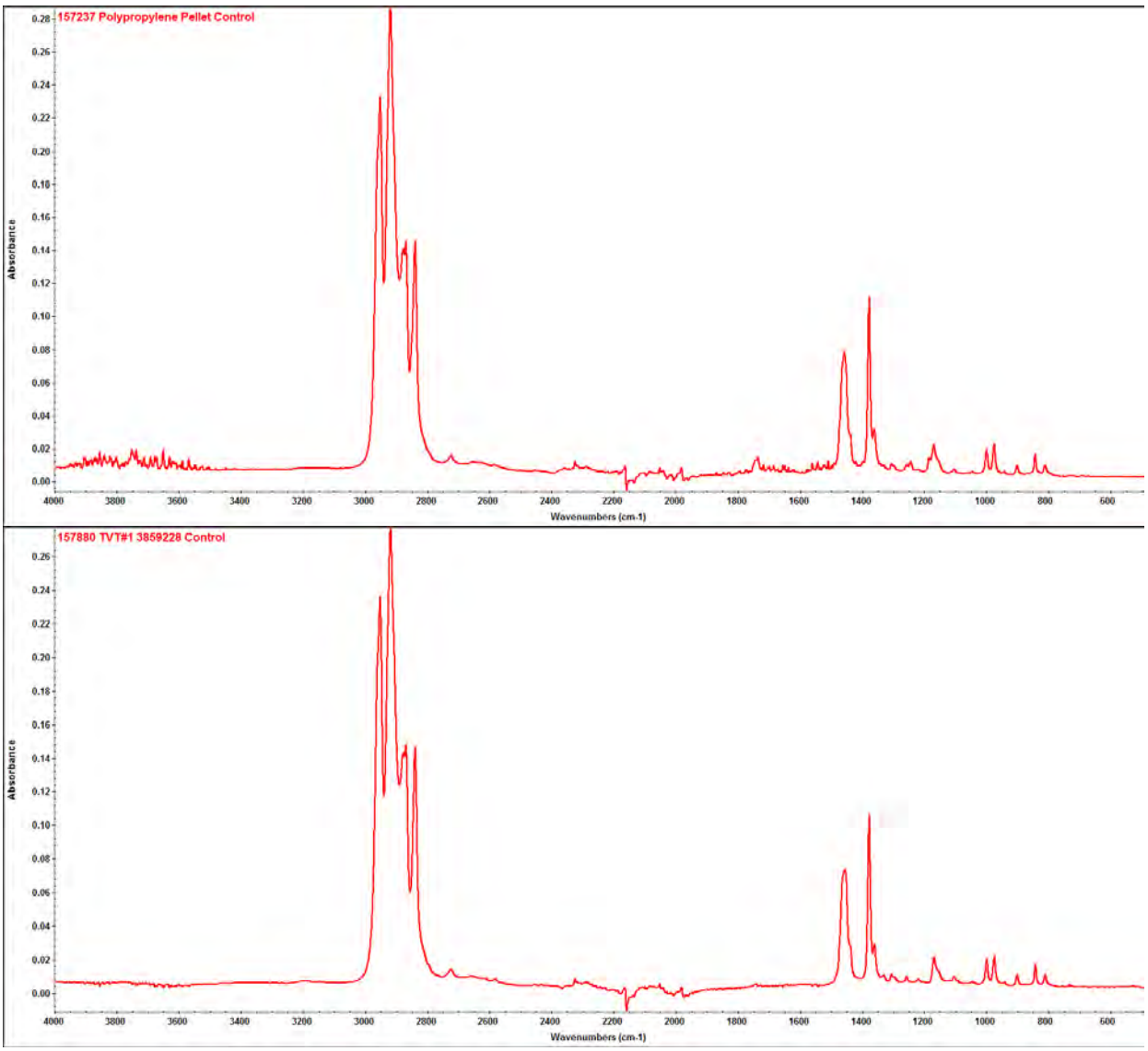
157237 Polypropylene Pellet Control
Absorbance
Wavenumbers (cm-1)
157880 TVT#1 3859228 Control
Absorbance
Wavenumbers (cm-1)

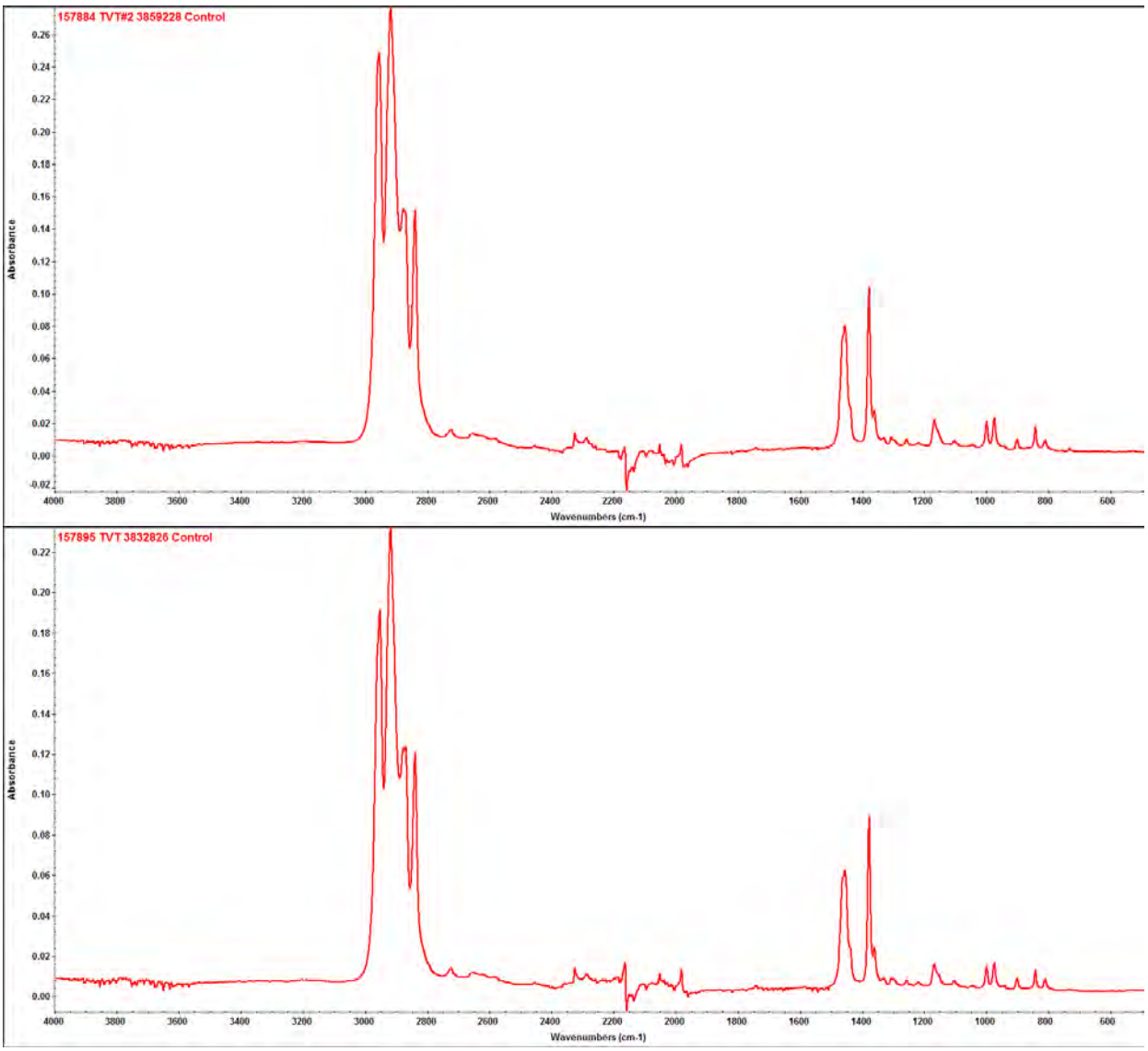
157884 TVT#2 3859228 Control
Absorbance
Wavenumbers (cm-1)
157895 TVT 3832826 Control
Absorbance
Wavenumbers (cm-1)

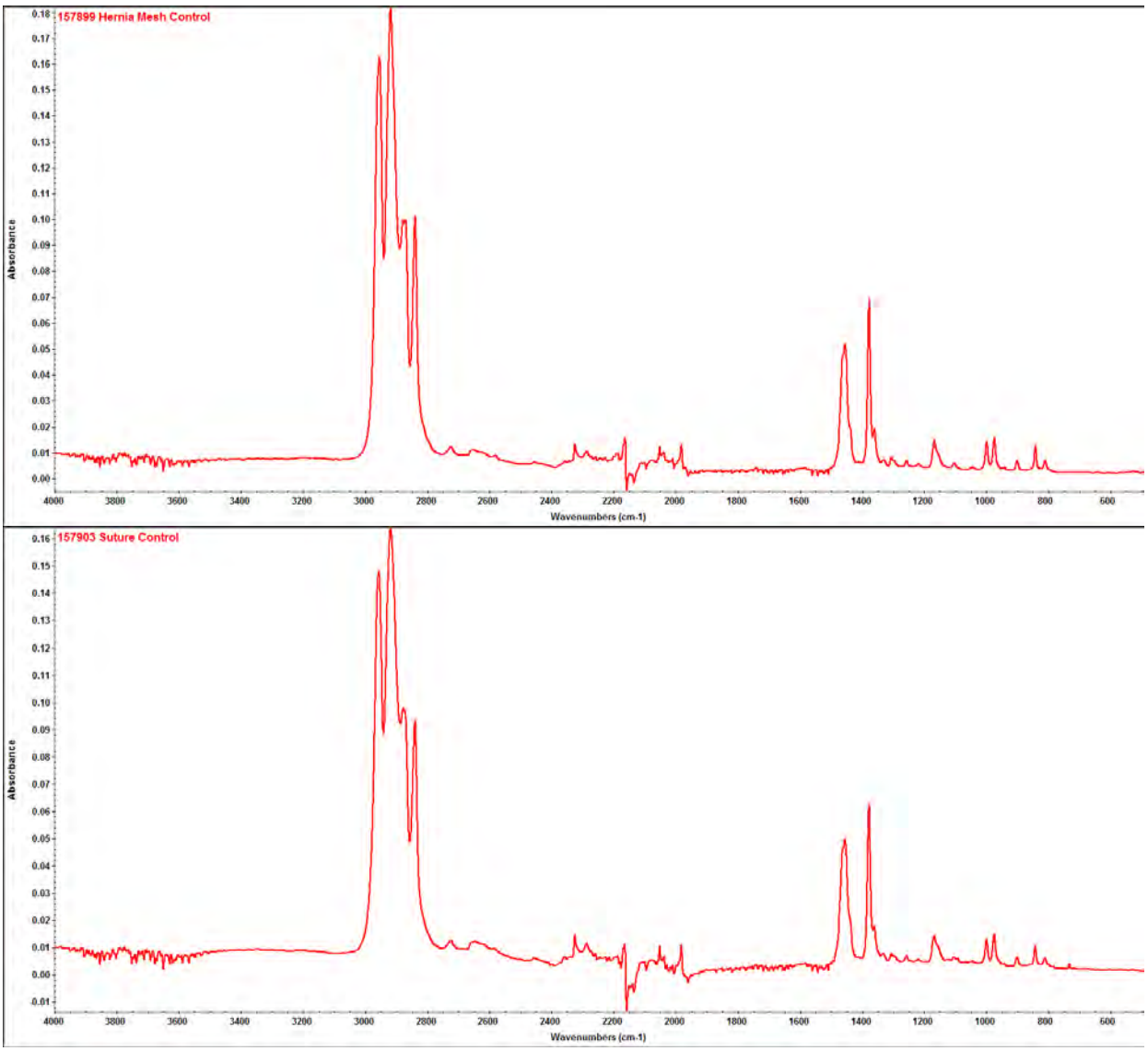
157899 Hernia Mesh Control
Absorbance
Wavenumbers (cm-1)
157903 Suture Control
Absorbance
Wavenumbers (cm-1)